

**Local auxin transport regulation in the
nascent nodule - an overview in nodulating
plants and an investigation into the cytokinin
receptor, CRE1-mediated control of auxin
transport in *Medicago truncatula***

A thesis submitted for the degree of

Doctor of Philosophy

of

The Australian National University



**Australian
National
University**

By

Liang Pin Jason Ng

Research School of Biology

March 2015

Local and systemic regulation in the
nervous system - an overview in regulatory
plants and an investigation into the cytoskeleton
mediated, ERK-mediated control of axonal
transport in *Medicago truncatula*

A thesis submitted for the degree of

Doctor of Philosophy

The Australian National University

Australian
National
University



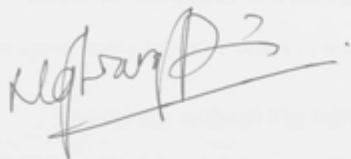
Living the Dream 1988

Research School of Biology



Declaration

This thesis is my own work and does not contain any results that have been generated by persons other than me, except where reference and acknowledgement have been made. Results presented in this thesis have not been used for the award of another degree at any other university.

A handwritten signature in black ink, appearing to read 'Liang Pin Jason Ng', with a long horizontal line extending from the end of the signature.

Liang Pin Jason Ng

Acknowledgements

I would like to thank my supervisor, Uli, for giving me the opportunity to pursue a PhD in her laboratory. Her expert guidance and advice in the last four years have made my PhD experience enjoyable. I would also like to thank her for her patience and understanding in some difficult moments during my PhD, and for supporting my conference attendance and laboratory visits. I am also grateful for being granted the opportunity to get involved in teaching activities.

I would like to thank Thy for her support and guidance in developing an LC-MS/MS method for auxin quantification. Her knowledge and input have been instrumental in making my project proceed smoothly. I am very grateful for her help and advice.

I would like to thank my laboratory members, Samira, Chooi, Deby, Sabrina, Giel, Lachy and Ethan for creating such a stimulating research environment. The organisational skills of Samira had made the running of the laboratory looked easy. I am also grateful to Samira, Chooi, Deby and Sabrina for their help, advice and banter. I would like to extend my gratitude to Britta, who had instilled me with scientific skills and discipline, both of which played important parts during my PhD. I would also like to thank past laboratory members, including Astrid, Nikki, Giulia, Irina, Sofia, Anton, Caesar and Wee Lin for their friendship and advice.

The project carried out during my PhD would not have been possible without the *cre1* mutant seeds, which were kindly provided by Dr Florian Frugier. I would like to thank him for his expert advice throughout my project, as well as the opportunity to visit his laboratory in Gif-sur-Yvette, Paris, to conduct some extremely engaging discussion about our work. I would also like to thank Professor Sofie Goormachtig for giving me the opportunity to visit her laboratory at the VIB, Ghent.

This PhD would not have been enjoyable and complete without my friends. I would like to extend my heartfelt appreciation to Kai Xun, Su Yin, Alvin, Wil, Kevin, Yi-leen, Nadia, Vinson, Richa, all of whom shared their PhD experiences with me. Their advice and friendship have been extremely helpful in aiding me overcome the difficulties I encountered. I am also very grateful to Nandha, Dartha and Boon for their friendship, and unrelentless patience and understanding.

Last but not least, I would like to say a big “thank you” to my parents and siblings, the cornerstones of my life. They have been the most caring, understanding and supportive people since my move to Australia. I am endlessly grateful to the freedom my parents have given me to do the things I want, and like. I will continue to strive for the best.

Publications

Published

- Mathesius U, Jin J, van Noorden GE, Ng JLP and Wasson AP. Regulation of nodule development by short and long distance auxin transport control. In: Biological Nitrogen Fixation. F. de Bruijn (Ed.). Wiley/Blackwell (in press).
- Ng JLP, van Noorden GE and Mathesius U (2013) Polar auxin transport regulation in plant-microbe interactions. In: Signaling and Communication in Plants. R. Chen and F. Baluška (eds.). Springer, Berlin, Heidelberg, pp. 201-219.

Accepted

Ng JLP, Hassan S, Truong T, Hocart C, Laffont C, Frugier F and Mathesius U (2015) Flavonoids and auxin transport inhibitors rescue symbiotic nodulation in the *Medicago truncatula* cytokinin perception mutant *cre1*. *Plant Cell*, in press.

Submitted

Ng JLP, Perrine-Walker F, Wasson AP and Mathesius U. Regulation of auxin transport in symbiotic and parasitic root-microbe interactions. *Plants* (invited review)

Manuscript in preparation

Winterberg B, Ng JLP and Mathesius U. Regulation of nodulation by a circadian rhythm in *Medicago truncatula*.

Contents

Declaration	iii
Acknowledgements	v
Publications	vii
Abstract	1
List of abbreviations	3
List of figures	5
List of tables	9
CHAPTER 1 General Introduction	11
1.1 Auxin homeostasis and signalling during plant development	13
1.1.1 Auxin transport carriers regulate plant development	13
1.1.1.1 <i>PIN proteins</i>	15
1.1.1.2 <i>P-glycoprotein / ATP-Binding Cassette proteins</i>	16
1.1.1.3 <i>PILS proteins</i>	17
1.1.2 Auxin biosynthesis	18
1.1.2.1 <i>Trp-independent pathway</i>	19
1.1.2.2 <i>Trp-dependent pathways</i>	21
1.1.3 Auxin conjugation	23
1.1.4 Auxin signalling	27
1.2 Auxin – central regulator of organogenesis	31
1.2.1 Organ initiation and development – the case of lateral roots	31
1.2.2 Auxin-cytokinin crosstalk	32
1.3 Biological nitrogen fixation and nodulation	36
1.3.1 Biological nitrogen fixation and its relevance	36
1.3.2 Non-symbiotic versus symbiotic nitrogen fixation	38
1.3.3 Nodule organogenesis in legumes	39
1.3.3.1 <i>Epidermal responses</i>	40
1.3.3.2 <i>Bacterial infection</i>	42
1.3.3.3 <i>Induction of cortical cell divisions</i>	44
1.3.3.4 <i>Regulation of nodulation by auxin and cytokinin</i>	45
1.4 Auxin transport regulation during nodulation	49
1.4.1 Flavonoids are natural auxin transport inhibitors	49
1.4.2 Regulation of local auxin transport	52
1.4.3 Involvement of auxin transport carriers	57
1.4.4 Regulation of long-distance auxin transport	59
1.5 Aims and hypotheses	60
1.5.1 Aim one - Establishment of an LC-ESI-Q-TOF MS/MS protocol for auxin quantification	61
1.5.2 Aim / hypothesis two – Do indeterminate and determinate nodule-forming legumes have different auxin requirements during nodulation?	62

1.5.3 Aim / hypothesis three – Does auxin transport inhibition act downstream of cytokinin signalling regulated by flavonoids in <i>Medicago truncatula</i>	63
CHAPTER 2 Materials and Methods	67
2.1 Plant materials and bacteria strains	67
2.2 Growth conditions	69
2.3 Bacterial inoculation conditions	70
2.4 Flood treatment with auxin transport inhibitors	71
2.5 Auxin quantification	72
2.5.1 Auxin standards	72
2.5.2 Auxin extraction protocol	72
2.5.3 Liquid chromatography-electrospray ionisation-tandem mass spectrometry quadrupole time-of-flight (LC-ESI-MS/MS Q-TOF) methodology	73
2.5.4 Data analysis	74
2.6 Flavonoid quantification	74
2.6.1 Flavonoid standards	74
2.6.2 Flavonoid extraction protocol	75
2.6.3 Liquid chromatography-electrospray ionisation-tandem mass spectrometry quadrupole time-of-flight (LC-ESI-MS/MS Q-TOF) methodology	76
2.6.4 Data analysis	76
2.7 Histochemistry and microscopy	76
2.8 Auxin transport studies	77
2.8.1 Preparation of agar blocks and pre-treatment of seedlings	77
2.8.2 Acropetal auxin transport studies	78
2.8.3 Basipetal auxin transport studies	78
2.8.4 Sample incubation and radioactivity measurement by scintillation proximity assay	79
2.9 RNA extraction, cDNA synthesis, and quantitative real-time PCR	79
2.10 Statistical analyses	80
CHAPTER 3 Bioanalytical Study Using Liquid Chromatography With Tandem Mass Spectrometry for the Quantification of IAA and Its Conjugates	83
3.1 Introduction	85
3.1.1 Extraction and purification procedures	90
3.1.2 Muller and Munne-Bosch (2011) extraction and purification method	91
3.1.3 Optimisation, method development and validation of the Agilent 1200 series HPLC and 6530 Accurate-Mass Q-TOF	92
3.2 Experimental procedure	96
3.2.1 Chemicals	96
3.2.2 Optimisation of the LC-ESI-Q-TOF	97

3.2.3	Extraction recovery experiment	98
3.3	Results and Discussion	100
3.3.1	Optimisation of the HPLC system	100
3.3.1.1	Reversed-phase HPLC column selection	100
3.3.1.2	HPLC mobile phase solvents	101
3.3.1.3	HPLC column temperature	109
3.3.1.4	HPLC gradients and flow rates	110
3.3.2	Optimisation of the ESI-Q-TOF	111
3.3.2.1	Optimisation of the Agilent ESI Jet Stream Ion Source	111
3.3.2.2	Optimisation of the Q-TOF	114
3.3.3	Validation of the positive and negative LC-ESI-Q-TOF MS/MS auxin methods	124
3.3.4	Quality parameters of an LC-ESI-Q-TOF MS/MS flavonoid method	126
3.3.5	Method validation of an existing auxin extraction protocol	128
3.3.6	Conclusion	131
CHAPTER 4	Comparison of Local Auxin Transport Control and Auxin Content in Indeterminate and Determinate Nodules	133
4.1	Introduction	135
4.2	Results	141
4.2.1	Auxin transport inhibitors induce pseudonodule formation in indeterminate nodule-forming legumes	141
4.2.2	Auxin transport regulation in response to <i>Rhizobium</i> inoculation is different in indeterminate and determinate nodule-forming legumes	150
4.2.3	Comparison of auxin content during nodule development and in mature nodules	158
4.2.4	Auxin content in nodulating and non-nodulating non-legumes	164
4.3	Discussion	168
4.3.1	Auxin transport regulation occurs bidirectionally during <i>Medicago truncatula</i> and <i>Lotus japonicus</i> nodule development	168
4.3.2	Nodule and pseudonodule formation involve an increased auxin response	170
4.3.3	Why do pseudonodules induced by ATIs form only in certain legumes?	171
4.3.4	Different auxins are more prominent at different stages of nodulation and across species	174
CHAPTER 5	Flavonoids and auxin transport inhibitors rescue symbiotic nodulation in the <i>Medicago truncatula</i> cytokinin perception mutant <i>cre1</i>	179
Author's note		181
5.1	Abstract	182
5.2	Introduction	183
5.3	Results	188
5.3.1	The <i>cre1</i> mutant is defective in acropetal and basipetal auxin transport regulation and auxin accumulation following <i>Rhizobium</i> inoculation	188

5.3.2	The <i>cre1</i> mutant shows an altered flavonoid profile	198
5.3.3	Nodulation in <i>cre1</i> mutants can be rescued by auxin transport inhibitors	208
5.4	Discussion	217
5.4.1	Cytokinin signalling is required for increased auxin accumulation at the infection site	217
5.4.2	Flavonoids rescue the <i>cre1</i> mutant	220
CHAPTER 6	General Discussion	227
6.1	Hypothesis one: Mass spectrometry complements qualitative / semi-quantitative results obtained through alternative approaches to study auxin	230
6.1.1	Challenges in the study of auxin at multiple levels	230
6.1.2	Advantages and disadvantages of quantitative hormone measurements using mass spectrometry	233
6.1.3	Advantages and disadvantages of hormone quantitation using alternative techniques	234
6.2	Hypothesis two: Auxin transport control is a general mechanism for increasing / decreasing auxin content during nodulation	237
6.2.1	Why does auxin transport inhibition occur?	237
6.2.2	The enigmatic pseudonodule	242
6.2.3	Lessons from computer models	243
6.3	Hypothesis three: Cytokinin perception triggers flavonoid-mediated regulation of auxin transport during nodulation	247
6.3.1	Auxin transport regulation - where do flavonoids fit in?	247
6.3.2	Mechanism of auxin transport regulation during nodulation	249
6.3.3	Nodulation - the big picture	253
6.4	Future perspectives	256
6.4.1	Improvements in experimental design, suggestions for further experiments and future direction	256
6.4.2	Conclusion	258
	Bibliography	259
	Appendix A Growth media	301
	Appendix B Quality parameters for auxin detection method using LC-MS/MS	305
	Appendix C Targeted MS/MS product ion spectra of auxin metabolites	307
	Appendix D Targeted MS/MS product ion spectra of flavonoid metabolites	315
	Appendix E Transcriptional changes in putative auxin synthesis genes in response to E65 inoculation	319

Abstract

Legumes form a symbiotic relationship with a group of bacteria, collectively known as rhizobia. The bacterial symbiont fixes atmospheric nitrogen within root nodules, thus providing the host with an assimilative nitrogen source. Nodule formation involves a complex signalling pathway within the legume host. The plant hormone auxin is involved in nodule organogenesis, but how auxin regulates nodulation is still poorly described. Several studies have found increased auxin signalling in nodule primordia, but so far auxin metabolites have never been quantified during the early stages of nodulation. Therefore, the first aim of this thesis was to establish methods for auxin quantification in legume roots. The presumed build-up of auxin in nodule primordia has been predicted to be due to inhibition of auxin export from cells at the nodule initiation site, but the regulation of auxin transport has not been tested systematically in different legumes. Therefore, the second aim was to compare auxin concentrations and auxin transport changes during nodulation in different legumes. Third, the regulation of auxin transport and auxin accumulation was placed into the known signalling pathway of nodulation in the model legume, *Medicago truncatula*.

Auxins are naturally present in low quantities in the root. We developed an LC-MS/MS method for the accurate and sensitive quantification of auxins in root tissues. The method was validated and produced sensitive limits of detection / quantification and correlation coefficients.

To compare the role of auxin between indeterminate and determinate nodule types, we measured auxin transport and auxin content in *M. truncatula* (forming indeterminate nodules) and *Lotus japonicus* (forming determinate nodules). In addition to acropetal auxin transport, basipetal auxin transport was regulated in response to rhizobia inoculation in both legumes. Different auxins with distinct levels of abundance were detected in separate legumes, with some

unique to the nodule tissues. Auxin concentrations increased at the early stages of nodule formation in *M. truncatula*, but not *L. japonicus*. The inhibition of acropetal polar auxin transport by rhizobia occurred only in indeterminate nodule-forming legumes and correlated with the ability of synthetic auxin transport inhibitors to induce pseudonodules in those legumes.

Finally, we investigated the role of the cytokinin receptor CRE1 in modulating auxin transport during nodulation in *M. truncatula*. We found that cytokinin signalling through CRE1 is necessary for inhibition of acropetal auxin transport, increased auxin concentration and auxin signalling in response to rhizobia. The CRE1 receptor was also required for the correct induction of several flavonoids, which could act as endogenous auxin transport inhibitors. External application of those flavonoids rescued nodulation in the *cre1* nodulation-deficient mutant.

In conclusion, we demonstrated that the auxin transport machinery is a crucial component in the host legume that is regulated in response to rhizobia. Auxin transport changes could explain measured changes in auxin concentrations during nodule initiation of *M. truncatula*, but not *L. japonicus*. Auxin transport control is mediated by endogenous flavonoids, and both flavonoid induction and auxin transport control are regulated by cytokinin signalling in *M. truncatula*.

List of abbreviations

[M+H] ⁺	protonated pseudomolecular ion
[M-H] ⁻	deprotonated pseudomolecular ion
ABCB	ATP-binding cassette subfamily B
AHK	Arabidopsis histidine kinase
ANOVA	analysis of variance
ARF	auxin response factor
ATI	auxin transport inhibitor
AUX	auxin-resistant
AUX/IAA	auxin/indole acetic acid
B&D	Broughton and Dilworth
BMM	Bergensen's modified medium
CCaMK	calcium and calmodulin-dependent protein kinase
CE	collision energy
CHI	chalcone isomerase
CHR	chalcone reductase
CHS	chalcone synthase
CPM	counts per minute
CRE	cytokinin response
d.p.i.	days post-inoculation
d.p.t.	days post-treatment
D5-IAA	indole-2,4,5,6,7-d5-3-acetic acid
EIC	extracted ion chromatogram
ENOD	early nodulin
F	Fabraeus
F3'H	flavonoid 3'-hydroxylase
FLS	flavonol synthase
GH3	gretchen hagen 3
h.p.i.	hours post-inoculation
h.p.t.	hours post-treatment

IAA	indole-3-acetic acid
IBA	indole-3-butyric acid
IMGAG	International Medicago Genome Annotation Group
IPyA	indole-3-pyruvic acid
LAX	like AUX
LC-ESI-MS/MS	liquid chromatography-electrospray ionisation-tandem mass spectrometry
LHK	Lotus histidine kinase
LOD	limit of detection
LOQ	limit of quantification
<i>m/z</i>	mass-to-charge ratio
MDR	multidrug-resistant
NFP	Nod factor perception
NIN	nodule inception
NPA	1-N-naphthylphthlamic acid
NSP	nodulation signalling pathway
PAA	phenylacetic acid
PAT	polar auxin transport
PGP	P-glycoprotein
PIN	pinformed
Q-TOF	quadrupole time-of-flight
S/N	signal-to-noise ratio
TAA	tryptophan aminotransferase of Arabidopsis
TAR	TAA-related
TIBA	2,3,5-triiodobenzoic acid
TIR1	transport inhibitor resistant 1
t_R	retention time
TY	tryptone-yeast

List of figures

1.1	Localisation and regulation of auxin transport facilitators
1.2	Auxin (IAA) biosynthesis in higher plants
1.3	Auxin (IAA) conjugation
1.4	Auxin (IAA) signalling pathway
1.5	Auxin-cytokinin crosstalk in the root
1.6	Schematic representation of the nodulation process and regulatory pathways involved in legumes
1.7	Natural and synthetic polar auxin transport inhibitors
1.8	Auxin transport inhibition in response to rhizobia infection in indeterminate nodule-forming legumes
3.1	Flow diagram describing the extraction protocol adapted from Muller and Munne-Bosch (2011) in this study
3.2	Schematic diagram describing major components of the Agilent 6530 ESI-Q-TOF system
3.3	Components of an Agilent Jet Stream electrospray
3.4	Schematic diagram describing the experimental design for determining the extraction efficiency of the modified extraction protocol from Muller and Munne-Bosch (2011)
3.5	Peak heights of auxins detected in acetonitrile or methanol with 0.1 % formic acid as the mobile phase B
3.6	Peak heights of auxins detected in 0.1 % formic acid or 0.1 % acetic acid as the additive in mobile phases A (water) and B (90 % methanol / water)
3.7	Positive ion mode extracted ion chromatograms (EIC) of IAA, D5-IAA and IBA
3.8	Positive ion mode extracted ion chromatograms (EIC) of IAA, D5-IAA and IBA
3.9	T-piece set up for post-column infusion of modifiers for negative ion polarity ESI targeted MS/MS
3.10	Effect of post-column modifiers on negative ion ESI targeted MS/MS
3.11	Column temperature selection of auxin compounds
3.12	Work flow for the optimisation of the ESI Jet Stream ion source and the Q-TOF
3.13	Fragmentor voltage optimisation
3.14	Collision energy optimisation
3.15	Positive targeted MS/MS extracted ion chromatograms (top) and MS/MS product ion spectra (bottom) of (A) D5-IAA and (B) IAA, respectively, using a 5 $\mu\text{g ml}^{-1}$ auxin standard mixture
3.16	Negative targeted MS/MS extracted ion chromatograms (top) and MS/MS product ion spectra (bottom) of (A) D5-IAA and (B) IAA, respectively, using a 5 $\mu\text{g ml}^{-1}$ auxin standard mixture
3.17	Location of fragmentation via collision induced dissociation (CID) on each auxin protonated molecule $[\text{M}+\text{H}]^+$ to produce the respective most abundant product ion in the positive ESI mode

3.18	Location of fragmentation via collision induced dissociation (CID) on each auxin deprotonated molecule [M-H] ⁻ to produce the respective most abundant product ion in the negative ESI mode
3.19	Detector saturation at high concentrations of analytes
3.20	Extracted ion chromatograms and MS/MS product ion spectra of flavonoid analytes analysed in the negative ion polarity with LC-ESI-Q-TOF-MS/MS using a 5 µg ml ⁻¹ commercial flavonoid standard mixture
4.1	Primary root growth in response to TIBA and NPA treatment at various concentrations
4.2	Pseudonodule formation in response to TIBA and NPA treatment at various concentrations
4.3	Pseudonodule formation in response to TIBA and NPA treatment on <i>Medicago truncatula</i> roots
4.4	Pseudonodule formation in response to TIBA and NPA treatment on subclover roots
4.5	Pseudonodule formation in response to TIBA and NPA treatment on <i>Sesbania rostrata</i> roots
4.6	Nodulation efficiency on A17 roots in response to local application of rhizobia
4.7	Cross sections of pseudonodules induced by TIBA and NPA treatment
4.8	Bump-like structures formed on the stems of <i>Sesbania rostrata</i> treated with TIBA and NPA
4.9	Auxin response as seen by <i>GH3::GUS</i> expression on <i>Medicago truncatula</i> roots
4.10	Cartoon showing auxin transport measurements performed in this thesis
4.11	Auxin transport measurements in <i>Medicago truncatula</i> root segments
4.12	Nodulation on <i>Lotus japonicus</i> roots 20 d.p.i. with <i>Mesorhizobium loti</i>
4.13	Auxin transport measurements in <i>Lotus japonicus</i> root segments
4.14	Auxin transport inhibition in <i>Lotus japonicus</i> roots in response to rhizobia inoculation
4.15	Nodule development in <i>Medicago truncatula</i>
4.16	Nodule development in <i>Lotus japonicus</i>
4.17	Auxin content in developing <i>Medicago truncatula</i> nodules
4.18	Auxin concentration in TIBA-treated <i>Medicago truncatula</i> root segments of similar developmental stage as those for nodules in Figure 4.17
4.19	Auxin content in developing <i>Lotus japonicus</i> nodules
4.20	Auxin content in mature 4-week-old nodules
4.21	Auxin measurements with LC-MS/MS in <i>Datisca glomerata</i> root tissue
4.22	Auxin measurements with LC-MS/MS in root tissue
5.1	Nodulation efficiency on WT and <i>cre1</i> mutant roots spot-inoculated with <i>Sinorhizobium meloti</i> strains Rm1021 and E65
5.2	Relative auxin transport changes in WT (A17) and <i>cre1</i> mutant roots
5.3	Auxin concentration in WT (A17) and <i>cre1</i> mutant roots at 6 and 24 h post mock- or E65 inoculation

5.4	Combined auxin concentrations (sum of IAA, IBA and IAA-Ala) in WT (A17) and <i>cre1</i> mutant roots mock-treated or inoculated with E65 rhizobia
5.5	Auxin response (<i>GH3:GUS</i> expression) is localised to dividing cells during the early stages of nodule and pseudonodule development
5.6	Quantitative RT-PCR showing transcript abundance in root segments of WT (A17) and <i>cre1</i> mutants inoculated for 6 and 24 h with E65 relatively to mock-treated roots
5.7	Quantitative RT-PCR of MtPIN genes
5.8	Quantitative RT-PCR of MtLAX genes
5.9	Concentrations of major flavonoids in WT (A17) and <i>cre1</i> mutant root segments 24 h after mock- or E65 inoculation
5.10	Concentrations of total flavonoid aglycones following acid hydrolysis of flavonoid glycosides in WT and <i>cre1</i> roots
5.11	Schematic overview of the flavonoid biosynthesis pathway in <i>Medicago truncatula</i>
5.12	Quantitative RT-PCR showing relative transcript abundance of flavonoid-related genes in roots treated with cytokinin (Benzylaminopurine, BAP)
5.13	Quantitative RT-PCR showing transcript abundance of flavonoid-related genes in root segments
5.14	Quantitative RT-PCR showing transcript abundance of flavonoid-related genes in root segments
5.15	Complementation of nodulation in <i>cre1</i> mutants using flavonoids or the synthetic auxin transport inhibitor TIBA
5.16	Root growth (change in tap root length) on <i>Medicago truncatula</i> WT plants with or without flavonoids and E65
5.17	Nodulation on WT and <i>cre1</i> mutant roots treated with or without quercetin or hesperetin, in the presence of E65
5.18	Nodules restored on <i>cre1</i> mutant roots treated with selected flavonoids are infected by rhizobia
5.19	Nodules formed on <i>cre1</i> mutant roots with addition of auxin transport inhibitors are infected by rhizobia
5.20	Acropetal auxin transport measurements in roots of WT (A17) and the <i>cre1</i> mutant
5.21	Acropetal auxin transport in roots treated with or without flavonoids, in the presence of E65
5.22	Basipetal auxin transport in WT and <i>cre1</i> mutant roots in response to auxin transport inhibitors at 24 h.p.i.
5.23	Relative flavonoid abundance (free aglycones) in WT and <i>cre1</i> mutant roots in control or E65-inoculated roots
5.24	Proposed model for the action of cytokinin on auxin transport and accumulation during nodule initiation in <i>Medicago truncatula</i>
6.1	Complementary approaches to study auxin regulation of nodulation in <i>Medicago truncatula</i>
6.2	Comparison of various techniques to measure auxin transport and concentration

6.3	Differences in auxin regulation at the site of nodule initiation between indeterminate and determinate nodule-forming legumes
6.4	Schematic model for auxin transport routes before and after <i>Rhizobium</i> infection in <i>Medicago truncatula</i>
6.5	Cytokinin regulation of nodule organogenesis and lateral root initiation share many similarities
6.6	Challenges in the identification of signals which are necessary and sufficient for nodulation

List of tables

1.1	Auxin transport facilitators involved in nodulation
2.1	Primer sequences of genes used in this study and their gene IDs (v4.0)
3.1	Agilent 6530 Accurate-Mass Q-TOF acquisition modes
3.2	Auxin compounds targeted for investigation in this study
3.3	Flavonoid compounds targeted for investigation in this study
3.4	Function of each component of the ESI Jet Stream ion source
3.5	Optimised Agilent Jet Stream ESI-Q-TOF parameters in the positive and negative full MS scan ion modes
3.6	Fragmentor voltage optimisation for individual auxin compounds in the positive and negative ion polarities
3.7	Quality parameters for auxin detection using LC-MS/MS in our study
3.8	Correlation coefficient (R^2 values) of auxin compounds
3.9	Quality parameters for flavonoid detection using LC-MS/MS in our study
3.10	Extraction recoveries of auxin metabolites
4.1	An overview of the similarities and differences that have so far been documented between indeterminate and determinate nodule-forming legumes
5.1	Induction of flavonoid-related genes by the cytokinin BAP, extracted and modified from the publication by Ariel et al. (2012)
5.2	Summary table showing the roles of different flavonoid aglycones identified in this study

CHAPTER 1



General Introduction



1.1 Auxin homeostasis and signalling during plant development

1.1.1 Auxin transport carriers regulate plant development

Auxin is primarily synthesised in young shoot tissues, although other plant tissues are capable of producing auxin, too. Aerially-synthesised auxin is transported to lower parts of the plant (Ljung et al., 2001, Ljung et al., 2005, Petersson et al., 2009). The transport of auxin can occur through two possible mechanisms: (1) passive transport from source to sink tissues through the phloem and, (2) active transport across membrane barriers (Aloni, 2004, Baker, 2000). The latter, known as polar auxin transport (PAT), requires energy from ATP hydrolysis and is strictly regulated by auxin transport proteins. Due to the large sizes of many land plants, the requirement of auxin in lower body parts spells for the need of a quick transport stream. The phloem is capable of carrying auxin up to a speed of 7 cm h^{-1} (Eliasson, 1972), whereas PAT has been measured at about a tenth of that, i.e. $\sim 1 \text{ cm h}^{-1}$ (Kramer et al., 2011). Thus, passive transport through the phloem is the likely route opted for long-distance transport (Baker, 2000). However, because genetic, molecular and biochemical evidence over the years have so successfully shed light on the nuts and bolts of polar auxin transport, the focus on auxin transport studies has largely remained in this domain (Friml, 2003, Krecek et al., 2009).

The auxin indole-3-acetic acid (IAA) is a weak acid ($\text{pK}_a=4.75$). Due to the slightly acidic apoplastic pH of ~ 5.5 , it largely remains in the protonated form and can partly diffuse across the hydrophobic plasma membrane. There remains a population of deprotonated IAA, which is actively taken up into the cell by auxin facilitators (Terasaka et al., 2005, Yang et al., 2006). In *Arabidopsis*, there are at least four auxin importers known, represented by *AUXIN-RESISTANT1* (*AUX1*) and *LIKE-AUX1* (*LAX1*), *LAX2* and *LAX3* (Parry et al., 2001). The *AUX1* and *LAX3* proteins are located at the plasma membrane. These importers function to translocate auxin into the cytoplasm via a proton gradient (Bennett et al., 1996,

Swarup et al., 2008, Swarup et al., 2004, Yang et al., 2006). The AUX1 protein mobilises between plasma membrane and internal compartments dynamically (Grebe et al., 2002, Kleine-Vehn et al., 2006).

Once inside the cytoplasm, the more alkaline (~ pH 7) environment means auxin is present in the deprotonated form and has to be exported actively. The PINFORMED (PIN) family of proteins, of which eight members have been identified in *Arabidopsis* (PIN1-8) are crucial for auxin export. Orthologs have been discovered in many other plant species, including *Medicago truncatula*, *Populus trichocarpa*, *Solanum lycopersicum*, *Oryza sativa* and *Zea mays* (Carraro et al., 2012, Forestan et al., 2012, Nishio et al., 2010, Pattison and Catalá, 2012, Schnabel and Frugoli, 2004, Wang et al., 2009). The name owes its roots to the PINFORMED inflorescence phenotype observed in the *Arabidopsis* mutant lacking PIN1, the primary auxin export facilitator (Figure 1.1). The PIN proteins can be further subdivided into full-length proteins (PIN1, 2, 3, 4, 7) and truncated forms (PIN5, 6, 8) (Zažímalová et al., 2010). Members of the former group are localised to the plasma membrane and their auxin export capabilities have been well-characterised in multiple heterologous systems (Chen et al., 1998, Geisler et al., 2005, Petrasek et al., 2006). Although auxin moves through the vascular tissue from shoot to root, it can be transported back up along the root cap cells and epidermis by PIN2 in *Arabidopsis* (Friml et al., 2004, Rashotte et al., 2000). This reflux / fountain model provides an additional source of auxin in the elongation zone and the early differentiation zone of the root, where priming and initiation of lateral roots may occur. PIN8, a truncated PIN protein, has been found in the nuclear membrane, in addition to the plasma membrane (Ganguly et al., 2010). The authors postulate the organelle-localised PIN8 possibly functions to sequester auxin from the nucleus, thus controlling nuclear auxin signalling. Another atypical efflux carrier, PIN5, localises to the endoplasmic membrane, presumably to control the translocation of auxin from the cytoplasm into the lumen of the endoplasmic reticulum (Mravec et al., 2009).

1.1.1.1 PIN proteins

An important characteristic of the full-length PIN proteins is their polar localisation in the cell. This gives directionality to auxin flow and underlines the role of PINs in creating auxin maxima, such as during the initiation of lateral roots, formation of nematode galls and meristem maintenance (Benková et al., 2003, Blilou et al., 2005, Grunewald et al., 2009, Wisniewska et al., 2006). The asymmetric distribution of PIN proteins, especially PIN1, is modulated by actin filaments via rapid recycling of the proteins into endosomal vesicles and subsequent plasma membrane domain repositioning (Geldner et al., 2001). The endosomal protein GNOM is involved in the polar recycling of PIN (Geldner et al., 2003, Kleine-Vehn et al., 2009). Drdová et al. (2013) recently postulated that PIN recycling involves an exocyst complex, similar to those functioning in exocytosis in animals and yeasts, which acts downstream of GNOM. Phosphorylation of PIN by PINOID relocates the auxin transport protein to the basipetal side of root cells through a GNOM-independent pathway. This process is negatively regulated by phosphatase 2A (PP2A) (Michniewicz et al., 2007). Hence, this mechanism allows plants to respond quickly by channelling auxin into the responding tissues upon receiving external stimuli.

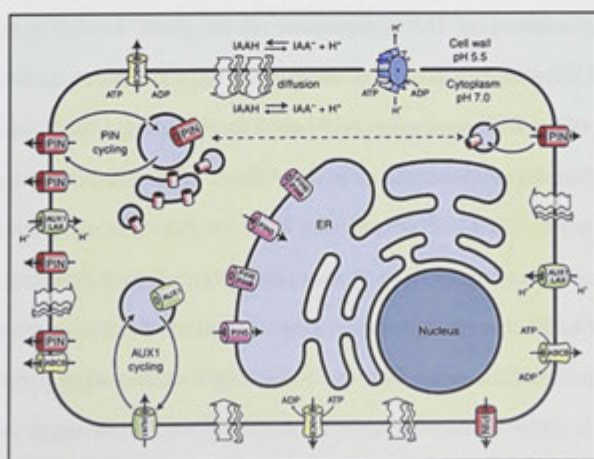


Figure 1.1 Localisation and regulation of auxin transport facilitators. Auxin (IAA), a weak acid, can diffuse across the hydrophobic plasma membrane. However, the majority of auxin exists in the deprotonated form and thus requires assistance to traverse the hydrophobic plasma membrane. Auxin transport proteins have been identified in various plant species. The PIN and AUX1 / LAX families of auxin transporters are mainly associated with auxin efflux and influx activities, respectively. Members of the ATP-binding cassette subfamily B (ABCB) have been shown to exhibit auxin transport capacity and in one case, acts synergistically with a PIN protein. So far, "full-length" PIN proteins (long central hydrophilic loop) are primarily found at the plasma membrane, whereas "truncated" PIN proteins (short central hydrophilic loop) are mainly located in the ER membrane. The most well-characterised plasma-membrane bound PIN protein is PIN1 (represented by the red PIN). The endocytic recycling of PIN and AUX1 proteins bypasses transcriptional regulation and presents a rapid mechanism to adjust auxin levels, or to redirect auxin flow during plant development. Image was adapted from Zažímalová et al. (2010).

1.1.1.2 *P-glycoprotein / ATP-Binding Cassette proteins*

A second group of transporters involved in auxin export is the family of P-glycoproteins (PGP)/ATP-Binding Cassette subfamily B (ABCB) transporters. However, unlike PINs, their arrangement at the plasma membrane is more homogenous (Zažímalová et al., 2010). P-glycoproteins function in non-polar efflux of auxin. PGP1 and PGP19/MDR1 (MULTIDRUG RESISTANT1) both interact and form complexes with the immunophilin-like protein TWISTED DWARF1 (TWD1). Disruption of this interaction affects plant development, including epinastic and inflorescence growth (Geisler et al., 2003, Geisler et al., 2005). At least one member of the PGP family, i.e. PGP4 exhibits auxin import activity, in addition to its export capability in certain cells (Santelia et al., 2005, Terasaka et al., 2005, Yang and Murphy, 2009). PGP4 appears to be an inducible exporter. Under low IAA concentrations, it operates as an auxin importer, whereas it reverts to being an exporter when IAA concentrations increase. Direct evidence suggests the primary role of PGP is to restrict auxin flow in the vascular bundle and to prevent reflux of auxin. This is observed in small cells, where PGPs and auxin occur at high levels

(Bandyopadhyay et al., 2007, Blakeslee et al., 2007, Mravec et al., 2008). Models for PIN-PGP crosstalk have been drawn. In cases where PGP co-localises with PIN, they work in tandem to direct auxin translocation into specific cells. Nevertheless, their mostly homogenous distribution in cells means that PGPs primarily regulate the effective cellular auxin concentration by importing / exporting auxin, according to cellular stimuli (Blakeslee et al., 2007, Mravec et al., 2008, Titapiwatanakun et al., 2009, Yang and Murphy, 2009).

1.1.1.3 PILS proteins

A novel group of putative intracellular auxin transport regulators was identified through *in-silico* analysis. The *PIN-LIKES* (*PILS*) family of genes encodes proteins with similar topology to the PIN proteins, i.e. they contain a predicted central hydrophilic loop flanked by five transmembrane domains on both sides (Barbez et al., 2012, Krecek et al., 2009). In addition, PILS contain the InterPro auxin carrier domain. Barbez and colleagues showed that the loss-of function insertion mutants and overexpression lines exhibited defects in auxin-dependent cellular growth and cellular auxin homeostasis. Despite sharing similar topology to PINs, the amino acid sequences between these two families of proteins have very low similarity (< 20 %), limiting the usefulness of conventional BLAST approaches to search for homologs (Barbez et al., 2012). Nevertheless, Feraru et al. (2012) analysed the diversification of PILS and found that they are generally conserved throughout the plant lineage. Putative PILS members in other model organisms were also highlighted (Feraru et al., 2012). PILS are evolutionarily older because PILS are present in ancient plants, such as the unicellular algae *Ostreococcus tauri* and *Chlamydomonas reinhardtii*, where PINs are absent (Barbez et al., 2012; Mravec et al., 2009). The importance of intracellular auxin homeostasis was given further weight by the discovery of a tonoplast-localised auxin carrier, WALLS ARE THIN1

(WAT1), which is a plant-specific protein and is also the first vacuolar auxin transport protein to be identified (Ranocha et al., 2013).

Intercellular auxin transport is controlled by the three groups of auxin carriers mentioned above, i.e. AUX1/LAXs, PINs and PGP/ABCs. This clearly demonstrates auxin transport as a complex system, and one of many plant-evolved mechanisms controlling a plethora of developmental responses. Their roles in stem cell maintenance, organ initiation, growth and tropic responses were discovered owing to rigorous studies since the turn of the century. However, there are still questions unanswered. Based on current knowledge in a few model systems, their roles during plant-microbe interactions are evident but genetic and biochemical evidence are lacking. Furthermore, it remains to be seen whether other carrier-carrier interactions exist apart from the currently known PIN1-PGP19 coupling. It is also worthwhile to note that research has so far focussed on the transport of the most abundant active auxin, IAA. Transport of other auxin metabolites, such as IBA (Liu et al., 2012, Strader and Bartel, 2011), will require further studies. Liu et al. (2012) demonstrated a lower transport occurrence of IBA than IAA in *Arabidopsis*, but this could differ in other plant species.

1.1.2 Auxin biosynthesis

Auxin biosynthesis has been proposed to occur primarily in young shoot tissues. Aerially-produced auxins are then translocated to other plant parts via a very efficient transport stream (Ljung et al., 2001, Ljung et al., 2005, Petersson et al., 2009). However, there is now evidence pointing towards alternative major biosynthesis hubs, such as the root meristem (Ljung et al., 2005). Auxin was the first phytohormone to be discovered more than 80 years ago (Went, 1926). Compounded by the astonishing fact that auxin is implicated in literally almost every aspect of plant development, it is surprising that the auxin biosynthesis

pathways are still poorly defined. This is due to the lack of auxin biosynthesis mutants, and that clear phenotypes might be difficult to obtain because of potential functional redundancy / lethality of such mutants. Work over the last two decades has unravelled many components of the auxin biosynthesis machinery (Tivendale et al., 2014). Intriguingly, microorganisms also possess similar pathways (Spaepen and Vanderleyden, 2010). Today, it is known that four main naturally-occurring active auxins are present in land plants, with indole-3-acetic acid (IAA) being the most abundant and biologically active auxin form in plant tissues. Other active auxins are indole-3-butyric acid (IBA), 4-chloro-indole-3-acetic acid (4-Cl-IAA) and phenylacetic acid (PAA). Auxin biosynthesis can be classified into two branches: the tryptophan (Trp)-independent and the Trp-dependent pathways (Figure 1.2).

1.1.2.1 Trp-independent pathway

The Trp-independent pathway for auxin biosynthesis was first demonstrated in the tryptophan auxotroph mutant of *Zea mays*, *orange pericarp*. This mutant is unable to produce tryptophan as a result of mutations in two unlinked loci encoding TRYPTOPHAN SYNTHASE β (Wright et al., 1991). Despite this, *orange pericarp* accumulated 50 times higher total IAA than WT plants. Comparable results were demonstrated in *Arabidopsis* (Normanly et al., 1993). Furthermore, one of Trp precursors, indole, is suggested to be an intermediate in auxin biosynthesis not involving Trp. Östin et al. (1999) showed that feeding *Z. mays* seedlings with [^{14}C]indole resulted in the production of [^{14}C]IAA and this process is not inhibited by unlabelled Trp. Similar feeding experiments with [^{14}C]Trp did not yield the same outcome. Later, it was shown that indole-3-glycerol-phosphate may act as the branch point in Trp-independent auxin synthesis. *Arabidopsis* transgenic plants carrying an indole-3-glycerol-phosphate synthase (*IGS*) RNAi construct had significantly less IAA compared to WT plants (Ouyang et al., 2000). Interestingly,

the authors also showed that the Trp biosynthetic mutant lines *trp2-1* and *trp3-1* had higher IAA levels than WT. The tomato mutant *sulfurea* exhibits paramutation and is auxin deficient (Ehlert et al., 2008). A suppressor mutation resulted in overaccumulation of IAA and the pathway involved is thought to be independent of Trp. Although multiple lines of evidence suggest the existence of a Trp-independent pathway, the molecular characterisation and enzymology of this pathway is still barely explored.

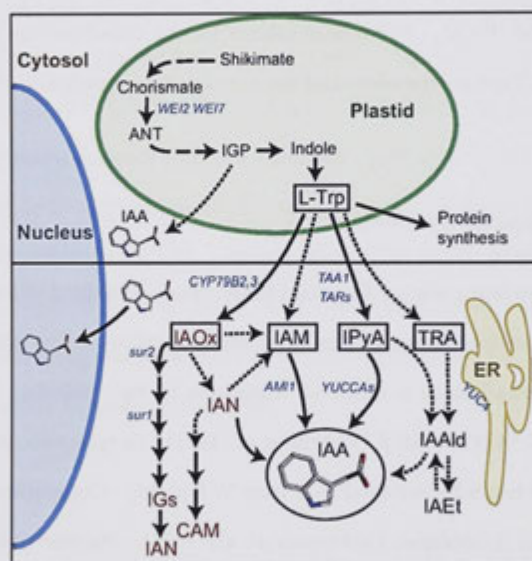


Figure 1.2 Auxin (IAA) biosynthesis in higher plants. The biosynthesis of auxin can occur via a Trp-independent or Trp-dependent pathway (separated by horizontal black line). Trp is produced in the plastid via the Shikimate pathway. So far, four Trp-dependent pathways have been proposed, each named after the immediate metabolite downstream of Trp, i.e. the IPyA, IAOx, IAM and TRA / TAM pathways. The IPyA pathway, which operates through a simple two-step process, is thought to be the major IAA biosynthetic pathway in plants. Trp is converted to IPyA by the TRYPTOPHAN AMINOTRANSFERASE OF ARABIDOPSIS (TAA) or the TAA-RELATED (TAR) family of proteins. The biosynthesis of IAA from IPyA is catalysed by the YUCCA (YUC) family of flavin monooxygenase-like enzymes. Abbreviations: ANT, anthranilate; IGP, indole-3-glycerol phosphate; Trp, tryptophan; IPyA, indole-3-pyruvic acid; IAOx, indole-3-acetaldoxime; IAM, indole-3-acetamide; TRA / TAM,

tryptamine; IAN, indole-3-acetonitrile; IG, indole-3-glucosinolates; CAM, camalexin; IAAld, indole-3-acetaldehyde; IAEt, indole-3-ethanol. Image was modified from Ljung (2013).

1.1.2.2 Trp-dependent pathways

At least four Trp-dependent pathways have been proposed to occur in land plants. Each of them is named after the intermediate directly below Trp. These are the indole-3-pyruvic acid (IPyA), indole-3-acetaldoxime (IAOx), indole-3-acetamide (IAM) and the tryptamine (TAM) pathways (Tivendale et al., 2014). The most widely-studied among these four pathways is the IPyA pathway. A complication arises here because IPyA is unstable and spontaneously converts into IAA. Hence, at times it is challenging to show experimentally that the conversion from IPyA to IAA is enzymatically-driven. At the turn of the decade, several studies shed light on the genetic position of the enzymes involved in the IPyA pathway. It turns out to be a simple two-step process. Independent studies have demonstrated that in this branch, Trp is converted into IPyA by TRYPTOPHAN AMINOTRANSFERASE OF ARABIDOPSIS1 (TAA1) and TAA1-related (TAR1-3) (Mashiguchi et al., 2011, Stepanova et al., 2011, Won et al., 2011). From here, the flavin-monooxygenase-like enzyme family of YUCCA (YUC) proteins convert IPyA into IAA. Evidence for the repositioning of *TAA*, *TAR* and *YUC* in the same auxin biosynthesis pathway can be found. Phenotypic characteristics of *taa* and *yuc* mutants are very similar. Moreover, a study of auxin-related phenotypes between the *taa1 tar2-1* double mutant and another mutant carrying additional mutations on four *YUC* genes revealed no additional phenotypic alterations in the latter (Stepanova et al., 2011, Won et al., 2011). Internal IPyA levels decreased in the *taa1 tar2-1* double mutant and accumulation of IPyA was recorded in the *yuc1/2/4/6* quadruple mutant. Mashiguchi et al. (2011) showed that YUC converts IPyA into IAA in a heterologous *Escherichia coli* system and also proposed this as the rate-limiting step of IAA synthesis in *Arabidopsis*.

Regulation of TAA and TAR involves hormonal crosstalk. Ethylene positively regulates these genes. The *taa1* mutant was originally isolated as an ethylene insensitive mutant, *wei8*. Ethylene-insensitive phenotypes of *taa1*, including defective gravitropism, embryo patterning and vasculature development, were accompanied by a reduction in IAA levels (Stepanova et al., 2008, Tao et al., 2008). Although ethylene positively regulates these auxin transport proteins, auxin can also regulate ethylene-related genes (Stepanova et al., 2007). *TAA1* is also positively regulated by cytokinin. A mutant affected in the same gene was isolated by Zhou et al. (2011). The authors demonstrated that this mutant has reduced IAA induction upon cytokinin treatment.

The IPyA pathway has been proposed to be the major pathway for auxin synthesis in *Arabidopsis*. Evidence for IAOx, IAM and TAM pathways operating in plants are more sporadic. Zhao et al. (2002) demonstrated *in vitro* and *in vivo* that the cytochrome p450 enzymes CYP79B2 and CYP79B3 are responsible for catalysing conversion of Trp to IAOx. The *superroot1* (*sur1*) and *sur2* mutants have elevated levels of IAOx, which culminates in much higher IAA levels (Mikkelsen et al., 2004), suggesting that the IAOx pathway could be a major source for IAA synthesis, and that the WT genes negatively regulate IAA.

Studies in bacteria showed that Trp is converted to IAM by tryptophan-2-monooxygenase, *iaaM*. IAM is then hydrolysed to IAA by the IAM hydrolase, *iaaH* (Tivendale et al., 2014). In *Arabidopsis*, the major source of IAM seems to originate from IAOx (Sugawara et al., 2009). However, because several plant species, such as maize, rice and tobacco lack the CYP79B2/3 enzymes, the endogenous IAM detected in these species is likely to be synthesised via a distinct route. In these plants, IAM is most likely converted from Trp by *iaaM*-like enzymes and then to IAA by the AMI1 protein (Lehmann et al., 2010).

Interest in the TAM pathway gained momentum in the early 2000's following the discovery of the *YUC* family of enzymes (Zhao et al., 2001). Initially, NHT was proposed to be a product of TAM through *YUC* activity. This study, however, did not utilise authentic NHT standards for comparison. A subsequent mass spectrometry study using authentic NHT standards showed that the previously proposed mechanism was incorrect (Tivendale et al., 2010). The TAM pathway might still be a source of IAA in certain plant species, as Quittenden and colleagues showed that in pea roots, TAM is converted to IAA (Quittenden et al., 2009). Interestingly, this pathway does not seem to operate in pea seeds (Tivendale et al., 2010).

1.1.3 Auxin conjugation

Although IAA is widely-regarded as the most abundant form of active auxin in higher land plants, its occurrence inside plants is less than half of the total auxin pool. Auxins are by and large conjugated to amino acids and sugars (Bajguz and Piotrowska, 2009). These compounds serve various functions, mostly for storage and as degradation intermediates. More recently, conjugated forms of auxins to peptides and proteins have been discovered, although their functions are unknown (Figure 1.3). From an evolutionary perspective, auxin conjugates are likely to play an equally important role as IAA, considering they are present in the most ancient land plants (e.g., moss), whereas IAA is not. Apart from IAA, other auxinic compounds with auxin activity, including IBA, indole-3-propionic acid (IPA), 4-Cl-IAA and PAA can also form conjugates with amino acids and sugars (Bajguz and Piotrowska, 2009, Ludwig-Müller and Cohen, 2002).

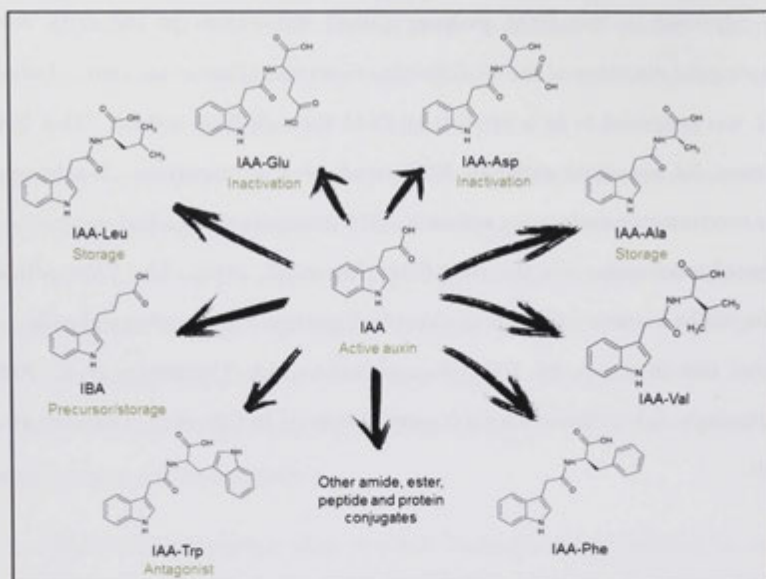


Figure 1.3 Auxin (IAA) conjugation. IAA, an active auxin, can be conjugated to esters, amino acids, peptides and proteins. Several forms of auxin conjugates have been identified, although not all of them appear at similar concentrations in different plant species. The function of auxin conjugates is still poorly understood. However, the roles of a few IAA-amide conjugates have been proposed. For example, IAA-Ala and IAA-Leu are thought to be storage forms, whereas IAA-Glu and IAA-Asp are proposed to be intermediates for IAA degradation. Abbreviations: IAA, indole-3-acetic acid; IBA, indole-3-butyric acid; IAA-Ala, indole-3-acetyl-L-alanine; IAA-Asp, indole-3-acetyl-L-aspartate; IAA-Glu, indole-3-acetyl-L-glutamate; IAA-Leu, indole-3-acetyl-L-leucine; IAA-Trp, indole-3-acetyl-L-tryptophan; IAA-Phe, indole-3-acetyl-L-phenylalanine; IAA-Val, indole-3-acetyl-L-valine.

There is a huge range of auxin conjugates that exists in plants. Auxin conjugates comprising different permutations of the indole moiety (IAA, IBA, IPA, 4-Cl-IAA and PAA) and the attached groups (amino acid, sugar, peptide and proteins) are possible. It is likely that these auxin conjugates play specific but overlapping roles during plant development (Ludwig-Müller, 2011). Several low molecular weight auxin conjugates (indole moiety attached to amino acids and sugars) have been discovered in plants. Amide conjugates seem to be ubiquitous

among land plants investigated thus far. In *Arabidopsis*, a broad range of amide conjugates have been detected, including IAA-Alanine (IAA-Ala), IAA-Leucine (IAA-Leu), IAA-Glutamate (IAA-Glu), IAA-Aspartate (IAA-Asp) and 2-oxoindole-3-acetic acid (Kowalczyk and Sandberg, 2001, Ludwig-Müller, 2011). Detection of amide conjugates has also been reported in Scots pine (IAA-Asp), soybean and cucumber (IAA-Glu and IAA-Asp), spruce (IAA-Ala), tobacco and tomato (IAA-Asp) (Bajguz and Piotrowska, 2009, Ludwig-Müller, 2011, Korasick et al., 2013).

Increasing experimental evidence has arisen in recent years for the presence of high molecular weight auxin conjugates. These compounds consist of an indole moiety attached to peptides and / or proteins (Ludwig-Müller, 2011). Interest in the search for new forms of auxin conjugates stemmed from inconsistencies in the total constituent of compounds before and after hydrolysis. Furthermore, an example of such a conjugate in the form of an IAA-bound peptide has been reported in bean (Bialek and Cohen, 1986). Later, a gene encoding a protein modified by IAA, *IAP1*, was cloned from *Phaseolus vulgaris* (Walz et al., 2002). However, when this gene was heterologously expressed in *Arabidopsis* and *M. truncatula* under the control of the bean endogenous promoter, the resulting protein was not modified by IAA, suggesting a species specific conjugation form (Walz et al., 2008). Proteins modified by IAA have also been identified in pea and strawberry (Ludwig-Müller, 2011). In strawberry, the protein in question has been identified as an ATP synthase, based on LC-MS/MS analysis (Park et al., 2006). More work is required to identify the peptide / protein moiety and to elucidate the function of this class of compounds.

Our understanding of the function of auxin conjugates was boosted by the discovery of the *GRETCHEN HAGEN3* (*GH3*) gene family. The proteins encoded by this family of genes are responsible for conjugating auxins and other hormones (Korasick et al., 2013). The crystal structures of an IAA conjugating GH3 enzyme (Peat et al., 2012), as well as an IAA-amino acid hydrolase protein have been resolved (Bitto et al., 2009). These findings have improved our knowledge on the

interconversion between free auxins and their conjugate forms. The number of *GH3* and hydrolase gene copies in different species varies. For *GH3*, certain plants like *Arabidopsis* and *Brassica rapa* contain 24 and 41 entries, respectively, based on a current NCBI database analysis. On the other hand, lower numbers were found for *Physcomitrella patens* (two). As a result, single mutants in *Arabidopsis* usually do not show clear phenotypes, most likely due to the high redundancy in protein function (Ludwig-Müller, 2011). Recently, Yang et al. (2014) characterised the expression patterns of 17 *GH3* genes in *M. truncatula*.

Although IAA-amino acid conjugates have been detected in an array of plant species, there is currently limited information describing the direct biological role of auxin conjugates. As mentioned earlier, this is due in part to the high redundancy in protein function. In *Arabidopsis*, the clubroot disease induced by the protist *Plasmodiophora brassicae* caused an upregulation in the transcription of several *GH3* genes, with a 100-fold induction for one of the genes (Siemens et al., 2006). Interestingly, Reddy et al. (2006) found that mRNA levels of *Pinus pinaster GH3.16* reduced upon interaction with the ectomycorrhizal fungus *Hebeloma cylindrosporum*. The reduction in transcription was more drastic when the interaction took place with an IAA-overproducing strain of *H. cylindrosporum*, suggesting a need for increased levels active auxin during the symbiotic interaction. During *Arabidopsis-Pseudomonas syringae* interaction, *GH3.5* was upregulated (Zhang et al., 2007). The authors showed that induction of this gene is linked to an increased IAA synthesis during pathogen interaction. So far, the conjugation of auxin has largely been viewed as a mechanism to sequester active auxins inside the cell (Korasick et al., 2013). However, a direct activity of the auxin conjugates on target molecules cannot be overlooked.

Nevertheless, the current hypothesis is that certain auxin conjugates serve as storage compounds, including IAA-Ala and IAA-Leu (Korasick et al., 2013). IAA-Glu and IAA-Asp are thought to be intermediates for auxin degradation because

they are not hydrolysed significantly compared to the other auxin conjugates during *Arabidopsis* germination (Rampey et al., 2004). On the contrary, Campanella et al. (2008) demonstrated that IAA-Asp in *M. truncatula* can be easily hydrolysed to IAA, indicating the possibility of species specificity in terms of active auxin-auxin conjugate interconversion, or even different roles for the same compound in separate species. Finally, IAA-tryptophan (IAA-Trp) has been proposed to be an auxin antagonist, such as during the inhibition of IAA-induced lateral root production in *Arabidopsis* (Staswick, 2009).

1.1.4 Auxin signalling

In order for auxin to cause cellular changes, a complex signalling network is activated upon auxin perception. To date, several auxin receptors have been identified (Peer, 2013). The best studied receptor is the TRANSPORT INHIBITOR RESISTANT1 (TIR1) nuclear receptor, along with its downstream components (Dharmasiri et al., 2005). When auxin binds to TIR1, it does not cause a conformational change to the receptor (Tan et al., 2007). Rather, this interaction promotes the complex to bind to the AUXIN / INDOLE ACETIC ACID (AUX/IAA) family of transcriptional repressors. Under low IAA conditions, the AUX/IAA proteins repress the *AUXIN RESPONSE FACTOR* (*ARF*) genes. An increase in endogenous IAA levels initiates the interaction between TIR1 and the AUX/IAA repressors, causing the latter to be ubiquitinated and subsequently degraded by the 26S proteasomes (Figure 1.4). This promotes the transcription of the *ARF* genes, which facilitates further auxin responses (Sauer et al., 2013).

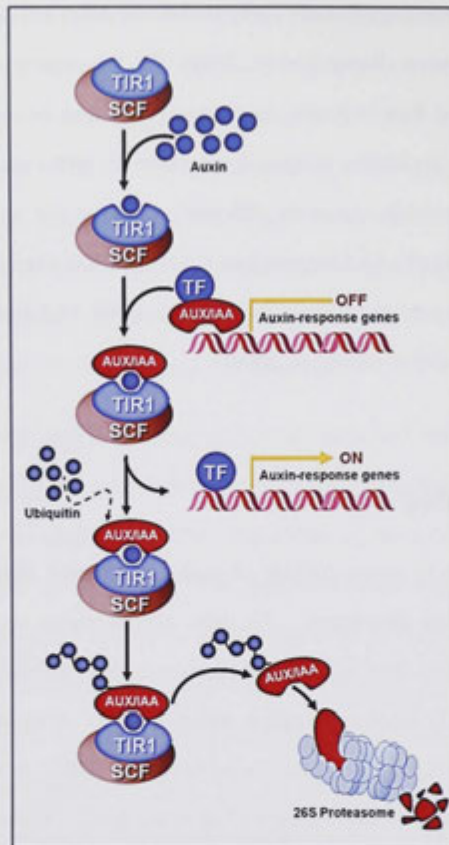


Figure 1.4 Auxin (IAA) signalling pathway. The most well-characterised auxin signalling pathway is the $SCF^{TIR1/AFB}$ -mediated signalling cascade. The membrane receptor TIR1 binds auxin and this reaction triggers the formation of the $SCF^{TIR1/AFB}$ complex inside the cell. Before a cellular auxin response is activated, the family of AUX/IAA transcriptional repressors blocks the promoters of auxin-responsive genes. The $SCF^{TIR1/AFB}$ complex removes AUX/IAA from the transcription start site and catalyses the ubiquitination of AUX/IAA proteins and subsequent degradation by the 26S proteasomes. In the meantime, the removal of AUX/IAA proteins activates transcription of auxin-responsive genes. Image was modified from Freschi (2013).

A huge amount of effort has been invested into uncovering the components of auxin signalling. Although there is currently an established understanding in how the pathway works, there are still many questions to be answered (Sauer et al.,

2013). The large family of proteins involved at every level of signal transfer is complicating our understanding of the pathway. For example, in *Arabidopsis*, there are five other paralogs of TIR1, namely AFB1-5, which all bind auxin with different affinities (Calderon-Villalobos et al., 2010). Based on crystallography, auxin binds into the substrate pocket of TIR1 and then interacts with Domain II of AUX/IAA (Tan et al., 2007). Because there are 29 members of AUX/IAA in *Arabidopsis*, the range of TIR1-auxin-AUX/IAA combination is large. Indeed, Calderón Villalobos et al. (2012) showed that the AFB5-AUX/IAA combination selectively binds the auxin herbicide picloram. This large variation in interactions may explain the range of auxin responses observed during different plant developmental programs and depending on cellular auxin concentrations.

When complexity like the auxin signalling machinery involving redundancy, interactions and feedback presents a hurdle, the value of heterologous systems targeting isolated pathways is highlighted. For instance, using the yeast expression system, Havens et al. (2012) showed that the rate of AUX/IAA degradation is faster when auxin is perceived by TIR1 and AFB2, compared to AFB1 / 3. The auxin receptor TIR1 has a distinct function from AFB1 *in vivo*, as miR393 post-transcriptionally regulates TIR1 and AFB2 / 3, but not AFB1 (Parry et al., 2009). These findings were recently supported by Shimizu-Mitao and Kakimoto (2014). The authors investigated the effect of all possible TIR/AFB-auxin-AUX/IAA combinations on the rate of AUX/IAA degradation. This work will be a valuable resource for further studies on auxin-mediated responses in various developmental processes.

Our relatively detailed understanding of the TIR/AFB-AUX/IAA signalling has paved the way for the development of useful reporters. The *GH3*- and *DR5*-based reporters have been widely used for studying auxin responses in plants. In addition to showing a local response, the output is usually also interpreted as depicting local auxin concentrations. Such interpretations can be misleading, as

complex signalling pathways are sandwiched between the initial input and final output. The novel DII-VENUS sensor is a much-improved tool for measuring auxin gradient and distribution in real-time (Brunoud et al., 2012). It utilises the auxin-interacting DII domain of AUX/IAA proteins fused to the fast-maturing VENUS yellow fluorescent protein, thus giving a more controlled and linearised measurement of auxin.

The S-PHASE ASSOCIATED KINASE 2A (SKP2A) receptor is suggested to be an alternative auxin receptor. This protein has high homology to the mammalian SKP2 protein involved in degradation of cell cycle transcription factors (del Pozo et al., 2006). Auxin has been shown to bind directly to SKP2A (Jurado et al., 2010). This interaction is abolished when amino acid residues in the binding site are mutated. Furthermore, *skp2a* mutants show auxin resistant growth phenotypes. Although direct links of SKP2A function to cell cycle factor degradation has not been established, circumstantial evidence suggests that SKP2A is likely to be an auxin receptor linked to cell cycle control (Sauer et al., 2013). A third auxin receptor, AUXIN BINDING PROTEIN1 (ABP1), has been known for decades but still poorly understood. It is the first auxin receptor to be identified (Napier et al., 2002). Unlike TIR1/AFBs and SKP2A, both of which function at the nuclear membrane, ABP1 is believed to be secreted from the endoplasmic reticulum to the extracellular space, where it functions. Indeed, Tian et al. (1995) showed that the maximum binding activity of ABP1 to auxin occurs at a pH of 5.5, which is similar to the apoplasmic pH. It is thought that ABP1 could act as an auxin sensor, such as to determine auxin gradient and transport direction outside the cell, thus serving as the first point of auxin regulation before a signal is transduced into the nucleus. This is supported by a recent finding that ABP1 forms a complex with a plasma membrane located receptor-like kinase, regulating rapid non-transcriptional responses near the cell surface (Xu et al., 2014). Interestingly, though, ABP1 seems unnecessary for *Arabidopsis* development (Gao et al., 2015). By comparing two

separately-generated *abp1* null mutants with the WT plant, the authors could not find any difference between the common auxin-inducible genes in both genotypes, as well as no observable developmental defects in the *abp1* mutants, at various growth stages. The role of ABP1 in plants is still a mystery.

1.2 Auxin - central regulator of organogenesis

1.2.1 Organ initiation and development - the case of lateral roots

Auxin is a key player in founder cell specification and organ development. In the last few years, there has been an increasing shift in research focus towards understanding organ development as an output from coordination between multiple hormonal networks (Chandler, 2011a). However, multiple lines of evidence exist showing that auxin is the main actor in the complex orchestration involved in organ formation. Perhaps the most well-studied system in this context is the initiation of lateral roots in *Arabidopsis* (Lavenus et al., 2013, Péret et al., 2009). However, extensive studies have also been performed on the role of auxin in root development, flower development and meristem maintenance (Bishopp et al., 2011, Chandler, 2011b, Su et al., 2011). In most cases, the initiation of lateral organs is associated with the formation of auxin maxima.

Lateral root formation in *Arabidopsis* has been rigorously investigated. The initiation of lateral roots is highly regular and tends to follow a rhythmic pattern in *Arabidopsis* (De Smet et al., 2007). The authors showed that this regular pattern is correlated with an elevated auxin response in the basal meristem. Each consecutive auxin pulse is spaced consistently ~ 15 h apart. The spots of increased auxin response are where lateral roots primordia will form (De Smet et al., 2007). Later, Dubrovsky et al. (2008) elegantly demonstrated that the earliest lateral root initiation event is an increased auxin response in a single pericycle cell and this is

sufficient to convert it into a lateral root founder cell. This suggests that auxin alone could act as a trigger for lateral organ formation. Several other reports support auxin as a positive regulator of lateral root initiation and development. The *superroot1* (*sur1*) mutant has an increased aldehyde oxidase activity, which resulted in higher IAA biosynthesis and lateral root numbers (Seo et al., 1998). Similarly, the *sur2* mutant displays elevated IAA production and lateral root formation (Barlier et al., 2000). Acro- and basipetal auxin transport are required for lateral root initiation (Casimiro et al., 2001). Mutants with defects in the auxin transport machinery have clear lateral root phenotypes. The AUX1 permease translocates IAA into the cytoplasm and is involved in root gravitropism (Bennett et al., 1996, Yang et al., 2006). Loss-of-function in this gene reduced lateral root initiation (Marchant et al., 2002). Another auxin importer, LAX3, has been proposed to translocate auxin from the developing lateral root into cortical and epidermal cells overlaying the lateral root primordium (Swarup et al., 2008). This promotes auxin-dependent expression of cell wall remodelling enzymes, which are likely to separate cells in the outer cell layers prior to lateral root emergence. In agreement with this positive role, the *lax3* mutant has reduced numbers of emerged lateral roots, but is not defective in lateral root primordia initiation (Swarup et al., 2008). Finally, various mutants of the PIN family involved in auxin export, including *pin1*, *pin3/pin7* double mutant, and the *pin1/pin3/pin4* triple mutant have retarded lateral root primordia formation associated with aberrant auxin response (Benková et al., 2003). Defects in the auxin transport machinery could affect the creation of auxin maxima in the correct cells and consequently impact lateral root initiation and development.

1.2.2 Auxin-cytokinin crosstalk

Cytokinins, together with auxins, fine tune the processes of cell division and differentiation. These two hormones act antagonistically during plant development.

Auxin and cytokinin interaction has been investigated in embryonic meristem formation, shoot and root meristem development (Bishopp et al., 2011). Several reports have shown that the antagonism between auxin and cytokinin in the root meristem is determined by certain integrators, which mutually control the signalling pathways or homeostasis of both hormones (Figure 1.5) (Dello Ioio, 2008, Marhavý et al., 2011, Marhavý et al., 2014, Moubayidin, 2009, Růžicka et al., 2009).

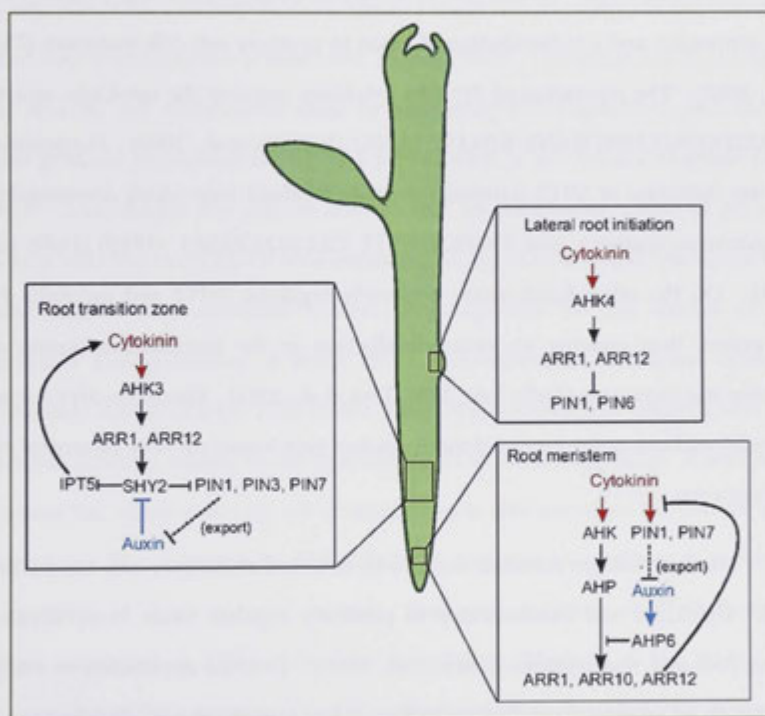


Figure 1.5 Auxin-cytokinin crosstalk in the root. Auxin and cytokinin act antagonistically in the root to control lateral root emergence, the transition zone and root meristem maintenance. The genetic components involved are distinct, but overlap in each case. In general, cytokinin is perceived by a receptor-like kinase and the resulting signal causes an inhibition of auxin transport. Abbreviations: AHK, *Arabidopsis* Histidine Kinase; ARR, *Arabidopsis* Response Regulator; SHY2, Short Hypocotyl 2; IPT, Isopentenyl transferase; AHP, *Arabidopsis* Histidine Phosphotransfer protein. Image was modified from El-Showk et al. (2013).

A genetic framework has been proposed describing auxin-cytokinin interaction in root meristem maintenance. Dello Ioio (2008) demonstrated that *SHORT HYPOCOTYL2 (SHY2/IAA3)* acts at the convergence of auxin-cytokinin signalling to control cell division and differentiation. The *SHY2* gene is a member of the *AUX/IAA* gene family encoding transcriptional repressors functioning in the TIR1/AFB-dependant auxin signalling cascade (Tian et al., 2003). At the root transition zone, the cytokinin-induced transcription factor ARR1 binds directly to the promoter of *SHY2*. An increase in *SHY2* expression results in the reduction of *PIN* expression and a redistribution of auxin to promote cell differentiation (Dello Ioio, 2008). The repression of *PIN1* by cytokinin requires the cytokinin receptor ARABIDOPSIS HISTIDINE KINASE (AHK) (Růžicka et al., 2009). Furthermore, positive induction of *SHY2* activates a negative feedback loop which downregulates the cytokinin synthesis gene *ISOPENTENYL TRANSFERASE5 (IPT5)* (Dello Ioio, 2008). On the other hand, auxin negatively regulates *SHY2* and increases *PIN* expression, thus creating an auxin distribution in the meristem favouring cell division and expansion (Dello Ioio, 2008, Tian et al., 2003). Therefore, *SHY2* acts as a regulatory knob at the proximal meristem and root transition zone to control root meristem size.

Auxin-cytokinin crosstalk can also be observed at the hormone biosynthesis level. Cytokinin was demonstrated to positively regulate auxin biosynthesis in young root and shoot tissues (Jones et al., 2010). External application or ectopic expression of cytokinin resulted in increased auxin biosynthesis. Furthermore, a decrease in cytokinin biosynthesis, either through loss-of-function mutations of *IPT* genes, or induction of the cytokinin degrading enzyme, *CYTOKININ OXIDASE (CKX)*, resulted in a downregulation of auxin biosynthesis. Transcript profiling indicated that certain auxin biosynthesis genes, including *YUC6*, were upregulated after cytokinin treatment (Jones et al., 2010). Consistent with this, Zhou et al. (2011) showed an increase in *TAA1* expression after cytokinin treatment in

Arabidopsis roots. This was accompanied by a decrease in polar auxin transport and both of these cytokinin-induced responses were dependent on the *AHK3-ARR1* signalling module. Previously, auxin biosynthesis has been shown to rapidly downregulate cytokinin production (Nordström et al., 2004). Hence, a model has been proposed where cytokinin acts as a positive regulator of auxin biosynthesis but auxin represses cytokinin synthesis (Jones et al., 2010).

Lateral root formation is induced by auxin and inhibited by cytokinin. Clearly, plants have to balance the actions of these two hormones in the context of lateral root organogenesis (Fukaki and Tasaka, 2009). Cytokinin acts at the lateral root founder cell specification stage by perturbing *PIN* expression, such that an auxin gradient promoting lateral root primordium is not formed (Laplaze et al., 2007). Accordingly, the authors showed that transactivating *CKX1* in pericycle founder cells increased lateral root numbers. Using *in vitro* assays, Pernisová et al. (2009) showed that cytokinin controls organogenesis via the control of *PIN* expression and inhibition of auxin efflux. Moreover, an additional cytokinin modulator, *ARABIDOPSIS HISTIDINE PHOSPHOTRANSFER6 (AHP6)*, acts as a cytokinin inhibitor during lateral root initiation (Moreira et al., 2013). It is required to orient the initial pericycle cell divisions and is also necessary for correct *PIN1* patterning. The reduction in *PIN* activity in response to cytokinin is rapid and independent of transcriptional control. Endocytic recycling of *PIN1* from the plasma membrane is followed by lytic degradation (Marhavý et al., 2011). The susceptibility of *PIN* proteins at certain polar domains to degradation is dependent on its phosphorylation status (Marhavý et al., 2014). Phosphomimicking experiments and enhanced phosphorylation of *PIN1* due to modified activities of *PIN*-specific kinases and phosphatases desensitised *PIN1* to cytokinin (Marhavý et al., 2014). A mechanism bypassing transcriptional control such as this is useful for a rapid initial response, while a more elaborate and complex network of gene regulation may produce a synergistic output at a later stage.

1.3 Biological nitrogen fixation and nodulation

1.3.1 Biological nitrogen fixation and its relevance

Nitrogen is one of the most essential elements for plant growth. It is required as a building block for nucleic acids, amino acids and many secondary metabolites. Nitrogen limitation is a frequent and major problem in many soil ecosystems (Herridge et al., 2008). Although the atmosphere comprises 78 % nitrogen (N_2), this is not accessible to plants. Plants can only assimilate soluble nitrogen in the soil. Atmospheric nitrogen is converted into these accessible forms in a process known as nitrogen fixation. This process can happen naturally, such as through lightning and biological processes, or by human intervention through industrial nitrogen conversion. Enhanced efforts from governmental and private organisations have improved estimates of fixed nitrogen from various sources, thus giving a better overview of the scale of natural and anthropogenic inputs (Fowler et al., 2013).

In the last few decades, soil infertility has been overcome by widespread application of nitrogenous fertilisers. The discovery of the Haber-Bosch process was a major breakthrough in the early 1900s, and instrumental for the advent of industrial fertiliser production (Erisman et al., 2008). However, the extreme conditions required for breaking the inert nitrogen molecule to make ammonia, coupled with the low yield, have increased production costs of nitrogenous fertilisers. Small scale farmers are finding it increasingly difficult to cope with the price hike of synthetic fertilisers. With the rising challenge of feeding an ever-expanding human population, food security is becoming a serious issue, especially amongst third-world populations (Godfray et al., 2010). The available tools for increasing crop yield, including plant breeding, fertiliser application and pest control are simply not sufficient to cope with the current upward trend in human growth. What we need is a technological advance that can allow us to make the

quantum leap forward in agriculture, in the same manner as fertilisers did with the green revolution 50 years ago.

Biological nitrogen fixation is an astonishing naturally-occurring process because it can perform nitrogen fixation at ambient conditions, instead of the extreme pressures and temperatures that the Haber-Bosch process requires. The ability to fix nitrogen is only present in a subset of bacteria. According to recent estimates, biological nitrogen fixation contributed by terrestrial and marine ecosystems accounts for 200 Tg N year⁻¹, half of the total fixed nitrogen on earth (Vitousek et al., 2013, Voss et al., 2013). The idea of engineering cereal crops that have the ability to fix nitrogen through symbiosis with nitrogen-fixing bacteria has been discussed for some time (Oldroyd and Dixon, 2014). If nitrogen fixation capability can be transferred to food crops, not only will the yield and nutritional value of crops likely increase, but importantly, the price of food will fall. On top of that, environmental and health issues resulting from nitrogen leaching from fertiliser use, such as water eutrophication and the blue baby syndrome, can be avoided (Holloway et al., 1998).

The challenge of engineering symbiotic pathways into crops is not menial. Plants usually enter a symbiotic relationship with bacteria. The host plant harbouring the bacterial symbiont will then benefit from the nitrogen fixing activity of the microbe. Hence, it is imperative to dissect bacterial and plant signalling pathways before we can fully engineer biological nitrogen fixation in a new plant system. Over the last three decades, our understanding on both sides of the biological nitrogen fixation equation has made significant inroads. Model organisms have been adopted, which greatly accelerated research progress. Biological nitrogen fixation is now truly recognised as one of the answers to the future of sustainable agriculture and food security (Beatty and Good, 2011).

1.3.2 Non-symbiotic versus symbiotic nitrogen fixation

The ability to fix atmospheric nitrogen is present in a range of bacteria. Nitrogen-fixing bacteria can be loosely classified as non-symbiotic and symbiotic (requiring extensive differentiation into a specialised form). Examples of non-symbiotic nitrogen-fixing bacteria include cyanobacteria, proteobacteria and firmicutes (Zhan and Sun, 2012). The process of nitrogen fixation is energy expensive. Thus, non-symbiotic nitrogen fixers thrive in soils rich in organic matter. They usually also occur in high densities in the rhizosphere, where they can feed off plant exudates (Orr et al., 2011). Nitrogen-fixing ability is conferred by the nitrogenase enzyme present in the bacteria. The function of nitrogenase is tightly controlled by the *nif* regulon. Expression of this enzyme complex and subsequently nitrogen-fixing function is only activated under low fixed nitrogen conditions in the soil. Furthermore, the enzyme complex is highly sensitive to oxygen and must therefore operate in an anaerobic environment (Schmitz et al., 2002).

Symbiotic nitrogen fixation involves a host organism and a nitrogen-fixer. The host obtains nitrogen metabolites from the bacteria, and in exchange, the bacteria benefit from photosynthates and protection from the host. Cyanobacteria, for instance, can also form a symbiosis with *Azolla* and cycads, in addition to their nitrogen-fixing capability in free-living form (Herridge et al., 2008). The legume-*Rhizobium* symbiosis is a very controlled interaction between a leguminous host and *Rhizobium* symbiont. Two model systems have been widely used in recent years to study this interaction, namely the *Medicago truncatula* - *Sinorhizobium meliloti* and *Lotus japonicus* - *Mesorhizobium loti* interactions. An initial signal exchange occurs between the host plant and *Rhizobium*. The symbiont will then enter the host plant root. A structure, termed nodule, concurrently initiates inside the host plant, which will eventually house the symbiont (Oldroyd et al., 2011). At least one non-legume, *Parasponia* sp., has been shown to form symbiosis with *Rhizobium*. This interaction also culminates in the formation of a nodule, albeit the *Rhizobium* infection process

differs (Santi et al., 2013). The nodule provides an optimum environment for nitrogen fixation. A very similar process occurs between non-legumes and a group of actinorhizal bacteria, called *Frankia*. Entry of bacteria into the host plant occurs intracellularly in plants of the Fagales order and intercellularly in Rosales (Pawlowski and Demchenko, 2012). In Datisceae and Coriariaceae, the process is unclear, due to the difficulty in studying the early infection processes. In legumes, nodules have a peripheral vasculature instead of a central vasculature, as formed by *Frankia* association with non-legumes (Guan et al., 2013, Santi et al., 2013). Another marked difference is the formation of a pre-nodule, which has not been observed in legume-*Rhizobium* symbiosis.

1.3.3 Nodule organogenesis in legumes

Nodulation in legumes involves signal exchange with a group of bacteria, collectively known as rhizobia. The *M. truncatula* and *L. japonicus* nodulation programs represent the two most extensively studied systems (Desbrosses and Stougaard, 2011). Nonetheless, work on other legume species, notably on *Medicago sativa* (alfalfa), *Glycine max* (soybean), *Pisum sativum* (pea), *Trifolium repens* (white clover) and *Sesbania rostrata* have also provided useful insights on similarities and differences between nodulating plants. Currently, there is a general consensus that leguminous nodules can be divided into two types, i.e. indeterminate and determinate nodules (Oldroyd et al., 2013). Indeterminate nodules contain a persistent meristem and can grow into larger, elongated structures. On the other hand, determinate nodules have a temporary meristem, which disappears early during nodule development, causing determinate nodules to be spherical in shape. Despite of this difference, there is a lot of overlap in indeterminate and determinate nodulation. The epidermal and cortical responses in both nodulation programs have been the subjects of rigorous investigations.

1.3.3.1 Epidermal responses

Symbiosis between legumes and rhizobia is initiated when flavonoids are secreted by host plants into the rhizosphere. Flavonoids are plant secondary metabolites acting as *Rhizobium* chemoattractants (Aguilar et al., 1988, Dharmatilake and Bauer, 1992, Hassan and Mathesius, 2012). Upon perception of flavonoid compounds, the corresponding *Rhizobium* species synthesises Nod factors (lipochitin oligosaccharides). Nod factors are highly specific and unique to each *Rhizobium* species. These compounds are detected by N-acetylglucosamine-binding lysin motifs (LysM) receptor-like kinases (RLK) located at the epidermis (Arrighi et al., 2006, Radutoiu et al., 2003). In *L. japonicus*, the NOD FACTOR RECEPTOR1 (NFR1) and NFR5 are crucial for detection of Nod factors from *Mesorhizobium loti* (Madsen et al., 2003, Radutoiu et al., 2003). Transferring *NFR1* and *NFR5* to *M. truncatula* allowed its symbiosis with *M. loti* (Radutoiu et al., 2007). Moreover, a difference in a single amino acid residue within *NFR5* of *L. japonicus* and *Lotus filicaulis* confers specificity for different symbionts. Later, Broghammer et al. (2012) showed that these receptors directly bind Nod factors. In *M. truncatula*, NOD FACTOR PERCEPTION1 (NFP1) and LYK3 are orthologs of *NFR1/5*, as well as being strong LysM-RLK candidates for binding Nod factors from *S. meliloti*. However, direct evidence for Nod factor binding is still missing.

Nod factor perception is followed by a series of phosphorylation events. Pharmacological and biochemical evidence suggest a role for phospholipase C/D (PLC/D) in symbiotic nodulation. Charron et al. (2004) showed that by blocking the activities of PLC/D with inhibitors, expression of the nodulation marker *EARLY NODULIN11* (*ENOD11*) was abolished, and nodulation failed to occur in *M. truncatula*. Den Hartog et al. (2001) also showed the importance of PLC/D activity in *Vicia sativa* (vetch) nodulation, specifically for root hair deformation.

These two proteins are proposed to be secondary messengers linking plasma membrane ligand perception with nuclear activity (Oldroyd and Downie, 2008).

Calcium spiking in the nuclear region of cells associated with, and in the vicinity of Nod factor perception, is a hallmark of nodule organogenesis. This phenomenon occurs inside and around the nucleus, which explains why secondary messenger(s) carrying information upon Nod factor perception from the plasma membrane into the nucleus was proposed (Charpentier and Oldroyd, 2013, Oldroyd and Downie, 2008). Specific calcium oscillation signatures within the nucleus are interpreted and decoded by the calcium and calmodulin-dependent protein kinase (CCaMK), a central player of nodule formation, encoded by the *DMI3* gene in *M. truncatula*. Indeed, an autoactive form of CCaMK is sufficient to induce spontaneous nodule formation on *M. truncatula* and *L. japonicus* roots (Gleason et al., 2006, Tirichine et al., 2006). Recently, Singh et al. (2014) demonstrated that CCaMK phosphorylates CYCLOPS, a process essential for its function as a transcription activator for nodulation-related genes, such as *NODULE INCEPTION* (*NIN*). Phosphomimetic forms of CYCLOPS were sufficient to cause spontaneous nodule formation independent of CCaMK. The GRAS-family transcription factors *NODULATION SIGNALING PATHWAY1* (*NSP1*) and *NSP2* form a heteropolymer, which binds directly to DNA and activates the nodulation marker *ENOD11* (Hirsch et al., 2009, Kaló et al., 2005, Smit et al., 2005). Many of the genetic components above are also required during mycorrhization (the formation of a symbiotic relationship between the mycelium of a fungus and the roots of a plant), and hence are not nodulation-specific. However, a study by Soyano et al. (2013) suggested that the legume-specific *NIN* transcription factor could be one of the determinants of nodulation (Figure 1.6).

1.3.3.2 Bacterial infection

Nod factor perception also leads to invasion of the correct *Rhizobium* species into host roots. The process is facilitated by cytoskeletal changes in root hair cells, causing deformation of the root hair, resulting in the formation of an infection thread. Rhizobia in the vicinity of the curled root hair are entrapped within the structure. The cell wall of the root hair grows inwards, forming a tunnel-like structure, called an infection thread that rhizobia migrate into. During infection thread growth, rhizobia undergo replication and increase Nod factor concentration by further synthesis, a process important for inducing plant responses in the latter stages of infection (Oldroyd et al., 2011).

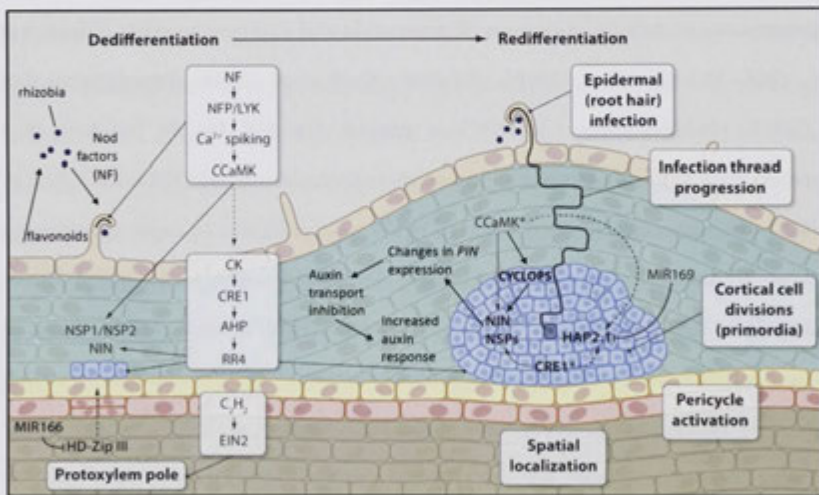


Figure 1.6 Schematic representation of the nodulation process and regulatory pathways involved in legumes. Here, a *Medicago truncatula* nodule forming at the early stages is shown. The host plant exudes flavonoids, which act as chemoattractants to the corresponding *Rhizobium* species (*Sinorhizobium meliloti*). In addition, flavonoids induce Nod factor (NF) synthesis in *Rhizobium*. At the epidermis, NF is perceived by receptors, NOD FACTOR PERCEPTION (NFP) / LYK located in the root hairs. NF perception activates calcium spiking, which is decoded by calcium and calmodulin-dependent protein kinase (CCaMK). CCaMK activates transcription of nodulation-related transcription factors, including NODULATION SIGNALLING PATHWAY1 (NSP1), NSP2 and NODULE

INCEPTION (NIN). At the inner cortex, CCaMK also plays similar roles. In addition, it was recently shown that CCaMK directly phosphorylates CYCLOPS, which then directly activates NIN. An autoactive form of CCaMK is sufficient to induce nodule organogenesis. Hormones play important roles during nodulation. Cytokinin signalling is induced in the inner cortex and cytokinin signalling through CYTOKININ RESPONSE1 (CRE1) is essential for nodulation in *M. truncatula*. CRE1 positively regulates *RESPONSE REGULATOR4* (RR4) and *NSP2*. Cytokinin signalling via CRE1 is also essential for auxin transport inhibition, which is correlated with changes in *PIN* expression. This is followed by an increase in auxin response, cell divisions and development of a nodule primordium. Ethylene (C₂H₂) is a negative regulator of nodulation and controls the positioning of nodules through the ETHYLENE INSENSITIVE2 (EIN2) regulator. Ethylene signalling is controlled by the HD-ZIP III transcription factor, which in turn is post-transcriptionally regulated by MIR166. Concurrent with the cortical responses, rhizobia infect the curled root hair with the aid of an infection thread, a tunnel-like structure composed of plant cell wall material. Once inside the nodule primordium, rhizobia are released from the infection thread into nodule cells, where they further differentiate into bacteroids, which is the nitrogen-fixing form of the symbiont. The meristem-specific transcription factor, HAP2.1 is controlled post-transcriptionally by MIR169 to promote nodule differentiation. Image was modified from Crespi and Frugier (2008).

Root hair curling and cortical cell divisions are proposed to occur via independent pathways. The Nod factor receptor NFP is required for root hair deformation in *M. truncatula* (Esseling et al., 2003). Using various mutants defective in the early nodulation signalling pathway, Miwa et al. (2006) showed that there is no correlation between calcium spiking and induction of root hair curling. Hence, downstream responses after calcium spiking are not essential for root hair curling, which is likely to be controlled by a parallel pathway after Nod factor perception (Oldroyd et al., 2011).

Infection thread formation and growth are tightly controlled by the host plants. Only the correct structure of the Nod factor from the specific symbiont will elicit normal infection thread formation and growth (Oldroyd and Downie, 2008). Studies in *S. meliloti* and *Rhizobium leguminosarum* (pea symbiont) showed that Nod factors with the incorrect side groups and modifications were able to induce

calcium spiking and *ENOD* expression, but progression of the infection threads was aborted in root hairs (Ardourel et al., 1994, Walker and Downie, 2000). This has led to a two-stage control hypothesis of nodulation. First, an initial stage of non-stringent Nod factor recognition for calcium signalling and the expression of early response genes occur. Next, a stringent Nod factor recognition stage for bacterial invasion is required (Desbrosses and Stougaard, 2011). In *M. truncatula*, the NFP protein is proposed to be the initial ligand receptor and later forms a complex with LYK3 to perform higher stringency recognition of Nod factors during nodulation (Pietraszewska-Bogiel et al., 2013).

1.3.3.3 Induction of cortical cell divisions

While the epidermal layer controls the initial physical contact with *Rhizobium*, early responses and bacterial infection, the making of a nodule is controlled by the cortical and other inner cell layers. Initial cell divisions occur in the inner cortex and outer cortex of *M. truncatula* and *L. japonicus*, respectively (Mathesius, 2008). Recently, Xiao et al. (2014) has meticulously described the contribution of every cell layer to the formation of a mature nodule structure, including the fate of the pericycle and endodermal cells. Using cell-specific markers, they were able to trace the entire developmental journey taken by individual cells during nodule formation in *M. truncatula*. Studies in nodulation-defective mutants showed that the inner layer cell divisions and epidermal responses can occur independently of each other. Cortical cell divisions may proceed normally when bacterial infection has failed (Gleason et al., 2006, Tirichine et al., 2006), and the opposite is true as well (Murray et al., 2007, Plet et al., 2011). However, to form a functional nodule that contains nitrogen-fixing rhizobia, these two parallel processes must be coordinated so that they happen close to one another (Ferguson et al., 2010).

Several reports suggest that the onset of nodule organogenesis is to a large extent plant autonomous. In alfalfa and white clover, spontaneous nodules can form on WT plants in the absence of rhizobia. Spontaneous nodules do not contain the microsymbiont and are white in colour, instead of the typical pinkish appearance of a nitrogen-fixing nodule (Blauenfeldt et al., 1994, Joshi et al., 1991). Interaction between mutant symbionts and WT host plants can also result in similar structures (Imaizumi-Anraku et al., 2000, Tansengco et al., 2003). A genetic screen in *L. japonicus* and directed mutagenesis in *M. truncatula* identified the CCaMK protein as sufficient to induce nodule organogenesis in the absence of rhizobia (Gleason et al., 2006, Tirichine et al., 2006). Autoactivation of CCaMK, as shown in these two studies, activated *ENOD11* expression in the same spatio-temporal manner as Nod factor perception does (Journet et al., 1994). Hence, the Nod factor signalling pathway downstream of CCaMK is predefined, regardless of whether rhizobia or a signal is recognised at the root surface.

1.3.3.4 Regulation of nodulation by auxin and cytokinin

Hormones, in particular auxin and cytokinin, are intrinsic players of nodule organogenesis. The participation of hormones in nodulation has been proposed a while back (Libbenga et al., 1973). Application of auxin transport inhibitors was able to induce expression of early nodulins and nodule-like structures on alfalfa (Hirsch et al., 1989). An *S. meliloti* strain overproducing IAA induced more nodules on *M. truncatula* than a WT strain (Pii et al., 2007). Interestingly, *S. meliloti* mutants that synthesise higher levels of cytokinin could also induce formation of nodule-like structures (Cooper and Long, 1994). Other hormones have also been implicated in nodulation control (Ferguson and Mathesius, 2014).

The importance of cytokinin signalling as a positive cue for nodule formation has been highlighted by several studies. Soybean roots overexpressing

miR160 are hyposensitive to cytokinin and have reduced nodule primordia formation (Turner et al., 2013). Gain-of-function mutation in the cytokinin signalling receptor gene *LOTUS HISTIDINE KINASE1 (LHK1)* in *L. japonicus* was sufficient to induce spontaneous nodule formation in the absence of rhizobia or Nod factors (Tirichine et al., 2007). Conversely, loss-of-function in *LHK1* and the ortholog in *M. truncatula*, *CYTOKININ RESPONSE1 (CRE1)*, greatly diminished nodulation capability in the respective host plants, in the presence of rhizobia (Murray et al., 2007, Plet et al., 2011). Interestingly, the *Arabidopsis* ortholog of *LHK1*, *ARABIDOPSIS HISTIDINE KINASE4 (AHK4)*, was able to functionally complement nodulation in the *lhk1* mutant, indicating the absence of legume-specific features of *LHK1* (Held et al., 2014). Furthermore, nodules can still form on the *lhk1* and *cre1* mutants, indicating that other cytokinin receptors work partially redundantly in *L. japonicus* (Held et al., 2014), which is most likely the case in *M. truncatula* as well (Frugier, 2008).

In *M. truncatula*, cytokinin induction is observed at the earliest stages following Nod factor perception, preceding cell divisions. Expression studies of the cytokinin primary response regulator *RESPONSE REGULATOR4 (RR4)* showed that after Nod factor application, the first point of cytokinin action is in the inner cortical cells, but not in the outer cell layers in *M. truncatula* (Plet et al., 2011). The *MtRR4*, *MtNSP2* and a gene encoding a basic Helix-Loop-Helix (bHLH) transcription factor loci are direct targets of cytokinin signalling (Ariel et al., 2012). Loss-of-function and knockdown of *MtNSP2* and the bHLH transcription factor, respectively, reduced nodulation (Ariel et al., 2012, Murakami et al., 2007, Oldroyd and Long, 2003). Although the point of cytokinin action has been investigated, whether cytokinin synthesis occurs in the same cells is unclear. However, Chen et al. (2013) demonstrated that a cytokinin synthesis gene, *ISOPENTENYL-TRANSFERASE3 (IPT3)*, positively regulates nodulation locally in the root. Intriguingly, another study showed that shoot-derived cytokinin is transported

towards the root and act as a negative regulator of nodulation (Sasaki et al., 2014). The authors proposed that cytokinin translocation from shoot to root as one of the components involved in controlling nodule numbers, a process termed autoregulation of nodulation. More recently, cytokinin synthesis was shown to increase as early as 3 h in response to Nod factor treatment (van Zeijl et al., 2015).

Several reports suggest an important role for auxin during nodulation. One of the consequences of cytokinin signalling is the transient inhibition of auxin transport in indeterminate nodule-forming legumes (Plet et al., 2011). This phenomenon has been reported in multiple studies and the significance of auxin transport inhibition during nodulation will be discussed in section 1.4. Interestingly, auxin transport inhibition has not been observed during nodulation in determinate nodule-forming legumes. The temporary blockage of acropetal auxin transport is followed by an increased expression of the auxin response gene, *GH3*, in the nodule primordia of *M. truncatula* (Mathesius et al., 1998a, van Noorden et al., 2007). Observations of these auxin maxima have also been reported in the nodule primordia of *L. japonicus* and soybean, where they occur in the dividing outer cortical cells (Pacios-Bras et al., 2003, Suzuki et al., 2012, Takanashi et al., 2011, Turner et al., 2013).

Despite the lack of auxin transport inhibition preceding cortical cell divisions in *L. japonicus* and soybean, it seems that an increased auxin response is conserved among indeterminate and determinate nodule-forming legumes. Suzuki et al. (2012) also found increased expression of the TRYPTOPHAN AMINOTRANSFERASE-RELATED (TAR) genes in response to rhizobia infection, which correlated with an increase in auxin response, as indicated by the *DR5:GFP-NLS* signal. In line with this finding, it was reported that the proteome changes in response to rhizobia infection and exogenous auxin treatment highly overlap (van Noorden et al., 2007). However, external auxin treatment reduced nodulation on *M. truncatula* roots, as did the application of the auxin action inhibitor PCIB (van

Noorden et al., 2007). Such an observation can be explained by the differential requirement of auxin gradient and signalling during different stages of nodulation, which cannot be mimicked by external chemical treatments (Ferguson and Mathesius, 2014). Indeed, the requirement for a “window” of auxin sensitivity is supported by several other studies. Surprisingly, overexpression of miR160, which targets and degrades AUX/IAA transcriptional repressors of auxin response genes and thus enhances auxin response, resulted in reduced nodulation in *M. truncatula* and soybean (Bustos-Sanmamed et al., 2013, Turner et al., 2013). Finally, downregulation of the *M. truncatula* cell-cycle regulator, *CELL DIVISION CYCLE16* (*CDC16*) attenuates auxin signalling and resulted in higher nodule numbers (Kuppusamy et al., 2009).

In addition to auxin sensitivity, induction of genes by auxin is also affected by the availability of internal auxin. Auxin breakdown by peroxidases, which are regulated by flavonoids, is part of auxin homeostasis and could control effective auxin levels inside cells (Peer et al., 2013). In white clover, specific flavonoids have been localised in the dividing cortical cells during nodule organogenesis (Mathesius et al., 1998a). It was found that the flavonoid 7,4-dihydroxyflavone and its derivative decelerated auxin breakdown by peroxidases *in vitro*, whereas the flavonoid formononetin sped up the process (Mathesius, 2001). Nevertheless, *in vivo* experimental evidence showing the control of auxin breakdown by specific flavonoids is still lacking. A computational model was produced to elucidate the likely events during nodulation that could explain the distribution of auxin maxima at various stages of nodule formation in indeterminate nodule-forming legumes (Deinum et al., 2012). For simplification, auxin maxima could arise from three basic mechanisms, namely (1) increased auxin influx, (2) decreased auxin efflux or, (3) elevated local auxin biosynthesis. The authors determined that the diffused and broad auxin response pattern observed during nodule primordia formation, coupled with the speed and timing in which it occurs, is most-likely contributed by a

decrease in auxin export. Relocalisation of auxin efflux carriers can also contribute to differential auxin maxima observed in the inner and outer cortex of indeterminate and determinate nodule primordia, correspondingly (Deinum et al., 2012). The authors concluded that auxin breakdown is unlikely to be quick enough to reconcile the auxin patterns that experimental evidence has uncovered so far.

1.4 Auxin transport regulation during nodulation

1.4.1 Flavonoids are natural auxin transport inhibitors

Flavonoids form one of the best-studied groups of secondary metabolites. The flavonoid biosynthesis pathway forms part of the phenylpropanoid pathway. The roles played by flavonoids are diverse, ranging from pathogen defence, UV protection, symbiosis, allelopathy and quorum sensing (Hassan and Mathesius, 2012). Flavonoids also function as natural auxin transport inhibitors (Jacobs and Rubery, 1988). Flavonoid-biosynthesis mutants have altered auxin transport capacity. Apart from flavonoids, other naturally occurring auxin transport inhibitors exist. Recently, Ueda and coworkers identified two novel natural auxin transport inhibitors, namely dehydrocostus lactone and 4-hydroxy- β -thujone, using a radish hypocotyl bioassay system (Ueda et al., 2013).

Not all flavonoids have been shown to exhibit auxin transport inhibition activities. The flavonoid subclass flavonols in particular, such as kaempferol and quercetin, show the strongest inhibition (Figure 1.7) (Jacobs and Rubery, 1988, Murphy et al., 2000). Flavonoid overaccumulating mutants show decreased auxin transport rate, whereas the opposite is true for flavonoid-deficient mutants (Brown et al., 2001, Peer et al., 2004, Wasson et al., 2006). Flavonols inhibit auxin transport by competing with synthetic auxin transport inhibitors (including NPA and TIBA) for plasma membrane and microsomal binding sites (Bernasconi, 1996, Jacobs and

Rubery, 1988, Stenlid, 1976). *Arabidopsis* mutants lacking flavonoids have altered PIN expression and localisation (Peer et al., 2004). The PID/WAG kinases regulate PIN subcellular localisation and are flavonoid-sensitive (Benjamins et al., 2001, Christensen et al., 2000, Santner and Watson, 2006, Sukumar et al., 2009). As mentioned before, PID and PP2A act antagonistically to regulate polar localisation of PIN1 (Michniewicz et al., 2007). Hence, flavonoids may indirectly modulate PAT via inhibition of PID/WAG. Flavonoids were also able to partially restore asymmetric PIN1 subcellular localisation and lateral redirection of auxin transport in the *pin2/eir1* mutant (Santelia et al., 2008).

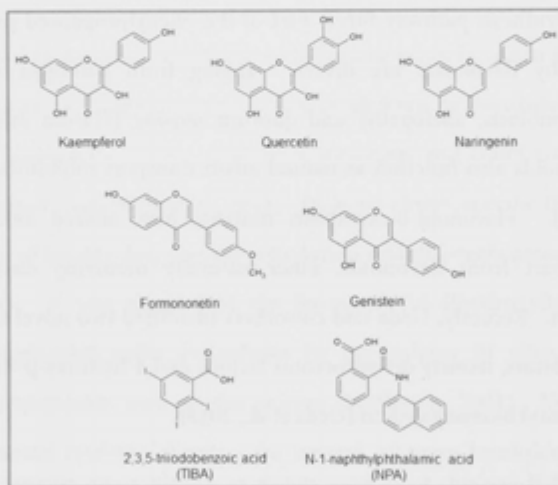


Figure 1.7 Natural and synthetic polar auxin transport inhibitors. Flavonoids represent a large group of secondary metabolites that can inhibit auxin transport. In particular, flavonols (a subclass of flavonoids), such as kaempferol and quercetin, have a strong capacity in inhibiting auxin transport. In addition to exhibiting auxin transport inhibition capabilities, the isoflavones, such as formononetin and genistein, are also unique to legumes. Synthetic auxin transport inhibitors, including TIBA and NPA, have been widely used to investigate the role of polar auxin transport during plant development.

Flavonoids may also act on PGP-mediated auxin transport. The binding of flavonols to mammalian and plant PGP transporters inhibits their activity, both *in vivo* and in heterologous systems (Brown et al., 2001, Ferte et al., 1999, Murphy et al., 2002, Peer et al., 2001, Terasaka et al., 2005). Mammalian PGPs are regulated through phosphorylation and flavonoids were found to disrupt ATPase activity through phosphorylation and allosteric binding (Szabó et al., 1997). Since PGPs are highly conserved between species, flavonoids might regulate plant PGPs via phosphorylation (Bernasconi, 1996, Carrera et al., 2007, Verrier et al., 2008). Moreover, the flavonols kaempferol and quercetin have been demonstrated to disrupt the binding between PGP1 and its activator, TWISTED DWARF (Bailly et al., 2008).

Flavonoids and auxin seem to be closely associated in several developmental responses. Accumulation of auxin and expression of auxin transport carriers are accompanied by an increase in flavonoid concentration (Grunewald et al., 2012, Noh et al., 2001, Peer et al., 2001, Terasaka et al., 2005). Flavonoid aglycones are present in low concentrations in cells (Buer et al., 2013). The majority of flavonoids exist as glycosides stored in vacuoles. The active form of flavonoids involved in auxin transport inhibition is still questionable, and recently a glycoside form of kaempferol was shown to inhibit auxin transport in *Arabidopsis* shoots (Yin et al., 2014). In the *Arabidopsis* mutant *rol1-2* (*repressor of lrx1*), flavonols specifically inhibit cellular export of naphthalene acetic acid (NAA), but not IAA, suggesting a possible developmental or tissue-specific mode of action of flavonols (Kuhn et al., 2011). Although flavonoids affect auxin transport, their mechanism of action is still unknown and auxin transport carriers are not their direct targets. Most likely, flavonoids are not direct regulators of auxin transport, especially when experimental results suggest they target a range of different processes, including auxin transporters, kinases and the trafficking machinery. Interestingly, flavonoids accumulate in plant tissues during interactions with bacteria, nematodes and fungi

(Dakora and Phillips, 1996, Hassan and Mathesius, 2012, Hutangura et al., 1999, Mathesius et al., 1998b). The function of flavonoids in nodulation, in particular their effect on auxin transport, was further examined in this thesis.

1.4.2 Regulation of local auxin transport

Two major forms of nodules have been described. Indeterminate nodules can be found on temperate legumes, such as white clover (*Trifolium repens*), pea (*Pisum sativum*) and barrel medic (*Medicago truncatula*). Nodules formed on these plants originate from pericycle and inner cortical cell divisions. They are characterised by a persistent meristem, resulting in an elongated nodule form. On the other hand, determinate nodules do not have a persistent meristem and are defined by a globular shape. Determinate nodules are initiated by outer cortical cell divisions, which subsequently fuse with the pericycle. Such nodules are seen on (sub)tropical legumes, for instance, common bean (*Phaseolus vulgaris*), soybean (*Glycine max*) and birdsfoot trefoil (*Lotus japonicus*). Indeterminate and determinate nodules represent the best-studied forms of nodulation, although many other shapes and forms of nodulation have been identified. Interestingly, formation of uninfected nodule-like structures can be mimicked by external application of synthetic auxin transport inhibitors to the roots, suggesting that polar auxin transport inhibition is part of rhizobia's toolbox in making a nodule (Hirsch et al., 1989, Wu et al., 1996).

Evidence for the occurrence of a transient auxin transport inhibition during indeterminate nodule formation can be found in multiple studies. In the model legume *M. truncatula* and vetch (*Vicia sativa*), the amount of radiolabelled auxin detected below the site of rhizobia or Nod factor treatment was reduced within 24 h (Figure 1.8) (Boot et al., 1999, Plet et al., 2011, Prayitno et al., 2006, Wasson et al., 2006). Furthermore, auxin response studies using a *proGH3:GUS* construct, where *proGH3* is an auxin-responsive promoter, showed reduced GUS staining below the

site of rhizobia infection and Nod factor application in white clover. This was consistent with results obtained from application of synthetic auxin transport inhibitors (Mathesius et al., 1998). The reduced staining does not last, however, as staining could be observed below the infection site following a short period of inhibition, and enhanced staining was observed later at the infection zone. Intriguingly, attempts to find evidence for a similar pattern in determinate legumes have fallen short. Studies in *L. japonicus* and soybean did not yield similar results (Pacios-Bras et al., 2003, Subramanian et al., 2006). On the contrary, an increase in radiolabelled auxin was measured in root segments encompassing the spot-inoculated site of *L. japonicus* at an equivalent time point when inhibition is observed in *M. truncatula* and white clover (Pacios Bras et al., 2003).

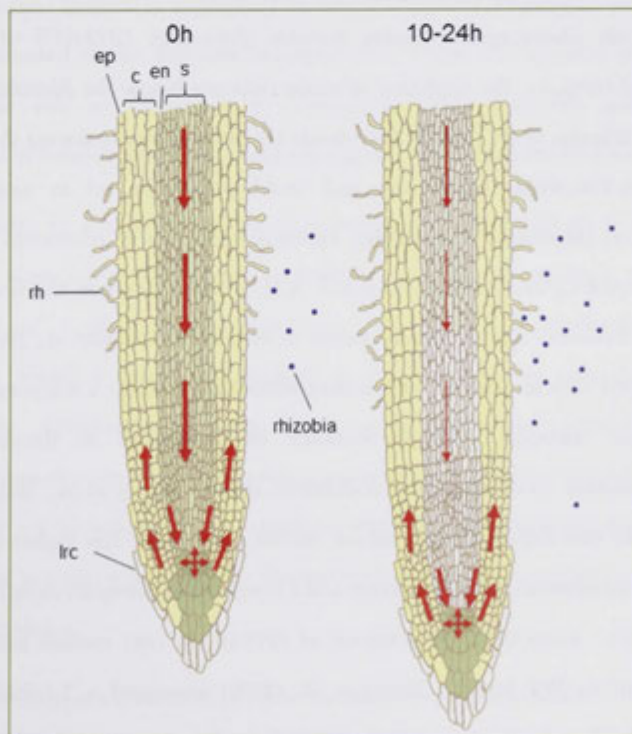


Figure 1.8 Auxin transport inhibition in response to rhizobia infection in indeterminate nodule-forming legumes. One of the characteristic responses in indeterminate nodule-forming legumes, which has so far not been observed in determinate nodule-forming legumes, is the transient inhibition of acropetal auxin transport following rhizobia or Nod factor treatment to the roots. This phenomenon has been recorded in *Medicago truncatula*, white clover and vetch, as early as 10 h after rhizobia / Nod factor treatment. The inhibition of acropetal auxin transport is short-lived, and normal auxin transport rate resumes thereafter. Abbreviations: ep, epidermis; c, cortical cell layers; en, endodermis; s, stele; rh, root hair; lrc, lateral root cap. Red arrows indicate polar auxin transport, with the thickness proportional to auxin transport capacity. Arrows pointing downwards and upwards represent acropetal and basipetal auxin transport, respectively. Shades of green indicate auxin (IAA), with the darkness proportional to concentration.

As described earlier, flavonoids have been implicated as endogenous auxin transport regulators, affecting multiple developmental programs. Flavonoids are one of the major players in nodulation control. External application of certain flavonoids phenocopied staining patterns driven by *GH3:GUS* of *Rhizobium*-infected roots, i.e. the depletion of auxin response below the *Rhizobium* infection site (Mathesius et al., 1998b). Flavonoids are induced locally during the early stages of host-*Rhizobium* interaction, and could potentially act as auxin transport regulators (Mathesius et al., 1998a). Flavonoid-deficient *M. truncatula* roots lacking the enzyme CHALCONE SYNTHASE (CHS), which catalyses the first committed step in flavonoid synthesis, were unable to nodulate (Wasson et al., 2006). This was associated with an inability of infecting *Rhizobium* to elicit a temporary inhibition of auxin transport. Supplementation of kaempferol to flavonoid-deficient *M. truncatula* roots reinstated nodulation ability (Zhang et al., 2009). The *cra1* (*compact root architecture1*) mutant, on the other hand, has higher CHS activity, higher formononetin concentration and a lower auxin transport capacity (Laffont et al., 2010). Accordingly, knockdown of *CHS* in the *cra1* mutant increased auxin transport to WT levels. Zhang et al. (2009) measured a 2.5-fold increase in kaempferol concentration during nodulation. Since auxin transport inhibition is

observed at 24 h post-infection, it is possible that kaempferol (or its derivatives) is the active auxin transport inhibitor during *M. truncatula*-*S. meliloti* interaction.

In comparison to indeterminate nodulation, auxin transport inhibition has not been observed in determinate legumes, such as soybean and *Lotus japonicus* (Pacios-Bras et al., 2003; Subramanian et al., 2006). An increase in auxin transport was observed in *L. japonicus* following *Rhizobium* infection (Pacios-Bras et al., 2003). Reduction in nodule numbers on isoflavonoid-deficient soybean roots was attributed to the inability of the host plant to induce Nod factor production in the symbiont *Bradyrhizobium japonicum*, rather than a host defect in isoflavonoid-mediated auxin transport inhibition (Subramanian et al., 2006). Rípodas et al. (2013) reported a reduction in nodule numbers in the isoflavonoid RNAi-silenced roots of common bean (*Phaseolus vulgaris*, a determinate legume). The difference in auxin transport control in indeterminate and determinate nodulation programs could be attributed to the different location where initial cell division happens. However, the role of flavonoids in controlling auxin transport and / or accumulation in determinate nodule-forming legumes remains to be clarified.

Recently, in a different nodulation program, Abdel-Lateif et al. (2013) showed that silencing of *CHS* in the actinorhizal tree *Casuarina glauca* reduced nodule numbers. *C. glauca* forms a symbiosis with actinorhizal *Frankia* bacteria. The authors found a three-fold decrease in concentration of two quercetin glycosides in RNAi-silenced roots, and nodulation was restored after supplementation of roots with naringenin, a precursor to flavonols (Abdel-Lateif et al., 2013). It will be interesting to investigate whether auxin transport inhibition occurs, and if it does, which specific flavonoid(s) are involved in this process in actinorhizal nodules.

Auxin transport control is likely to occur downstream of early Nod factor signalling. In *M. truncatula*, it is possible to induce formation of pseudonodules

after treatment with synthetic auxin transport inhibitors (NPA and TIBA) on the roots of *nfp*, *lyk3*, *dmi1*, *dmi2*, *dmi3*, *nin*, and *rit1*, but not the ethylene-insensitive mutant *skl* (Rightmyer and Long, 2011). Nodulation in the *skl* mutant is insensitive to NPA in the presence of rhizobia, suggesting that auxin transport control during nodulation requires ethylene signalling (Prayitno et al., 2006). The *M. truncatula* cytokinin-insensitive mutant *cre1*, which is a non-nodulating mutant, exhibits aberrant *PIN* expression after Nod factor treatment, compared to WT (Gonzalez-Rizzo et al., 2006, Plet et al., 2011). Hence, it is plausible that auxin transport inhibition during nodulation in *M. truncatula* is mediated by PIN proteins and this is also partially regulated by cytokinin signalling.

ATI-induced pseudonodulation has also been demonstrated in alfalfa, white sweetclover and pea (Hirsch et al., 1989, Scheres et al., 1992, Wu et al., 1996). These nodule-like structures usually form through cortical cell division and subsequent expansion, with a final globular structure usually containing lobes. However, ATI-induced pseudonodules share some structural features with *Rhizobium*-induced nodules, such as a central tissue, (pseudo)nodule cortex and an equivalent tissue of the nodule parenchyma (Hirsch et al., 1989). Synthetic auxin transport inhibitor treatments to *Lotus japonicus* roots did not induce pseudonodule formation (Kawaguchi et al., 1996). Intriguingly, Takanashi et al. (2011) discovered that cotreatment of rhizobia with high concentrations of TIBA (100 μ M) significantly increased nodule primordia formation in *L. japonicus*, despite a significant reduction in root growth.

It is fascinating to observe a difference in auxin transport regulation between indeterminate and determinate nodule formation. The common theme in the two nodulation programs is an increase in auxin response. Perhaps the inhibition of auxin transport in certain nodulating plants serves as a mechanism to increase auxin concentration and response during nodule initiation. Indeed, auxin response (as indicated by *Pro_{GUS}::GUS*) intensified at the earliest dividing pericycle and inner

cortical cells of white clover and *M. truncatula* (Huo et al., 2006, Mathesius et al., 1998b, van Noorden et al., 2007). As the nodule develops and matures, auxin response is confined to a small group of meristematic cells at the tip of the nodule. In *L. japonicus*, elevated auxin response is found in dividing cortical cells early on and later restricted to the mature nodule vasculature near the base (Pacios-Bras et al., 2003, Suzaki et al., 2012, Takanashi et al., 2011). The spatio-temporal specificity of auxin response, which is to a considerable extent related to auxin localisation, may be governed by dynamic changes in auxin transporters, thus giving rise to directional auxin flow and asymmetric auxin responses. The observed changes in auxin response could also be attributed to local auxin biosynthesis, by both the legume host and / or rhizobia.

1.4.3 Involvement of auxin transport carriers

Several auxin export facilitators of the PIN family have been identified in legumes. Based on sequence similarities, Schnabel and Frugoli (2004) have identified ten *PIN* genes in *M. truncatula* and two in *L. japonicus*. Using reporter analyses, it was found that the expression pattern of *MtPIN2* is similar to *AtPIN2* in their corresponding plants (Huo et al., 2006). Moreover, *MtPIN2* expression during nodule initiation strongly mirrors that found during lateral root initiation, supporting the hypothesis that *Rhizobium* hijacked the developmental pathway of the closely-related process of lateral root organogenesis. Knockdowns of *MtPIN2*, *MtPIN3* and *MtPIN4* reduced nodulation (Huo et al., 2006). These results support the role of PINs in nodulation, presumably through coordination of polar auxin transport (Table 1.1). The fact that *MtPIN2* is also highly expressed in root nodules suggests that *MtPIN2*-mediated auxin transport control is important throughout nodule development (Huo et al., 2006). Plet et al. (2011) found differential changes

in expression of certain *PIN* genes between WT and the non-nodulating *cre1* mutant, indicating the roles of *PIN* in auxin transport control during nodulation.

There are five auxin importers of the *LAX* family (*LIKE AUX1*) in *M. truncatula* and at least one in *L. japonicus*. One study found that the expression of *MtLAX* genes is concentrated in dividing cells of a developing nodule and lateral root (de Billy et al., 2001, Schnabel and Frugoli, 2004). In the latter stages, the expression domains shifted toward the peripheral and central region of a nodule and lateral root, respectively. The authors concluded that *LAX* could play a role in primordia development and vasculature differentiation (de Billy et al., 2001). In *L. japonicus*, *LjABCBI* was found to be highly expressed in nodules, expressed at low levels in roots and not expressed in other tissues (Takanashi et al., 2012). Localisation of this transporter exclusively to uninfected cells adjacent to infected cells suggested that *LjABCBI* exports auxin into symbiont-containing cells.

During the symbiosis between the actinorhizal tree *C. glauca* and actinomycete *Frankia*, expression of *CgAUX1* was found in *Frankia*-infected cells throughout the infection process, and that treatment with the auxin influx inhibitor 2-naphthoxyacetic acid severely reduced nodule numbers, suggesting the importance of auxin influx in actinorhizal nodulation (Péret et al., 2007). It was later discovered that *C. glauca* *PIN1*-like proteins were selectively localised to uninfected cells (Perrine-Walker et al., 2010). Coupled with computer simulations, the authors suggested that *CgAUX1* and *CgPIN1*-like proteins are arranged in this manner to direct auxin accumulation in *Frankia*-infected cells. Isoflavonoids have the capability to control auxin transport, and transcript profiling during *C. glauca*-*Frankia* association suggested a role for isoflavonoids during nodulation in this system (Auguy et al., 2011). However, whether isoflavonoids play a role in actinorhizal nodulation through auxin transport control remains a black box.

Table 1.1 Auxin transport facilitators involved in nodulation. The role of auxin transport during legume-*Rhizobium* and actinorhizal plant-*Frankia* symbioses is supported by molecular data. Several auxin exporters from the PIN family and auxin importers from the AUX1/LAX family have been shown to positively regulate nodulation. In addition, multidrug-resistant transporters from the ABCB subfamily may also play critical roles during nodulation.

Gene / Protein	Host organism	Type of interaction	Role / Phenotype	Reference(s)
MtPIN2	<i>Medicago truncatula</i>	<i>Sinorhizobium meliloti</i> inoculation	- Expressed in peripheral vasculature in early nodule primordium - Expressed at the base of mature nodule - Knockdown of MtPIN2 reduced nodulation	Huo et al. (2006)
MtPIN3	<i>Medicago truncatula</i>	<i>Sinorhizobium meliloti</i> inoculation	- Knockdown of MtPIN3 reduced nodulation	Huo et al. (2006)
MtPIN4	<i>Medicago truncatula</i>	<i>Sinorhizobium meliloti</i> inoculation	- Knockdown of MtPIN4 reduced nodulation	Huo et al. (2006)
		<i>Sinorhizobium meliloti</i> Nod factor treatment	- Increased expression after Nod factor treatment	Plet et al. (2011)
MtPIN10	<i>Medicago truncatula</i>	<i>Sinorhizobium meliloti</i> Nod factor treatment	- Increased expression after Nod factor treatment	Plet et al. (2011)
MtLAX1-3	<i>Medicago truncatula</i>	<i>Sinorhizobium meliloti</i> inoculation	- Transcripts are localised to early dividing cells and to cells near the vasculature of early nodule primordium	de Billy et al. (2001)
LjABCB1	<i>Lotus japonicus</i>	<i>Mesorhizobium loti</i> inoculation	- Localised to uninfected cells adjacent to rhizobia-infected cells - Exports IAA from uninfected cells into adjacent rhizobia-infected cells	Takanashi et al. (2012)
CgPIN1	<i>Casuarina glauca</i>	<i>Frankia</i> inoculation	- Localised to uninfected cells adjacent to <i>Frankia</i> -infected cells - Exports IAA into <i>Frankia</i> -infected cells	Perrine-Walker et al. (2010)
CgAUX1	<i>Casuarina glauca</i>	<i>Frankia</i> inoculation	- Localised to <i>Frankia</i> -infected cells - Imports IAA into <i>Frankia</i> -infected cells	Peret et al. (2007)

1.4.4 Regulation of long-distance auxin transport

In addition to the local control of auxin transport and signalling at the nodule initiation site, the involvement of shoot-derived auxin at the nodulation site has also been suggested. The hypernodulating, ethylene-insensitive *sk1* mutant is defective in long-distance auxin transport regulation following rhizobia infection, although the mechanism by which ethylene signalling affects long-distance auxin transport control remains a question (Prayitno et al., 2006). Plant hosts control the number of nodules being formed according to their nitrogen requirements, in a process that

involves systemic signals and known as autoregulation of nodulation (AON) (Caetano-Anolles and Gresshoff, 1991). AON mutants are unable to limit nodule numbers and supernodulate (Stacey et al., 2006). This mechanism is governed by a leucine-rich repeat receptor-like kinase that acts in the shoot (SUNN, for SUPER NUMERIC NODULES, in *Medicago*). Upon rhizobia infection at the root, a root-to-shoot signal is mobilised and perceived by the receptor and subsequently a reciprocal, yet-to-be-identified signal is transmitted to the root. In the *M. truncatula sunn1* mutant, shoot-to-root auxin transport is higher than WT plants under uninfected conditions (van Noorden et al., 2006). Moreover, this long-distance auxin transport is reduced in WT plants after rhizobia infection, but not in the *sunn1* mutant, suggesting that systemic auxin transport is part of the AON (van Noorden et al., 2006). The supernodulation phenotype in the *sunn1* mutant can be rescued by application of the auxin transport inhibitor NPA at the shoot / root junction, suggesting that long-distance auxin transport control is PIN-mediated. Nonetheless, it is possible that SUNN-mediated auxin transport is a more generalised mechanism for controlling root architecture in response to nitrogen. This is supported by the failure of the *sunn1* mutant to control lateral root density in response to nitrate through the modulation of shoot-to-root auxin transport (Jin et al., 2012).

1.5 Aims and hypotheses

This thesis contains three aims. Firstly, a method for quantifying auxin using LC-ESI-Q-TOF MS/MS was optimised and established to quantify auxins during nodulation in legumes. Secondly, a comparison between indeterminate and determinate nodule-forming legumes in the context of auxin requirements during nodulation was performed. Thirdly, using a *Medicago truncatula* cytokinin

perception mutant *cre1*, we attempted to elucidate downstream auxin transport components defective in the *cre1* mutant.

1.5.1 Aim one - Establishment of an LC-ESI-Q-TOF MS/MS protocol for auxin quantification

The plant hormone auxin is essential for organ formation. Organ development is tightly regulated by auxin gradients (Su et al., 2011). At different stages of organ development, cellular auxin concentrations change dynamically as a result of auxin homeostatic control, including auxin biosynthesis and conjugation. Auxin represents a class of hormones, where the most abundant form of active auxin in most land plants examined hitherto is indole-3-acetic acid (IAA) (Tivendale et al., 2014). However, several other active auxin species exist and they can be conjugated to amino acids. In *M. truncatula* roots, several auxins are thought to exist based on expression studies of auxin conjugation and hydrolase enzymes (Ludwig-Müller, 2011). Nevertheless, direct measurement of auxins, in particular during various stages of *Rhizobium*-legume interaction, is still missing. Several questions have to be addressed to unravel the role of auxins in nodulation. Firstly, it is still unclear which auxins are important for nodulation and whether their concentrations change during nodulation. Secondly, the contradictory reports for the requirement of auxin transport control in determinate and indeterminate nodulation warrant further investigation. Thirdly, the control of auxin transport in indeterminate nodule-forming legumes needs to be placed in the known signalling pathway of nodulation. Here, we aimed to develop a method for auxin quantification in *M. truncatula* roots during nodulation. Various methods exist in the literature but adaptation and optimisation for different instruments are necessary. We took advantage of a highly sensitive and specific LC-ESI-Q-TOF MS/MS system available at The Australian National University. By using a targeted MS/MS approach with

commercial standards available for comparison, we aimed to develop a method for unbiased quantification of endogenous auxin compounds.

1.5.2 Aim / hypothesis two – Do indeterminate and determinate nodule-forming legumes have different auxin requirements during nodulation?

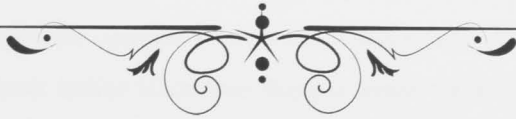
Nitrogen-fixing nodules in legumes can be loosely divided into two types, namely indeterminate and determinate nodules. Some examples of legumes which form indeterminate nodules include *Medicago* sp., clovers and pea. Determinate nodules form on *L. japonicus*, soybean and common bean (Hirsch, 1992). The difference between these two nodule types is the presence of a persistent nodule meristem in indeterminate nodules and the absence of it in determinate nodules. Moreover, auxin transport inhibition has only been observed in indeterminate legumes (Ferguson and Mathesius, 2014). However, detailed and localised measurements of auxin transport is lacking in the literature, with only one direct measurement in *L. japonicus* representing the available auxin transport data for determinate nodule-forming legumes (Pacios-Bras et al., 2003). Here, we hypothesised that a transient acropetal auxin transport inhibition occurs in indeterminate, but not in determinate nodule-forming legumes, using *M. truncatula* and *L. japonicus* as our model systems, respectively. Furthermore, we investigated changes in basipetal auxin transport, which has been largely overlooked in legume-*Rhizobium* symbiosis. Auxin quantification was performed at sequential time points. Together with the auxin transport measurements, the requirement for auxin during early nodulation stages of *M. truncatula* and *L. japonicus* were compared. We also hypothesised that if auxin transport inhibition is specific to indeterminate nodule formation, application of synthetic auxin transport inhibitors would induce pseudonodules on the roots of indeterminate nodule-forming legumes, but not on the roots of determinate nodule-forming legumes. Crossing the legume boundary, we

investigated auxin content in a few non-leguminous species which do or do not nodulate. Here, we tested whether different auxin compounds might be present or absent, in comparison to legumes.

1.5.3 Aim / hypothesis three – Does auxin transport inhibition act downstream of cytokinin signalling regulated by flavonoids in *Medicago truncatula*?

The *cre1* mutant is cytokinin insensitive, displays increased lateral root formation and has greatly diminished nodulation capacity. Previously, it was shown that rhizobia inoculation on WT *M. truncatula* roots caused a reduction in acropetal polar auxin transport. However, this was not observed in the *cre1* mutant (Plet et al., 2011). Thus, acropetal auxin transport inhibition likely occurs downstream of cytokinin signalling. Here, we aimed to investigate the molecular processes behind auxin transport inhibition, as well as downstream responses, which are dependent on this physiological response. We hypothesised that auxin transport inhibition is controlled by the *PIN* and *LAX* family of auxin exporters and importers, respectively, in *M. truncatula* (Schnabel and Frugoli, 2004). Flavonoids might be involved in this process, as they were previously shown to inhibit auxin transport (Brown et al., 2001). In addition, flavonoid-deficient *M. truncatula* roots exhibit increased auxin transport and failed to inhibit auxin transport in response to rhizobia treatment (Wasson et al., 2006). We hypothesised that selected flavonoids are induced in response to rhizobia treatment in WT roots, but this would be unaltered in the *cre1* mutant. Moreover, exogenous application of flavonoids deficient in the *cre1* mutant would complement nodulation. An increase in auxin response observed in WT would be absent in the *cre1* mutant, and this is associated with an increase in local auxin biosynthesis in WT plants, but not in the *cre1* mutant.

CHAPTER 2



Materials and Methods



2.1 Plant materials and bacterial strains

Plant materials used in this study include *Medicago truncatula* wild type cultivar Jemalong A17 (The South Australian Research and Development Institute, Adelaide), *Lotus japonicus* ecotype Gifu B-129 (Biological Resource Center In *Lotus* and *Glycine*, University of Miyazaki, Japan), *Acacia longifolia* (Royston Petrie Seeds, NSW, Australia), *Trifolium subterraneum* (subclover) cv Karridale (Clean Seeds, Australia), *Glycine max* (soybean) cv Bragg (Prof. Peter Gresshoff, University of Queensland), *Sesbania rostrata* (Prof. Sofie Goormachtig, Ghent University, Belgium), *Cucumis sativus* (cucumber; Royston Petrie Seeds, NSW, Australia), *Begonia cleopatra* (courtesy of Steve Dempsey, ANU), *Datisca glomerata*, *Casuarina glauca*, and *Coriaria myrtifolia* (Prof. Katharina Pawlowski). The *M. truncatula* cytokinin perception mutant *cre1-1* (kindly provided by Dr. Florian Frugier) was used for experimental studies described in Chapter 5 of this dissertation (Le Signor et al., 2009).

The *Sinorhizobium meliloti* strain A2102, a triple nod mutant for *nodD1*, *nodD2* and *nodD3* derived from the WT strain Sm1021, containing the pE65 plasmid encoding a constitutively overexpressed copy of *nodD3* (Barnett et al., 2004) was used for all inoculations on *M. truncatula* (kindly provided by Melanie Barnett and Sharon Long, Stanford University), unless otherwise stated in individual sections below and / or in Chapter 4. This strain produces Nod factors in the absence of nod gene-inducing flavonoids from the legume host (Barnett et al., 2004) and was used to exclude the possibility that defects in flavonoids in the *cre1* mutant prevented proper nod gene activation in the symbiont (e.g., Zhang et al. 2009). For standardisation of results in this thesis, this strain, hereafter referred to as "E65", was used for inoculation as opposed to a WT strain, unless otherwise stated. The E65 strain was maintained on Bergensen's Modified Medium (BMM) (Rolfe and Gresshoff, 1988) supplemented with 10 µg ml⁻¹ tetracycline and 100

$\mu\text{g ml}^{-1}$ streptomycin (Sigma Chemicals). For subclover, *L. japonicus* and soybean, inoculation ($\text{OD}_{600\text{nm}} = 0.05$) was performed with *Rhizobium leguminosarum* bv *trifolii*, *Mesorhizobium loti* WT strain MAFF303099 and *Bradyrhizobium japonicum* WT strain USDA110, respectively. All three *Rhizobium* strains were maintained on tryptone-yeast (TY) medium.

To generate a *gfp*-labelled E65 strain, the plasmid pTE3 containing the *nodD3* expression cassette driven by the *tcp* promoter was isolated from *S. meliloti* A2102 (Barnett et al., 2004). A 957 bp region from the plasmid pHc60 containing *gfp* under a constitutive promoter (Cheng and Walker, 1998) was excised using BglII (New England Biolabs, USA), ligated into the pTE3 vector containing *nodD3* expression cassette using T4 DNA ligase (New England Biolabs, USA), and electroporated into competent Sm1021. The colonies were cultured on BMM with $10 \mu\text{g ml}^{-1}$ tetracyclin (Sigma, USA) and screened for GFP fluorescence to confirm insertion of *gfp* fragment. This was done by Samira Hassan (ANU)

The overexpression vector for MtFLS (flavonol synthase) was generated by amplifying the MtFLS full length sequence (IMGAG Gene ID Medtr5g059140) using the primers MtFLSox listed in Table 2.1. The PCR product was introduced into the overexpression vector pK7WG2D using Gateway cloning (Karimi et al., 2002). The MtFLS overexpression vector was introduced into *Agrobacterium rhizogenes* strain ARqual using the freeze-thaw method (Hofgen and Willmitzer, 1988). Plant transformation of A17 or the *cre1* mutants with MtFLSox was done by *A. rhizogenes* hairy root transformation (Boisson-Dernier et al., 2001). The overexpression of MtFLS was confirmed through qRT-PCR. This was done by Samira Hassan (ANU).

2.2 Growth conditions

M. truncatula, *L. japonicus* and subclover seeds were scarified with sand paper, surface-sterilized in 6 % (w/v) sodium hypochlorite for 10 min, then washed with sterilised milliQ water five times. Next, *M. truncatula* and *L. japonicus* seeds were imbibed in sterilised milliQ water containing 0.25 mg ml⁻¹ augmentin (further disinfection) for six hours, on a rotating wheel. Sterilised seeds were washed once with sterilised milliQ water and then plated on F medium (Fahraeus, 1957) for *M. truncatula*, or ¼ strength Broughton and Dilworth medium (Broughton and Dilworth, 1971) for *L. japonicus*. For subclover, seeds were sown straight onto F plates without the augmentin incubation step. Seeds were incubated at 4 °C in the dark for 48 h. Germination of seeds was synchronised by incubating the plates at 25 °C for 24-48 h with plates inverted. Seedlings with radical length of approximately 5-10 mm were transferred onto F plates (*M. truncatula* and *T. subterraneum*) or ¼ B&D plates (*L. japonicus*). Plates were semi-sealed with parafilm, placed vertically in a container with a black cardboard interspersed between each plate to shield roots from direct light. Plates were incubated at 25 °C (*M. truncatula* and *T. subterraneum*) or 20 °C (*L. japonicus*), with a 16 h light and 8 h dark period at 150 µmol m⁻² s⁻¹ light intensity.

For *A. longifolia*, a minute portion of the hard seed coat was chipped off with a scalpel. Seeds were then sterilised for 10 min in 6 % (w/v) sodium hypochlorite. Sterilised seeds were washed five times with sterilised milliQ water and then imbibed overnight in sterilised milliQ water on the bench. Imbibed seeds were plated onto F plates and left at 25 °C in the dark for germination over several days. Germinated seedlings were transferred into vermiculite (Grade 3) pots, watered with F medium, and grown at 16 h light and 8 h dark period at 150 µmol m⁻² s⁻¹ light intensity.

For soybean, the germination protocol was based on Brechenmacher et al. (2009). Seeds were soaked in 0.1 N HCl for 10 min and then washed with tap water

five times. Seeds were then surfaced-sterilised with 6 % (w/v) sodium hypochlorite for 15 min and then washed with sterilised water five times, air dried for 20 min, and subsequently sown on $\frac{1}{4}$ B&D plates. Seeds were left at 25 °C in the dark for germination over several days. Germinated soybeans were transferred into vermiculite (Grade 3) pots, watered with $\frac{1}{4}$ B&D medium and grown at 16 h light and 8 h dark period at $150 \mu\text{mol m}^{-2} \text{s}^{-1}$ light intensity.

For *S. rostrata*, the germination protocol was modified from Goethals et al. (1989). Seeds were immersed in ~ 4 M sulphuric acid for one hour and washed five times with tap water. This was followed by surface-sterilisation with 6 % (w/v) sodium hypochlorite for 15 min and then five washes with sterilised miliQ water. Sterilised seeds were imbibed overnight in sterilised miliQ water. Imbibed seeds were plated onto F plates and left at 25 °C in the dark for germination over several days. Germinated seedlings were transferred into vermiculite (Grade 3) pots, watered with F medium and grown at 16 h light and 8 h dark period at $150 \mu\text{mol m}^{-2} \text{s}^{-1}$ light intensity.

Cucumber and begonia were germinated directly in pots in fine sand without pre-treatment. Seeds were sown approximately 1 cm below the surface. *D. glomerata*, *C. glauca* and *C. myrtifolia* were grown at Stockholm University and the root materials directly shipped to The Australian National University for analysis, as part of a collaborative study with Prof. Katharina Pawlowski and Dr. Irina Demina.

2.3 Bacterial inoculation conditions

For plant inoculation, an overnight culture of *S. meliloti* strain E65 in BMM at 28 °C was used. The optical density ($\text{OD}_{600\text{nm}}$) of the culture was adjusted to 0.1 for spot-inoculation and 0.01 for flood-inoculation. Spot-inoculation was performed by

placing ~ 1 μ l of *S. meliloti* culture or BMM, 2 mm above the root tip, corresponding to the nodulation-susceptible zone (Bhuvanewari et al., 1981). For analyzing *GH3::GUS* expression, spot-inoculation was performed with a glass capillary pulled into a fine tip over a flame and glued to a hypodermic needle. Flood inoculation (1 ml / plate) used for complementation assays is described below.

For inoculation of *L. japonicus* and subclover, a liquid culture of *M. loti* (*L. japonicus*) and *R. leguminosarum* (subclover) in TY medium were incubated for three days at 28 °C. The OD_{600nm} of the cultures were adjusted to 0.05. Inoculation was performed by placing 1 μ l of *Rhizobium* culture or TY control, 3 mm above the root tip.

For inoculation of soybean, a liquid culture of *B. japonicum* in TY medium was incubated for three days at 28 °C. The OD_{600nm} of the culture was adjusted to 0.05. Inoculation was performed by pouring 50 ml of *B. japonicum* culture into individual pots.

2.4 Flood treatment with auxin transport inhibitors

Seeds were germinated as described above. At one week post-transfer onto agar medium, seedlings were treated by flooding, as described in Rightmyer and Long (2011). Diluted solutions of NPA (100 μ M), TIBA (50 μ M) (Sigma), kaempferol (3 μ M), quercetin (3 μ M), naringenin (3 μ M), isoliquiritigenin (3 μ M) and hesperetin (3 μ M) (Sigma) were made in sterile 50 ml Falcon tubes. Control treatments contained equivalent dilutions of methanol used as a solvent for stock solutions. The concentrations of auxin transport inhibitors and flavonoids were chosen because they were previously demonstrated to induce pseudonodules and to complement nodule formation, respectively, in *M. truncatula* (Rightmyer and Long, 2011, Zhang et al., 2009). Seedlings were flooded with 20-30 ml of diluted ATIs or

flavonoids for 10 s, and then the solution was decanted. Following flooding, the entire root of individual seedlings was inoculated with BMM (mock-inoculation) or strain E65 adjusted to 0.01 (OD_{600nm}) (~ 1 ml). Similar treatments were performed on *L. japonicus* and subclover roots. For plants grown in pots (*A. longifolia*, soybean, *S. rostrata*), 100 ml of auxin transport inhibitor diluted in growth medium was applied to each pot, once.

2.5 Auxin quantification

2.5.1 Auxin standards

Commercial auxin standards and a deuterated internal standard were used to determine elution times, collision energies, detection limits and for absolute quantification. Auxin standards were obtained from OlChemim (IAA-Phenylalanine, IAA-Leucine, IAA-Valine, IAA-Tryptophan, 4-Cl-IAA), Sigma (IAA-Aspartate, IAA-Alanine, IAA-Isoleucine, IAA, IBA, PAA) and Cambridge Isotope laboratories (Indole-2,4,5,6,7-d5-3-acetic acid).

2.5.2 Auxin extraction protocol

The extraction protocol used was adapted from Muller and Munne-Bosch (2011). Plant roots were collected at 6, 24, and 48 h post-treatment with rhizobia or auxin transport inhibitors. Root segments of 4-5 mm spanning the inoculation spot (or in the case of ATI treatment, a segment corresponding to a rhizobia-treated root) were collected and snap-frozen immediately in liquid nitrogen. A total of 30-40 root segments (70-90 mg) were collected for each treatment, for each biological replicate. The frozen tissue samples were mechanically lysed with stainless steel beads in a Qiagen TissueLyser LT with a pre-cooled tube holder. To each tube 20 μ L of the

internal standard ($1 \mu\text{g mL}^{-1}$ of 3- $^{3}\text{H}_5$ indolylic acid) followed by $500 \mu\text{l}$ extraction solvent (methanol:propanol:glacial acetic acid, 20:79:1, v/v/v) were added and auxin extraction was performed in a sonicator bath for 30 min at 4°C . Samples were then centrifuged at $16100 \times g$ for 15 min. The supernatant was transferred to a fresh tube and subsequently dried in a Speedvac centrifuge. Extraction was repeated once and the supernatant combined with the (dried) supernatant from the first extraction, and subsequently evaporated in a Speedvac centrifuge. Vacuum-dried samples were resuspended with 100% methanol, vortexed for five seconds, and filtered through a Nanosep MF GHP $0.45 \mu\text{m}$ filter (Pall Life Sciences) by centrifugation at $16100 \times g$, for 1 min. The resuspension step was repeated once. The eluent containing the auxin extracts was transferred to an amber vial and vacuum-dried. Samples were stored at -80°C until analysis. Prior to analysis, samples were taken out from the freezer to equilibrate with room temperature. Each sample was resuspended with $50 \mu\text{l}$ methanol (Acros Organics) and water (60:40, v/v).

2.5.3 Liquid chromatography - electrospray ionisation - tandem mass spectrometry quadrupole time-of-flight (LC-ESI-MS/MS Q-TOF) methodology

Tandem mass spectrometry was performed using an Agilent 6530 Accurate Mass LC-MS Q-TOF (Santa Clara, CA, USA). Samples were subjected to ESI in the Jet Stream interface in both ion positive and negative polarities. Based on optimised LC-ESI-Q-TOF parameters using auxin standards, the auxins IAA, IBA and IAA-Ala had better sensitivity in the positive mode. The other auxin species were better detected in the negative mode. Optimised conditions in the positive mode were as follow: gas temperature 250°C , drying gas 5 L min^{-1} , nebulizer 30 psig, sheath gas temperature 350°C and flow rate of 11 L min^{-1} , capillary voltage 2500 V, nozzle voltage 500 V and fragmentor voltage 138 V. Conditions in the negative mode were

as follow: gas temperature 300 °C, drying gas 9 L min⁻¹, nebulizer 25 psig, sheath gas temperature 350 °C and flow rate of 11 L min⁻¹, capillary voltage 3000 V, nozzle voltage 500 V and fragmentor voltage 140 V. Samples were injected (7 µl) onto an Agilent Zorbax Eclipse 1.8 µm XDB-C18 2.1 × 50 mm column. Solvent A consisted of 0.1 % aqueous formic acid and solvent B, 90 % methanol/ water with 0.1 % formic acid. Free auxins and conjugates were eluted with a linear gradient from 10-50 % solvent B over 8 min, 50-70 % solvent B from 8-12 min (then held at 70 % from 12-20 min) at a flow rate of 200 µl min⁻¹. The Q-TOF was run in targeted MS/MS mode using collision induced dissociation (CID; N₂ collision gas supplied at 18 psi with *m/z* 1.3 isolation window) where the MS extended dynamic range (2 Hz) was *m/z* 100-1000 with an acquisition rate of 3 spectra s⁻¹ and MS/MS at *m/z* 50-1000 at 3 spectra s⁻¹.

2.5.4 Data analysis

Data were analysed using Agilent Technologies MassHunter software (ver. B.5.0). Commercial auxin standards and deuterated internal standard were used to determine elution times, collision energies, limit of detections (LODs) and limit of quantifications (LOQs) in order for subsequent quantification of the endogenous auxins.

2.6 Flavonoid quantification

2.6.1 Flavonoid standards

Commercial flavonoid standards and an analog internal standard, luteolin (Sigma) were used to determine elution times, collision energies, detection limits and for absolute quantification. Flavonoid standards were obtained from Sigma

(kaempferol, naringenin, quercetin, morin, hesperetin), Fluka (apigenin), ICN biomedical (genistein) and Indofine Chemicals (luteolin).

2.6.2 Flavonoid extraction protocol

Plant roots inoculated and mock-inoculated with rhizobia, as described above, were collected 24 h.p.i.. Root segments of 2 cm length starting from the root tip (including the inoculation site) were collected and snap-frozen immediately in liquid nitrogen. To determine the total content (free form and glycosides) of flavonoids, 30 root segments were collected for each treatment in each biological replicate and flavonoid concentration from 3 biological replicates were analysed. The frozen tissue samples were mechanically lysed with stainless steel beads in a Qiagen TissueLyser LT, with a pre-cooled tube holder. Extraction of total flavonoids was based on Farag et al. (2007), with some modifications. As an internal standard, 20 ng luteolin (Indofine Chemicals) was added to each tube and 1 ml of 80 % methanol/water was used as the extraction solvent. Flavonoids were extracted overnight on a rotating wheel at 4 °C in the dark. Tubes were centrifuged at 16100 × g for 30 min and the supernatant transferred to a fresh tube and evaporated in a Speedvac centrifuge. The residue was redissolved in 100 µl of 2 N HCl and heated at 80 °C for 90 min to deglycosylate flavonoids. The acid hydrolysed sample was mixed with 200 µl of ethyl acetate, vortexed, and the ethyl acetate fraction (containing flavonoid aglycones) was transferred to a separate tube before being dried in a Speedvac centrifuge. Samples were resuspended in 50 µl of 45 % methanol, passed through a Nanosep MF GHP (hydrophilic polypropylene) 0.45 µm filter (Pall Life Sciences) and analysed by targeted LC-ESI-MS/MS.

To determine the concentration of selected flavonoid free aglycones, 15 root segments were collected for each treatment in each biological replicate and flavonoid concentration from five biological replicates were analysed. Extraction

was similar to total flavonoids, but without the acid hydrolysis and ethyl acetate fractionation step, i.e. following overnight extraction, samples were dried and resuspended for targeted LC-ESI-MS/MS analysis.

2.6.3 Liquid chromatography - electrospray ionisation - tandem mass spectrometry quadrupole time-of-flight (LC-ESI-MS/MS Q-TOF) methodology

LC-ESI-MS/MS analysis was performed as described above in the negative mode, with collision energies optimized for the targeted flavonoids. Samples were injected (7 μ l) onto an Ascentis[®] Express 2.7 μ m C18 2.1 \times 50 mm column (Supelco). Mobile phase A consisted of 0.1 % aqueous formic acid and mobile phase B consisted of 90 % acetonitrile/water with 0.1 % formic acid. The applied gradient was as described above.

2.6.4 Data analysis

Absolute quantification was performed as described above. For identification and relative quantification (peak area ratio of the endogenous analyte/internal standard) of flavonoid compounds where commercial standards were not available, the mass spectra of flavonoid compounds detected in samples were compared to the MassBank database (Horai et al., 2010) and the literature (Guo et al., 2008, Li et al., 2013).

2.7 Histochemistry and Microscopy

GUS staining was performed as described in van Noorden et al. (2007). Sections were made using a Vibratome 1000 (Vibratome Company, St. Louis, MO, USA), and viewed under brightfield using a DMLB microscope (Leica Microsystems,

Wetzlar, Germany) and images were collected with a mounted CCD camera (RT Slider; Diagnostic Instruments, Sterling Heights, MI, USA).

For complementation of nodulation by flood treatment, whole roots were viewed under a Leica M205 FA stereomicroscope. GFP fluorescence was visualized using an ET Blue LP filter system (max. excitation at 470 nm with a 515 nm long pass filter). Nodule sections were viewed under a Leica DM5500 epifluorescence microscope. GFP fluorescence was visualized using a +L5 filter cube (Leica Microsystems) with a blue excitation range (max. excitation at 480 nm, band pass filter at 527 +/- 30 nm). Photos were taken with a Leica DFC550 high-speed digital camera.

2.8 Auxin transport studies

2.8.1 Preparation of agar blocks and pre-treatment of seedlings

Tritium-labelled indole-3-acetic acid (^3H -IAA) solution ($7.5 \mu\text{l}$ of 1 mCi ml^{-1}) (American Radiolabelled Chemicals, St Louis, MO, USA) was diluted in $20 \mu\text{l}$ ethanol and mixed with 1.5 ml of melted and cooled 1 % agarose at pH 4.8, in a petri dish. The pH was chosen as it is close to the isoelectric point of IAA. The ^3H -IAA block was left to cool in the dark for 10 minutes with the lids off before transferring to 4°C until use to prevent degradation. Small blocks with dimensions of $2 \text{ mm} \times 2 \text{ mm} \times 2 \text{ mm}$ were cut with a scalpel. This standardised the amount of ^3H -IAA supplied to plants. Seedlings were pre-treated with *Rhizobium*/auxin transport inhibitors prior to auxin transport study, as described below.

2.8.2 Acropetal auxin transport studies

Acropetal auxin transport was strictly performed in relation to the spot-inoculation site. Where three segments were analysed, roots were cut 10 mm from the inoculation spot in the shootward direction (approximately 16 mm from the root tip); where two segments were analysed, roots were cut 8 mm from the inoculation spot in the shootward direction (approximately 12 mm from the root tip). The shoot-containing segment was discarded, a small ^3H -IAA block (2 mm \times 2 mm \times 2 mm) placed on the cut end of the root-tip containing segment. A parafilm strip was placed underneath the root segments to prevent diffusion of ^3H -IAA from the growth media directly into parts of the root. Samples were incubated vertically for 6 h (*M. truncatula*) or 12 h (*L. japonicus*) in the dark to allow ^3H -IAA to diffuse from the agar block through the cut end. The first 4 mm segment touching the ^3H -IAA agar block was discarded. For analysis of three segments, the subsequent 12 mm was divided into three segments; for analysis of two segments, the subsequent 8 mm was divided into two segments. These root segments were transferred into individual scintillation vials containing 2 ml scintillation fluid (Perkin-Elmer).

2.8.3 Basipetal auxin transport

For basipetal auxin transport measurements, ^3H -IAA agar blocks were placed touching the root tip of intact seedlings, which were also placed on parafilm strips. After 6 h (*M. truncatula*) or 12 h (*L. japonicus*) vertical incubation in the dark, the first 2 mm root segment from the agar block was discarded. Subsequent 2 mm segments were collected into four separate vials containing scintillation fluid, with each vial containing one segment.

2.8.4 Sample incubation and radioactivity measurement by scintillation proximity assay

Samples for both acropetal and basipetal transport measurements (in scintillation fluid) were incubated on an INOVA 2100 platform shaker (New Brunswick Scientific) overnight at room temperature. Radioactivity was measured in a scintillation counter (Tri-Carb[®] Liquid Scintillation Analyzer B2810TR, Perkin-Elmer) over 1 min each. The default settings for tritium decay measurement were used. A vial containing just the scintillation fluid was used as a blank for background subtraction during analysis. Raw data were exported in Excel format and analysed with Excel. In Chapter 5, data was represented as “auxin relative transport change”. These were calculated by dividing each data point with the untreated control for each genotype.

2.9 RNA extraction, cDNA synthesis, and quantitative real-time PCR

Frozen root samples were ground in liquid nitrogen with a pre-cooled mortar and pestle. Total RNA extraction was performed with an RNeasy[®] Plant Mini Kit (Qiagen) or Spectrum[™] Plant Total RNA kit (Sigma). RNA quality and quantity were analysed with a NanoDrop[®] ND-1000 (Labtech International). First-strand cDNA synthesis was performed using a SuperScript[™] First-strand Synthesis System for RT-PCR kit (Invitrogen). RNA quantity from each sample in each biological replicate was standardized prior to first-strand cDNA synthesis. Primers were designed using Clone Manager for Windows version 9.0 (GE Healthcare Life Sciences) or Primer 3. The list of gene primers and other relevant information are listed in Table 2.1. Standard criteria for quantitative RT-PCR primer design were used, based on Udvardi et al. (2008). Sample mix for qRT-PCR was prepared in

384-well plates using standard reaction mixture from Power/Fast SYBR® Green (Applied Biosystems) and analysed with an Applied Biosystems 7900HT or ViiA™ 7 Real-Time PCR System. Raw data were analysed in Excel using a relative quantification method based on (Pfaffl, 2001), with *GLYCERALDEHYDE-3-PHOSPHATE DEHYDROGENASE (GAPDh)* or *RIBOSOME BINDING PROTEIN1 (RBP1)* as the reference genes.

2.10 Statistical analyses

Statistical analyses were carried out with Genstat 15th Edition (VSN International, Hemel Hempstead, UK), Prism version 5.02 and InStat version 3.06 (Graphpad Software, La Jolla, CA, USA).

Table 2.1 Primer sequences of genes used in this study and their gene IDs (v4.0). *MtPIN5* and *MtPIN8* mRNAs were not detected in *M. truncatula* roots (Schnabel and Frugoli, 2004).

Gene	Gene ID (Medicago v4.0)	Sequences of primer pairs
<i>MtPIN1</i>	Medtr4g084870	5'-TGCCCTGAACAAGCTAGGAG-3' ; 5'-GAGACGGGTGATAACACTTGC-3'
<i>MtPIN2</i>	Medtr4g127100	5'-AGCCTAAGCTGATTGCATGTGG-3' ; 5'-TGCTATTGAGGTTGCCGCAATC-3'
<i>MtPIN3</i>	Medtr1g030890	5'-CTTCGCCGGTTTCGGAAAG-3' ; 5'-GTTTCATCAGCCACCACCATC-3'
<i>MtPIN4</i>	Medtr6g069510	5'-GCATGGCTATGTTTCAGTCTTGG-3' ; 5'-GACCAACAAGGAATCTCACACC-3'
<i>MtPIN6</i>	Medtr1g029190	5'-CAGCCTCGTATCATTGCTTGTG-3' ; 5'-CGGCAATCGAGGATAAGGAC-3'
<i>MtPIN7</i>	Medtr4g127090	5'-TGTGATTGCGGCAACCTC-3' ; 5'-TGGCAAACACAAAGGGAACG-3'
<i>MtPIN9</i>	Medtr7g079720	5'-ATGGGTGTGGATCTTGTG-3' ; 5'-CCCTCTATTCCCGTCTTC-3'
<i>MtPIN10</i>	Medtr7g089360	5'-TGCCACCTGCTAGTGTATG-3' ; 5'-GGGACCAGGTAAGACCAATAAG-3'
<i>MLAX1</i>	Medtr5g082220	5'-CTTGGCCTGGCATGACTAC-3' ; 5'-TCTTTGGACCCGAGTGAACC-3'
<i>MLAX2</i>	Medtr4g415390	5'-TGGGTTTGGGTTTGGAGGATGG-3' ; 5'-GACTGGTGGTGGTTTGCATTGG-3'
<i>MLAX3</i>	Medtr3g072870	5'-GACAGGCTGAGGATGTGAAG-3' ; 5'-AACAGCATGCCACCAAAGG-3'
<i>MLAX4</i>	Medtr4g415390	5'-TGGAGGATGGGCTAGTATGACC-3' ; 5'-ATGGTCTTGAGGTGGTGGTGG-3'
<i>MLAX5</i>	Medtr4g073770	5'-CCACCGTTGGATCTCTACTTG-3' ; 5'-CATTCTGTCGAGCAGAGGATG-3'
<i>MGH3</i>	Medtr5g016320	5'-CTCAGAGTTTCTGACCAGTTCAG-3' ; 5'-AGTAGGCTGTACAATAACTGACGAC-3'
<i>MtCHS</i>	Medtr7g016780	5'-CACCTTCGTGAAGCTGGACT-3' ; 5'-GTGGCTCAAAGCGTCAACC-3'
<i>MtCHR</i>	Medtr5g097900	5'-TTGGCCACTTAGCTCTCAGC-3' ; 5'-CCATGGATTCCCAAACACCC-3'
<i>MtCHI</i>	Medtr1g115870	5'-CCACCAGGCTCCTCTATCCT-3' ; 5'-ACTGCTGTCTCAACCTCTGG-3'
<i>MtF3H</i>	Medtr3g025230	5'-CACCTTATGGTCCGCGGTG-3' ; 5'-TACCTCTCCTGACGCAAGT-3'
<i>MtFLS</i>	Medtr5g032870	5'-GTGACCAACAATGTGCAACC-3' ; 5'-TTGGGAGGGTGTCTTCAATC-3'
<i>MtFLS</i>	Medtr4g100590	5'-GGTGCCTCTGCTCATTGAGA-3' ; 5'-CCACACCTGAGGTTGCTTCA-3'
<i>MtGAPDh</i>	Medtr3g085850	5'-TGCCCTACCGTCGATGTTTCAGT-3' ; 5'-TTGCCCTCTGATTCTCCTTG-3'
<i>MtRBP1</i>	Medtr6g034835	5'-AGGGGCAAGTTCCTTCATT-3' ; 5'-GGTAGAAGTGCTGGCTCAGG-3'
<i>MtFLSox</i>	Medtr3g072820	5'-ATGGAGGTAGAAGGGTACA-3' ; 5'-TTATTGAGGGATCTTATTA-3'

CHAPTER 3



Bioanalytical Study Using Liquid
Chromatography With Tandem Mass
Spectrometry for the Quantification of
IAA and Its Conjugates



3.1 Introduction

Auxin precursors, conjugates and catabolites have been found to significantly influence several physiological stages during a plant's life cycle, including germination, growth, differentiation, immunity, senescence, tropic and environmental stress responses. Like most other phytohormones, IAA metabolites are usually present at very low concentrations *in planta*, with a typical range of between 0.1 – 50 ng g⁻¹ fresh weight (Davies, 2010, Liu et al., 2013), or 10⁻⁹ M to 10⁻⁶ M (Muller and Munne-Bosch, 2011). Molecular biology has provided semi-quantitative tools for hormone quantitation, such as immunoassays and promoter:reporter systems. However, immunoassays rely on specific antibody-antigen interactions in sample detection, which have led to problems with inconsistent results due to cross-reactivities, and therefore lack validation. On the other hand, the relationship between promoter:reporter signal input and output is not linear, due to the complex pathways involved in between both ends of the signal transduction chain / network. Therefore, developing high-throughput and comprehensive analytical methods are required to reproducibly isolate and accurately quantitate these chemically diverse IAA metabolites, as well as to validate and complement the conclusions derived from classical immuno- and reporter assays. Unfortunately, developing these analytical methodologies is highly challenging, not only due to the chemical diversity of these compounds, but also because some of these analytes are highly unstable and may degrade during extraction and purification procedures. To date, due to their different chemistries and varying concentrations in different plant tissues, most published studies have focussed on only small subsets of these compounds in a given plant tissue (Kai et al., 2007, Mashiguchi et al., 2011, Tam et al., 2000). Novák et al. (2012) successfully profiled a large subset of known auxin precursors and conjugates / catabolites in *Arabidopsis* tissue. Plant tissues are complex biological matrices comprising constituents with different chemistries, such as proteins, carbohydrates, lipids,

pigments and ligands (Villagrasa et al., 2007). Depending on the class(es) of compounds of interest (analytes), the other constituents must be removed from the crude plant extract using suitable solvents to obtain a sufficiently pure sample. If this is achieved, the interfering effects of these constituents plus the solvents (a.k.a. matrix effects) will be minimised during analysis, which may otherwise potentially modify the results (e.g., physical or chemical reactions with the analytes) or produce an enhanced or suppressed response from an instrument detector (Villagrasa et al., 2007).

Mass spectrometry (MS) and nuclear magnetic resonance (NMR) are two techniques conferring superior accuracy for the study of plant hormones (Kueger et al., 2012). These two technologies utilise physico-chemical detectors that can distinguish structurally similar compounds from one another. Due to the very low concentrations of auxins in complex plant extracts, NMR is not suitable as a quantification tool, as it lacks sensitivity. However, NMR is required for comprehensive structural elucidation of compounds, such as determining sugar positions in hormone conjugate identification (Östin et al., 1995). At the turn of the century, MS has emerged as the primary tool for phytohormone analyses (Pan and Wang, 2009). Mass spectrometry is a highly sensitive and selective analytical tool for hormone profiling that can reliably complement immuno- and reporter-based techniques. Coupled with extraction and purification technologies, MS-based analytical methods are highly sensitive and selective for identifying and quantifying plant hormones, such as IAA metabolites.

A mass spectrometer is an analytical instrument where molecules are ionised in an ion source by different kinds of energy sources, depending on the instrument (Ljung et al., 2010). The subsequent masses of the ions produced are detected, and a mass spectrum unique to the compound is generated. The mass spectrum is compared to either a commercial and / or synthesised standard, matching with existing MS libraries (MassBank, Wiley and NIST), if available, or by interpreting

the mass spectra using first principles calculations (Grimme, 2013). Molecules can be ionised in the liquid phase, such as liquid chromatography with electrospray ionisation (ESI), atmospheric pressure chemical ionisation (APCI), or frit-fast atom bombardment (frit-FAB). Alternatively, molecules can be introduced into the ion source in the gas phase, such as gas chromatography with electron ionisation (EI) or chemical ionisation (CI) (Pan and Wang, 2009). Gas chromatography (GC) and gas chromatography-mass spectrometry (GC/MS) were once widely used for IAA metabolite profiling (Engelberth et al., 2003, Schmelz et al., 2004). These techniques are suitable for volatile compounds, and therefore non-volatile hormones would usually have to undergo time-consuming steps of purification and derivatisation (e.g., methylation, silylation, and oximation) in order to increase their volatility and to enhance chromatographic behaviour and sensitivity for analysis. However, high injection temperatures during GC operation pose difficulties for analysing compounds that could be thermally labile (Birkemeyer et al., 2003). High performance liquid chromatography (HPLC) coupled to different detectors (e.g., conventional UV, fluorescence, or photodiode array) is a common technique employed for polar and thermally labile IAA metabolites in plant samples (Dai and Mumper, 2010). However, HPLC alone is usually not sensitive and selective enough for accurate determination of endogenous plant hormones. For instance, interferences by the matrix coextractives with the target HPLC-UV signals may lead to a longer separation analysis time, or a more complex purification procedure (Li et al., 2015).

Like GC/MS, high throughput profiling of phytohormones using LC/MS has become popular and routine these days (Liu et al., 2013, Muller and Munne-Bosch, 2011, Pan et al., 2010). Unlike GC/MS, however, LC/MS involves simple sample preparation, high sensitivity, and can cover a wide range of compound polarities operating under ambient temperatures, with no further need for derivatisation (Pan and Wang, 2009). However, the sensitivity of single mass spectrometers is usually

not high enough for hormone detection in low tissue quantities. Extensive optimisation of sample amount, extraction and purification techniques, as well as optimisation and method development of the chromatographic technique with a mass spectrometer are often required to achieve acceptable levels of sensitivity (Ribnicky et al., 1997). In addition, sample matrix that can coelute with the targeted compounds can cause ionisation suppression / enhancement during the ionisation process in the mass spectrometer, which can affect the quantification data (Gamoh et al., 1996, Novák et al., 2003).

Tandem mass spectrometry (MS/MS) or high resolution mass spectrometry (HRMS) could circumvent the need for extensive purification and other issues encountered by single MS by adding another layer of selection in the analytical process. Examples of tandem mass spectrometers are ion trap, triple quadrupole (QQQ), quadrupole time-of-flight (Q-TOF) and other hybrid instruments (e.g., triple quadrupole system coupled with a quadrupole-linear ion trap). These techniques improve the selectivity and sensitivity of the analysis. Several methodologies for hormone identification and quantification using these modules have been published (Pan and Wang, 2009). A triple-quadrupole mass spectrometer is often used in hormonal profiling due to its high selectivity (Muller and Munne-Bosch, 2011, Pan et al., 2010). The first quadrupole (Q_1) serves as a mass analyser to select the specific parent (precursor) ion(s) unique to each target compound whilst filtering out interfering ions; Q_2 acts as a collision cell to break the precursor ions selected in Q_1 into fragments; Q_3 is a second mass analyser that detects the product ions produced from the fragmentation of the parent ion from Q_2 . The terms selected reaction monitoring (SRM) or multiple reaction monitoring (MRM) are often used for triple-quadrupole instruments, because they monitor precursor-to-product ion pairs, providing superior sensitivity and selectivity during analysis (Pan et al., 2010).

The roles of auxin in growth, development and tropic responses in *Arabidopsis* have been studied extensively (Ljung, 2013, Overvoorde et al., 2010). However, less is known about how auxin regulates nodulation in legumes. The most abundant form of active auxin in most land plants appears to be indole-3-acetic acid (IAA). Indole-3-acetic acid can be conjugated to amino acids, of which their functions are still open to investigation (Korasick et al., 2013). In *M. truncatula*, there is currently no study showing the direct detection of these conjugates, nor any study investigating the changes in auxin concentrations during nodulation. Enzyme feeding assays suggest the presence of IAA-Alanine, IAA-Phenylalanine, IAA-Aspartate, IAA-Leucine, IAA-Isoleucine, and IAA-Valine in *M. truncatula* (Campanella et al., 2008). Auxin conjugates have been postulated to serve various functions, for instance, as storage compounds, degradation intermediates and auxin antagonists (Korasick et al., 2013, Ludwig-Müller, 2011). Investigating the changes in auxin concentrations during nodulation will potentially give new insights into the roles of auxin / auxin conjugates during nodulation, and plant development in general.

The objectives of this chapter were: (1) to validate the IAA extraction and purification procedure published by Muller and Munne-Bosch (2011); (2) to develop and validate fast and accurate HPLC-MS/MS methods using electrospray ionisation (ESI) with Q-TOF MS technology for IAA metabolites and flavonoids and; (3) to apply these methods to identify and quantify IAA metabolites and flavonoids in root tissues of *M. truncatula* (as discussed in subsequent chapters, respectively). The primary focus of this thesis was to investigate the role of local auxin concentration changes during nodule development, with a secondary aim of elucidating the interaction between auxin and flavonoids as endogenous modulators of auxin transport.

3.1.1 Extraction and purification procedures

The first step in any analytical study involving identifying and / or quantifying IAA and IAA conjugates / catabolites is sample preparation, where, if a large amount of sample is used, homogenisation is often performed by grinding the frozen plant material using a mortar and pestle. When only small amount of plant tissue is available, homogenisation can be more conveniently performed directly in tubes using ball grinders (Ernst et al., 2014). During homogenisation and extraction, the plant tissue must be kept at ≤ 4 °C to prevent enzymatic or chemical degradation of the plant hormones. Antioxidants, such as diethyldithiocarbamic acid (DIECA), may also be added to prevent enzymatic metabolism of the hormones (Jackson et al., 2002). One or more internal standards (e.g., D5-IAA, $^{13}\text{C}_6$ -IAA, $^{13}\text{C}_8$, $^{15}\text{N}_1$ -IBA) are often added to the biological material, either prior to or after plant hormone extraction and derivatisation (Novák et al., 2012). Internal standards are needed for the final quantitative analysis of plant hormones (Castillo et al., 2011), account for losses of analytes during the extraction, purification and instrumental analysis, as well as to aid in determining the recovery efficiency of the extraction method. The internal standard is preferably similar in chemical structure and mimics the behaviour of the targeted endogenous analytes during extraction and purification. They could be a radiolabelled / stable isotope or an analogue compound, but must not occur naturally in the plant. Following homogenisation and internal standard(s) addition, an appropriate extraction solvent is added to the plant sample. The extraction solvent(s) used must efficiently isolate most of the target analytes away from the interfering substances (e.g., carbohydrates, proteins, pigments) from the plant sample that could contribute to matrix effects during analysis (Ljung et al., 2010). Methanol, methanol / water, acetonitrile / water / formic acid mixtures or neutral pH buffers (e.g., 50 mM sodium phosphate) are common solvents used for auxin extraction (Pan et al., 2010). The extraction period should be long enough to allow the internal standard to equilibrate with the endogenous analytes in the plant

matrix, and then to subsequently extract most of the analytes from the medium. If the extraction period is too long, the analyte may degrade, or increase the chances of hydrolysing the hormone conjugates into free hormones in the resultant extract.

The sample extract may further undergo another step of purification (e.g., solid phase extraction (SPE), preparative HPLC or immunoaffinity chromatography) prior to analysis (Ernst et al., 2014). Purification techniques, such as solvent partitioning and preparative HPLC are often sufficiently replaced by SPE methods alone. Examples of SPE columns with silica-based packing material include octadecyl carbon chain bonded silica (C18), strong ion exchange (SAX, SCX) and silica (Si). Target analytes are bound to the SPE column by retention-chemical interactions (e.g., non-polar, polar or ionic) with the solid stationary phase. A suitable solvent is used to wash off the interfering substances before applying a stronger solvent to elute the analytes off the column for analysis (Huie, 2002).

3.1.2 Muller and Munne-Bosch (2011) extraction and purification method

For our purpose, we chose an extraction method reported in Muller and Munne-Bosch (2011). A flow diagram describing the extraction protocol is shown in Figure 3.1. For their phytohormonal profiling of abscisic acid (ABA), salicylic acid (SA), indole-3-acetic acid (IAA) and gibberellins (GAs - GA₄, GA₉) in rosemary leaves, the authors used methanol:isopropanol:glacial acetic acid, 20:79:1 (v/v/v) as the preferred solvent extraction mixture. The reported recoveries for these analytes were > 80 %.

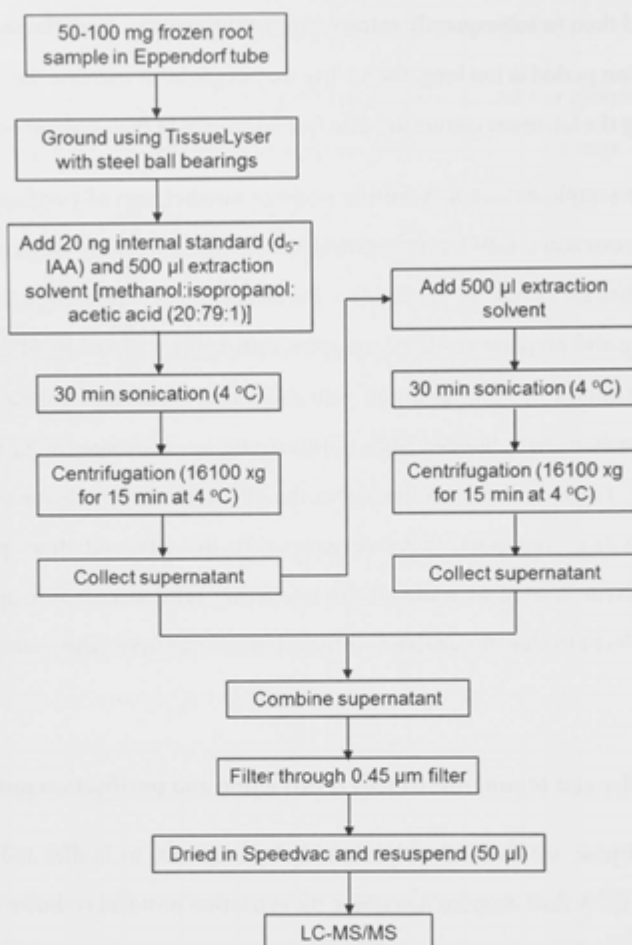


Figure 3.1 Flow diagram describing the extraction protocol adapted from Muller and Munne-Bosch (2011) in this study.

3.1.3 Optimisation, method development and validation of the Agilent 1200 series HPLC and 6530 Accurate-Mass Q-TOF

For our study, IAA and IAA conjugates were identified and quantified using an Agilent 1200 series HPLC and a 6530 Accurate-Mass Q-TOF LC/MS (Agilent Technologies, Inc. Santa Clara, USA). Standards and samples were subjected to

pneumatic electrospray ionisation (ESI) dual spray Jet Stream ion source interface, in both positive and negative ion polarities after separation on an Agilent ZORBAX Eclipse XDB-C18 column (2.1 × 50 mm; 1.8 μm). Figure 3.2 shows a schematic diagram of the ESI-Q-TOF system used at the Mass Spectrometry Facility, Research School of Biology, The Australian National University.

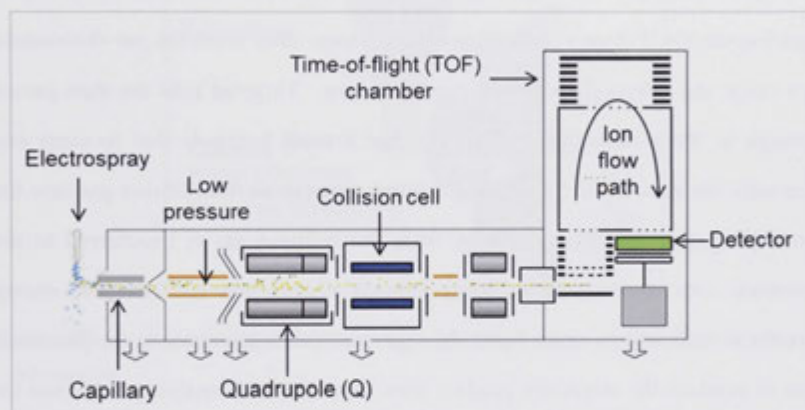


Figure 3.2 Schematic diagram describing major components of the Agilent 6530 ESI-Q-TOF system. Image was adapted from Agilent technologies.

Electrospray ionisation (ESI) is regarded as a soft ionisation technique, which utilises strong electrical fields to produce charged gas phase ions. The LC effluent is subjected to a high voltage as it exits through the nebulising needle which is set at ground potential (Figure 3.3). The LC liquid phase, which contains the IAA and IAA conjugate analytes, sprays into the source chamber from the nebuliser needle that is surrounded by a counter electrode, where high voltage is applied. The potential difference between the counter electrode and the nebulising needle creates a strong electric field that charges the surface of the emerging LC liquid to form a fine ionising spray of charged droplets (aerosols). The evaporation process is assisted by the application of high pressure and super-heated sheath nitrogen gas.

As the evaporated droplets move towards the dielectric platinum-plated capillary sampling orifice, counter-flow heated nitrogen drying gas removes uncharged particles and solvent, while continuing to repeatedly shrink the droplets until the repulsive electrostatic forces exceed the droplet surface tension to bring about droplet explosions (Figure 3.2 and 3.3). The gas-phase charged ions are transmitted through the capillary into the low atmospheric pressure region of the ion source, and then eventually into the higher vacuum region of the first MS analyser (quadrupole, Q) (Figure 3.2). The quadrupole mass filter scans the pre-determined m/z range and selects the targeted precursor ions. Targeted ions are then passed through to the collision cell, which also has a small hexapole that focusses and transmits the ions, while introducing neutral nitrogen as the collision gas into the ion flight path. The kinetic energy from the collision gas is transferred to the precursor ions to promote collision induced dissociation (CID). The energy transfer is sufficient to cause bond cleavages and rearrangements in the precursor ions to produce the respective product ions unique to each analyte. Precursor-to-product ion formation can be represented by the following equation:



Finally, fragmented ions generated in the collision cell enter the time-of-flight (TOF) chamber, where they are subjected to a fixed electric field and travel a known distance. The speed at which an ion travels is inversely proportional to its mass-to-charge (m/z) ratio. At the end of the flight path, a detector recognises and amplifies the signal, which is then converted into a mass spectrum.

The Agilent 6530 Accurate-Mass Q-TOF can operate in three operational modes, as explained in Table 3.1.

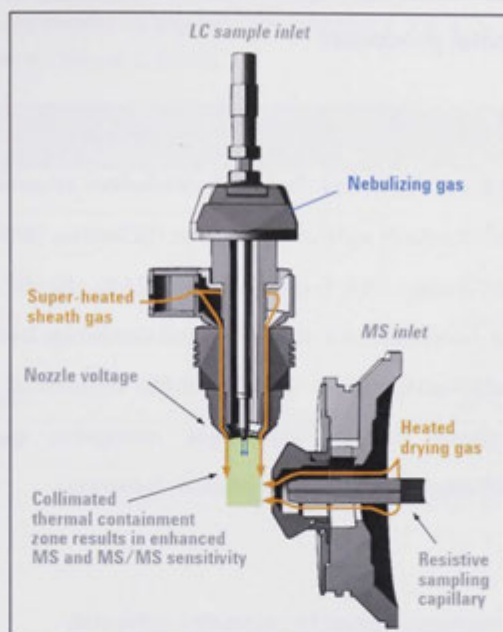


Figure 3.3 Components of an Agilent Jet Stream electrospray. Image taken from Agilent Technologies.

Table 3.1 Agilent 6530 Accurate-Mass Q-TOF acquisition modes.

Total transmission ion (TTI) mode	All ions are passed through the quadrupole (which is in the TTI mode) to the TOF. No voltage difference. No collision energy applied in the collision cell, so only low energy collision occurs. Time-of-flight performs as a stand-alone mass analyser providing high resolution data.
Product ion scan auto MS/MS	The software algorithm automatically selects the precursor ions (based on the highest ions detected) and fragments them. Signal-to-charge is compromised as this is used for method development or identification of unknown compounds.
Product ion scan targeted MS/MS	The quadrupole is directed to pass pre-selected precursor ions only into the collision cell. The TOF analyses all the resulting product ions. This sensitive mode is used for quantitative analysis, identification of known analytes and structural elucidation.

Therefore, for our auxin analyses, we were only interested in the TTI (full scan MS) and targeted MS/MS modes.

3.2 Experimental procedure

3.2.1 Chemicals

Table 3.2 and 3.3 list auxin and flavonoid metabolites targeted in this study. Commercial auxin standards were obtained from OlChemim (IAA-Phenylalanine, IAA-Leucine, IAA-Valine, IAA-Tryptophan, 4-Cl-IAA), Sigma (IAA-Aspartate, IAA-Alanine, IAA-Isoleucine, IAA, IBA, PAA) and Cambridge Isotope laboratories (Indole-2,4,5,6,7-d5-3-acetic acid). For flavonoids, commercial standards were obtained from Sigma (luteolin, kaempferol, naringenin, quercetin, morin, hesperetin), Fluka (apigenin) and ICN biomedical (genistein).

Table 3.2 Auxin compounds targeted for investigation in this study.

Auxin compound	Molecular formula	Molecular weight (g mol ⁻¹)
Indole-2,4,5,6,7-d5-3-acetic acid (D5-IAA)	C ₁₀ H ₄ D ₅ NO ₂	180.21
Indole-3-acetic acid (IAA)	C ₁₀ H ₉ NO ₂	175.19
Indole-3-butyric acid (IBA)	C ₁₂ H ₁₃ NO ₂	203.24
Phenylacetic acid (PAA)	C ₈ H ₈ O ₂	135.05
4-chloro-indole-3-acetic acid (4-Cl-IAA)	C ₁₀ H ₈ ClNO ₂	208.02
Indole-3-acetyl-alanine (IAA-Ala)	C ₁₃ H ₁₄ N ₂ O ₃	246.27
Indole-3-acetyl-aspartate (IAA-Asp)	C ₁₄ H ₁₄ N ₂ O ₅	290.28
Indole-3-acetyl-leucine (IAA-Leu)	C ₁₆ H ₂₀ N ₂ O ₃	288.35
Indole-3-acetyl-isoleucine (IAA-Ile)	C ₁₆ H ₂₀ N ₂ O ₃	288.35
Indole-3-acetyl-phenylalanine (IAA-Phe)	C ₁₉ H ₁₈ N ₂ O ₃	322.37
Indole-3-acetyl-tryptophan (IAA-Trp)	C ₂₁ H ₁₉ N ₃ O ₃	361.40
Indole-3-acetyl-valine (IAA-Val)	C ₁₅ H ₁₈ N ₂ O ₃	274.32

Table 3.3 Flavonoid metabolites targeted for investigation in this study, based on flavonoid aglycones identified in Farag et al. (2007).

Flavonoid compound	Molecular formula	Molecular weight (g mol ⁻¹)
Luteolin	C ₁₅ H ₁₀ O ₆	286.24
Kaempferol	C ₁₅ H ₁₀ O ₆	286.24
Naringenin	C ₁₅ H ₁₂ O ₅	272.26
Quercetin	C ₁₅ H ₁₀ O ₇	302.24
Morin	C ₁₅ H ₁₀ O ₇	302.24
Hesperetin	C ₁₆ H ₁₄ O ₆	302.27
Genistein	C ₁₅ H ₁₀ O ₅	270.24
Apigenin	C ₁₅ H ₁₀ O ₅	270.24

3.2.2 Optimisation of the LC-ESI-Q-TOF

Liquid chromatography-tandem mass spectrometry (LC-MS/MS) is regarded as an effective and sensitive analytical technique to study auxin metabolites. To optimise the LC-ESI-Q-TOF, we used a 2 µg mL⁻¹ standard mixture of all the auxin analytes, including the D5-IAA internal standard (Table 3.2). Parameters of both ion polarities (positive and negative) were optimised to enhance sensitivity for the better detection of these analytes. As reported and discussed later in more detail, some analytes were more sensitive in one polarity than the other. We compared acetonitrile and methanol gradients, with and without formic acid or acetic acid as additives. In order to further improve the sensitivity in the negative mode, we also compared post-column addition via a T-piece of ammonium hydroxide, 2,2,2-trifluoroethanol, 2,2,3,3,3-pentafluoro-1-propanol, triethylamine acetic acid or formaldehyde. Other LC parameters optimised included column temperatures and flow rates. With respect to the MS, we optimised the ESI dual spray Jet Stream Q-TOF parameters, i.e. fragmentor voltage, sheath gas temperature, nebuliser pressure, etc., as outlined in Figure 3.12. Once both ion polarities were optimised, calibration

standards (0.01, 0.05, 0.1, 0.5, 1.0, 2.0 and 5.0 ng μL^{-1} with the internal standard fixed at a known concentration of 0.4 ng μL^{-1}) were analysed to determine the linear regressions, correlation coefficients, limits of detection (LOD, $3 \times S/N$), and limits of quantification (LOQ, $5 \times S/N$) for each hormone analyte. It is from optimising these specific parameters that we achieved the sensitivity we needed for the detection of trace plant IAA metabolites in the small amounts of plant tissues used.

3.2.3 Extraction recovery experiment

Commercial auxin standards were used to assess reproducibility and extraction recoveries of the extraction protocol from Muller and Munne-Bosch (2011). As shown in Figure 3.4, approximately 2 g of *M. truncatula* roots were pooled and snap-frozen immediately in liquid nitrogen to inhibit enzymatic degradation of auxins. The frozen root sample was then ground, using a pre-cooled mortar and pestle, in liquid nitrogen. The homogenised, ground sample was subsequently equally subdivided into two sets ($n=5$) in 2 mL Eppendorf tubes. One set was labelled as "spiked", and the other "unspiked", with ~ 100 mg accurately weighed tissue in each tube. To the samples labelled "spiked" 20 μL of 2.5 $\mu\text{g ml}^{-1}$ auxin standard mix and 20 μL of 1 $\mu\text{g mL}^{-1}$ D5-IAA internal standard were added. To the samples labelled "unspiked" only 20 μL of 1 $\mu\text{g mL}^{-1}$ D5-IAA was added. In addition, five laboratory control blanks (empty 2 mL Eppendorf tubes) were also conducted in parallel to the plant samples to assess any cross contamination during the extraction procedure. Next, 500 μL of methanol:isopropanol:glacial acetic acid, 20:79:1 (v/v/v) extraction solvent was added into each tube. Subsequent steps in the modified Muller and Munne-Bosch (2011) protocol were followed (Figure 3.1). To calculate the recovery of each analyte, the following equation was applied:

$$\text{Recovery (\%)} = [(\text{spiked amount} - \text{unspiked amount}) / \text{spiked amount}] \times 100 \%$$

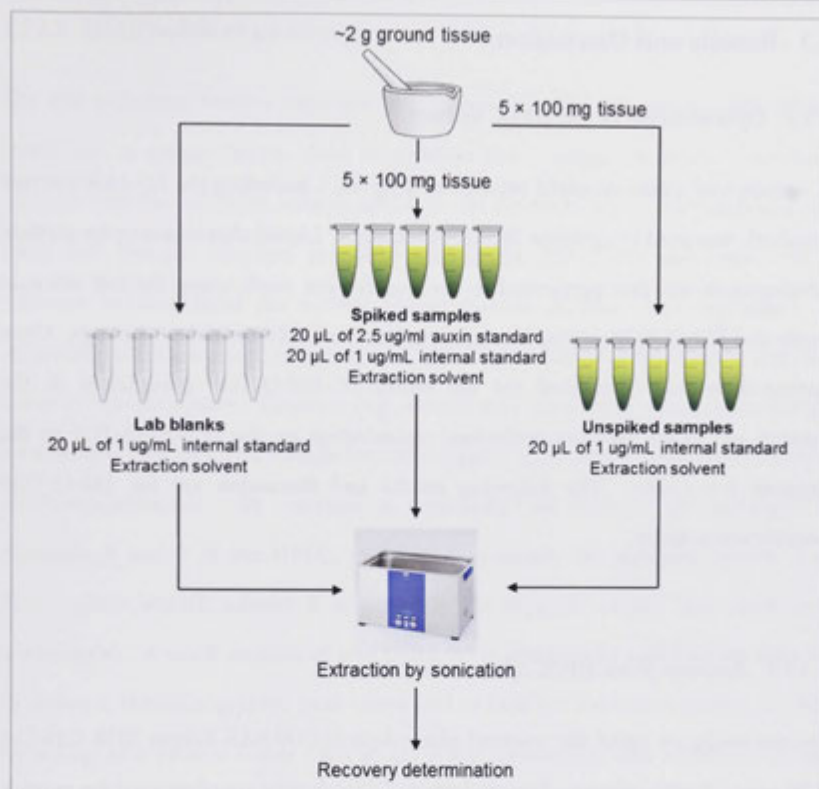


Figure 3.4 Schematic diagram describing the experimental design for determining the extraction efficiency of the modified extraction protocol from Muller and Munne-Bosch (2011), as shown in the flow diagram above (Figure 3.1).

3.3 Results and Discussion

3.3.1 Optimisation of the HPLC system

A commercial auxin standard mixture of $2 \mu\text{g mL}^{-1}$, including the D5-IAA internal standard, was used to optimise the LC parameters. Liquid chromatography method development was first performed in the positive ion mode using the full MS scan mode and ESI-Q-TOF parameters were Agilent Technologies default settings. Once optimisation was completed for the entire LC-ESI-Q-TOF parameters in the positive ion mode, we then performed optimisation on the LC-ESI-Q-TOF in the negative ion mode. The following results and discussion are for ESI-Q-TOF positive ion polarity.

3.3.1.1 Reversed-phase HPLC column selection

For our study, we opted the reversed-phase Agilent ZORBAX Eclipse XDB-C18 ($2.1 \times 50 \text{ mm}$, $1.8 \mu\text{m}$) column. Reversed-phase C18 columns are often used for peptide and small molecule (e.g., auxins) separation, where the stationary phase is generally comprised of hydrophobic alkyl chains ($-\text{CH}_2-\text{CH}_2-\text{CH}_2-\text{CH}_3$) that interact with the analytes by retaining and separating them according to their degree of hydrophobicity (Itoh et al., 1993). Compounds tend to be retained on the reversed-phase column in high aqueous mobile phase and then eluted from the column using high organic mobile phase. The Agilent ZORBAX Eclipse XDB-C18 ($2.1 \times 50 \text{ mm}$, $1.8 \mu\text{m}$) reversed-phase column offers high performance over a wide pH range (pH 2-9) by providing good peak shape, rapid compound separation due to its short length, high resolution chromatograms and a low internal diameter to enhance MS response (Mack, 2011). These columns are extra densely bonded and double end-capped to cover as many active residual silanols as possible, which would otherwise cause peak tailing at mid pH region.

3.3.1.2 HPLC mobile phase solvents

The ESI technique ionises relatively high polar molecules by spraying the mobile phase into a strong electric field to produce fine charged droplets. Therefore, solvents with low viscosity, volatile salts that can dissolve polar compounds and can form fine charged droplets, are only suitable for ESI (Cech and Enke, 2001). Solvents recommended for mobile phases include alcohols (e.g., methanol, 2-propanol), polar aprotic (e.g., acetonitrile, dimethyl sulfoxide, ethyl acetate, acetone), water or volatile aqueous solutions (e.g., formic acid, acetic acid, ammonium acetate, ammonium formate), and volatile ion pair reagents (e.g., dibutyl ammonium acetate, perfluorocarbonate). By convention, reversed-phase solvents are installed on channels A and B of the HPLC. Solvent A is usually the aqueous solvent (e.g., HPLC-grade water); solvent B is generally the organic solvent (e.g., methanol, acetonitrile). A small amount of acid (~ 0.1 %) is also usually added to the solvents to improve chromatographic peak shape and to facilitate ionisation during LC/MS, by acting as a proton donor (Wu et al., 2004). Common acid additives include formic acid, acetic acid and trifluoroacetic acid, although the latter is commonly avoided in Q-TOF because it has been reported to cause ion suppression during MS ionisation (Annesley, 2003, Chan et al., 2012).

Methanol (protic) and acetonitrile (aprotic) are the two most common organic mobile phases used in reversed-phase HPLC. We compared methanol and acetonitrile with 0.1 % formic acid to determine best chromatographic performance. For solvent A, we used HPLC grade water with 0.1 % formic acid. Acetonitrile, due to its lower viscosity, has higher ESI ionisation efficiency than methanol (Herrera et al., 2008). In aqueous mixtures (i.e. acetonitrile or methanol mixed with water), acetonitrile tends to have higher elution strength than methanol as well (Gilar et al., 2014). However, the elution strength of methanol is higher when the organic composition gets closer to 100 %. As a result of this knowledge, it was important that we compared these organic solvents on our LC-ESI-Q-TOF performance. We

validated that methanol gave rise to better peak signals for D5-IAA, IAA and IBA, in accordance with previous reports that favoured methanol as the solvent of choice for IAA metabolite analysis (Figure 3.5) (Durgbanshi et al., 2005, Kallenbach et al., 2009, Ma et al., 2008). Our primary compound of interest, IAA, had a four-fold higher peak height signal in methanol in comparison to acetonitrile. Indole-3-butyric acid had nearly a 20-fold improvement in detection sensitivity in methanol. We then varied methanol composition with water such as 50/50, 70/30, 90/10 methanol/water (v/v), and found that the composition 90/10 provided better separation, peak shape and signal.

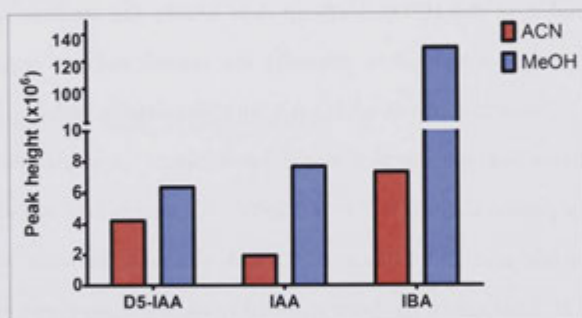


Figure 3.5 Peak heights of auxins detected in acetonitrile or methanol with 0.1 % formic acid as the mobile phase B. Mobile phase A was water with 0.1 % formic acid. Higher peak height corresponds to enhanced sensitivity. Abbreviations: ACN, acetonitrile; MeOH, methanol.

Next, we compared the effects of different acid additives on chromatographic performance. Formic acid and acetic acid, two widely used additives that are known to aid in improving compound separation, peak shape and protonation in LC/MS (Durgbanshi et al., 2005, Ma et al., 2008), were compared. Mobile phase A was water with 0.1 % acid and mobile phase B was 90% methanol/water with 0.1 % acid. Among the eight auxin compounds tested, five

(IAA, IBA, IAA-Asp, IAA-Phe and IAA-Trp) were better detected in 0.1 % formic acid, whereas the internal standard D5-IAA had similar detection sensitivity with either 0.1 % formic acid or acetic acid (Figure 3.6), suggesting that 0.1 % formic acid is a better overall option for further method development. Formic acid has a lower molecular weight than acetic acid and during negative ion analysis, these lower molecular weight deprotonated molecules and deprotonated dimers will cause less interferences (Annesley, 2003, McMaster, 2005). Furthermore, commercial formic acid solvents generally contain much less contaminants than acetic acid mobile phases. Solvent purity (HPLC or LC/MS grade) is particularly crucial during sensitive LC/MS analysis.

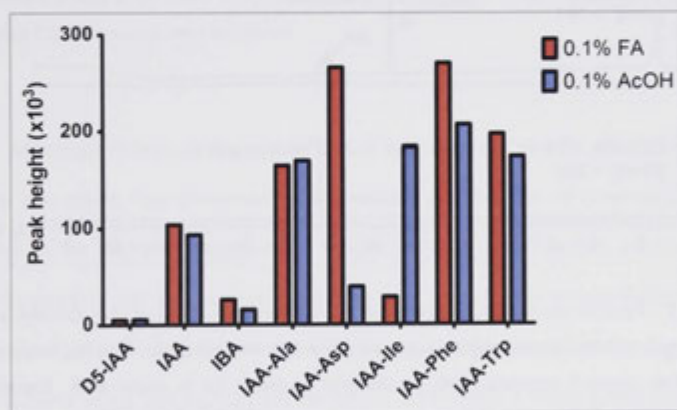


Figure 3.6 Peak heights of auxins detected in 0.1 % formic acid or 0.1 % acetic acid as the additive in mobile phases A (water) and B (90 % methanol/water). Higher peak height denotes enhanced sensitivity. Abbreviations: FA, formic acid; AcOH, acetic acid.

In addition, we found that acetic acid is an inferior acid for chromatographic peak shape and elution selectivity. A comparison of 0.1 % formic acid or acetic acid as the additive for the mobile phases suggested that formic acid was the better

option for fully resolving D5-IAA and IAA, which eluted within seconds of each other. Using acetic acid resulted in unresolved D5-IAA and IAA peaks (Figure 3.7) but Gaussian (bell-curve) and baseline resolved peaks were attained with formic acid (Figure 3.8). Our preferred solvent system for ESI LC/MS was: Solvent A - HPLC grade water with 0.1 % formic acid; Solvent B - HPLC grade 90 % methanol / water with 0.1 % formic acid.

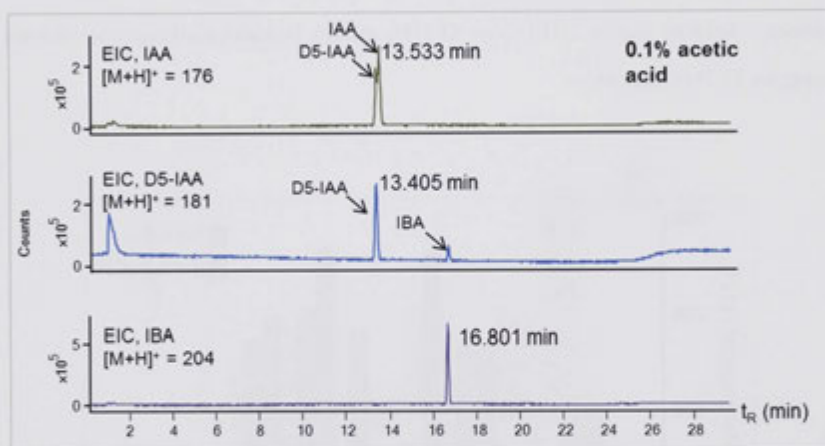


Figure 3.7 Positive ion mode extracted ion chromatograms (EIC) of IAA, D5-IAA and IBA. Chromatograms show peak height counts on the y-axis and retention time (t_R , min) on the x-axis. Mobile phase B consists of 90 % methanol / water + 0.1 % acetic acid. Extracted ion chromatogram for IAA shows IAA peak unresolved from D5-IAA peak.

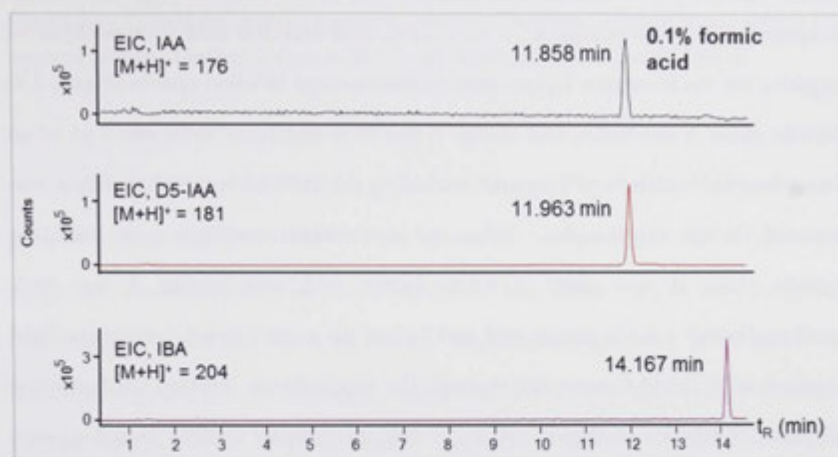


Figure 3.8 Positive ion mode extracted ion chromatograms (EIC) of IAA, D5-IAA and IBA. Chromatograms show peak height counts on the y -axis and retention time (t_R , min) on the x -axis. Mobile phase B consists of 90 % methanol / water + 0.1 % formic acid. Full resolution of IAA and D5-IAA peaks was achieved.

Although formic acid and acetic acid are common mobile phase additives in positive ion mode, less information is available for the use of common, versatile additives in the opposite negative ion mode. As mentioned earlier, acids are often added to positive ion ESI to provide a source of protons for reversed-phase HPLC (Wu et al., 2004). By logic, bases would serve as suitable modifiers for negative ion ESI to achieve good ESI LC/MS performance. However, a study using ammonium hydroxide as a basic modifier yielded poor detection limits and less sample stability in methanolic or aqueous solutions (Cech and Enke, 2001). On the other hand, fluorinated solvents like 2,2,2-trifluoroethanol were reported to improve negative ion ESI response (Cech and Enke, 2001). To select a potentially more suitable modifier for negative ion ESI targeted MS/MS, we performed some quick experiments following Wu et al. (2004) experimental design of post-column infusion of several acidic and basic modifiers, including water, 1 mM ammonium hydroxide, 100 mM 2,2,2-trifluoroethanol, 100 mM 2,2,3,3,3-pentafluoro-1-

propanol, 0.01 % triethylamine, 1 mM acetic acid and 100 mM formaldehyde in negative ion mode using a T-piece post-column syringe infusion system (Figure 3.9). Mobile phase A was water, and mobile B was 90 % methanol/water and 7 μL of an auxin standard mixture of 1 $\mu\text{g mL}^{-1}$, including the D5-IAA internal standard, was injected via the autosampler. When no post-column modifiers were used, the mobile phase A was water + 0.1 % formic acid, and mobile B was 90 % methanol/water + 0.1 % formic acid and 7 μL of the same 1 $\mu\text{g mL}^{-1}$ auxin standard mixture with D5-IAA were run through the post-column infusion configuration (Figure 3.9; labelled in Figure 3.10 as "None") to compare results. In some cases, modifiers marginally improved detection of auxin compounds. Ammonium hydroxide (1 mM), for example, increased ESI⁻ responses for D5-IAA, IAA, IBA and PAA (Figure 3.10). In general, however, the detection sensitivity of auxin compounds was quite comparable with or without additional modifiers. We therefore opted to proceed with future analyses without a post-column modifier.

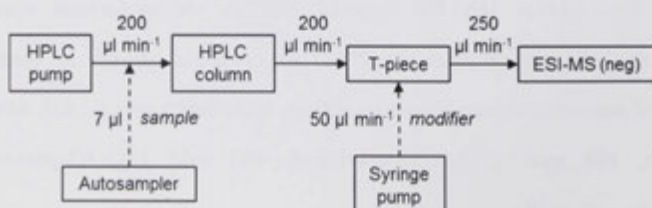
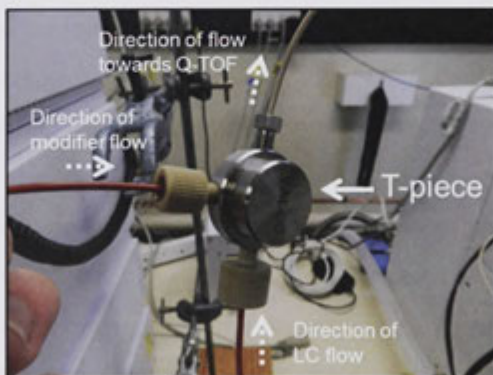


Figure 3.9 T-piece set up for post-column infusion of modifiers for negative ion polarity ESI targeted MS/MS. (A) Photo of actual set-up; (B) Schematic diagram of the set-up.

We are aware that this was not an exhaustive investigation of the effects of post-column modifiers on ESI⁻ MS performance. For example, we did not test a range of concentrations for each modifier, but rather chose the optimum concentration based on Wu et al. (2004). The authors, however, investigated the effects of negative ESI on androgen compounds that do not have acidic functional groups, and therefore, very different in chemical properties to auxins and thus reacted differently with the modifiers tested. In addition, they stated in their study that formic acid suppressed ionisation, while in our normal LC/MS configuration (without post-column infusion system), we found that formic acid used in negative ESI provided enhanced sensitivity for the detection of many IAA conjugates. Formic acid is a weak acid that has a small anion molecular volume (HCOO^- , 37.74 Å) with high gas-phase proton affinity, unlike acetic acid (CH_3COO^- , 54.97 Å). As all auxins have a carboxylic acid group, formic acid would likely retain them longer during reversed-phase HPLC and therefore, improve their separation and negative ESI response. However, in the future, it would be interesting to perform a more detailed survey of different modifiers on negative ESI response, particularly when the method can be potentially expanded to include analysis of different classes of plant hormones.

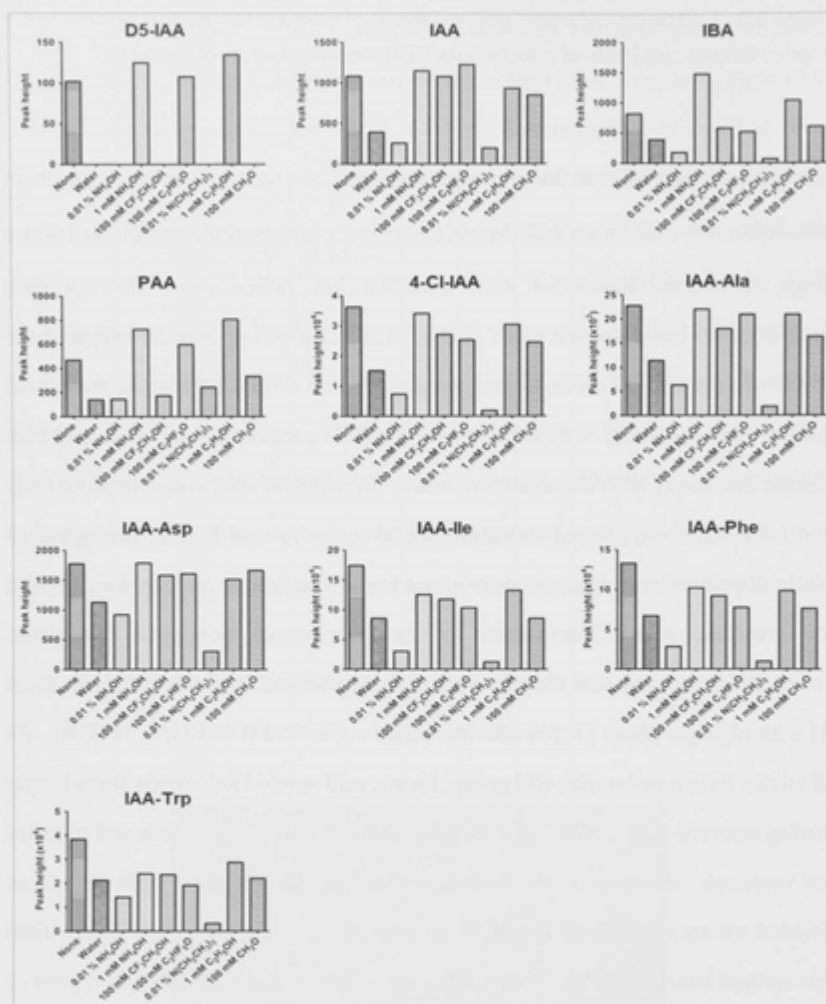


Figure 3.10 Effect of post-column modifiers on negative ion ESI targeted MS/MS. Histograms show raw peak height counts on the y-axis and different modifiers on the x-axis. Different auxin compounds were better detected with different post-column modifiers. Key: NH_4OH , ammonium hydroxide; $\text{CF}_3\text{CH}_2\text{OH}$, 2,2,2-trifluoroethanol; $\text{C}_2\text{HF}_5\text{O}$, 2,2,3,3,3-pentafluoro-1-propanol; $\text{N}(\text{CH}_2\text{CH}_3)_3$, triethylamine; $\text{C}_2\text{H}_5\text{OH}$, acetic acid; CH_2O , formaldehyde.

3.3.1.3 HPLC column temperature

Column temperature is an essential parameter of HPLC. Peak retention time shift due to fluctuations in ambient temperature is common (Barwick, 1999). To circumvent this problem, many HPLC systems have controlled-temperature compartments. Besides maintaining a constant temperature to be able to reproduce peak retention times, column temperature can affect chromatographic separation. The temperature operation range of individual columns differs and extreme temperatures may not be suitable for some columns (Barwick, 1999). The column used in this study can tolerate temperatures up to 90°C. Higher temperature results in more rapid elution and sharper peaks, but may shorten column lifetime due to the deterioration of the stationary phase.

We selected the optimum column temperature based on the detection sensitivity of the auxin compounds. The column temperature range investigated was between 30-50 °C. Higher temperatures resulted in more rapid compound elution and better separation. However, the higher or lower temperatures tested favoured detection of different subset of auxin compounds. We therefore opted for a compromise of 35 °C in the positive ion polarity, which conferred the best detection sensitivity for IAA (Figure 3.11), which is also our primary compound of interest, and most other auxin compounds. In the negative polarity, it was a straightforward selection of 35 °C due to maximal sensitivity of all but one compound (IAA-Trp) at this temperature.

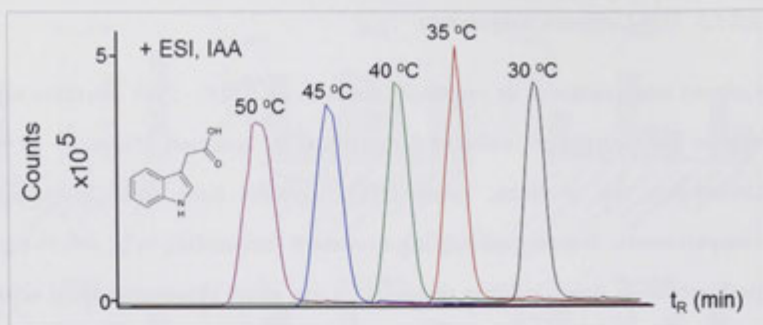


Figure 3.11 Column temperature selection of auxin compounds. Graph shows raw peak height counts on the y-axis and retention time (t_R , min) on the x-axis. Chromatogram shows an example of the column temperature selection for IAA in the positive ion polarity. Detection sensitivity is proportional to peak height. Most auxin compounds analysed have an optimum column temperature close to 35°C. Analytes eluted faster at higher column temperatures, as indicated by the shorter retention times as temperature increased.

3.3.1.4 HPLC gradients and flow rates

Optimisation of HPLC gradient would serve to provide sufficient separation of compounds within the least amount of time possible. When large numbers of samples are involved, a shortened sample run would greatly improve the efficiency of the whole analytical process. At the start of the run, typically a low organic solvent (higher solvent A composition) is run through the column. Due to the relatively less polar nature of auxins, they can be retained on the C18 stationary phase (Ljung et al., 2010). As the organic solvent B composition increases, auxins are eluted from the stationary phase due to the increasingly favourable interaction with the high organic mobile phase. We compared several elution gradients in search for an optimal gradient that would provide separation, resolution and good peak shape of IAA and its conjugates. The mobile phase A was water + 0.1 % formic acid, and mobile phase B was 90 % methanol/water + 0.1 % formic acid. Aliquots of 7 μL of the 1 $\mu\text{g mL}^{-1}$ auxin standard mixture with D5-IAA were repeatedly injected. We varied the start of the gradient at 10 or 15 % B at 0 min, steadily took the

gradient to either 70 or 80 % B to ensure everything was eluted from the column, and determined the run time between 30 and 40 min to observe when the last peak eluted to subsequently shorten the run time, if possible. The optimal gradient conferring total compound separation and good chromatographic peaks was determined to be a linear gradient from 10-50 % solvent B over 8 min, 50-70 % solvent B from 8-12 min (then held at 70 % from 12-20 min) at a flow rate of 200 $\mu\text{l min}^{-1}$. All compounds were eluted between 8-18 min. Total run time was 30 min. Note that the starting composition of solvent B was not 0 % because this would cause the C18 alkyl chains to repel from the high polar aqueous mobile phase and “collapse” (Bidlingmeyer and Broske, 2004). This would result in inefficient binding of analytes to the stationary phase.

For 2.1 mm diameter reversed-phase columns, such as the one used in our study, the typical flow rate is 200 $\mu\text{l min}^{-1}$. A flow rate at 160 $\mu\text{l min}^{-1}$ gave rise to broad, poor chromatographic peak shapes and lower peak height counts. Minor, poor peak shapes occurred at 180 $\mu\text{l min}^{-1}$ flow rate, although peak heights were similar to the 200 $\mu\text{l min}^{-1}$ flow rate. We opted for 200 $\mu\text{l min}^{-1}$ flow rate because it was the most sensitive and produced Gaussian peaks. Higher flow rates have the potential of increasing work efficiency by reducing run times, without compromising chromatographic peak performance (Cabo-Calvet et al., 2014), but might also increase the back pressure load on the system and cause leaks. However, future trials of highly porous monolith HPLC columns can overcome this issue by allowing much higher flow rates without increasing backpressure significantly (Svec, 2010).

3.3.2 Optimisation of the ESI-Q-TOF

3.3.2.1 Optimisation of the Agilent ESI Jet Stream Ion Source

Optimisation of the Agilent ESI Jet Stream ion source and Q-TOF were performed according to manufacturer's suggestion, as outlined in Figure 3.12. The sheath gas temperature, sheath gas flow, nebuliser pressure, capillary voltage, nozzle voltage, drying gas temperature and drying gas flow were sequentially investigated to obtain optimised conditions to maximise detection sensitivity of all auxin compounds. The test range and increments investigated are shown in brackets next to each parameter. The function of each component in the ESI Jet Stream Q-TOF is detailed in Table 3.4. For each parameter tested, an average value was selected because each auxin compound had a different optimal detection condition. Whilst quantification is based on peak area, to enhance sensitivity, optimisation was based on peak height. Detection in the positive and negative full MS scan modes displayed different optimal values for each ESI Jet Stream source component and therefore, Table 3.5 summarises the optimised conditions for both ion polarities.

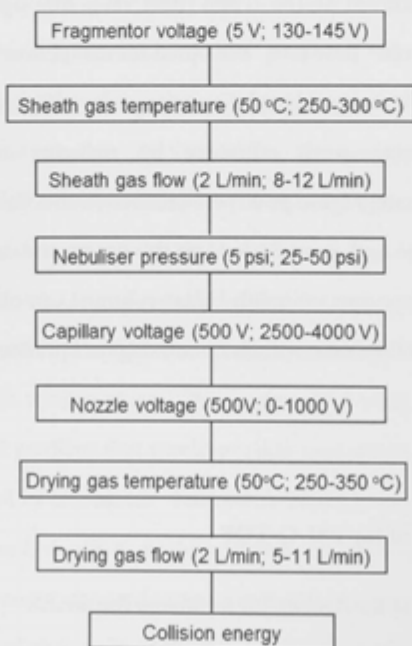


Figure 3.12 Work flow for the optimisation of the ESI Jet Stream ion source and the Q-TOF.

Table 3.4 Function of each component of the ESI Jet Stream ion source.

ESI Jet Stream Source component	Function/Description
Sheath gas temperature / flow	Sets the temperature and flow rate of the nitrogen drying gas and depends on the LC flow rate. Confines the nebulizer spray to more effectively dry and desolvate ions and concentrate them in a thermal confinement zone
Nebuliser pressure	Controls the pressure of the nitrogen nebulizing gas and is dependent on the LC flow rate to determine the speed at which the sample is aspirated into the electrospray chamber
Capillary voltage	Applied at the entrance of the capillary in the ionisation chamber to transmit ions into the sampling capillary
Nozzle voltage	Voltage applied between the electrospray needle and the skimmer
Drying gas temperature / flow	Nitrogen drying gas facilitates drying of droplets formed in the ionisation chamber by carrying away excess charges and solvent until only "naked" charged sample ions are formed

Table 3.5 Optimised Agilent Jet Stream ESI-Q-TOF parameters in the positive and negative full MS scan ion modes.

ESI Jet Stream component	Optimised positive ion polarity	Optimised negative ion polarity
Sheath gas temperature (°C)	350	350
Sheath gas flow (L min ⁻¹)	11	11
Nebuliser pressure (psig)	30	25
Capillary voltage (V)	2500	3000
Nozzle voltage (V)	500	500
Drying gas temperature (°C)	250	300
Drying gas flow (L min ⁻¹)	5	9

3.3.2.2 Optimisation of the Q-TOF

The function of the fragmentor (at the end of the capillary) is to control the speed at which an ion travels from the electrospray chamber (atmospheric pressure) to the mass spectrometer. The voltage applied to the fragmentor must be sufficiently high to produce good and strong MS signals but should not fragment the ions travelling through the capillary (Hua and Jenke, 2012). Fragmentation of ions occurs in the collision cell. The collision cell contains neutral nitrogen gas molecules which bombard precursor ions to produce fragments. Each target auxin analyte produces a distinct set of product ions (characteristic fragmentation spectrum) used for identification and quantification. An optimal collision energy must be sufficiently high to fragment individual precursor ions (10 % of the original precursor ion signal) to produce strong and reproducible product ions. Collision energies that are too high might over-fragment precursor ions to produce many indistinct and weak “noise-like” fragments (MacLean et al., 2010). We determined the optimal fragmentor voltage for individual auxin compounds in full MS scan mode. After varying the fragmentor voltage based on manufacturer’s suggestion for each compound, we selected voltages which conferred maximum peak sensitivity. For example, D5-IAA and IAA had optimal fragmentor voltages of 130 and 140 V in the positive polarity, respectively (Figure 3.13). The optimal fragmentor voltage for all auxin compounds are listed in Table 3.6. As the Q-TOF can only operate with one fragmentor voltage in each ion polarity, we arrived at an average value of 138 and 140 V for the positive and negative ion modes, respectively.

Next, we optimised the collision energies of individual auxin compounds. Optimal collision energy was chosen on the basis of near-complete fragmentation of precursor ions to produce the most intense product ions in both positive and negative targeted MS/MS scan modes. For example, the optimum collision energies for D5-IAA and IAA in positive ESI were 12 and 10 eV, respectively (Figure 3.14B and 3.14E). Lower collision energies insufficiently fragment the precursor ions, thus

affecting the quantitation process, which relies on good product ion peaks (Figure 3.14A and 3.14D). On the contrary, higher collision energy over-fragmented the precursor ions (Figure 3.14C and 3.14F).

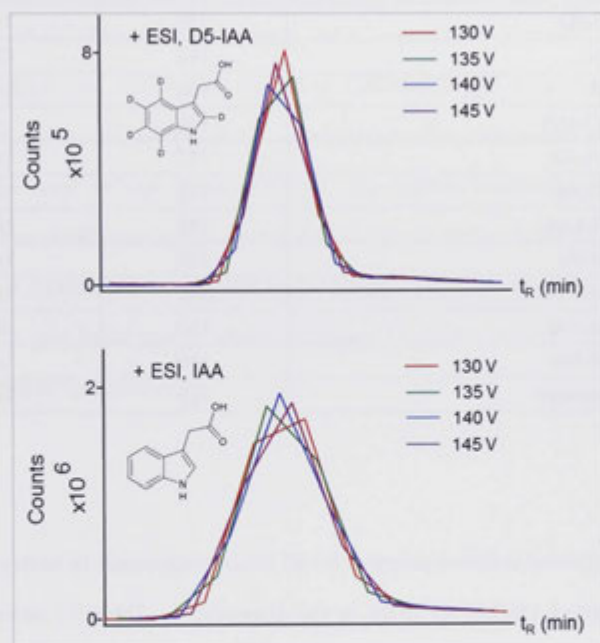


Figure 3.13 Fragmentor voltage optimisation. Graphs show raw peak height counts on the y-axis and retention time (t_R , min) on the x-axis. Optimal fragmentor voltage for each auxin compound was investigated. Examples for fragmentor voltage tested for D5-IAA and IAA are shown. Maximum sensitivity was achieved for D5-IAA and IAA with fragmentor voltages of 130 and 140 V, respectively.

Table 3.6 Fragmentor voltage optimisation for individual auxin compounds in the positive and negative ion polarities. An average fragmentor voltage value was calculated and used for subsequent LC/MS analyses, as the instrument can only operate at one fragmentor voltage in each ion polarity mode.

Auxin compound	Fragmentor voltage (V)	
	Positive	Negative
D5-IAA	130	140
IAA	140	135
IBA	130	145
4-Cl-IAA	145	140
IAA-Ala	145	145
IAA-Asp	140	135
IAA-Leu	145	NA
IAA-Ile	130	140
IAA-Phe	140	140
IAA-Trp	130	140
IAA-Val	140	140
Average	138	140

The optimal collision energies for all auxin compounds in both positive and negative targeted MS/MS are listed in the Appendix B. Table 3.7 summarises the analytes that were best analysed in the positive and the negative ion modes, based on their limits of detection (LOD, $3 \times S/N$; S/N, signal-to-noise ratio). For subsequent quantification in standards and real samples, the most intense product ion for each auxin compound was selected as the quantification (quant) ion, and the other product ions were confirmation (qualifier) ions. For D5-IAA and IAA, the quant ion would be m/z 134.09 and 130.06, respectively. Figures 3.15 and 3.16 show examples of targeted MS/MS extracted ion chromatograms (EIC) and MS/MS (MS2) product ion spectra for D5-IAA and IAA, in the positive and negative ion modes, respectively. Figures 3.17 and 3.18 show the fragmentation location on each auxin protonated, $[M+H]^+$ and deprotonated, $[M-H]^-$ molecules to produce the most intense product ion observed in the positive and negative ion modes, respectively.

The major precursor-to-product transition for D5-IAA was 181→134 (positive scan mode) and 179→135 (negative scan mode). In the positive ion mode, apart from IBA (204→186) and 4-Cl-IAA (210→164), all other auxin species had precursor ion→130 (quinolinium ion) transitions. In the negative ion mode, the most intense transitions were as follow: IAA (174→130), IBA (202→116), PAA (135→91), 4-Cl-IAA (208→164), IAA-Ala (245→88), IAA-Asp (289→88), IAA-Leu/IAA-Ile (287→130), IAA-Phe (321→164), IAA-Trp (360→203) and IAA-Val (273→116). Phenylacetic acid could not produce a good peak in the positive ion MS/MS mode. The column used in our analyses could not resolve leucine and its isoform isoleucine, nor could mass spectrometry differentiate between these two compounds. Thus, future quantification of these compound(s) must be carefully interpreted. Alternatively, ion-exchange or chiral columns could be used to separate these isoforms prior to quantification.

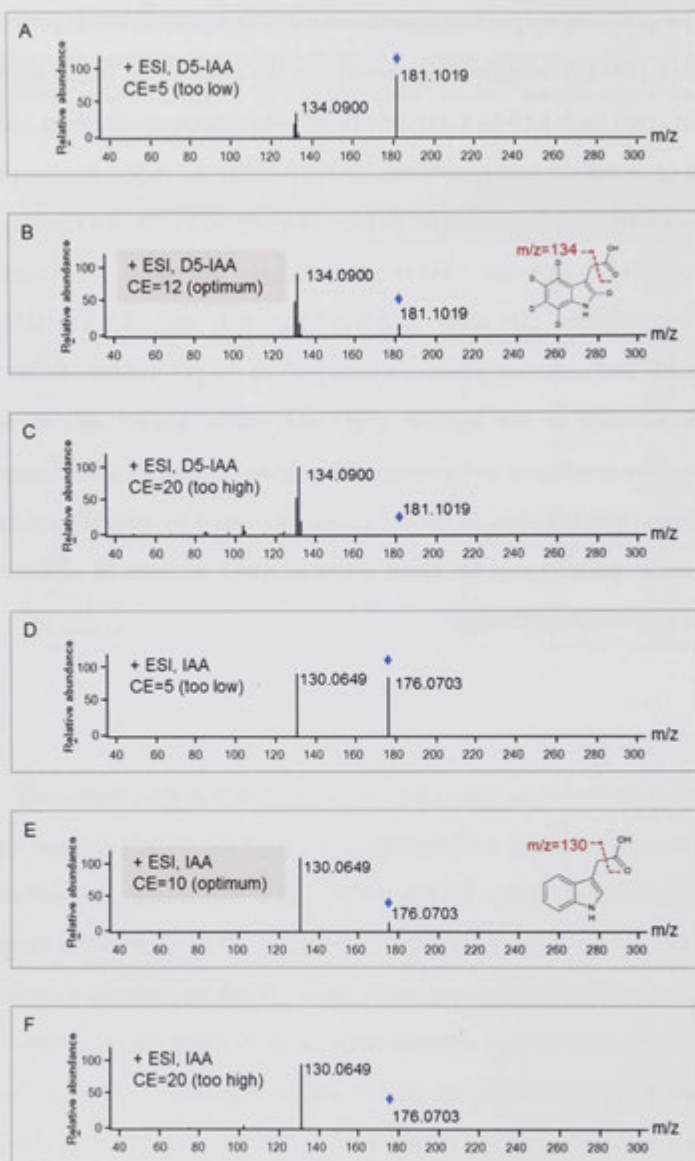


Figure 3.14 Collision energy optimisation. Mass spectra show relative abundance on the y-axis and mass-to-charge (m/z) ratio on the x-axis. Product ion spectra of (A-C) D5-IAA and (D-F) IAA under different collision energies (CE) in positive ESI. The optimum collision energy dissociates the precursor ion to ~10% of its original abundance (B,E). Lower collision energies promote insufficient fragmentation (A,D). Higher collision energies promote additional “noise-like” fragments (C,F). Blue diamonds indicate precursor ions.

Table 3.7 Quality parameters for auxin detection using LC-MS/MS in our study. Commercial auxin standards used in this study and their respective retention times, optimised collision energies, collision induced dissociation high resolution product ions, LODs^a, LOQs^b, linearity and correlation coefficients for identification and quantification in positive and negative ion polarity ESI targeted MS/MS.

Analyte	Molecular formulae	MW (g/mol)	Parent Ion [M+H] ⁺	Collision energy (eV)	t _R (min)	Product ions (from most intense to least)					LOD ^a (pg/mg)	LOQ ^b (pg/mg)	Linearity (y =)	Correlation coefficient (R ²)
D5-IAA	C ₁₀ H ₄ D ₅ NO ₂	180.21	181.1014	12	12.3 ± 0.004	134.0892	133.0826	135.0961	116.9742	95.9716	0.54	0.91	-	-
IAA	C ₁₀ H ₉ NO ₂	175.19	176.0710	10	12.4 ± 0.005	130.0643	131.0663	158.0582	103.0522	77.0336	1.01	1.69	20.9120x - 0.1716	0.9991
IBA	C ₁₂ H ₁₃ NO ₂	203.24	204.1033	12	15.7 ± 0.007	186.0890	130.0624	168.0787	158.0934	144.0790	0.20	0.51	34.5990x - 0.3430	0.9976
IAA-Ala	C ₁₃ H ₁₄ N ₂ O ₃	246.27	247.1095	10	11.7 ± 0.014	130.0651	90.0553	131.0686	201.1019	-	0.75	1.26	30.9550x - 0.1009	0.9991
Analyte	Molecular formulae	MW (g/mol)	Parent Ion [M-H] ⁻	Collision energy (eV)	t _R (min)	Product ions (from most intense to least)					LOD ^a (pg/mg)	LOQ ^b (pg/mg)	Linearity (y =)	Correlation coefficient (R ²)
D5-IAA	C ₁₀ H ₄ D ₅ NO ₂	180.21	179.0874	10	12.2 ± 0.020	135.0960	90.9979	159.6305	59.1363	104.9311	3.71	6.18	-	-
PAA	C ₈ H ₈ O ₂	136.05	135.0452	3	11.7 ± 0.047	91.0526	72.0207	117.4564	50.2836	-	6.90	11.50	1.2736x - 0.0050	0.9922
4-Cl-IAA	C ₁₀ H ₈ ClNO ₂	209.63	208.0171	8	15.0 ± 0.006	164.0287	165.0275	128.0468	-	-	0.25	0.41	21.5260x + 0.1375	0.9956
IAA-Asp	C ₁₄ H ₁₄ N ₂ O ₅	290.28	289.0830	17	9.6 ± 0.059	88.0423	132.0311	115.0051	173.0723	156.0472	1.55	2.58	9.1470x + 0.0279	0.9975
IAA-Ile	C ₁₆ H ₂₀ N ₂ O ₃	288.35	287.1361	15	16.5 ± 0.002	130.0854	131.0887	156.0425	243.1475	-	0.05	0.09	97.2150x + 1.1548	0.9959
IAA-Leu	C ₁₆ H ₂₀ N ₂ O ₃	288.35	287.1385	10	16.5 ± 0.002	130.0854	131.0887	156.0425	243.1475	-	0.05	0.09	97.2150x + 1.1548	0.9959
IAA-Phe	C ₁₉ H ₁₈ N ₂ O ₃	322.37	321.1245	15	16.9 ± 0.007	164.0718	165.0749	147.0453	103.0548	277.1341	0.14	0.24	45.3370x + 0.3456	0.9974
IAA-Trp	C ₂₁ H ₁₈ N ₃ O ₃	361.39	360.1354	17	16.4 ± 0.003	203.0829	204.0864	74.0254	116.0514	156.0455	0.76	1.27	6.3667x + 0.1310	0.9914
IAA-Val	C ₁₅ H ₁₈ N ₂ O ₃	274.32	273.1243	15	15.1 ± 0.006	116.0739	117.0765	156.0478	128.0522	229.1371	0.11	0.18	58.1590x + 0.3346	0.9987

Injection precision (n=10), data shows mean and SD

^a Limit of detection (LOD) ≥ 3 x S/N, ^b Limit of quantification (LOQ) ≥ 5 x S/N

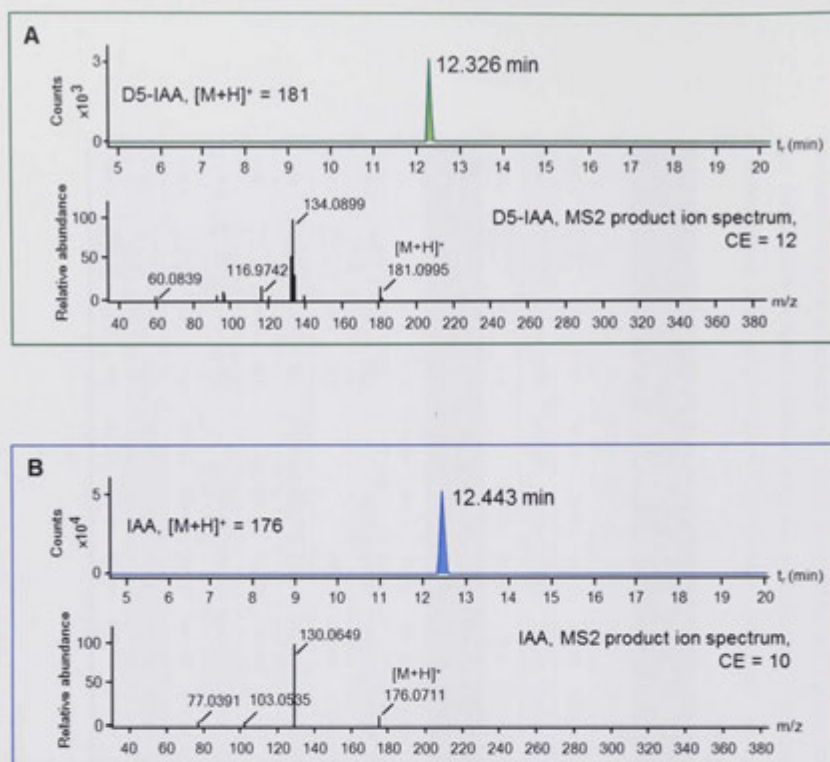


Figure 3.15 Positive targeted MS/MS extracted ion chromatograms (top) and MS/MS product ion spectra (bottom) of (A) D5-IAA and (B) IAA, respectively, using a 5 $\mu\text{g ml}^{-1}$ auxin standard mixture. Extracted ion chromatograms show the retention time of individual auxin analytes. Product ion spectra show the precursor ion and the three most abundant product ions unique to each analyte.

3.3 Results and discussion

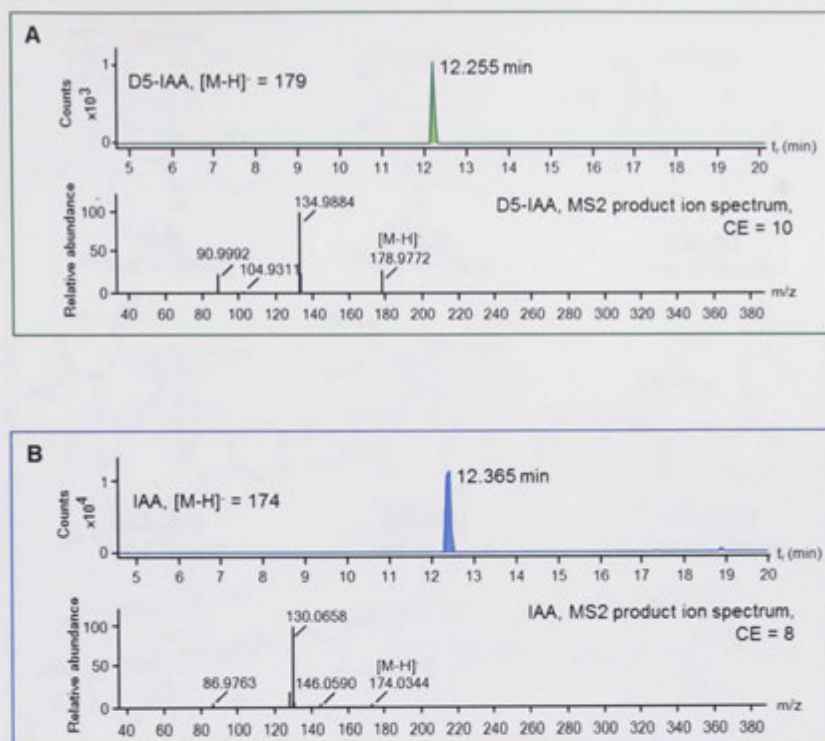


Figure 3.16 Negative targeted MS/MS extracted ion chromatograms (top) and MS/MS product ion spectra (bottom) of (A) D5-IAA and (B) IAA, respectively, using a $5 \mu\text{g ml}^{-1}$ auxin standard mixture. Extracted ion chromatograms show the retention time of individual auxin analytes. Product ion spectra show the precursor ion and the three most abundant product ions unique to each analyte.

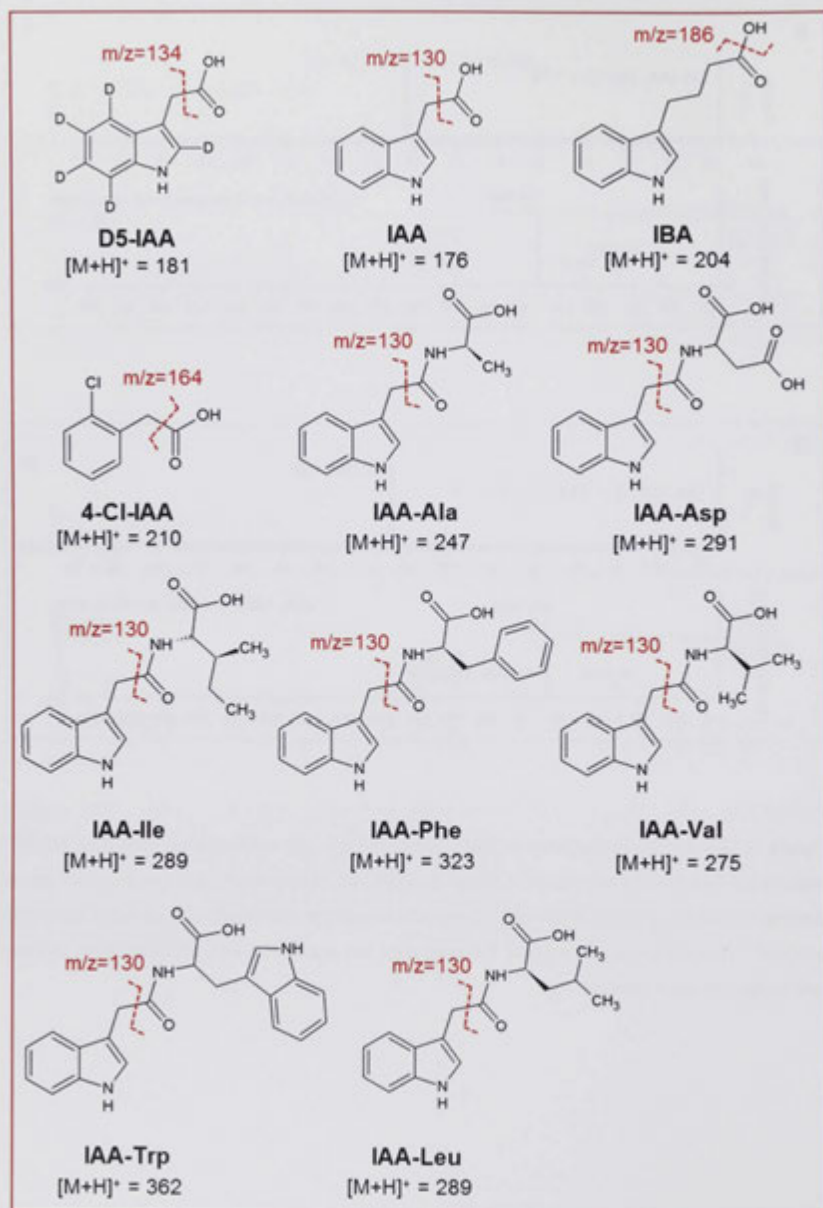


Figure 3.17 Location of fragmentation via collision induced dissociation (CID) on each auxin protonated molecule $[M+H]^+$ to produce the respective most abundant product ion in the positive ESI mode. Mass-to-charge (m/z) = 130 is a quinolinium ion.

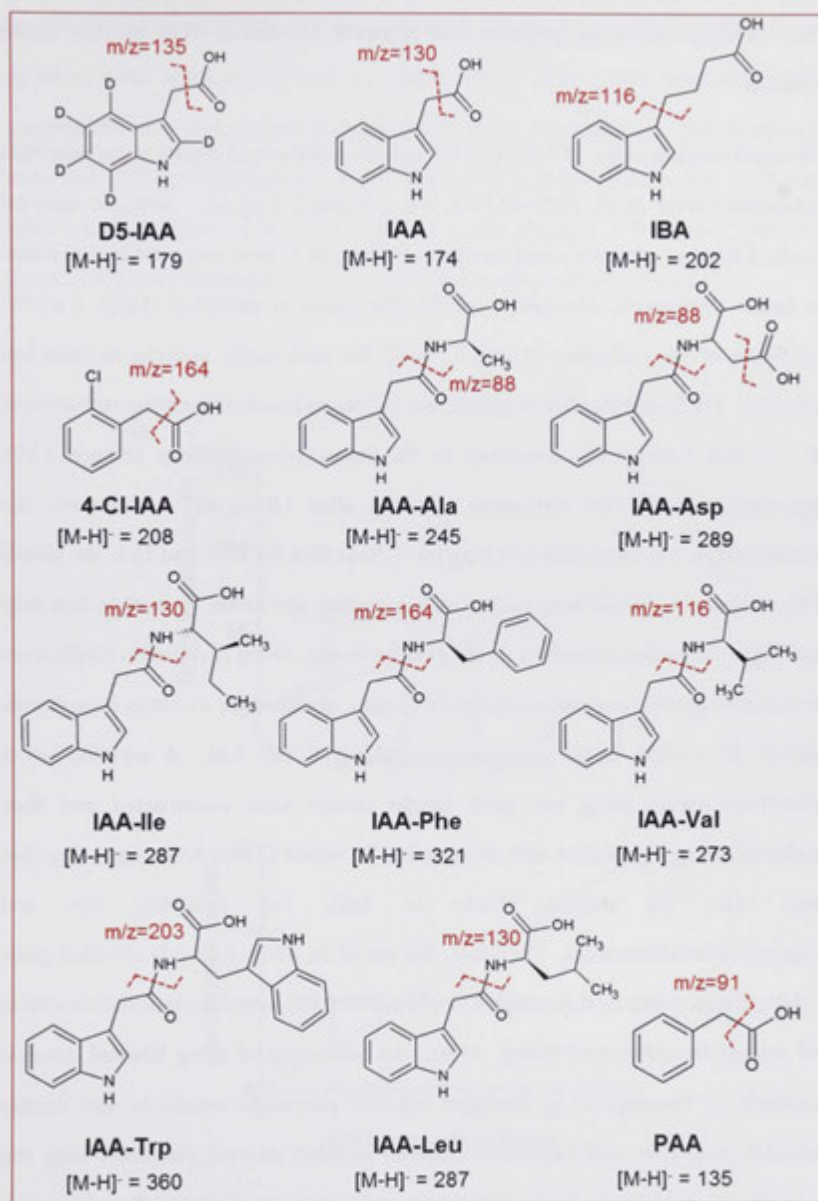


Figure 3.18 Location of fragmentation via collision induced dissociation (CID) on each auxin deprotonated molecule $[M-H]^-$ to produce the respective most abundant product ion in the negative ESI mode.

3.3.3 Validation of the positive and negative LC-ESI-Q-TOF MS/MS auxin methods

After optimisation of the LC-ESI-Q-TOF in both positive and negative ion polarities, calibration curves (0.01, 0.05, 0.1, 0.5, 1.0, 2.0 and 5.0 ng μL^{-1} , with the internal standard fixed at a known concentration of 0.4 ng μL^{-1}) were analysed to determine the linear regressions, correlation coefficients, limits of detection (LOD, $3 \times \text{S/N}$) and limits of quantification (LOQ, $5 \times \text{S/N}$) for each auxin analyte, in both ion polarities. We found that MS response was no longer linear at the concentrations of 1.0, 2.0 and 5.0 $\mu\text{g ml}^{-1}$, compared to the lower concentrations (Figure 3.19), suggesting that detector saturation occurred after 1.0 $\mu\text{g ml}^{-1}$. Therefore, the linearity range was from 0.01 to 1.0 $\mu\text{g ml}^{-1}$. Note that for IAA and IBA, the slopes of the calibration curves were steeper in the positive ion mode, indicating that they have higher detection sensitivity in the positive mode. Good correlation coefficients for standard curves (normalised to D5-IAA) were obtained for all auxin compounds studied ($R^2 > 0.99$), in the optimal scan polarity (Table 3.8). A separate set of calibration curves using raw peak height counts were constructed and they produced linear regressions with comparable R^2 values (Table 3.8), suggesting that there were no matrix effects in both ion polarities (i.e. ion suppression/enhancement). Therefore, the use of an internal standard added prior to the extraction step in real samples would account for complex plant matrix effects and sample loss (Pan and Wang, 2009). An advantage of using labelled internal standards in comparison to analogue internal standards would be the similar chemical properties and behaviour between labelled internal standards with the endogenous compounds during extraction and analysis procedures (Lanckmans et al., 2007). Good reproducibility for retention times was observed with a relative standard deviation (% RSD) ranging from 0.01-0.70 % for run-to-run precision ($n=10$) (Table 3.7). In addition, the internal standard D5-IAA displayed reproducibility in peak area counts with a % RSD of 13% (run-to-run, $n=10$). The

limits of detection (LOD) and quantification (LOQ) were calculated based on a signal-to-noise ratio of 3:1 and 5:1, respectively. The LODs and LOQs of all compounds were determined and are listed in the Appendix B. The compounds IAA, IBA and IAA-Ala had lower LODs and LOQs in the positive ESI mode while other auxin analytes were better detected in the negative ESI mode (Table 3.7). Good LODs were obtained with our optimised methods ($0.05\text{--}6.90\text{ ng g}^{-1}$).

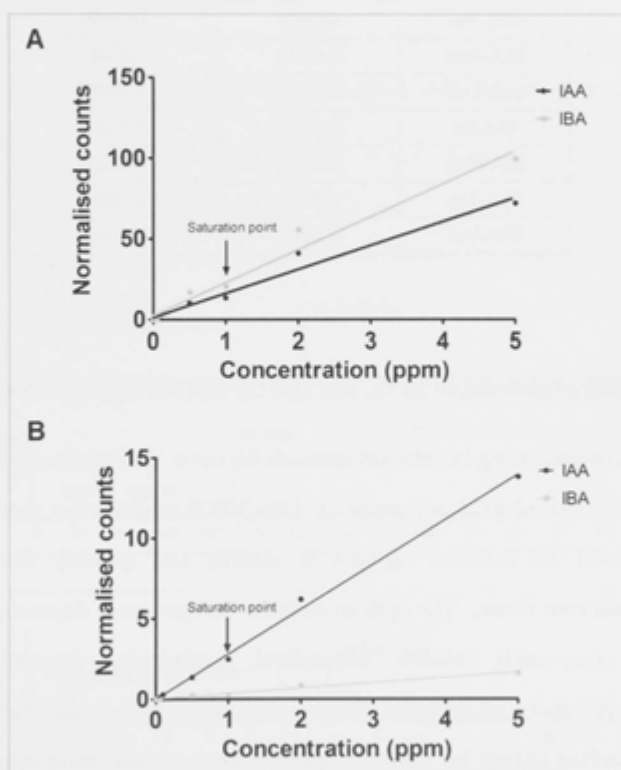


Figure 3.19 Detector saturation at high concentrations of analytes. Examples of IAA and IBA standard curves ($0\text{--}5\ \mu\text{g ml}^{-1}$) in the (A) positive and (B) negative scan polarities. Analyte counts were normalised to the D5-IAA internal standard. The detector saturation point occurs at around $1\ \mu\text{g ml}^{-1}$.

Table 3.8 Correlation coefficient (R^2 values) of auxin compounds. Correlation coefficients were calculated from calibration curves generated from raw peak height counts, which were or were not normalised to the D5-IAA internal standard. Comparable R^2 values indicate no matrix effects (i.e. ion suppression / enhancement) during MS ionisation.

Auxin compound	Correlation coefficient (R^2)	
	Normalised	Not normalised
IAA	0.9991	0.9988
IBA	0.9976	0.9974
PAA	0.9922	0.9949
4-CI-IAA	0.9956	0.9992
IAA-Ala	0.9991	0.9999
IAA-Asp	0.9975	0.9997
IAA-Leu	0.9959	1.0000
IAA-Ile	0.9959	1.0000
IAA-Phe	0.9974	0.9998
IAA-Trp	0.9914	0.9991
IAA-Val	0.9987	0.9997

3.3.4 Quality parameters of an LC-ESI-Q-TOF MS/MS flavonoid method

In addition to optimising LC-MS/MS methods for auxin identification and absolute quantification, we adopted our auxin LC-ESI-Q-TOF negative ion mode method and optimised the collision energies to identify and quantify flavonoids in *M. truncatula* root tissue. The optimal collision energies were determined for the flavonoid compounds luteolin, kaempferol, naringenin, quercetin, morin, hesperetin, genistein and apigenin. For our study, luteolin was used as an analogue internal standard (20 ng) for flavonoid quantification in calibration standards and real samples. Due to time constraints, only the negative targeted MS/MS mode was investigated for flavonoid compounds due to its good MS response in a previous work conducted on the same LC-MS system (Buer et al., 2013). Samples were injected (7 μ l) onto an Ascentis[®] Express 2.7 μ m C18 2.1 \times 50 mm column (Supelco). Mobile phase A consisted of 0.1 % aqueous formic acid and mobile phase B

3.3 Results and discussion

comprised of 90 % acetonitrile/water with 0.1 % formic acid, using the same gradient as for the auxin method. Chromatographic peak shapes, retention times and MS/MS product ion spectra of individual flavonoid compounds were good. Luteolin and naringenin are shown in Figure 3.20 as examples. Calibration curves from 0.01-5.0 ppm were generated and the linear range was found to be 0.01-2.0 ppm (Table 3.9). Good correlation coefficients were obtained ($R^2 > 0.98$) and the reproducibility of retention times was good with % RSDs of 0.09-1.37 % for run-to-run precision. Furthermore, the internal standard luteolin has an area count % RSD of 7.96 % (run-to-run). Finally, the LODs ($3 \times S/N$) and LOQs ($5 \times S/N$) were calculated as previously, with the former ranging from 5.47-45.91 pg mg^{-1} (Table 3.9).

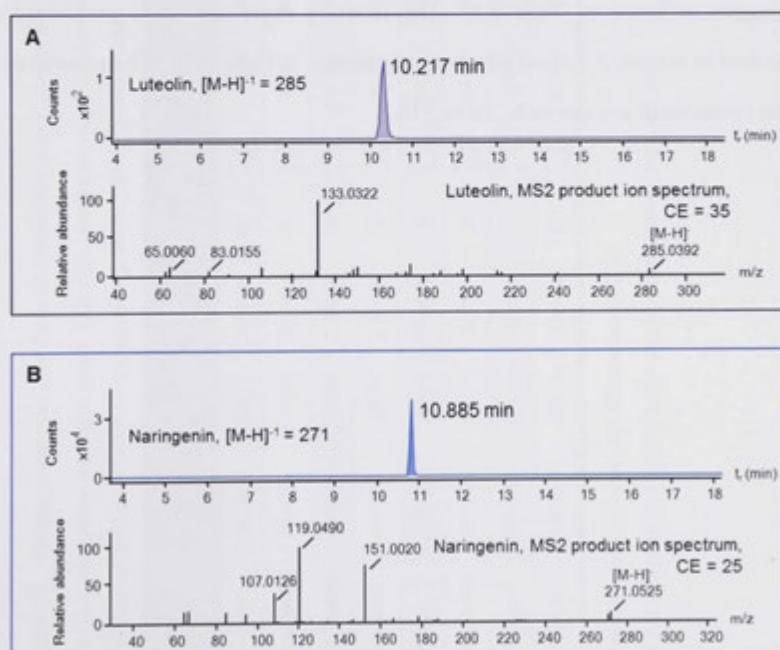


Figure 3.20 Extracted ion chromatograms and MS/MS product ion spectra of flavonoid analytes analysed in the negative ion polarity with LC-ESI-Q-TOF-MS/MS using a $5 \mu\text{g ml}^{-1}$ commercial flavonoid standard mixture. The compounds (A) luteolin and (B) naringenin are shown here. Chromatograms show the retention times (t_R , min) of individual flavonoid analytes. Product ion spectra show the precursor ion $[\text{M-H}]^-$, the characteristic most abundant product ions unique to each analyte and the collision energies applied.

3.3.5 Method validation of an existing auxin extraction protocol

Once all the LC-ES-Q-TOF method development and validation were completed we continued on to validate the extraction protocol for auxins. In the work conducted by Muller and Munne-Bosch (2011), it was reported that the recovery of IAA was > 80 %. An attempt was made in this study to reproduce the recovery for this analyte, as well as to investigate the suitability of this method in the extraction of auxin conjugates as listed in Table 3.2. The recovery experiment was performed as described in section 3.2.3 and schematically shown in Figure 3.4. The recoveries of auxin compounds are shown in Table 3.10.

Table 3.9 Quality parameters for flavonoid detection using LC-MS/MS in our study. Commercial flavonoid standards used in this study and their respective retention times, CID high resolution mass product ions, LODs^a, LOQs^b, linearity and correlation coefficients used for identification and quantification by negative polarity ESI Targeted MS/MS.

Analyte	Molecular formulae	MW (g/mol)	Parent Ion [M-H] ⁻	Collision energy (eV)	t _R (min)	Product ions (from most intense to least)					LOD ^a (pg/mg)	LOQ ^b (pg/mg)	Linearity	Correlation coefficient (R ²)
Luteolin	C15H10O6	286.24	285.0402	35	10.3 ± 0.010	133.0306	65.0043	83.0155	107.0141	175.0399	7.55	12.58	-	-
Kaempferol	C15H10O6	286.24	285.0394	45	11.1 ± 0.109	93.0318	117.0332	159.0429	65.0039	227.0369	8.61	14.35	0.6106x + 0.0608	0.9950
Naringenin	C15H12O5	272.26	271.0612	25	10.9 ± 0.112	119.0518	151.0058	107.0154	65.0043	83.0151	5.47	9.11	7.3793x + 0.0872	0.9985
Quercetin	C15H10O7	302.24	301.0354	35	10.2 ± 0.163	151.0042	107.0127	121.0291	65.0039	83.0142	6.53	10.89	31.4370x + 2.3750	0.9902
Morin	C15H10O7	302.24	301.0265	35	9.5 ± 0.196	149.0251	65.0039	83.0149	107.0144	125.0255	10.88	18.13	50.6800x + 1.4122	0.9993
Hesperetin	C16H14O6	302.27	301.0715	25	11.4 ± 0.097	164.0122	136.0173	108.0218	151.0047	134.0394	45.91	76.52	0.6527x + 0.0283	0.9896
Genistein	C15H10O5	270.24	269.0455	35	11.0 ± 0.035	117.0343	151.0034	107.0144	65.0026	83.0151	14.21	23.68	523.9500x - 3.4874	0.9992
Apigenin	C15H10O5	270.24	269.0455	30	11.0 ± 0.035	117.0343	151.0034	107.0144	65.0026	83.0151	14.21	23.68	523.9500x - 3.4874	0.9992

Injection precision (n=10); data shows mean and SD

^a Limit of detection (LOD) ≥ 3 x S/N, ^b Limit of quantification (LOQ) ≥ 10 x S/N

Table 3.10 Extraction recoveries of auxin metabolites (n=5).

Auxin compound	Recovery (%)	% RSD ^a
IAA	97.8	9.4
IBA	42.1	20.2
4-Cl-IAA	101.6	15.6
IAA-Ala	34.9	12.6
IAA-Asp	42.2	43.1
IAA-Phe	44.6	15.7

^a % Relative standard deviation (RSD) = (Standard deviation / Mean) × 100 %

Based on Table 3.10, recoveries of IAA and 4-Cl-IAA were close to 100%; IBA, IAA-Ala, IAA-Asp and IAA-Phe were < 50 %. Other auxins, such as PAA, IAA-Leu, IAA-Ile, IAA-Trp and IAA-Val were not detected. Although the recovery of IAA was similar to other studies (Matsuda et al., 2005, Novák et al., 2012), recoveries of other metabolites, such as IAA-Ala, IAA-Asp and IAA-Phe could be improved, as demonstrated by Matsuda et al. (2005), which attained recoveries between 91-99 %. Suboptimal analyte recoveries suggest that matrix effects (ion suppression) from interfering compounds in the sample extract were affecting the recovery of these analytes (Annesley, 2003). Nevertheless, the recovery of IAA, the primary active auxin, was comparable with other auxin extraction methods (Liu et al., 2012, Novák et al., 2012), where different methanol compositions (5-80 %) were used as the extraction solvent. Although the IAA conjugates in this study were all acidic in chemical characteristics, it was discovered by Novák et al. (2012) that the stability of these analytes only occurred over a pH range of 4-12, where compounds like IAA-Trp, IBA and IAA-Phe were only stable when the pH was at 8. One of the strengths of the Muller and Munne-Bosch (2011) method adopted in this study was the speed, and avoidance of additional steps, such as derivatisation and purification. However, adapting the Novák et al. (2012) extraction method, which incorporated a derivatisation step using cysteamine for the thermally labile auxins (0.25 M, pH 8.0,

incubation for 1 hour) and SPE purification in this study could have potentially improved the detection and quantification of auxins in *M. truncatula* root tissues.

3.3.6 Conclusion

It is from optimising these specific LC-ESI-Q-TOF parameters in both positive and negative ion polarities that we could achieve the sensitivity we needed for the reproducible detection and quantification of trace IAA and IAA conjugates in the small amounts of plant tissues used, within a relatively short analysis time. We did not, however, do an exhaustive survey and development of alternative extraction methods. The extraction efficiencies obtained in our study could be improved, for example, by modifying the Muller and Munne-Bosch (2011) extraction protocol, or adopting the Novák et al. (2012) method, which reported good recoveries for various auxin metabolites. An improved method which allows simultaneous hormone profiling with improved analyte recovery will accelerate our understanding of hormonal (inter)action during legume development.

CHAPTER 4



Comparison of Local Auxin Transport Control and Auxin Content in Indeterminate and Determinate Nodules



4.1 Introduction

Nodulation in legumes is tightly regulated by plant hormones. Positive regulators of nodulation include auxin, cytokinin, gibberellic acid and brassinosteroids. Ethylene, jasmonic acid and abscisic acid are generally considered negative regulators of nodulation (Ferguson and Mathesius, 2014). Auxin is one of the most widely studied hormones during nodulation. The plant hormone auxin is a key regulator of meristem maintenance and organogenesis (Overvoorde et al., 2010). These two important functions are particularly relevant to nodulation, given that it involves: 1) the dedifferentiation of mature cells and the establishment of a new group of meristematic cells, forming the nodule meristem and; 2) a controlled auxin response in specific tissues as a nodule grows and differentiates outwards from the inner layers of the root to form a new organ (Mathesius, 2008, Oldroyd and Downie, 2008). Even though the study of auxin has taken centre stage, many questions remain about its regulation during nodule development, including the similarities or differences in different nodulating species.

Regulation of auxin takes place at multiple levels within a plant. Auxin can be synthesised locally or at a distant location and subsequently transported to the target tissue (Ljung, 2013). In addition, the vacuole is a store of inactivated/conjugated auxins, which can be hydrolysed into active, free forms (Korasick et al., 2013, Ludwig-Müller, 2011). Although IAA is the most abundant active, free auxin in most land plants, possible direct activity of auxin conjugates, which are generally present at levels many folds higher than free IAA, cannot be ruled out (Siemens et al., 2006). Other active auxin forms, such as IBA and 4-Cl-IAA, are also able to form conjugates with sugars and amino acids. However, their function in plant development is even more under-explored. Given the variety of auxin species present in plants, it is imperative that we understand their biological function and

behaviour *in planta*, including their concentration and localisation patterns during lateral organ formation.

During the legume-*Rhizobium* symbiosis, the auxin response at the early stages of nodule development changes dynamically. In white clover, auxin response indicated by *GH3:GUS* expression decreased at and below the *Rhizobium trifolii*-inoculated site at 10 h post inoculation (h.p.i.) (Mathesius et al., 1998). Between 20–30 h.p.i., an enhanced auxin response was visualised at the site of rhizobia inoculation. In *M. truncatula*, an increased auxin response at the pericycle, endodermis and cortex was detected at 24 h.p.i. with *S. meliloti* (van Noorden et al., 2007). This enhanced auxin response was later localised to a cluster of dividing cells in the pericycle, endodermis and inner cortex at 48 h.p.i. The development of a nodule in *L. japonicus* is slower, as a visible auxin response was only seen after 5 d.p.i. (Suzaki et al., 2012). Similar to *M. truncatula*, auxin response is detected in cortical cells at the early primordia stage of *L. japonicus* (Pacios-Bras et al., 2003, Takanashi et al., 2011) and soybean (Turner et al., 2013). This enhanced auxin response is maintained in the entire nodule until it matures approximately a week later, where auxin response is primarily focussed at the periphery of the nodule, corresponding to the nodule vasculature (Suzaki et al., 2012, Takanashi et al., 2011). So far, the investigation of auxin response in other nodulating species is lacking. One open question is how the increased auxin response in the nodule primordia is achieved. Modelling suggests that it is most likely a result of reduced auxin export from the cortical cells (Deinum et al., 2012). Thus, we investigated auxin transport control during nodulation.

The importance of polar auxin transport regulation in root development has been highlighted in multiple studies. Mutants in the *PIN* and *AUX/LAX* family (auxin efflux and influx facilitators, respectively; see section 1.1.1) show root growth and lateral root developmental defects (Overvoorde et al., 2010). In *M. truncatula*, knockdown of various *PIN* genes reduced nodule numbers on transgenic roots (Huo

et al., 2006). By comparing with a non-nodulating mutant of *M. truncatula*, it was subsequently suggested that a transient inhibition of acropetal auxin transport after Nod factor treatment on WT *M. truncatula* roots was a prerequisite for nodule formation (Plet et al., 2011). This temporary inhibition of acropetal auxin transport has also been shown in vetch (Boot et al., 1999). So far, this phenomenon seems to be exclusive to indeterminate nodule formation. In *L. japonicus*, an increase in acropetal auxin transport capacity was measured at 48 h.p.i., but no inhibition was observed during the early stages of host-*Rhizobium* interaction in this legume (Pacios-Bras et al., 2003). Auxin transport inhibition is also likely not a requirement during soybean nodulation. Although RNAi-induced silencing of *ISOFLAVONE SYNTHASE* (catalyse isoflavonoid synthesis, which are capable of inhibiting auxin transport) in soybean hairy roots increased auxin transport rate and reduced nodulation, these soybean hairy roots could be rescued with a genistein (an isoflavone)-hypersensitive strain of *B. japonicum* or purified Nod factors, suggesting that auxin transport regulation by isoflavonoids is not essential for nodulation in soybean (Subramanian et al., 2006). However, changes in basipetal auxin transport during nodulation have not been investigated. Because knockdown of *PIN2* [auxin efflux facilitator orthologous to *AtPIN2*, which is involved in basipetal auxin transport in *Arabidopsis*; (Rashotte et al., 2000)] in *M. truncatula* roots reduced nodule numbers (Huo et al., 2006), it is likely that basipetal, in addition to acropetal auxin transport, plays a key role during nodulation.

The ability of synthetic auxin transport inhibitors to induce nodule-like structures on the roots of legumes further underlines the pivotal role of polar auxin transport (inhibition) in nodulation. Application of auxin transport inhibitors has successfully induced pseudonodule formation on the roots of alfalfa, *M. truncatula*, white sweetclover and pea (Hirsch et al., 1989, Rightmyer and Long, 2011, Scheres et al., 1992, Wu et al., 1996). Critically, all four mentioned legumes form indeterminate nodules and a similar treatment on *L. japonicus* roots (forming

determinate nodules) roots failed to induce pseudonodules (Kawaguchi et al., 1996). Coupled with the difference in polar auxin transport regulation between indeterminate and determinate nodulation (evidence present for *L. japonicus* only), this suggests the essential role of polar auxin transport inhibition for indeterminate but not determinate nodule formation. The temporary inhibition of polar auxin transport was initially proposed as a mechanism to redirect auxin flow into the incipient nodule primordium (Mathesius, 2008).

During lateral root formation in *Arabidopsis*, PIN1 auxin efflux carriers in lateral root primordia cells are depleted from the plasma membrane and undergo degradation, thus reducing polar auxin flow (Marhavý et al., 2011). In addition, the depletion of plasma membrane PIN1 from the vertical side of lateral root primordia cells also serves to reorganise the polarity of PIN1, i.e. to the horizontal sides, thus redirecting auxin flow in the horizontal direction (Marhavý et al., 2014). Although this has not been demonstrated during nodule formation in *M. truncatula*, the plausibility of such a mechanism was supported by the reorganisation of a PIN3-GFP fusion from basal-to-lateral configuration in the syncytium during nematode infection (Grunewald et al., 2009). Auxin transport inhibitors block endosomal recycling of PIN proteins (Geldner et al., 2001). Accordingly, application of auxin transport inhibitors to the roots blocks lateral root initiation (Casimiro et al., 2001). It is so far unclear how auxin transport inhibitors: 1) induce pseudonodule formation; 2) affect local and horizontal auxin flow in the nascent pseudonodule and; 3) regulate auxin response during pseudonodule development. Nevertheless, Suzuki et al. (2012) showed a localised auxin response during spontaneous nodule formation (an empty nodule-like structure not harbouring rhizobia, similar to pseudonodules) in the *L. japonicus snf2* mutant, similar to the auxin response seen during normal nodule formation.

A direct quantification of endogenous auxin concentration during nodule development will give us insights into changes of local auxin levels. This

information is missing from the literature hitherto. Although auxin response studies indicated by *GH3*- and *DR5*-driven auxin reporters give us information on auxin action, the changes in the reporter output does not necessarily translate linearly into alterations in endogenous auxin levels. Immunolabelling of IAA in mature *M. truncatula* nodules showed the localisation of IAA in the meristematic and invasion zones (Fedorova et al., 2005). Detection of IAA at the early stages of *M. truncatula* nodulation has so far not been demonstrated. In the actinorhizal plant *Casuarina glauca*, immunolocalisation experiments similarly demonstrated the presence of IAA in nodules (Perrine-Walker et al., 2010). In addition, a higher phenylacetic acid (PAA) signal was also detected in *C. glauca* (Perrine-Walker et al., 2010) and *Discaria trivernis* (Imanishi et al., 2014) nodules. This suggests that PAA (an active auxin) might play an important role inside actinorhizal nodules. In fact, PAA was detected at levels multiple fold higher than IAA in several plants, including pea, tobacco and maize (Wightman and Lighty, 1982). So far, however, its activity has been poorly defined. Identification of multiple auxin conjugate forms hints at a more complicated mode of auxin action in determining developmental outputs, rather than just by a few active auxin species (Korasick et al., 2013). Expression studies of several auxin conjugate hydrolases, as well as the corresponding enzyme-product specificity assays, suggest the presence of several auxin conjugates in the roots of *M. truncatula*, including IAA-Alanine, IAA-Phenylalanine, IAA-Aspartate, IAA-Leucine, IAA-Isoleucine and IAA-Valine (Campanella et al., 2008). The function of amino acid auxin conjugates is still unclear, but they have been proposed to serve as storage compounds, inactivation/degradation intermediates, or as an auxin antagonist to inhibit its own activity (Korasick et al., 2013). Having knowledge on the endogenous levels of auxins during nodulation will complement our understanding about the role of auxin during the legume-*Rhizobium* symbiosis.

Here, we tested the effects of two common auxin transport inhibitors, TIBA and NPA, on the roots of *M. truncatula*, subclover (*Trifolium subterraneum*), acacia, *Lotus japonicus*, soybean (*Glycine max*) and *Sesbania rostrata*. We chose *M. truncatula*, subclover and acacia to represent indeterminate nodule-forming legumes; determinate nodule-forming legumes were represented by *L. japonicus* and soybean; *S. rostrata* has been reported to form both nodule types, but potentially prefers to form indeterminate nodules under non-waterlogging and well-aerated conditions, similar to the short-termed flood treatment and growth system used in our study, respectively (Fernández-López et al., 1998). Changes in basipetal auxin transport have not been investigated during legume-*Rhizobium* symbiosis. We investigated acro- and basipetal auxin transport capacity in corresponding root segments in *M. truncatula* and *L. japonicus* to compare the effect of rhizobia infection on bidirectional auxin transport. Finally, we quantified endogenous auxin levels during legume-rhizobia symbiosis using liquid chromatography electrospray-ionisation quadrupole time-of-flight tandem mass spectrometry (LC-ESI-Q-TOF MS/MS) to investigate local changes in auxin concentrations.

4.2 Results

4.2.1 Auxin transport inhibitors induce pseudonodule formation in indeterminate nodule-forming legumes

Auxin transport inhibitors (ATIs), such as TIBA and NPA, have previously been shown to induce pseudonodule formation on the roots of the indeterminate nodule-forming legumes *Medicago truncatula*, alfalfa and pea (Hirsch et al., 1989, Rightmyer and Long, 2011, Scheres et al., 1992). We hypothesised that auxin transport inhibitors can only elicit pseudonodules in indeterminate but not determinate nodule-forming legumes. Because so far auxin transport inhibition has only been demonstrated during the formation of indeterminate nodules, we tested the effects of these auxin transport inhibitors at various concentrations on several indeterminate and determinate nodule-forming legume species, including *M. truncatula*, subclover, acacia, *Lotus japonicus*, soybean and *Sesbania rostrata*. First, we observed the effects of TIBA and NPA on the root growth of *M. truncatula* and *L. japonicus*, as the inhibition of auxin transport is expected to affect the root meristem (Sabatini et al., 1999). As predicted, the application of TIBA and NPA significantly inhibited primary root growth in *M. truncatula* and *L. japonicus* (Figure 4.1). *M. truncatula* root growth was significantly reduced at ATI concentrations starting from 1 μM . The highest TIBA concentration tested, 100 μM , significantly reduced root growth by approximately 45%. However, a ~80% reduction in root growth was already observed with a 10 μM NPA treatment on *M. truncatula* roots. *L. japonicus* was less sensitive towards the ATIs. NPA started inhibiting primary root growth at 10 μM . In comparison, TIBA only caused a slight but not significant growth reduction at 50 μM . Overall, primary root growth was inhibited by NPA more strongly than TIBA ($p < 0.0001$, two-way ANOVA), suggesting that NPA is a more potent auxin transport inhibitor at the expense of severe pleiotropic effects.

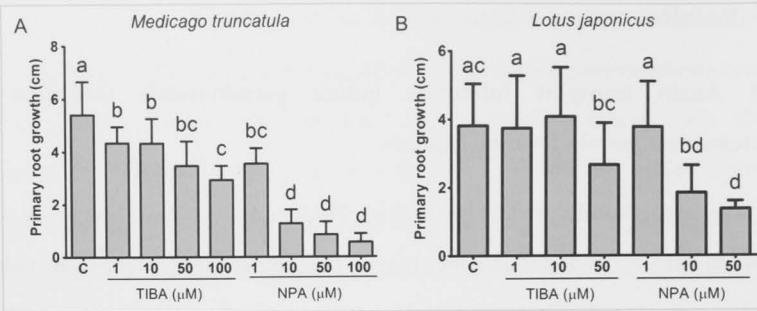


Figure 4.1 Primary root growth in response to TIBA and NPA treatment at various concentrations. Primary root growth was measured at 15 days post treatment for *Medicago truncatula* (A) and 25 days post treatment for *Lotus japonicus* (B). A two-way ANOVA with a Tukey-Kramer multiple comparison post-test was used for statistical analysis. Different lower case letter indicates statistically different root length ($p < 0.05$, $n = 15-20$). Abbreviations: C, control; TIBA, 2,3,5-triiodobenzoic acid; NPA, 1-naphthylphthlamic acid. Graphs show mean and SD. Abbreviation: C, control treatment.

We found that TIBA and NPA application in the concentration range of 1-200 μM induced formation of pseudonodules on the roots of *M. truncatula*, subclover and *S. rostrata*, but not on acacia, *L. japonicus* and soybean. In *M. truncatula* and subclover, there was a significant dose effect on the formation of pseudonodules by ATIs (Figures 4.2 A and B; $p < 0.0001$, two-way ANOVA). The auxin transport inhibitor TIBA showed a significantly higher pseudonodule-forming efficiency compared to NPA in both species (Figure 4.2A and B; $p < 0.001$, two-way ANOVA). The concentration of 50 μM of TIBA and NPA represents the optimal concentration for pseudonodule formation (Figures 4.2A and B).

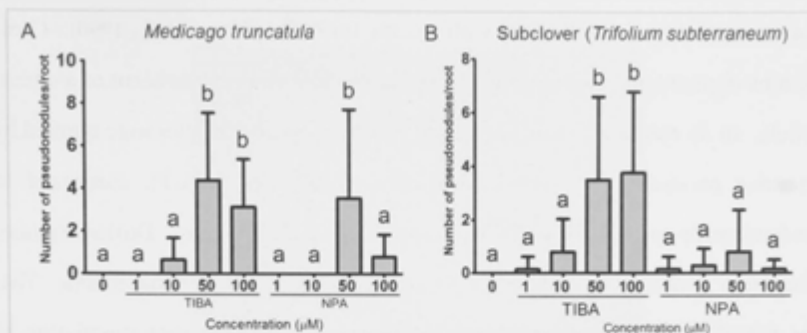


Figure 4.2 Pseudonodule formation in response to TIBA and NPA treatment at various concentrations. Pseudonodes were counted three-weeks post-treatment. Pseudonodule formation on the roots of (A) *Medicago truncatula* and (B) subclover, in response to TIBA and NPA treatment within the concentration range of 0-100 μM. A two-way ANOVA with a Tukey-Kramer multiple comparison post-test was used for statistical analysis. Different lower case letters indicate statistically different number of pseudonodes per plant ($p < 0.05$, $n = 20-25$). Graphs show mean and SD

We observed a variety of pseudonodulation patterns in *M. truncatula*, subclover and *S. rostrata*. The majority of pseudonodes were individual structures, similar to normal nodules (Figures 4.3A and B; 4.4A and B; 4.5A and B). There was a sizeable number of pseudonodes forming adjacent to (Figures 4.4C and D), as well as at the base of lateral roots (Figures 4.4E and F; 4.5C). There were a few pseudonodes forming at the tip of lateral roots (Figures 4.4G and 4.5D). Interestingly, pseudonodes were found along the entire roots of *M. truncatula* and subclover. We noticed that ATIs were even able to induce pseudonodes close to the stems of *M. truncatula* (Figure 4.3C) and subclover seedlings. In many cases, more than 10 pseudonodes were formed on a single seedling, which is far more than the mean nodule number (approximately four nodules / plant) usually obtained in our growth system (Figure 4.6). The external morphology of a pseudonodule was similar to a normal nodule but the internal features were distinct. A rhizobia-induced, functional nodule can be divided into several zones, with each

zone comprising a few cell layers with specific functions (Vasse et al., 1990). Cross sections of pseudonodules revealed a structure which is not reminiscent of a typical nodule. In *M. truncatula*, subclover and *S. rostrata*, pseudonodules were typified by extensive pericyclic and endodermal divisions (Figures 4.7A-F), compared to predominantly cortical cell divisions in rhizobia-induced nodules. During legume-*Rhizobium* symbiosis, a peripheral vasculature develops in a maturing nodule. This was not observed in pseudonodules. Moreover, the primary root vasculature of roots treated with TIBA and NPA was malformed.

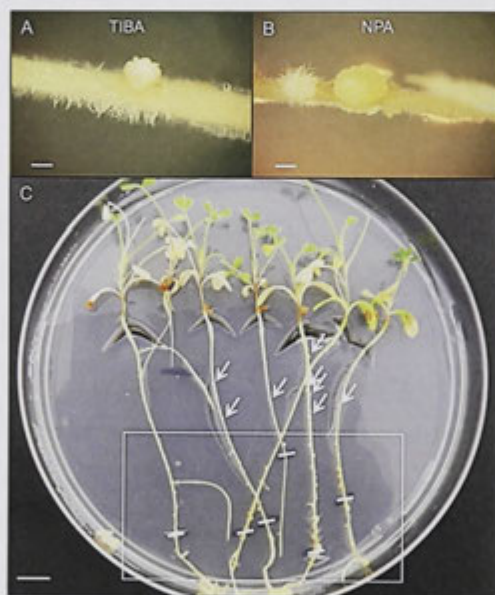


Figure 4.3 Pseudonodule formation in response to TIBA and NPA treatment on *Medicago truncatula* roots. (A) Pseudonodule formation in response to 50 μM TIBA treatment. (B) Pseudonodule formation in response to 50 μM NPA treatment. (C) Pseudonodules were formed along the entire length of the roots. Section encapsulated by the white box indicates the region where the majority of pseudonodules were found. White lines within the box indicate location of the root tip when the roots were first subjected to TIBA treatment. White arrows indicate pseudonodules found at distal parts of the roots. Scale bars represent 1 mm in (A) and (B), and 1 cm in (C).

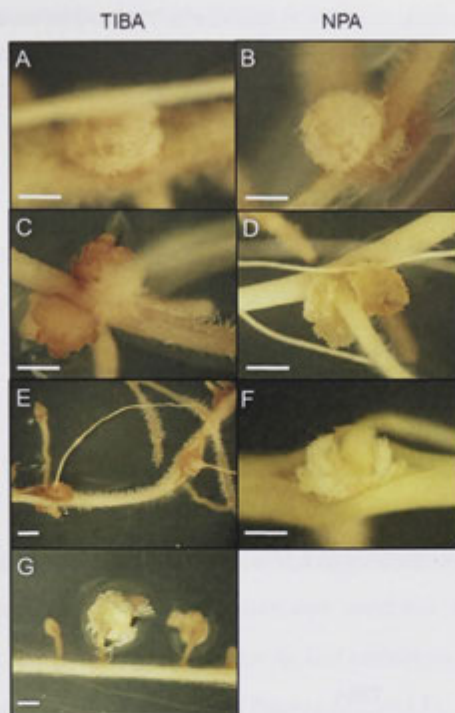


Figure 4.4 Pseudonodule formation in response to TIBA and NPA treatment on subclover roots. Pseudonodules were formed at different sites on the root. They were observed as singular structures (A-B), directly adjacent to a lateral root (C-D), at the base of a lateral root (E-F), and at the tip of a lateral root (G). Scale bars represent 500 μm .

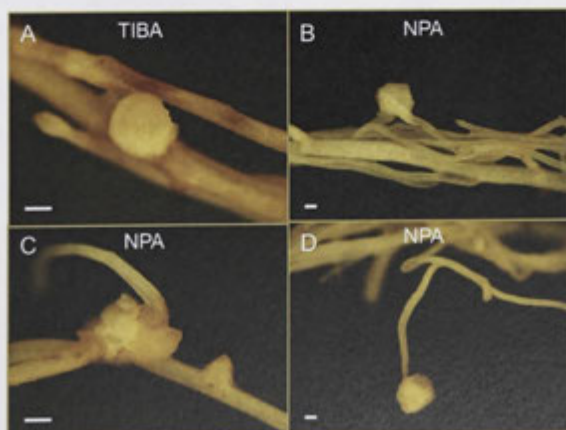


Figure 4.5 Pseudonodule formation in response to TIBA and NPA treatment on *Sesbania rostrata* roots. Pseudonodules were formed at different sites on the root. They were observed as singular structures (A-B), at the base of a lateral root (C) and at the tip of a lateral root (D). Scale bars represent 500 μm .

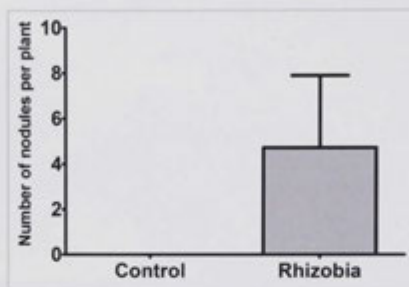


Figure 4.6 Nodulation efficiency on A17 roots in response to local application of rhizobia.

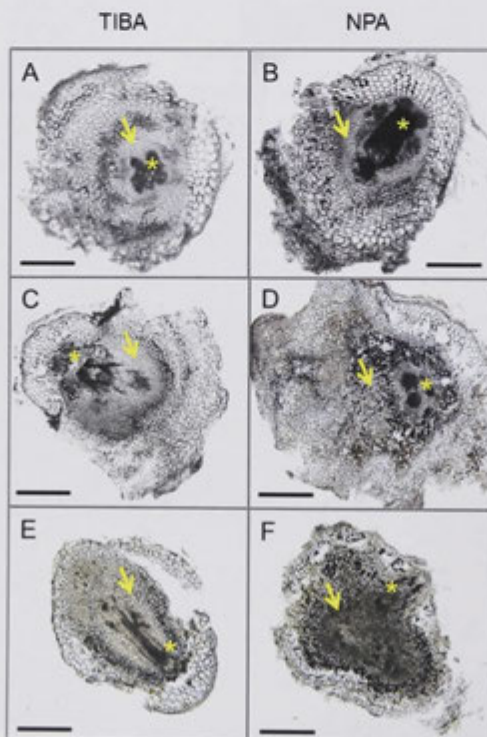


Figure 4.7 Cross sections of pseudonodules induced by TIBA and NPA treatment. Pseudonodules analysed were from *Medicago truncatula* (A-B), subclover (C-D) and *Sesbania rostrata* (E-F). Asterisks indicate location of the primary root vasculature. Arrows indicate pericyclic and endodermal cell divisions. Scale bars represent 500 μm .

Both *M. truncatula* and subclover were grown on petri dishes containing growth media. Due to the size and growth rate of *S. rostrata*, we used a potting system with vermiculite, instead of an *in vitro* system. Although we observed pseudonodules on the roots of *S. rostrata* between the TIBA and NPA concentration range of 10-200 μM , they were fewer compared to pseudonodules that were quantified on *M. truncatula* and subclover roots. Only 10 out of 96 *S. rostrata* plants at various TIBA and NPA concentrations formed pseudonodules on the roots. Similar to pseudonodules on *M. truncatula* and subclover roots, the observed internal structures displayed extensive pericyclic and endodermal divisions, with no apparent nodule vasculature development (Figures 4.7E and F). We did not observe pseudonodules on the stems of *S. rostrata*, despite of its ability to initiate stem nodules (Dreyfus and Dommergues, 1981). Nevertheless, we observed an elevated occurrence of bump-like structures on the stems of *S. rostrata* treated with TIBA and NPA (Figures 4.8D-I), instead of structures more resembling adventitious roots on the stems of mock-treated plants (Figures 4.8A-C). There was no clear central vasculature in these TIBA and NPA-induced bumps, as opposed to those observed in emerging adventitious roots (Figures 4.8B and C). Instead, there was an observable increase in cell divisions in the inner tissue layers (Figures 4.8E, F, H, I).

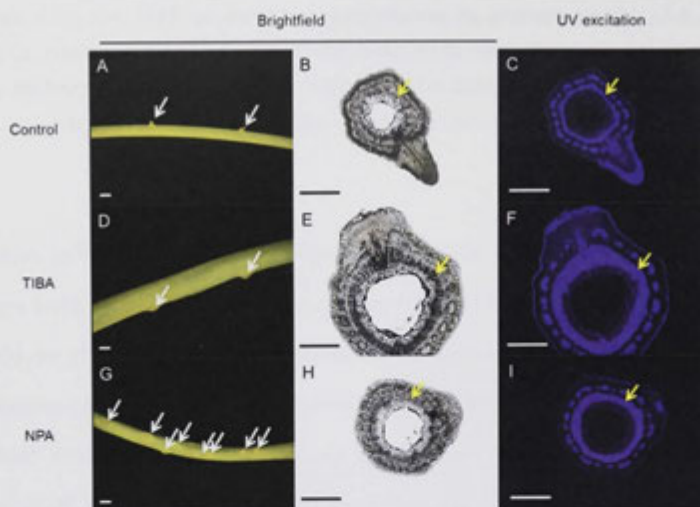


Figure 4.8 Bump-like structures formed on the stems of *Sesbania rostrata* treated with TIBA and NPA. Images show the morphology of lateral structures induced by water (mock treatment) (A-C), TIBA (D-F) and NPA (G-I). Ultraviolet light images highlight tissues with high wood/suberin content. White arrows indicate location of lateral structures. Yellow arrows highlight layers which differ in thickness between TIBA and NPA-treated stems compared to mock-treated stems. Scale bars represent 500 μm .

Finally, we compared changes in the auxin response during the development of a rhizobia-induced nodule, pseudonodule and a hijacked pseudonodule (nodule formed from a pseudonodule) on *M. truncatula* roots. During rhizobial nodule development, auxin response as seen by *GH3:GUS* expression was localised to the dividing pericycle, endodermal and inner cortical cells, at the early stage of nodulation (~ 48 h.p.i.; Figure 4.9B) and later restricted to the nodule meristem and vasculature in a late stage nodule (~ 10 d.p.i.; Figure 4.9C). In mock-inoculated (Figure 4.9A) and mock-flooded (Figure 4.9D) roots, auxin response was mainly observed in the primary root vasculature. Faint and diffuse auxin response was found in the cortical layers of mock-treated roots (Figure 4.9A and D). A distinct auxin response was also visualised in the primary root vasculature of early and late

stage rhizobia-induced nodules (Figure 4.9B and C), but could not be detected in the primary vasculature of the vast majority of roots treated with TIBA (Figure 4.9E, F, H, I, J, K, L). During the early stages of TIBA-induced pseudonodule development, auxin response was observed in the dividing pericycle, endodermis and inner cortex as well (between 5-10 d.p.t; Figure 4.9E-H). Auxin response remained in the inner layers of a late stage pseudonodule (~ 20 d.p.t; Figure 4.9I). It is hypothesised that rhizobia are able to hijack a developing lateral root to form nodules (Mathesius et al., 2000). When *M. truncatula* roots were co-treated with TIBA and *S. meliloti*, we observed that rhizobia were seemingly able to hijack pseudonodule formation to form a rhizobia-colonised nodule (Figure 4.9J-L). These structures are highly similar to rhizobia-induced nodules. Nonetheless, traces of pseudonodule origins could be observed in their slightly malformed primary root vasculature (increased number of protoxylem and xylem poles; Figures 4.9J-L), lack of auxin response in the central vasculature, as well as a slightly thicker outer cortical layer (Figure 4.9K and L). Interestingly, auxin response was observed in the “infection zone” of “hijacked pseudonodules”, but was absent in rhizobia-induced nodules.

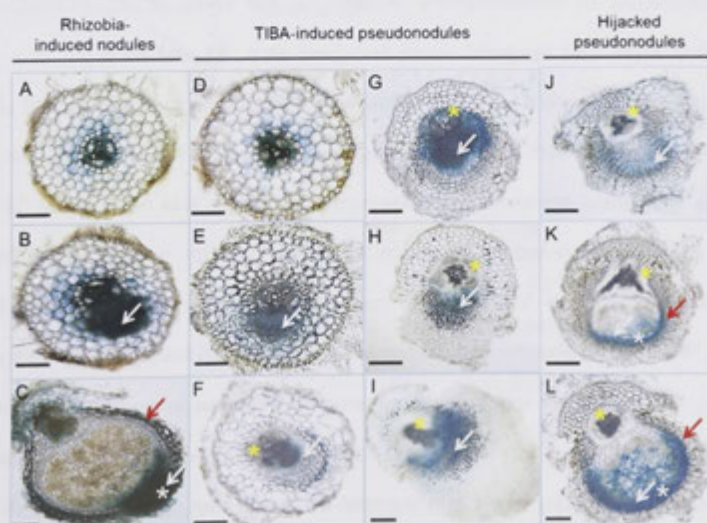


Figure 4.9 Auxin response as seen by *GH3::GUS* expression on *Medicago truncatula* roots. Auxin response in different tissues in a rhizobia-induced nodule (A-C), TIBA-induced pseudonodule (D-I), and a hijacked pseudonodule (J-L). Structures in J-L are possibly pseudonodules that were hijacked, and then rescued by *Sinorhizobium meliloti* during early development, as indicated by the thicker, outer cortical layer, typical of pseudonodules (H-I). White arrows indicate auxin response in dividing cells. Red arrows indicate auxin response in the nodule vasculature. White asterisks indicate the location of the nodule meristem, where an enhanced auxin response is observed. Yellow asterisks indicate malformed vasculature of the primary root. Scale bars represent 200 μm .

4.2.2 Auxin transport regulation in response to *Rhizobium* inoculation is different in indeterminate and determinate nodule-forming legumes

Auxin transport inhibition during legume-*Rhizobium* symbiosis is believed to occur exclusively in indeterminate nodule-forming legumes. However, a combined systematic analysis of auxin transport in both legume types during the early stages of symbiosis has not been published in the literature to date. Furthermore, basipetal auxin transport at the root tip, close to the nodulation susceptible zone, has been largely overlooked. We quantified changes in acro- and basipetal auxin transport in *M. truncatula* and *L. japonicus* in response to *Rhizobium* inoculation. Following spot-inoculation of *Sinorhizobium meliloti* on the roots of *M. truncatula*, we quantified acro- and basipetal auxin transport at 6, 24 and 48 h.p.i. in a 4 mm segment below (acropetal) or encompassing (basipetal) the inoculation spot (Figure 4.10). In agreement with previous findings (van Noorden et al., 2006, Wasson et al., 2006), a significant acropetal auxin transport inhibition was observed at 24 h.p.i., where a one third reduction in auxin transport capacity was measured in root segments treated with *S. meliloti*, in comparison to mock-treated roots (Figure 4.11A). We did not observe any change in acropetal auxin transport capacity at 6 or 48 h.p.i., although there was a significant overall reduction in response to *S. meliloti* treatment ($p < 0.05$; two-way ANOVA). For basipetal auxin transport, we quantified auxin transport capacity in a 4 mm segment above the root tip at 6, 24 and 48 h.p.i..

Here, we measured a significant increase in auxin transport capacity in *S. meliloti*-inoculated root segments compared to mock-treated root segments at 6 and 24 h.p.i. (Figure 4.11B). Interestingly, basipetal auxin transport underwent an even larger overall change (increase) in response to rhizobia inoculation ($p < 0.0001$; two-way ANOVA). Our results showed that in *M. truncatula*, basipetal auxin transport changes in response to *S. meliloti* treatment occur earlier than acropetal auxin transport. In addition, basipetal auxin transport changes were more sustained, as opposed to a more transient nature of acropetal auxin transport inhibition.

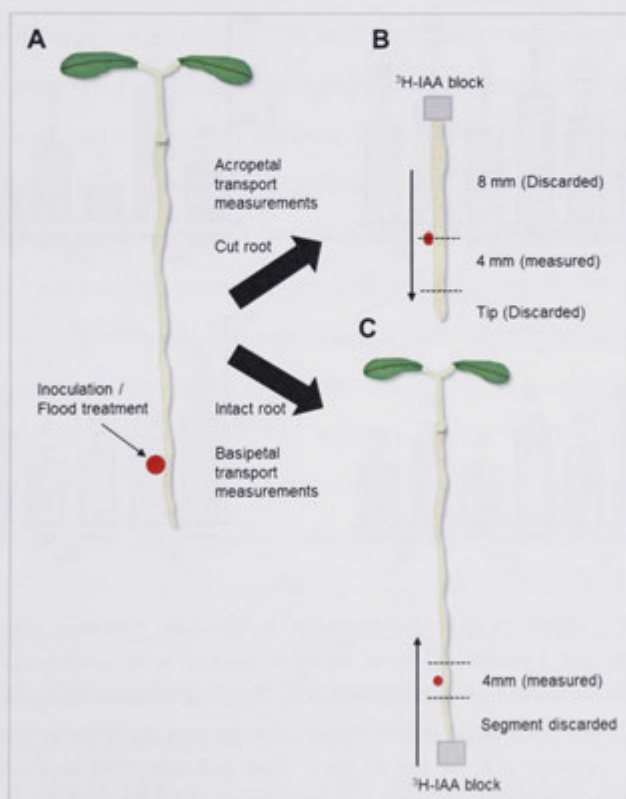


Figure 4.10 Cartoon showing auxin transport measurements performed in this chapter. (A) An intact seedling is treated with rhizobia/flavonoid, either by inoculation or flood treatment. For acropetal transport measurements (B), the root is excised 8 mm from the inoculation spot, or an equivalent spot in a flood-treated root. The cut root is incubated with a ^3H -IAA block touching the cut end. The 8 mm segment directly touching the block is discarded and radioactivity in the segment below the inoculation spot is measured. For basipetal auxin transport measurements (C), an intact seedling is incubated with a ^3H -IAA block touching the root tip. The segment directly touching the block (~4 mm, depending on root growth) is discarded and radioactivity of a 4 mm segment encompassing the inoculation spot is measured.

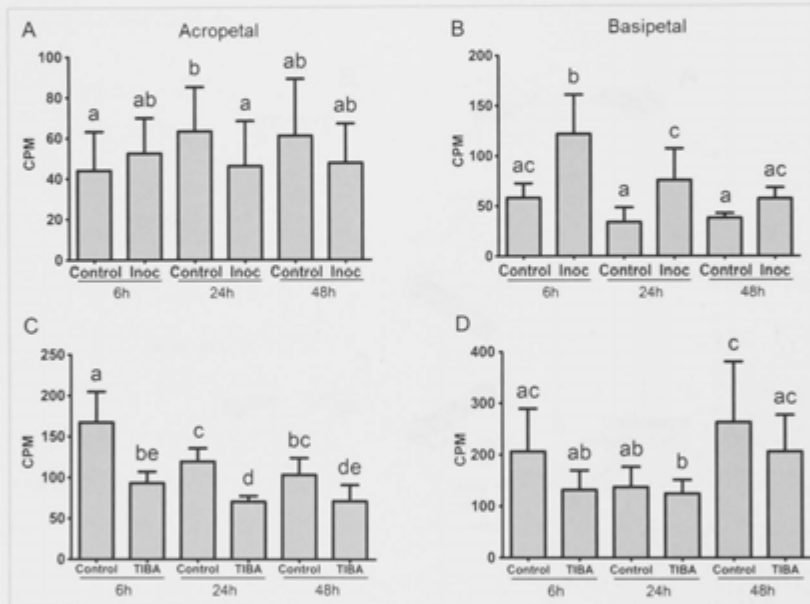


Figure 4.11 Auxin transport measurements in *Medicago truncatula* root segments. Acropetal (A) and basipetal (B) auxin transport capacity were quantified in mock or *Sinorhizobium meliloti*-treated root segments at 6, 24 and 48 hours post inoculation (h.p.i.). Acropetal (C) and basipetal (D) auxin transport capacity were quantified in mock or TIBA-treated root segments at 6, 24 and 48 h.p.i.. Note that total CPM does not reflect an absolute difference between acropetal and basipetal auxin transport. A two-way ANOVA with a Tukey-Kramer multiple comparison post-test was used for statistical analysis ($p < 0.05$, $n = 15-25$). Different lower case letters indicate statistically different auxin transport capacity. Graphs show mean and SD. Abbreviation: CPM, counts per minute.

Next, we performed equivalent measurements on *L. japonicus* roots. To establish the nodulation timeline in *L. japonicus in vitro*, we cultivated *L. japonicus* seedlings in petri dishes and studied nodule development after inoculation with *M. loti* (we did not replicate this study in *M. truncatula* because we have a well-established growth system in the lab for this legume species). We noticed that small but visible nodule bumps could be observed on the roots at the inoculated site at 7 d.p.i., which is similar to another publication (Suzaki et al., 2012). In addition, we consistently obtained nodules directly at, or in very close proximity (within 2 mm) to the inoculation site, indicating a reliable system for studying the nodulation stages (Figure 4.12A and B). An equivalent stage (visible nodule bumps) on *M. truncatula* roots can be seen as early as 72 h.p.i. using our growth system. We wanted to focus on auxin transport changes prior to the formation of visible nodule bumps. Hence, we focussed on measuring auxin transport capacity at the nodule developmental stages before it. Acro- and basipetal auxin transport capacities were quantified in root segments below the inoculation site of *L. japonicus* seedlings that were either mock-treated or inoculated with *M. loti* at 12, 24, 48, 72, 96 and 120 h.p.i.. Our data showed that there was a significantly higher acropetal auxin transport capacity in root segments treated with *M. loti*, in comparison to mock-treated root segments at 48, 96 and 120 h.p.i. (Figure 4.13A). Although no significant change was observed at either 6, 24 or 72 h.p.i., there was a general increase in acropetal auxin transport capacity across all measurements ($p < 0.0001$; two-way ANOVA). This is opposite to what was obtained in the case of *M. truncatula* roots in response to *S. meliloti* treatment. Similar results were obtained for basipetal auxin transport measurements. A significant elevation in basipetal auxin transport capacity in root segments in response to *M. loti* treatment occurred at 48 and 120 h.p.i. (Figure 4.13B). Furthermore, there was an overall significant inoculation effect on basipetal auxin transport capacity ($p < 0.01$; two-way ANOVA), albeit less profound than the changes in acropetal auxin transport (Figure

4.13A). Intriguingly, we could not fail to notice a slight but significant inhibition of both acro- and basipetal auxin transport between 24-33 h.p.i. in *L. japonicus* roots after *M. loti* treatment. Indeed, we quantified a significant decrease in acro- and basipetal auxin transport on separate occasions (Figure 4.14A and B). The fact that this trend was observed multiple times suggests it is not a coincidence.

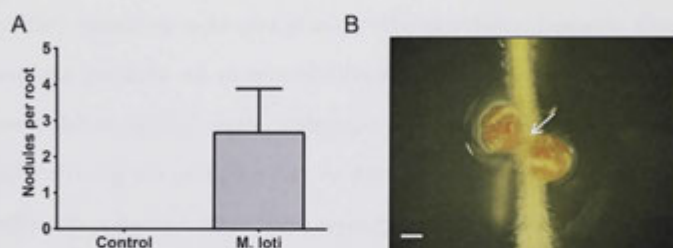


Figure 4.12 Nodulation on *Lotus japonicus* roots 20 d.p.i. with *Mesorhizobium loti*. (A) Nodules per root on *L. japonicus* roots spot-inoculated with *M. loti* ($n=40$). (B) Nodules forming at the site of *M. loti* inoculation. White arrow indicates the inoculation site. Scale bar represents 1 mm. Graph shows mean and SD.

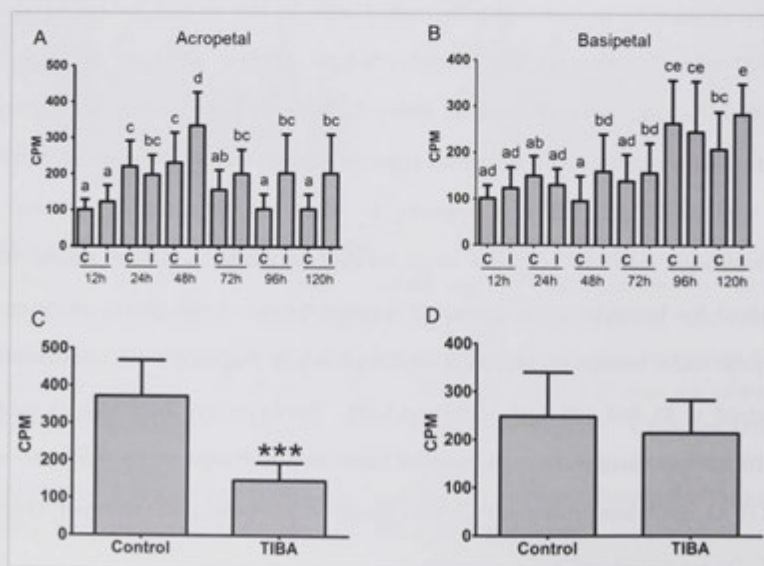


Figure 4.13 Auxin transport measurements in *Lotus japonicus* root segments. Acropetal (A) and basipetal (B) auxin transport capacity were quantified in mock or *Mesorhizobium loti*-treated root segments at 12, 24, 48, 72, 96 and 120 hours post inoculation (h.p.i.). A two-way ANOVA with a Tukey-Kramer multiple comparison post-test was used for statistical analysis ($p < 0.05$, $n = 25-30$). Acropetal (C) and basipetal (D) auxin transport capacity were quantified in mock or TIBA-treated root segments at 48 h.p.i.. A Student's *t*-test was used for statistical analysis ($p < 0.05$, $n = 25-30$). Note that total CPM does not reflect an absolute difference between acropetal and basipetal auxin transport. Different lower case letters in A and B indicate statistically different auxin transport capacity. In (C), *** indicates an extremely very significant change ($p < 0.0001$). Graphs show mean and SD. Abbreviations: CPM, counts per minute; C, control treatment; I, inoculated.

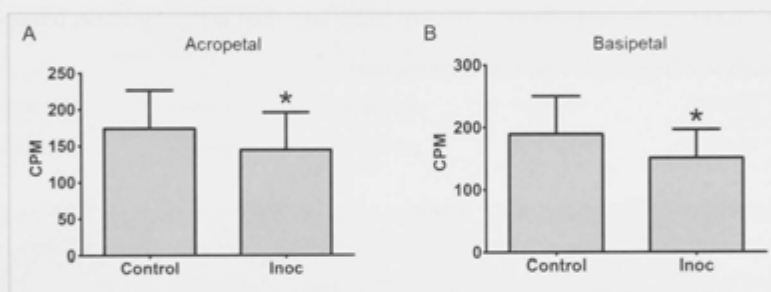


Figure 4.14 Auxin transport inhibition in *Lotus japonicus* roots in response to rhizobia inoculation. (A) Acropetal (at 33 h.p.i.) and (B) basipetal (at 24 h.p.i.) auxin transport capacity were quantified in mock or *Mesorhizobium loti*-inoculated root segments. A Student's *t*-test was used for statistical analysis ($p < 0.05$, $n = 25$). Asterisks indicate significant change in auxin transport capacity. Graphs show mean and SD. Abbreviation: CPM, counts per minute.

As mentioned in the previous paragraph, we have established growth systems which consistently produced localised nodule development in *M. truncatula* and *L. japonicus*. To reconcile the individual developmental stages with changes in auxin transport capacities, we examined root morphology of *S. meliloti*- and *M. loti*-treated roots of *M. truncatula* and *L. japonicus*, respectively. We confirmed the slower development of *L. japonicus* nodules compared to *M. truncatula* nodules, by visually assessing the extent of cortical cell divisions present at each individual stage.

In *M. truncatula* roots, the first visible cell division can be observed as early as 24 h.p.i. (Figure 4.15C), in agreement with a recent report by Xiao et al. (2014). This stage is also when acropetal auxin transport inhibition occurs (Figure 4.15C and 4.11A). At 48 h.p.i., multiple cell divisions had occurred at the pericycle and inner cortex (Figure 4.15D). At 0 and 6 h.p.i., cell division could not be observed, although basipetal auxin transport had increased at 6 h.p.i. (Figure 4.15A and B; 4.11B). In *L. japonicus*, cell division could not be observed at 0, 12, 24 and 48 h.p.i., although a single cortical cell division was possibly observed at 48 h.p.i. on one occasion (Figure 4.16A-D). Visible outer cortical cell divisions were reliably observed at 72, 96 and 120 h.p.i. (Figure 4.16E-G), when acropetal auxin transport capacity was increased in nodule-forming roots.

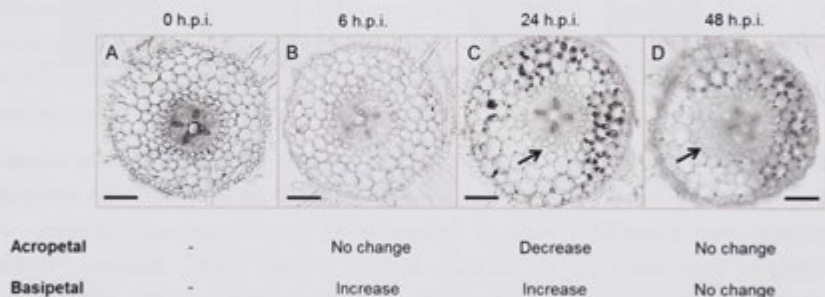


Figure 4.15 Nodule development in *Medicago truncatula*. Cross sections of roots showing the stages of nodulation at 0 hours post inoculation (h.p.i.) (A), 6 h.p.i. (B), 24 h.p.i. (C) and 48 h.p.i. (D). Changes in acro- and basipetal auxin transport at each individual stage are summarised below each figure. Approximately 10 roots were examined at each stage. Black arrows indicate pericyclic and cortical cell divisions. Scale bars represent 200 μm .

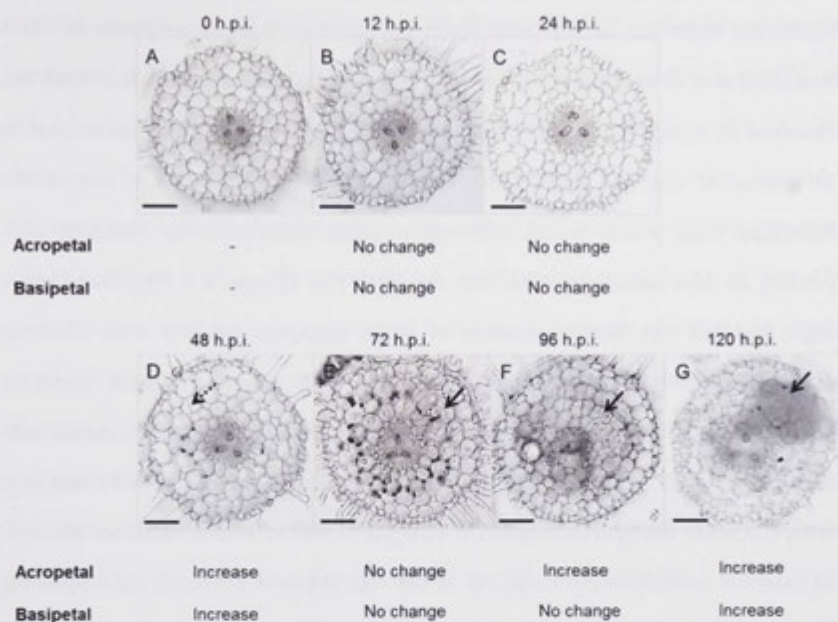


Figure 4.16 Nodule development in *Lotus japonicus*. Cross sections of roots showing the stages of nodulation with *Mesorhizobium loti* at 0 hours post inoculation (h.p.i.) (A), 12 h.p.i. (B), 24 h.p.i. (C), 48 h.p.i. (D), 72 h.p.i. (E), 96 h.p.i. (F) and 120 h.p.i. (G). Changes in acro- and basipetal auxin transport at each individual stage are summarised below each figure. Approximately 10 roots were examined at each stage. Black arrows indicate cortical cell divisions. Dotted black arrow in D indicates possible cortical cell division. Scale bars represent 200 μm .

In section 4.2.1, we demonstrated the ability of auxin transport inhibitors to induce pseudonodule formation on the roots of *M. truncatula*, but not *L. japonicus*. To confirm that the formation of pseudonodules was due to a reduction in auxin transport, we measured acro- and basipetal auxin transport capacity in root segments of *M. truncatula* and *L. japonicus* following TIBA treatment. We chose TIBA instead of NPA because it confers less pleiotropic effects on the roots at the concentrations that were being used to initiate pseudonodules (50 μM , Figure 4.1). We confirmed the reduction of acro-, but not basipetal auxin transport by TIBA in both *M. truncatula* and *L. japonicus* root segments. In *M. truncatula*, we observed a

significant reduction of acropetal auxin transport capacity in response to TIBA treatment at 6, 24 and 48 h.p.t. (Figure 4.11C). Similarly, a significant reduction was observed in *L. japonicus* at 48 h.p.t. (Figure 4.13C). Basipetal auxin transport in *M. truncatula* was not significantly affected by TIBA treatment at any of the individual time points tested, although a global reduction was observed after pooling all time points ($p < 0.01$; two-way ANOVA) (Figure 4.11D). There was a slight but not significant reduction of auxin transport capacity with TIBA in *L. japonicus* roots at 48 h.p.t. (Figure 4.13D). In summary, auxin transport regulation in *M. truncatula* and *L. japonicus* roots in response to treatments with their corresponding microsymbionts differ. Both legume species showed a transient acropetal auxin transport inhibition at 24 h.p.i., as well as a more sustained increase in basipetal auxin transport capacity in the root segment below, or encompassing the *Rhizobium*-inoculated spot, respectively. However, unlike *M. truncatula*, *L. japonicus* exhibited a longer and significant increase in acropetal auxin transport capacity below the *Rhizobium*-inoculated spot. This suggests an increased export of auxin from the site of nodule initiation in *L. japonicus*.

4.2.3 Comparison of auxin content during nodule development and in mature nodules

During nodule organogenesis, local auxin concentration in the nascent nodule could be affected by local auxin biosynthesis, conjugation/breakdown, and/or transport. These factors are hypothesised to contribute synergistically to a net change in auxin concentration. Liquid chromatography-mass spectrometry (LC/MS) is a sensitive analytical tool for measuring trace amounts of phytohormones (Pan and Wang, 2009). We used an LC-ESI-Q-TOF MS/MS system developed in Chapter 3 to measure changes in auxins during the earlier stages of nodulation in *M. truncatula* and *L. japonicus*. We quantified auxins in a segment surrounding the

inoculation spot at 6, 24 and 48 h.p.i. in *M. truncatula* roots. Our data showed a significant increase in IAA concentration in roots inoculated with *S. meliloti* at 24 h.p.i. (Figure 4.17A). This increase was not observed at either 6 or 48 h.p.i.. No change in IBA concentration was noted at any time point (Figure 4.16B). For IAA-Ala, there was a progressive decrease in concentration overtime ($p < 0.0001$, two-way ANOVA; Figure 4.17C). There was also a significant downregulation of IAA-Ala concentration at 48 h.p.i. in response to *S. meliloti* treatment. Although IAA-Asp could not be detected in our samples, we consistently measured relatively high levels of an IAA-Asp-like compound showing similar mass fragments to IAA-Asp, but eluting more than 1.5 s apart (Figure 4.17G). The auxins PAA, 4-Cl-IAA and IAA-Val were not consistently detected (Figures 4.17D-F). We could not detect IAA-Leu/Ile, IAA-Phe and IAA-Trp in *M. truncatula* root samples. Since TIBA treatment induces pseudonodule formation on *M. truncatula* roots, we investigated if a similar change in auxin concentration could be observed during pseudonodule formation. We quantified auxins in TIBA-treated *M. truncatula* roots at 6, 24 and 48 h.p.t.. The concentration of IAA was significantly reduced at 24 h.p.t. in response to TIBA treatment (Figure 4.18A). Although no significant reduction was measured at 6 and 48 h.p.t., an overall significant reduction in IAA concentration was observed ($p < 0.01$; two-way ANOVA). An IAA-Asp-like compound was also detected, albeit at levels much lower than in *S. meliloti*-treated roots (Figure 4.18B). Other auxins could not be detected in TIBA-treated *M. truncatula* roots.

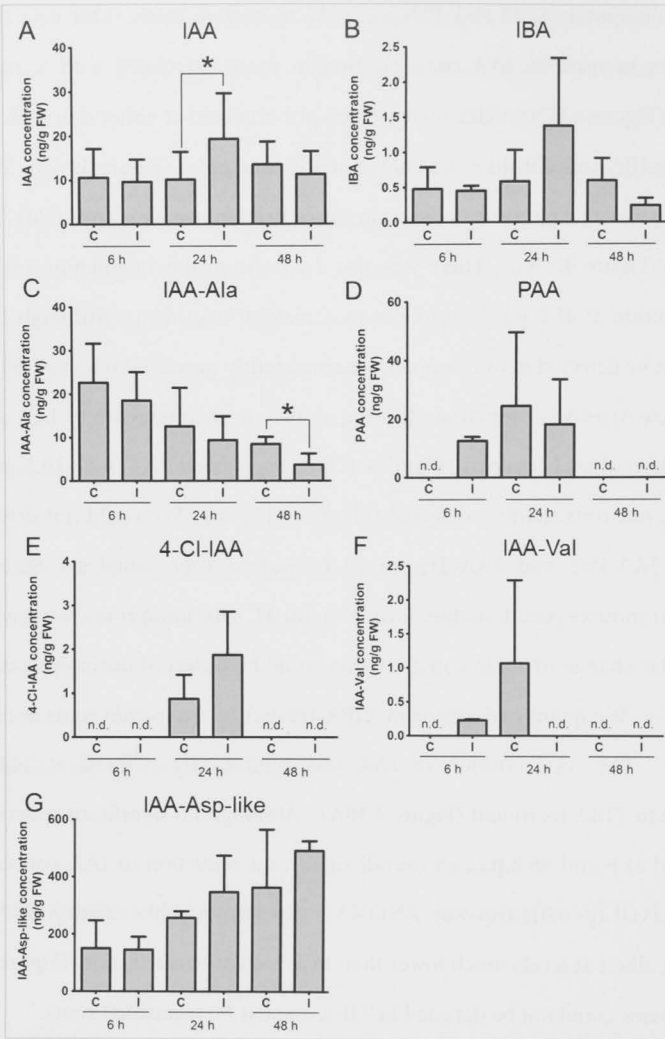


Figure 4.17 Auxin content in developing *Medicago truncatula* nodules (segments around the inoculation site). Endogenous auxin concentration (ng g^{-1} FW) in *M. truncatula* roots inoculated with *Sinorhizobium meliloti* and mock-treated roots were measured at 6, 24 and 48 hours post treatment (h.p.t.). Auxins detected in *M. truncatula* roots include (A) IAA, (B) IBA and (C) IAA-Ala. (D) PAA, (E) 4-Cl-IAA and (F) IAA-Val were not consistently detected at all time points. A compound hypothesised to have high structural similarity to IAA-Asp (G) was also detected. A two-way ANOVA and a Student's *t*-test were used for statistical analysis ($p < 0.05$; $n = 2-10$). Asterisks in (A) and (C) indicate significant difference in auxin concentration ($p < 0.05$). Graphs show mean and SD. Abbreviations: FW, fresh weight; C, control treatment; I, inoculated; n.d., not detected.

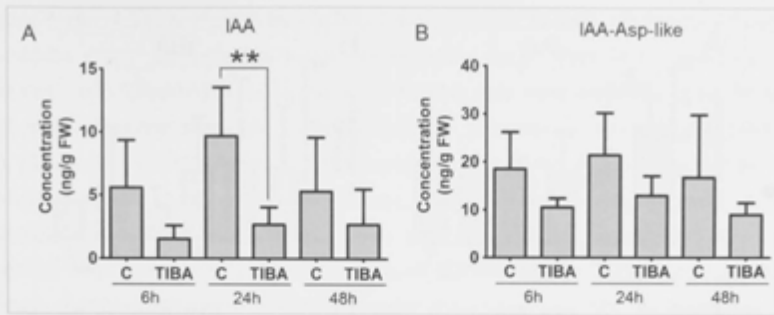


Figure 4.18 Auxin concentration in TIBA-treated *Medicago truncatula* root segments of similar developmental stage as those for nodules in Figure 4.17. IAA (A) and an IAA-Asp-like compound (B) were detected in *M. truncatula* roots at 6, 24 and 48 hours post treatment (h.p.t.). A two-way ANOVA and a Student's *t*-test were used for statistical analysis ($p < 0.05$; $n = 3-5$). Asterisks in A indicate a very significant change in IAA concentration. Graphs show mean and SD. Abbreviations: FW, fresh weight; C, control treatment.

To compare the auxin content in *L. japonicus* roots during nodule development, we quantified auxins in root segments surrounding the *M. loti* treated site at 24 h, 48 h and 5 d.p.i.. Opposite to what we found in *M. truncatula*, there was a slight but significant decrease in IAA concentration at 24 h.p.i. (Figure 4.19A). There was no significant change in IAA concentration at 48 h and 5 d.p.i. in response to *M. loti* treatment. The auxins IBA, IAA-Ala, IAA-Asp and IAA-Leu/Ile were detected in *L. japonicus* roots, although there were no significant changes in their respective concentrations following *M. loti* treatment (Figures 4.19B-E). Interestingly, we once again detected an IAA-Asp-like compound in the roots at relatively higher levels than other auxins (Figure 4.19I). Furthermore, there was a significant reduction in the concentration of the IAA-Asp-like compound at 48 h.p.i. in response to *M. loti* treatment (~ 3 fold) and a very significant overall reduction from *M. loti* treatment ($p < 0.01$, two-way ANOVA). The auxins 4-Cl-IAA, IAA-Phe and IAA-Trp were not consistently detected at all time points (Figures 4.18F-H). We could not detect IAA-Val in the roots of *L. japonicus*.

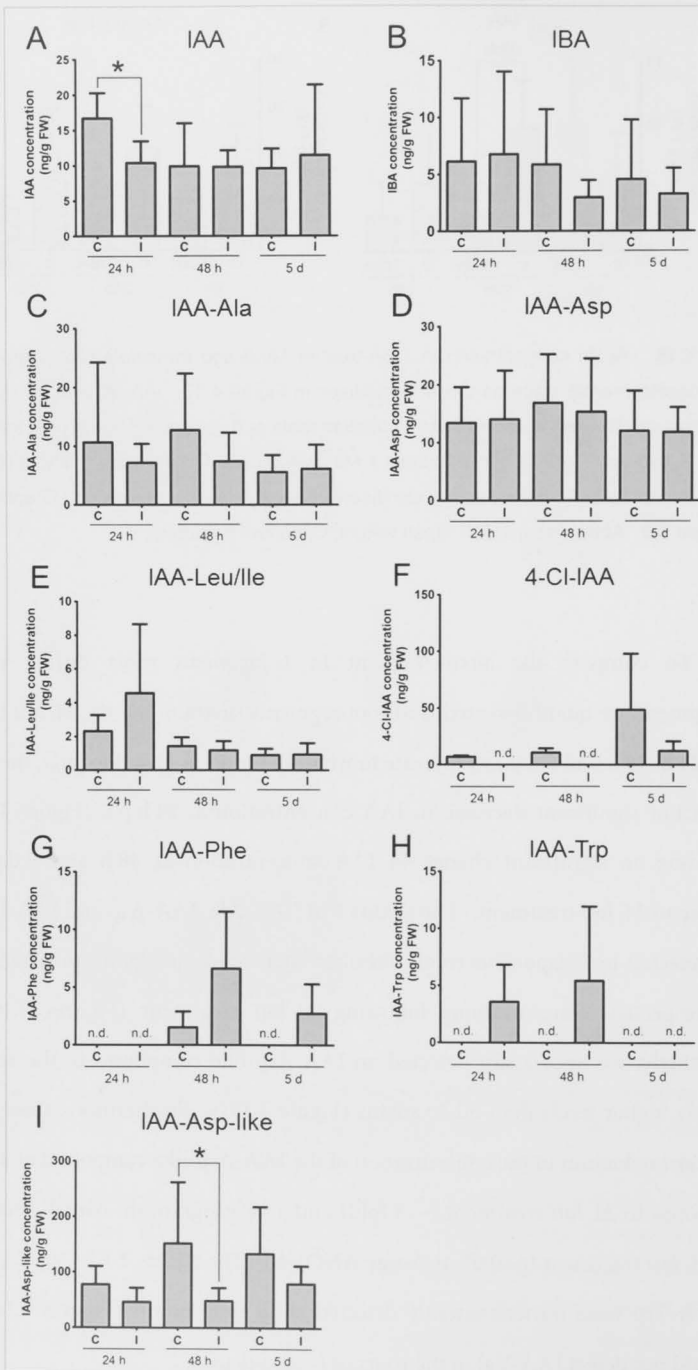


Figure 4.19 Auxin content in developing *Lotus japonicus* nodules (segments around the inoculation site). Endogenous auxin concentration (ng g^{-1} FW) in *L. japonicus* roots inoculated with *Mesorhizobium loti* and mock-treated roots were measured at 24, 48 hours post- and 5 days post treatment. Auxins detected in *L. japonicus* roots include (A) IAA, (B) IBA, (C) IAA-Ala, (D) IAA-Asp and (E) IAA-Leu/Ile. (F) 4-Cl-IAA, (G) IAA-Phe and (H) IAA-Trp were not consistently detected at all time points. A compound hypothesised to have high structural similarity to IAA-Asp (I) was also detected. A two-way ANOVA and a Student's *t*-test were used for statistical analysis ($p < 0.05$; $n = 2-6$). Asterisks in (A) and (I) indicate significant difference ($p < 0.05$). Graphs show mean and SD. Abbreviations: FW, fresh weight; C, control treatment; I, inoculated; n.d., not detected.

Next, we quantified auxins in mature nodules (four-week-old) of *M. truncatula*, *L. japonicus* and soybean. The auxins IAA, IAA-Ala, IAA-Asp, IAA-Val and PAA were detected in nodules of all three legumes (Figure 4.20A-C). Interestingly, the auxin PAA, which was not detected in the roots of *M. truncatula* and *L. japonicus*, was present at high quantities (176 and 460 ng g^{-1} FW, respectively) in the nodules of both legumes (Figure 4.20A and B). The auxin conjugate IAA-Asp, which was undetectable in *M. truncatula* roots, was present in *M. truncatula* nodules (8.8 ng g^{-1} ; Figure 4.20A) and was found at significantly higher levels in *L. japonicus* nodules ($> 2000 \text{ ng g}^{-1}$; Figure 4.20B). IAA was present at different concentrations in all three legumes, i.e. at 6.2 , 66.9 and 26.0 ng g^{-1} FW in *M. truncatula*, *L. japonicus* and soybean, respectively (Figure 4.20A-C). The auxin 4-Cl-IAA was only detected in the nodules of *M. truncatula* (4.3 ng g^{-1} FW; Figure 4.20A); IBA was only detected in soybean nodules (2.7 ng g^{-1} ; Figure 4.20 C); IAA-Trp was only detected in *L. japonicus* nodules (6.2 ng g^{-1} ; Figure 4.20B). We once again could not fail to notice the overwhelming presence of an IAA-Asp-like compound, which reached significantly higher concentrations of $> 9000 \text{ ng g}^{-1}$ FW in *M. truncatula* nodules (Figure 4.20D). It was also found at comparatively high levels in *L. japonicus* (97.2 ng g^{-1} FW) and soybean (415.2 ng g^{-1} FW).

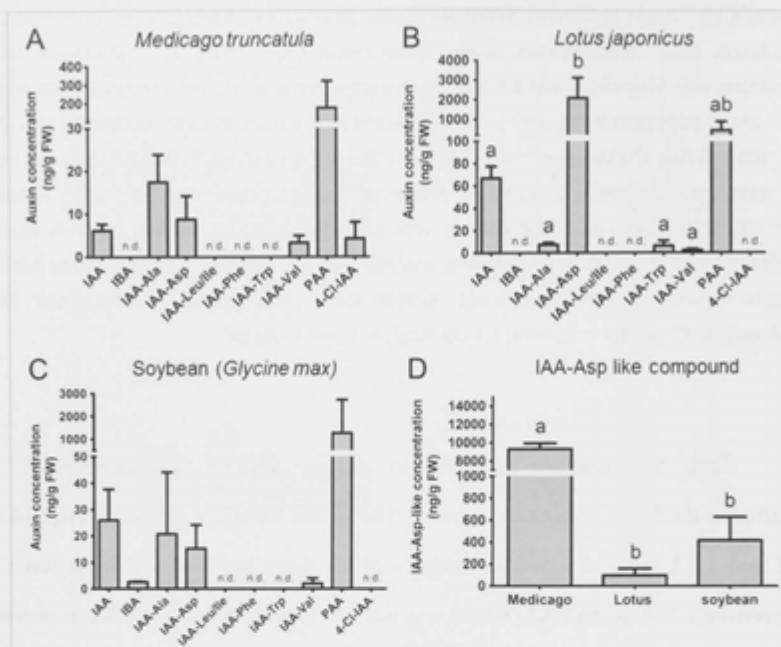


Figure 4.20 Auxin content in mature 4-week-old nodules. Endogenous auxin concentration (ng g^{-1} FW) in nodules of (A) *Medicago truncatula*, (B) *Lotus japonicus* and (C) soybean were quantified. (D) An IAA-Asp-like compound was detected in all three legumes. Auxin species detected in each legume differs. A one-way ANOVA was used for statistical analysis ($p < 0.05$; $n = 2-4$). Different lowercase letters indicate significant differences in auxin content. Graphs show mean and SD. Abbreviation: FW, fresh weight; n.d., not detected.

4.2.4 Auxin content in nodulating and non-nodulating non-legumes

It is generally thought that IAA is the primary active auxin during plant organogenic events (Overvoorde et al., 2010). A report by Perrine-Walker et al. (2010) suggests that PAA, another active auxin, might be as important as IAA during actinorhizal nodule formation, at least based on its abundance. Indeed, auxin measurements in *M. truncatula*, *L. japonicus* and soybean suggest a role for PAA, and other auxins, during nodule development and maintenance of mature nodules. To compare auxin requirements between legumes and non-legumes, we quantified auxins in the roots (non-symbiotic conditions) of a few nodulating non-

legumes, including the actinorhizal species *Datisca glomerata*, *Casuarina glauca* and *Coriaria myrtifolia*. In *D. glomerata*, PAA was consistently found at significantly higher concentrations than IAA in primary roots (52.7 vs 1.8 ng g⁻¹ FW; Figure 4.21A), hairy roots (119.9 vs 2.0 ng g⁻¹ FW; Figure 4.21B) and nodules (73.5 vs 1.5 ng g⁻¹ FW; Figure 4.21C). The auxin conjugate IAA-Asp was measured at 10.2 ng g⁻¹ FW in primary roots (Figure 4.21A) and 564.9 ng g⁻¹ FW in hairy roots (Figure 4.21B), suggesting an important role for IAA-Asp in hairy roots. IAA-Ala was found in the range of 1.0-2.5 ng g⁻¹ FW in all *D. glomerata* tissues. The auxins IAA-Phe and IAA-Val were only detectable in the primary roots of *D. glomerata* (Figure 4.21A).

Auxins were also quantified in the roots of the actinorhizal species *C. glauca* and *C. myrtifolia*. The main auxins detected in both species were PAA (57.9 ng g⁻¹ FW; Figure 4.22A) and IAA-Asp (8.7 ng g⁻¹ FW; Figure 4.22B), respectively. The auxins IAA, IBA and 4-Cl-IAA were detected at similar proportions in both species. Most other auxins were not detectable in *C. glauca* and *C. myrtifolia*, except for IAA-Ala and IAA-Phe, which were measured at 2.9 and 4.3 ng g⁻¹ FW, respectively, in *C. myrtifolia* (Figure 4.22B). Because PAA was present in the roots of *D. glomerata* in relatively high concentrations, we hypothesised that PAA might be a major auxin in plants belonging to the Cucurbitales order, in general. To test this hypothesis, we quantified auxins in two other non-nodulating species belonging to the Cucurbitales order, i.e. cucumber and begonia, which are non-actinorhizal species. Although PAA was the major auxin compound in cucumber (72.2 ng g⁻¹ FW; Figure 4.22C), PAA could not be detected in begonia (Figure 4.21D). Only the auxins IAA (3.8 ng g⁻¹ FW) and IAA-Asp (17.1 ng g⁻¹ FW) could be detected in begonia. In cucumber roots, IAA, IAA-Ala, IAA-Phe and IAA-Trp were all present in the range of 3.2-5.1 ng g⁻¹ FW (Figure 4.22C).

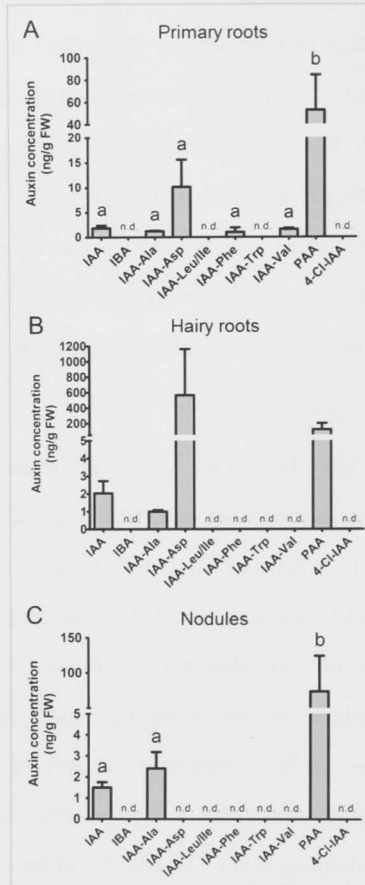


Figure 4.21 Auxin measurements with LC-MS/MS in *Datisca glomerata* root tissue. Concentrations of auxins were measured in the primary roots (A), hairy roots (B) and nodules (C). A one-way ANOVA with a Tukey-Kramer multiple comparison post-test was used for statistical analysis ($n=2-6$). Different lower case letters in (A) and (C) indicate statistically different auxin concentration in ng g^{-1} FW. Graphs show mean and SD. Abbreviation: FW, fresh weight; n.d., not detected.

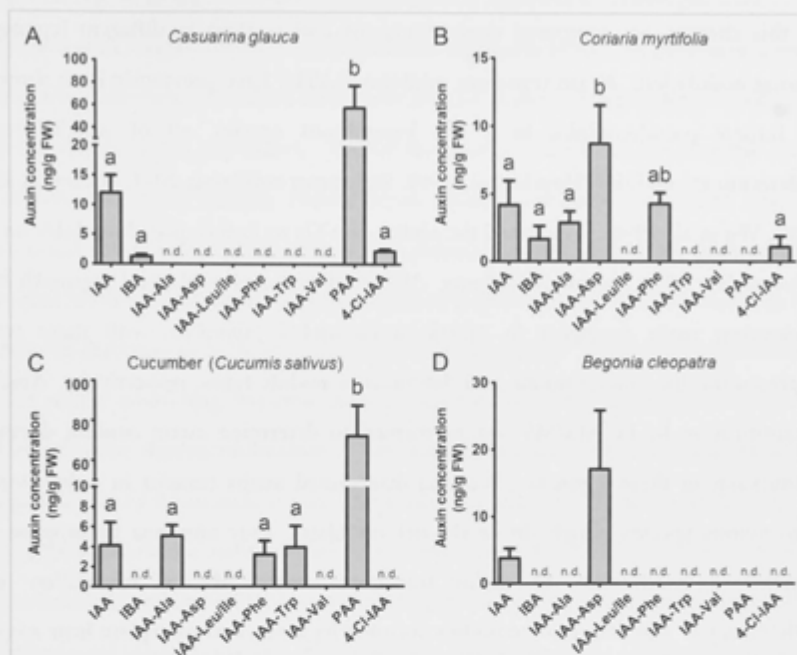


Figure 4.22 Auxin measurements with LC-MS/MS in root tissue. Concentrations of auxins were measured in the roots of *Casuarina glauca* (A), *Coriaria myrtifolia* (B), *Cucumis sativus* (C) and *Begonia cleopatra* (D). A one-way ANOVA with a Tukey-Kramer multiple comparison post-test was used for statistical analysis ($n=2-6$). Different lower case letters indicate statistically different auxin concentration in ng g^{-1} FW. Graphs show mean and SD. Abbreviation: FW, fresh weight; n.d., not detected.

4.3 Discussion

In this chapter, we compared auxin transport and content in different legumes during nodulation. Auxin transport inhibitors (ATIs) have previously been shown to initiate pseudonodules in a few leguminous species, all of which form indeterminate nodules (Hirsch et al., 1989, Rightmyer and Long, 2011, Scheres et al., 1992, Wu et al., 1996). We tested the ability of ATIs to induce pseudonodules on a selected few other leguminous plants. We employed a physiological approach by measuring auxin transport in *M. truncatula* and *L. japonicus*, with these two representing the indeterminate and determinate nodule types, respectively. Auxin quantification by LC-MS/MS was performed to determine auxin content during nodulation in these legumes. We also determined auxin content in a few non-leguminous species, which do or do not nodulate. Our aim was to propose a generalised mechanism of auxin transport control during nodulation in indeterminate and determinate nodule-forming legumes, and to explain how auxin transport regulation relates to auxin content and response at a given time. Furthermore, we hypothesised that different auxins may play a more prominent role in different nodulating plants.

4.3.1 Auxin transport regulation occurs bidirectionally during *Medicago truncatula* and *Lotus japonicus* nodule development

Our data showed that changes in auxin transport in response to rhizobia treatment occur in the acro- and basipetal directions. Consistent with previous results in *M. truncatula*, we observed a transient reduction in acropetal auxin transport following rhizobia treatment (Plet et al., 2011, van Noorden et al., 2006, Wasson et al., 2006). For *L. japonicus*, Pacios-Bras et al. (2003) previously demonstrated a significant increase in acropetal auxin transport capacity in response to Nod factor treatment at 48 h.p.i.. Here, we included two additional features to our

measurements: (1) we included additional time points at the early stages to assess if this increase in auxin transport capacity was of a transient or prolonged nature; (2) we measured auxin transport consistently in segments below the inoculation spot. Crucially, this study provides a direct comparison of two corresponding segments in *M. truncatula* and *L. japonicus*. Unlike the short-term nature of acropetal auxin transport inhibition during indeterminate nodule initiation, we found that an increased auxin transport capacity in *L. japonicus* was more sustained. Interestingly, we also found an increased auxin transport in response to rhizobia treatment in the basipetal direction in both *M. truncatula* and *L. japonicus*. We are not aware of any prior study examining basipetal auxin transport from the root tip towards the infection zone during nodulation. The requirement for basipetal auxin transport regulation in *M. truncatula* is consistent with two previous reports. Firstly, Huo et al. (2006) observed a reduced nodulation capacity in MtPIN2 knockdown roots of *M. truncatula*, where MtPIN2 is an ortholog of AtPIN2, an auxin carrier responsible for basipetal auxin transport in *Arabidopsis* (Rashotte et al., 2000). Secondly, a slight but significant increase in MtPIN2 mRNA expression was measured in *M. truncatula* WT roots in response to rhizobia treatment, and a ~ 5 fold increase was observed in the supernodulating *skl* mutant (Prayitno et al., 2006). These data strongly suggest a positive role for MtPIN2 and basipetal auxin transport during nodulation. Furthermore, knockdown of MtPIN4 (ortholog of AtPIN1 for acropetal auxin transport) in *M. truncatula* roots reduced nodulation (Huo et al., 2006), and transcription of this gene was one of the most highly upregulated by Nod factor treatment (Plet et al., 2011), strongly suggesting that acropetal auxin transport regulation might occur through MtPIN4.

Genetic studies on the role of auxin transport carriers during nodulation in *L. japonicus* are lacking. One report highlighted the role of an ABCB-type multidrug resistance protein, LjABCB1, in mature *L. japonicus* nodules, but did not examine its role during early nodule development. The authors proposed that

LjABCBI exports auxin towards infected cells in the nodule, based on the selective localisation of the protein at adjacent uninfected cells (Takanashi et al., 2012). In the current study, we demonstrated that basipetal auxin transport capacity in *L. japonicus* increased at two distinct early time points following rhizobia treatment. Surprisingly, we found an inhibition of acro- and basipetal auxin transport in *L. japonicus* roots in response to rhizobia treatment in separate experiments. The inhibition of auxin transport in both directions happened between 24-33 h.p.i., whereas auxin transport capacity was consistently increased at later time points. Identification and functional characterisation of the *L. japonicus* auxin carrier orthologs would advance our current knowledge of the role of auxin transport during nodulation in determinate legumes. Collectively, the results presented here highlight the importance of acro- and basipetal auxin transport regulation during nodulation, and point to a difference in acropetal auxin transport capacity between legumes forming indeterminate and determinate nodules.

4.3.2 Nodule and pseudonodule formation involve an increased auxin response

The results obtained suggest an increased basipetal auxin transport in response to rhizobia treatment as a common mechanism in indeterminate and determinate nodule-forming legumes. Indeed, we found an increased auxin response in the dividing cortical cells, endodermis and pericycle of *M. truncatula* nodule primordia (Figure 4.9), which was also observed at a similar stage during nodulation in *L. japonicus* (Suzaki et al., 2012, Takanashi et al., 2011). Although histological features of pseudonodules appear different to rhizobia-induced nodules, we also observed an increased auxin response in dividing cells of a developing pseudonodule. However, in a fully-developed pseudonodule, auxin response remains in the dividing pericycle and inner cortical cells, presumably due to the lack

of *S. meliloti*-mediated, coordinated cell divisions and a proper nodule meristem, as seen in a rhizobia-induced nodule (Guan et al., 2013). Studies in *L. japonicus* examining auxin response in spontaneous nodules induced by overexpression of *LHK1*, *NIN* (Suzaki et al., 2012) and *CCaMK* (Suzaki et al., 2013b) yielded results comparable to the auxin response observed during pseudonodule development (Figure 4.9). This suggests that despite the global and sustained auxin transport inhibition caused by ATI treatment, as well as a local reduction in IAA content early on, the host plant could increase auxin response locally at a later time to form a new lateral organ. Since *in silico* modelling suggests that during nodulation, a local increase in auxin is most likely caused by a local transient inhibition of acropetal auxin export and lateral redirection of auxin flow (Deinum et al., 2012), other components of auxin homeostasis, such as local synthesis and auxin breakdown, could play compensatory roles during pseudonodule formation.

4.3.3 Why do pseudonodules induced by ATIs form only in certain legumes?

The data obtained in this study further strengthen previous results showing the formation of ATI-induced pseudonodules only in indeterminate nodule-forming legumes. We observed pseudonodule formation in *M. truncatula*, subclover and *S. rostrata*. Although *S. rostrata* has the capacity to form both nodule types, it potentially prefers to form indeterminate-type nodules under non-waterlogging and well-aerated growth conditions (Fernández-López et al., 1998), and that our growth system and ATI assays simulated these conditions. Although we could not induce pseudonodules on *A. longifolia* roots, which form indeterminate-type nodules, it could likely be due to the suboptimal germination rates we encountered, which also resulted in poorly-developed seedling roots. In accordance with a previous study, we failed to observe any pseudonodule forming on *L. japonicus* roots in response to ATI treatment (Kawaguchi et al., 1996). To exclude the possibility that *L. japonicus*

could not inhibit acropetal auxin transport and thus failed to induce pseudonodules, we measured acropetal auxin transport following TIBA treatment and confirmed a reduction in acropetal auxin transport capacity in *L. japonicus* roots. This suggests that the inability of *L. japonicus* to form pseudonodules was not due to the inability of TIBA to inhibit acropetal auxin transport in this species. Curiously, gibberellins were able to induce pseudonodules on *L. japonicus*, but not alfalfa roots (Kawaguchi et al., 1996). The mode of action or physiological effects of gibberellins were however not examined. Nevertheless, gibberellins are not likely to inhibit acropetal auxin transport because of their failure to induce pseudonodules on alfalfa. Although acropetal auxin transport was reduced following TIBA treatment, basipetal auxin transport remained unchanged. This suggests that the formation of rhizobia-induced nodules, which involves changes in basipetal auxin transport, requires additional regulation compared to pseudonodules. Since Nod factor perception at the root hair activates a complex signalling pathway (Oldroyd et al., 2011, Suzaki et al., 2013a), basipetal auxin transport regulation might be controlled by an early signalling component following Nod factor perception. This would be difficult to mimic with a simple ATI treatment.

Aside from pseudonodules, we observed other structures forming on the roots of ATI-treated legumes. The induction of tumor-like structures, root bifurcation and swellings have been noted before in plants treated with growth-modulating chemicals, although the auxin transport inhibiting activities of these chemicals were not tested (Allen et al., 1953, Arora et al., 1959, Kawaguchi et al., 1996). However, ATI-induced pseudonodules have so far only form on plants capable of nodulation, suggesting that external ATI treatments can only elicit pseudonodules on species predisposed to nodulation. This hypothesis is supported by genetic studies in *M. truncatula* and *L. japonicus*. Overexpression of CCaMK resulted in spontaneous nodule formation in both legumes (Gleason et al., 2006, Tirichine et al., 2006). Although CCaMK is activated in response to a wide range of

biotic interactions with other organisms, including rhizobia, mycorrhizal fungi and pathogens, both legumes are predisposed to form nodule-like structures with an autoactive CCaMK. In the present study, we focussed on structures resembling nodules. Our findings showed that NPA causes severe inhibition of tap root growth, whereas TIBA results in less pleiotropic effects, suggesting that TIBA is more suited for studying ATI-effects on nodulation. TIBA, but not NPA, inhibits auxin export by stabilising actin filaments, and thus perturbs vesicle trafficking (Dhonukshe et al., 2008, Geldner et al., 2001, Petrasek et al., 2003). The mechanism of NPA in inhibiting auxin transport is still a question for further studies. Both ATIs are likely to induce side effects unrelated to auxin transport. For example, TIBA would affect the transport of additional cellular components, and not just auxin transport carriers. We noticed that a substantial number of pseudonodules resembled modified lateral roots. These structures could be analogous to nodules formed by rhizobia crack entry. Unlike the controlled process seen in infection thread-modulated rhizobia infection, the crack entry mechanism is less stringent and hypothesised to be a more evolutionarily ancient mechanism (Oldroyd et al., 2011). Rhizobia enter via cracks in the roots, such as at a lateral root emergence site, subsequently forming a nodule. Intriguingly, pseudonodules were found along the entire root axis, in large quantities. Under normal conditions, nodulation only initiates in a transient susceptible zone (Bhuvanewari et al., 1981), and the numbers are tightly controlled by a negative feedback mechanism termed autoregulation of nodulation (Ferguson and Mathesius, 2014). This phenomenon could be explained by the whole root application of concentrated ATIs used in this study. An alternative explanation is that these structures could be modified lateral roots. Unlike the localised nature of spot inoculation, rhizobia-induced nodule development, the site of pseudonodule initiation could not be predicted. In *M. truncatula*, visible pseudonodule bumps are typically seen after two weeks, which is longer than the development of rhizobia-induced nodule bumps (~ 72 h.p.i.).

Thus, the formation of rhizobia-induced nodules and pseudonodules is likely to involve different pathways.

4.3.4 Different auxins are more prominent at different stages of nodulation and across species

Our results show that several auxin species are present in *M. truncatula* and *L. japonicus* root tissue. In agreement with an increased auxin response observed in dividing cortical cells in the present and a previous study (van Noorden et al., 2007), we quantified an increase in IAA concentration at 24 h.p.i. in a root segment encompassing the inoculation spot of *M. truncatula* roots following rhizobia inoculation. Histological monitoring of nodulation progression in *L. japonicus* (Figure 4.16), and results from a previous report suggest that an increase in auxin response occurs at the onset of visible cell divisions, which corresponds to 5 d.p.i. (Suzaki et al., 2012). However, we did not observe a similar increase in IAA concentration in *L. japonicus* roots. It is possible that the increased auxin response seen in *L. japonicus* nodule primordia is in response to altered sensitivity to auxin in the primordia, or that small, local changes in auxin concentrations could not be detected by measuring auxin metabolites in root segments. There were two auxin conjugates, IAA-Phe and IAA-Trp that increased in concentrations in *M. loti*-inoculated roots. Although the increase in concentrations were non-significant, it is possible that they account for induction of auxin response. Intriguingly, a reduction in IAA content was measured at 24 h.p.i., which corresponded to the inhibition of basipetal auxin transport measured at the same time (Figure 4.14B). Present evidence suggests that the reduction of auxin signalling upon pathogen recognition is correlated with increased pathogen resistance in certain plants (Domingo et al., 2009, Wang et al., 2007, Wang and Fu, 2011). Here, it is tempting to speculate that rhizobia are first perceived by *L. japonicus* as invaders before subsequent symbiotic

signalling activation. Although auxin response increased at the inner cortical cells of developing pseudonodules, the concentration of IAA decreased in the TIBA-treated root segments at an equivalent time-point when IAA concentration increased in rhizobia-inoculated roots. However, the induction of pseudonodules is slower, and the initial increase in auxin response was only observed after 1-week post TIBA treatment.

The roles of other auxin compounds are largely unknown. The auxin conjugate IAA-Ala has been proposed to be a form of IAA storage compound (LeClere et al., 2002). A reduction in IAA-Ala concentration in *M. truncatula* roots at 48 h.p.i. to increase the active IAA pool in response to rhizobia treatment supports this hypothesis. The concentration of IAA in the mature nodules of *L. japonicus* was considerably higher than in *M. truncatula* nodules. This was surprising because at this stage, *M. truncatula* nodules maintain active meristems but nodules in *L. japonicus* would have been terminally differentiated and stop growing (Oldroyd et al., 2011). However, there could possibly be a role for auxin in regulating defence, rather than organogenesis in the mature nodule. The significantly higher concentration of PAA in the nodules of *M. truncatula*, *L. japonicus*, soybean and *D. glomerata* relative to other auxin species suggests a prominent role for PAA in mature nodules. Earlier studies showed that bacteria are able to synthesise auxins, including PAA (Slininger et al., 2004, Somers et al., 2005). This could explain the high levels of PAA in mature nodules, but its absence in uninfected *L. japonicus* roots and the occasional detection in uninfected *M. truncatula* roots. Strong PAA signals in *Frankia*-infected cells of *C. glauca* and *D. trinervis* nodules have also been reported (Imanishi et al., 2014, Perrine-Walker et al., 2010). However, plants are capable of synthesising PAA, too, as observed in the root tissues of *D. glomerata*, *C. glauca* and cucumber, as well as in the shoots of several higher plants (Wightman and Lighty, 1982). Intriguingly, PAA was reported to exhibit carrier-mediated IAA transport inhibition in pea stems (Morris and

Johnson, 1987). A similar role during nodulation and in mature nodules will have to be examined. The much higher IAA-Asp concentration found in mature *L. japonicus* nodules in comparison to nodules in other species examined in this study is also intriguing. Previous results suggest IAA-Asp as an auxin intermediate targeted for degradation (Rampey et al., 2004), which could explain the high levels in a terminally differentiated nodule. However, a similar observation should, in theory, be observed in determinate soybean nodules. Perhaps IAA-Asp performs additional roles in mature *L. japonicus* nodules. Moreover, future identification of an IAA-Asp-like compound observed in our study could help explain its high levels in all tissues where it was detected, especially in *M. truncatula* nodules.

Our results suggest that neither acro- nor basipetal auxin transport capacity is sufficient to explain the changes in auxin responses and auxin concentrations at the nodule initiation site. Despite an increase in auxin response in both indeterminate (e.g., *M. truncatula*, white clover) and determinate (e.g., *L. japonicus*, soybean) nodule primordia (Mathesius et al., 1998, Suzaki et al., 2012, Takanashi et al., 2011, Turner et al., 2013), regulation of acro- and basipetal auxin transport, as well as changes in auxin concentrations, are different in these legumes. Table 4.1 provides an overview of the similarities and differences between indeterminate and determinate nodule-forming legumes, based on results in this chapter and the literature. One plausible explanation for the increase in auxin response in determinate nodules, but not the IAA concentration (Figure 4.19A), is that sensitivities toward auxin in determinate nodules could account for the increase in auxin response in nodules (Mao et al., 2013, Turner et al., 2013). Other mechanisms, like auxin synthesis, could also contribute to the auxin pool in nodulating cells. It would also be interesting to investigate the role of lateral auxin transport in both *L. japonicus* and *M. truncatula* during nodule initiation by using PIN reporters or auxin biosensors.

Overall, we highlighted the importance of local, bidirectional auxin transport regulation during nodulation in indeterminate and determinate nodule-forming legumes. The role of acropetal auxin transport regulation has previously been investigated, but we showed that the scope of rhizobia manipulation on the host's auxin transport machinery is wider. Despite the difference in auxin transport regulation across different legumes, we propose a common response in legumes, whereby basipetal auxin transport is increased, followed by an elevation in auxin response, but not auxin content. During *Arabidopsis* lateral root initiation, a proper auxin gradient could not be established in the acropetal auxin transport-defective *pin1* mutant (Benková et al., 2003), suggesting that a functional auxin transport machinery is a prerequisite for proper auxin gradient and response during root development, in general. Finally, different auxin compounds are detected in root tissues and nodules, prompting the obvious question about their functions during root development. It is likely that some of them play overlapping roles, but a specific developmental stage function, such as PAA in nodules, is possible. The auxin measurements performed here has thus provided a very useful overview of candidate auxin compounds, and potentially the corresponding genes encoding enzymes for their synthesis /conjugation / breakdown, for future functional characterisations.

Table 4.1 An overview of the similarities and differences that have so far been documented between indeterminate and determinate nodule-forming legumes.

	<i>Medicago truncatula</i>	<i>Lotus japonicus</i>	Other indeterminate nodule-forming legumes	Other determinate nodule-forming legumes
Acropetal auxin transport inhibition	Yes. At 24 h.p.i..	Yes. Slightly at 24 h.p.i.. Increase at all later time points.	Yes. In <i>Vicia sativa</i> (common vetch) (Boot et al., 1999).	No. Increase in <i>Lotus japonicus</i> at 48 h.p.i. (Pacios-Bras et al., 2003).
Basipetal auxin transport increase	Yes. At several time points.	Yes. At several time points.	Not determined.	Not determined.
Auxin concentration at time just before cell division	Increase at 24 h.p.i..	No change, except maybe IAA-Trp and IAA-Phe.	Not determined.	Not determined.
Pseudonodulation with TIBA	Yes.	No.	Yes (subclover, alfalfa, pea etc.) (Hirsch et al., 1989, Scheres et al., 1992).	No.
Increased auxin response in primordia	Yes.	Yes.	Yes (white clover) (Mathesius et al., 1998).	Yes (soybean) (Turner et al., 2013).

CHAPTER 5



Flavonoids and auxin transport inhibitors
rescue symbiotic nodulation in the
Medicago truncatula cytokinin perception
mutant *cre1*



Author's Note

The results presented in this chapter were the author's own work, except for the following:

1. The GFP-expressing *Sinorhizobium meliloti* 1021 strain carrying the pE65 plasmid was generated by Ms. Samira Hassan.
2. Validation of the increased MtFLS mRNA levels from an MtFLS overexpression construct, and the LC-MS/MS confirmation of an increase in the concentration of the flavonol, quercetin, were conducted by Ms. Samira Hassan.
3. Quantitative RT-PCR of flavonoid-related genes in cytokinin-treated roots was conducted by Dr. Carole Laffont.

Results presented in this chapter have been accepted for publication.

Ng JLP, Hassan S, Truong T, Hocart C, Laffont C, Frugier F and Mathesius U (2015) Flavonoids and auxin transport inhibitors rescue symbiotic nodulation in the *Medicago truncatula* cytokinin perception mutant *cre1*. *Plant Cell*, in press.

5.1 Abstract

Initiation of symbiotic nodules in legumes requires cytokinin signalling, but its mechanism of action is largely unknown. Here, we tested whether the failure to initiate nodules in the *Medicago truncatula* cytokinin perception mutant *cre1* (*cytokinin response 1*) is due to its altered ability to regulate auxin transport, auxin accumulation, and induction of flavonoids. We found that in the *cre1* mutant, symbiotic rhizobia cannot locally alter acro- and basipetal auxin transport during nodule initiation, and that these mutants show reduced auxin (indole-3-acetic acid) accumulation and auxin responses, compared to the wild type. Quantification of flavonoids, which can act as endogenous auxin transport inhibitors, showed a deficiency in the induction of free naringenin, isoliquiritigenin, quercetin, and hesperetin in *cre1* roots compared to wild-type roots 24 hours after inoculation with rhizobia. Co-inoculation of roots with rhizobia and the flavonoids naringenin, isoliquiritigenin and kaempferol, or with the synthetic auxin transport inhibitor, 2,3,5-triiodobenzoic acid, rescued nodulation efficiency in *cre1* mutants and allowed auxin transport control in response to rhizobia. Our results suggest that CRE1-dependent cytokinin signalling leads to nodule initiation through the regulation of flavonoid accumulation required for local alteration of polar auxin transport and subsequent auxin accumulation in cortical cells during the early stages of nodulation.

5.2 Introduction

Symbiotic bacteria collectively called rhizobia can initiate the formation of nitrogen-fixing root nodules in many species of legumes. Nodule initiation involves the re-initiation of cell divisions in the cortex, endodermis, and pericycle of the root, followed by differentiation of the nodule primordium into a mature organ, similar to the process of lateral root formation (Herrbach et al., 2014, Hirsch et al., 1997, Mathesius, 2008, Xiao et al., 2014). Legume species differ in the types of nodules formed. Typically in temperate legumes, including the model legume *Medicago truncatula*, alfalfa (*Medicago sativa*), or clovers, indeterminate nodules are initiated from pericycle and inner cortical cell divisions, and nodules maintain a persistent meristem. In many tropical legumes however, including common bean (*Phaseolus vulgaris*) and soybean (*Glycine max*), determinate nodules form from outer cortical cell divisions, and the resulting nodules contain a temporary meristem that later differentiates (Hirsch, 1992, van Spronsen et al., 2001).

The mechanism of nodule initiation is only partially elucidated. Nod factors produced by rhizobia are in most cases necessary and in some legumes sufficient to induce nodules (Truchet et al., 1991). The signalling cascade mediating Nod factor action leads to the activation of cytokinin signalling in the cortex of the root (Crespi and Frugier, 2008, Oldroyd et al., 2011), which is accompanied by activation of the gene encoding the cytokinin biosynthesis enzyme LOG1, a cytokinin riboside 5-monophosphate phosphoribohydrolase (Mortier et al., 2014), and an increase in cytokinin concentration at the nodule initiation site in *M. truncatula* (van Zeijl et al., 2015). Several studies have implicated cytokinin as a central regulator in nodule development (Frugier, 2008). The expression of a cytokinin synthesis gene in *Sinorhizobium* nodulation mutants was sufficient to induce cortical cell divisions and expression of nodulation genes in alfalfa (Cooper and Long, 1994). Application of cytokinin can induce cortical cell divisions and expression of nodulation genes in

alfalfa (Fang and Hirsch, 1998, Hirsch et al., 1997), white clover (*Trifolium repens*) (Mathesius et al., 2000b) and *L. japonicus* (Heckmann et al., 2011), and pseudonodules on the actinorhizal plant *Alnus glutinosa* (Rodriguez-Barrueco and De Castro, 1973). Legume mutants impaired in cytokinin perception typically fail to initiate nodules (Gonzalez-Rizzo et al., 2006, Held et al., 2014, Murray et al., 2007, Plet et al., 2011), while constitutive cytokinin signalling was found to cause spontaneous nodule formation in the absence of rhizobia (*snf2* mutant, *spontaneous nodule formation*; Tirichine et al., 2007). In *M. truncatula*, the cytokinin receptor CRE1 is necessary for perceiving exogenous cytokinin in roots, and both mutation or local RNAi-induced silencing of *CRE1* in roots leads to the inhibition of nodule formation (Gonzalez-Rizzo et al., 2006, Plet et al., 2011). In response to rhizobia and cytokinins, the *cre1* mutant fails to induce several cytokinin primary response genes such as *RR4* (*RESPONSE REGULATOR 4*) and *NSP2* (*NODULATION SIGNALLING PATHWAY 2*) (Ariel et al., 2012). A recent transcriptome comparison of gene expression changes in wild-type and *cre1* mutant roots in response to a 3 h Nod factor treatment in *M. truncatula* demonstrated that cytokinin signalling is necessary for the majority (~75% or ~600 transcripts) of Nod factor-induced transcriptional changes (van Zeijl et al., 2015). However, the mechanism of how cytokinin controls nodule development is still not defined.

Previous studies have suggested that cytokinin signalling may regulate plant developmental processes through its action on auxin transport. Auxin transport is essential for establishing auxin gradients in the plant, leading to cell type specification and induction of meristematic cell divisions (Benková et al., 2003). Auxin transport regulation has been most closely studied for indole-3-acetic acid (IAA), which enters the cell partially by diffusion and by facilitated import via *AUX1/LAX* (*AUXIN RESISTANT1/LIKE AUX1*) and *ABCB* (*ATP Binding Cassette subfamily B*) related transporters. Auxin export is strictly regulated through *PIN* (*PIN-FORMED*) and *ABCB*-type transporters that are polarly inserted into the

plasma membrane on specific sides of the cell to control the direction of auxin transport in acropetal, basipetal or lateral direction (Petrášek and Friml, 2009). In the *Arabidopsis thaliana* root, auxin transport in the acropetal direction, from the root base to the root tip, is mainly mediated by PIN1, whereas basipetal auxin transport, from the root tip to the elongation zone, is mediated by PIN2 (Michniewicz et al., 2007, Rashotte et al., 2000).

Certain flavonoids act as modulators of auxin transport by affecting the expression (Peer et al., 2004) and localization of PIN proteins (Santelia et al., 2008), the cycling of PIN proteins to endosomal vesicles (Geldner et al., 2001), as well as modifying the activity of ABCB-type auxin transporters (Bailly et al., 2008, Di Pietro et al., 2002, Peer and Murphy, 2007). Flavonoids bind to two types of protein complexes, a low-affinity binding complex containing an aminopeptidase and a high affinity complex containing ABCB-type transporters (Murphy et al., 2002, Noh et al., 2001). External application of certain flavonoids, in particular flavonols, can inhibit auxin transport (Jacobs and Rubery, 1988), and auxin transport in flavonoid-deficient mutants or transgenic plants is altered (Brown et al., 2001, Buer and Muday, 2004, Laffont et al., 2010, Peer et al., 2004, Wasson et al., 2006). In addition, flavonoids are required to control auxin transport during nodule initiation in legumes forming indeterminate nodules (Wasson et al., 2006), and flavonols are the most likely subclass of flavonoids responsible for this auxin transport control (Zhang et al., 2009a).

Several studies indeed demonstrated that a local auxin transport inhibition is required for indeterminate nodule initiation. Early studies showed that application of synthetic auxin transport inhibitors can induce pseudonodules in some legumes that are characterized by a peripheral vasculature, which does not extend into the distal part of the nodule, an uninfected central zone and a diffuse meristem (Allen et al., 1953, Hirsch et al., 1989). During nodulation, acropetal root auxin transport is temporarily inhibited by rhizobia inducing indeterminate nodules, and this is

followed by a local increase in auxin response in the pericycle and inner cortex at the site of nodule initiation (Boot et al., 1999b, Mathesius et al., 1998, van Noorden et al., 2007). In the *cre1* mutant, rhizobia are unable to inhibit acropetal auxin transport and this is associated with a misregulation of some PIN auxin carrier-encoding gene expression and protein accumulation (Plet et al., 2011). The hypothesis that cytokinin acts upstream of auxin transport regulation is supported by studies from *Arabidopsis* showing that cytokinin regulates PIN expression, accumulation, selective degradation, and subsequently polar auxin transport (Marhavý et al., 2011, Marhavý et al., 2014, Pernisová et al., 2009, Ruzicka et al., 2009a). This is thought to regulate auxin accumulation during lateral root formation (Laplaze et al., 2007a, Marhavý et al., 2014). The finding that auxin transport inhibitors can cause pseudonodule formation in Nod factor signalling defective mutants acting downstream of CRE1, such as *nsp2* and *nin* (*nodule inception*), suggests that auxin transport control of nodulation acts downstream of cytokinin signalling (Rightmyer and Long, 2011). Furthermore, cytokinin application induces auxin responses in pseudonodule primordia in white clover (Mathesius et al., 2000b), and spontaneous nodules formed in the *L. japonicus* constitutively activated cytokinin signalling mutant, *snf2*, also show activation of auxin responses in dividing cortical cells during nodule primordium formation (Suzaki et al., 2012).

Collectively, these findings suggest that a crucial role of cytokinins may be to regulate auxin transport and/or response during nodule initiation. To investigate this hypothesis, we performed a detailed study of auxin transport, auxin response and auxin metabolite accumulation in the *M. truncatula cre1* mutant. We found that *cre1* mutant roots did not mediate rhizobia-induced changes in acro- as well as basipetal auxin transport, and had a limited activation of auxin response in the inner cortex. Following inoculation with rhizobia, *cre1* roots also showed reduced accumulation of the auxin indole-3-acetic acid (IAA) and of several flavonoids.

Nodule initiation was rescued by the application of synthetic auxin transport inhibitors, as well as certain flavonoids that also rescued auxin transport inhibition and auxin responses in rhizobia-infected *cre1* roots. These results suggest that cytokinins act through induction of flavonoids, which would alter auxin transport and accumulation during the initiation of indeterminate nodules.

5.3 Results

5.3.1 The *cre1* mutant is defective in acropetal and basipetal auxin transport regulation and auxin accumulation following *Rhizobium* inoculation

To investigate auxin transport control in the *cre1* mutant, we quantified acropetal and basipetal auxin transport using radiolabelled IAA applied either above the site of inoculation or at the root tip, respectively. To exclude the possibility that defects in flavonoids in the *cre1* mutant prevented proper *nod* gene activation in the symbiont (e.g. Zhang et al., 2009), we used, instead of a wild-type strain, a genotype of *Sinorhizobium meliloti* that constitutively expresses *nodD3*, i.e. that produces Nod factors in the absence of *nod* gene-inducing flavonoids from the legume host (Barnett et al., 2004); hereafter this strain is referred to as 'E65'. This strain formed a significantly higher number of nodules on wild-type (WT) roots compared to the reference strain *S. meliloti* 1021 (Figure 5.1). Under our growth conditions in agar plates, both strains usually did not lead to nodule formation in the *cre1* mutant (Figure 5.1), and when nodules formed, this was at a significantly lower level than in WT, as reported previously for the *cre1* mutant (Plet et al. 2011) and other cytokinin receptor mutants (e.g., Held et al., 2014; Murray et al., 2007).

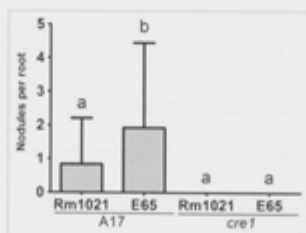


Figure 5.1 Nodulation efficiency on WT and *cre1* mutant roots spot-inoculated with *Sinorhizobium meliloti* strains Rm1021 and E65. Nodules were quantified two weeks post-inoculation. A two-way ANOVA with a Tukey-Kramer multiple comparison post-test was used for statistical analysis ($p < 0.05$, $n = 20$). Different lowercase letters indicate significant differences in nodule numbers per plant. Graphs show mean and SD.

Acropetal (from root base to root tip) auxin transport capacity was measured just below the site of inoculation with E65, where previous studies detected a reduction in auxin transport capacity following inoculation with strain 1021 (Wasson et al., 2006; Plet et al., 2011; Figure 5.2A). Consistent with those studies, the E65 *Rhizobium* strain led in WT roots to a significant reduction in acropetal auxin transport into a root segment below the inoculation site within 24 h. In the *cre1* mutant, inoculation with E65 failed to inhibit acropetal auxin transport (Figure 5.2A). Near the root tip, auxin transport also occurs in a basipetal (from the root tip upwards) direction and we therefore tested whether this basipetal auxin flow was also affected by rhizobia. We measured basipetal auxin transport capacity of the root segment just above the inoculation site (Figure 4.10). In WT roots, E65 inoculation significantly increased basipetal auxin transport capacity at 24 h p.i. (post inoculation), while in *cre1* mutant roots there was no significant difference between inoculated and control roots (Figure 5.2B).

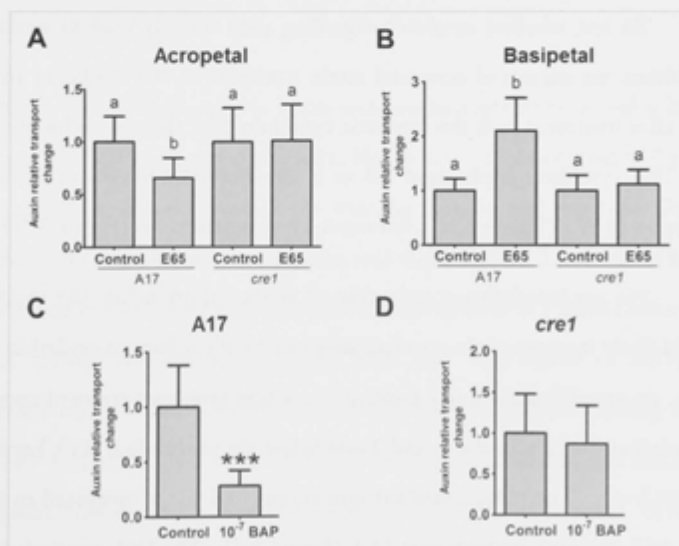


Figure 5.2 Relative auxin transport changes in WT (A17) and *cre1* mutant roots. (A) Acropetal and (B) basipetal auxin transport measurements 24 h after mock- or E65-inoculation in a segment just below (for acropetal) and above (for basipetal) the inoculation site, respectively. Acropetal auxin transport measurements in (C) A17 and (D) *cre1* mutant roots 24 h after mock- or benzylaminopurine (BAP) treatment (10^{-7} M) in a segment just below the mock or BAP application sites. Control treatments were set to "1" in each case. A two-way ANOVA with a Tukey-Kramer multiple comparison post-test was used for statistical analyses in (A-B) ($p < 0.05$, $n = 15-20$). Different lowercase letters indicate significant differences in relative auxin transport rate. A Student's *t*-test was used for statistical analyses in (C-D) ($p < 0.05$, $n = 20$), where asterisks in (C) indicate a significant difference in relative auxin transport rate ($p < 0.001$). Graphs show mean and SD.

Near the root tip, auxin transport also occurs in a basipetal direction, and we therefore tested whether this basipetal auxin flow was also affected by rhizobia. We measured basipetal auxin transport capacity of the root segment just above the inoculation site (Figure 4.10). In WT roots, E65 inoculation significantly increased basipetal auxin transport capacity at 24 h p.i., while in *cre1* mutant roots there was no significant difference between inoculated and control roots (Figure 5.2B).

To test whether cytokinin signaling may directly lead to auxin transport inhibition, we measured acropetal auxin transport in WT and *cre1* mutant roots 24 h after treatment with the synthetic cytokinin BAP (benzyl amino purine) at 10^{-7} M. This cytokinin application led to a significant inhibition of acropetal auxin transport in WT (Figure 5.2C), but not in *cre1* mutant roots (Figure 5.2D).

We predicted that a reduction of auxin export below the inoculation site would likely increase auxin concentrations at the *Rhizobium* inoculation site in WT. Thus, we quantified the auxin content in a 4 mm long root segment comprising the inoculation site (2 mm above and 2 mm below the inoculation site), harvested at 6 h and 24 h p.i.. The most abundant non-conjugated auxin measured in the roots of both WT and *cre1* mutants was IAA (Figure 5.3). The IAA concentration in WT root segments inoculated with rhizobia did not change at 6 h p.i., but significantly

increased at 24 h p.i. (Figure 5.3A). In *cre1* roots, no significant increase was measured at 6 h or 24 h p.i. (Figure 5.3B). Concentrations of indole-3-butyric acid (IBA) were not significantly changed in response to inoculation in WT or *cre1* mutants, but *cre1* roots showed elevated IBA concentrations compared to WT (Figure 5.3C, D). The conjugated auxin IAA-Alanine showed no significant changes in response to E65 inoculation in either genotype, but higher concentrations were observed in WT at 6 h p.i. compared to *cre1* roots (Figure 5.3E, F). Overall, combined auxin concentrations were higher in WT than in *cre1* roots under both control and inoculated conditions (Figure 5.4). We could not detect 4-chloro-IAA, phenylacetic acid (PAA), and the auxin conjugates IAA-Phenylalanine, IAA-Tryptophan, IAA-Leucine, IAA-Isoleucine, IAA-Valine or IAA-Aspartate in any of the root segments. These auxin metabolites were targeted for quantification because a previous study suggested their presence in *M. truncatula* based on enzyme feeding assays (Campanella et al., 2008). The detection limits for these auxins are shown in Table 3.7 and are below the concentrations measured for some of these auxins in other studies (e.g., Kowalczyk and Sandberg, 2001; Matsuda et al., 2005; Scheider et al., 1985).

Next, we visualized changes in auxin response in roots transformed with the auxin reporter *GH3:GUS* (Hagen et al., 1991; Figure 5.5). In uninfected WT roots, *GH3:GUS* expression was detected in the vascular bundle and pericycle (Figure 5.5A), similar to the expression in uninfected *cre1* roots (Figure 5.5E). At 24 h p.i., an auxin response was activated in the cortex and root hairs of WT plants before the initiation of cortical cell divisions (Figure 5.5B, C). The extent of *GH3:GUS* induction in the cortex varied between roots from partial to complete staining of the cortex. In *cre1* mutants, only a weak *GH3:GUS* response was seen in root hairs and cortical *GH3:GUS* expression was absent (Figure 5.5F, G). At 48 h p.i., dividing cortical and pericycle cells were detected in WT roots inoculated with E65, and these dividing cells, as well as cortical and epidermal cells surrounding the nodule

primordium, showed a strong auxin response (Figure 5.5D). In *cre1* roots, no activation of auxin response was observed in the cortex, which typically fails to induce cell divisions in response to E65 (Figure 5.5H). *GH3:GUS* expression was seen in epidermal cells of *cre1* mutants in the absence of cortical cell divisions (Figure 5.5H). However, in a few cases the *cre1* mutant did form small and delayed nodules, and in these cases *GH3:GUS* expression was found in dividing cells of the nodule primordia, as well as in overlying outer cortical and epidermal cells (Figure 5.5I), similar to the WT. Reverse transcription quantitative PCR (RT-qPCR) showed significantly higher expression of *GH3* inoculated in WT compared to *cre1* roots at 6 h p.i. (Figure 5.6A).

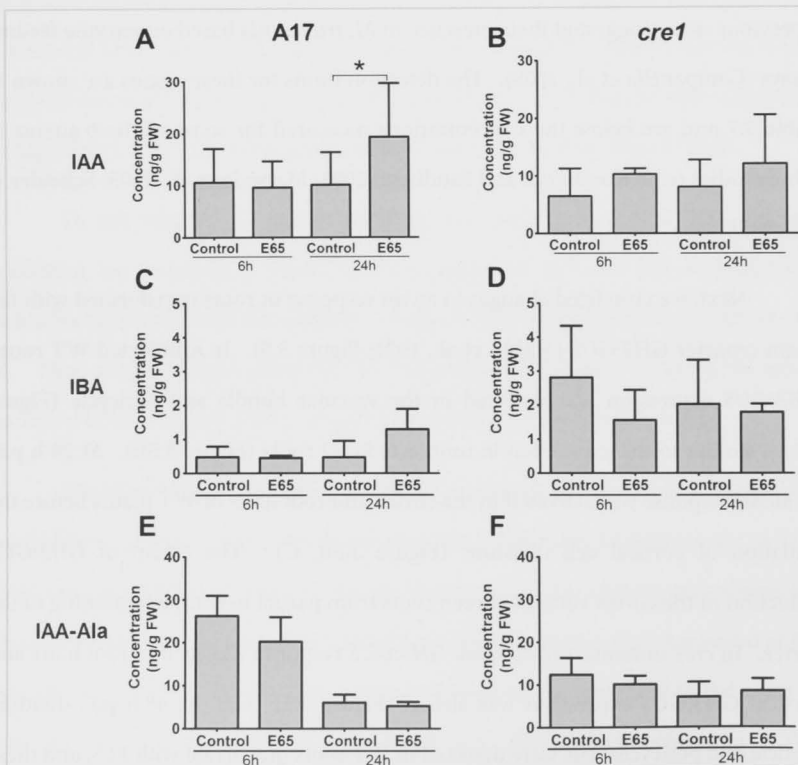


Figure 5.3 Auxin concentration in WT (A17) and *cre1* mutant roots at 6 and 24 h post mock- or E65 inoculation. (A-B) IAA concentration; (C-D) IBA concentration; (E-F) IAA-Ala concentration. A three-way ANOVA with a Bonferroni post-test was used for statistical analysis. Asterisk in (A) indicates a significant difference in auxin concentration with a Bonferroni post-test ($p < 0.05$; $n = 5-6$). Each biological replicate consists of at least 30 root segments. Graphs show mean and SD.

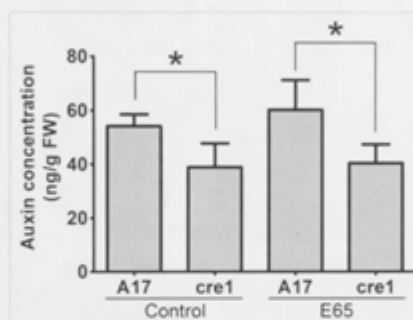


Figure 5.4 Combined auxin concentrations (sum of IAA, IBA and IAA-Ala) in WT (A17) and *cre1* mutant roots mock-treated or inoculated with E65 rhizobia. A Student's *t*-test was used for statistical analyses ($p < 0.05$, $n = 4-5$). Asterisks indicate significant differences in total root auxin concentrations between WT and *cre1* mutants.

To test whether changes in auxin transport and auxin accumulation were accompanied by changes in the expression of auxin transporter-encoding genes, we monitored the relative expression of all ten known *PIN* genes and of the five known *LAX* genes, using RT-qPCR (Schnabel and Frugoli, 2004a). A significantly higher *PIN4* and *PIN10* expression at 6 h p.i. and *PIN2* expression at 24 h p.i. was found in E65-inoculated WT roots compared to *cre1* roots (Figure 5.6B). None of the other *PIN* genes showed a significantly differential expression between WT and *cre1* roots in the first 24 h, while some minor changes in expression occurred at later time points (Figure 5.7). None of the *LAX* genes showed altered expression levels between genotypes or in response to inoculation with E65 (Figure 5.8).

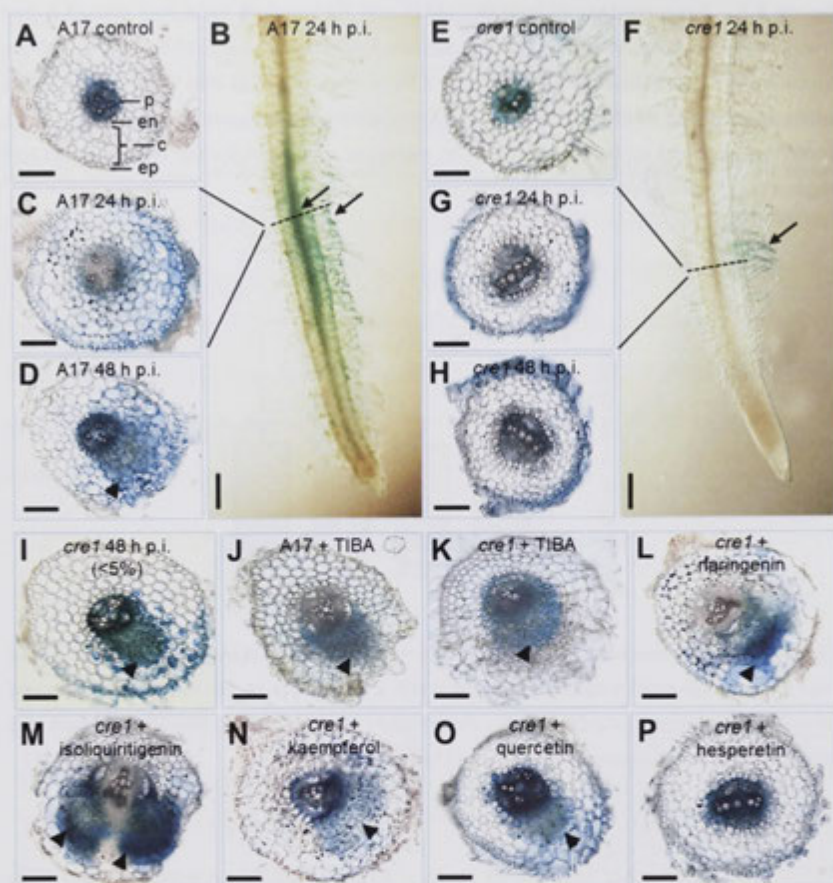


Figure 5.5 Auxin response (*GH3:GUS* expression) is localised to dividing cells during the early stages of nodule and pseudonodule development. (A) Auxin response in a mock-treated WT (A17) root. (B) Auxin response is localised to the root hairs and underlying cortex directly below the root hairs of a A17 root spot-inoculated with E65 at 24 h p.i.. (C) Cross-section of (B). (D) Auxin response in the dividing pericycle, endodermal and cortical cells during early symbiotic stages in an A17 root inoculated with E65 at 48 h p.i.. (E) Auxin response in a mock-treated *cre1* mutant root. (F) Auxin response is absent in the root cortex but present in the root hairs of a *cre1* mutant root spot-inoculated with E65 at 24 h p.i.. (G) Cross-section of (F). (H) In most of *cre1* mutant roots, no cell divisions occur in response to E65 inoculation at 48 h p.i.. (I) Dividing cells in *cre1* mutants are associated with an enhanced auxin response and are observed in less than 5% of *cre1* mutant roots inoculated with E65. Auxin response in the dividing cells of A17 (J) and *cre1* (K) roots in response to TIBA treatment. Auxin response in a *cre1* (L) naringenin-, (M) isoliquiritigenin-, (N) kaempferol-, and (O) quercetin-rescued nodule primordium. (P) No enhanced auxin

response or cell divisions were observed in hesperetin-treated roots. Arrowheads indicate nodule primordia. Arrows indicate auxin response in the root hairs and / or the root cortex. At least 30 individual samples were observed for each treatment. Horizontal and vertical scale bars represent 100 μm and 1 mm, respectively. Abbreviations: ep, epidermis; c, cortex; en, endodermis; p, pericycle.

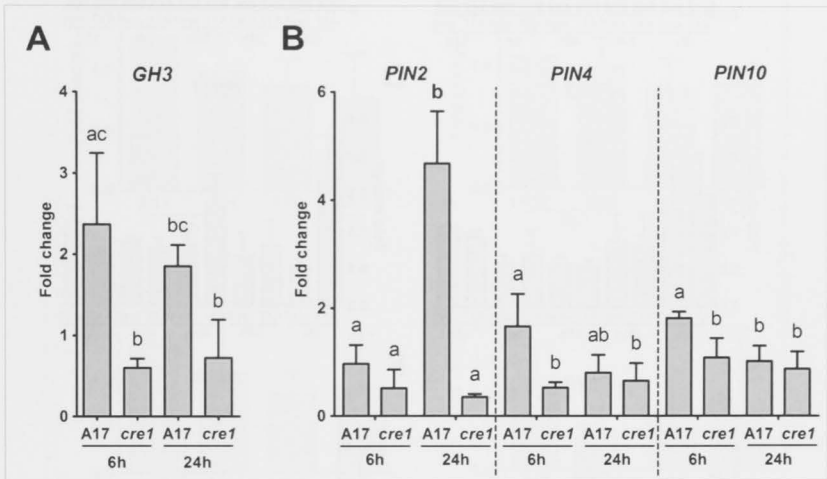


Figure 5.6 Quantitative RT-PCR showing transcript abundance in root segments of WT (A17) and *cre1* mutants inoculated for 6 and 24 h with E65 relative to mock-treated roots. Expression was normalised to the *GAPDh* reference gene. The auxin response gene *MtGH3* (A), and the IAA exporter-encoding genes *MtPIN2*, *MtPIN4* and *MtPIN10* (B) were analysed. A two-way ANOVA with a Tukey-Kramer multiple comparison post-test was used for statistical analyses ($p < 0.05$, $n=3$). Different lowercase letters indicate significant differences in transcript abundance within each gene. Each biological replicate consists of at least 50 root segments. Graphs show mean and SD.

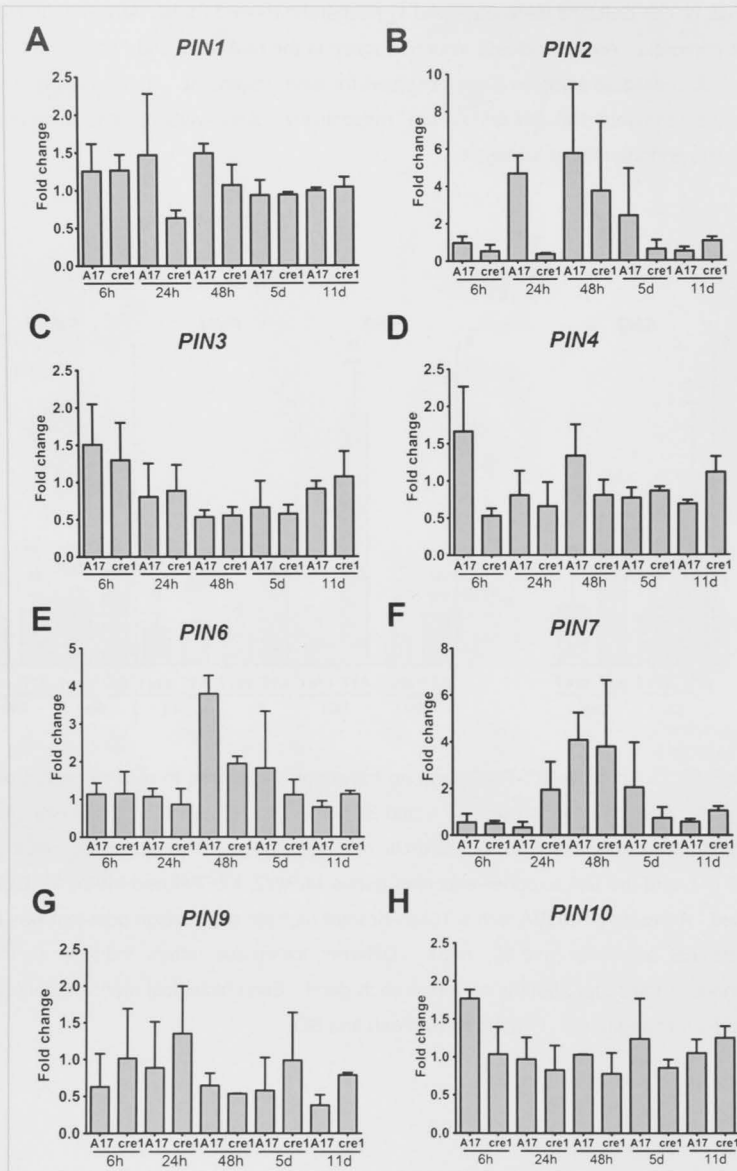


Figure 5.7 Quantitative RT-PCR of MtPIN genes. Transcript abundance was quantified in root segments inoculated for 6, 24, 48 h and 5 and 11 d with E65 relative to mock-treated roots. Expression was normalised to the *GAPdh* reference gene. IAA exporter-encoding genes *PIN1* (A), *PIN2* (B), *PIN3* (C), *PIN4* (D), *PIN6* (E), *PIN7* (F), *PIN9* (G) and *PIN10* (H) were analysed. *PIN5* and *PIN8* mRNAs were not detected in *M. truncatula* roots (Schnabel and Frugoli, 2004). A two-way ANOVA with a Tukey-Kramer multiple comparison post-test

was used for statistical analysis ($p < 0.05$, $n = 3$). No significant differences were found between any of the treatments. Three biological replicates consisting of at least 50 individual root segments were analysed. Graphs show mean and SD.

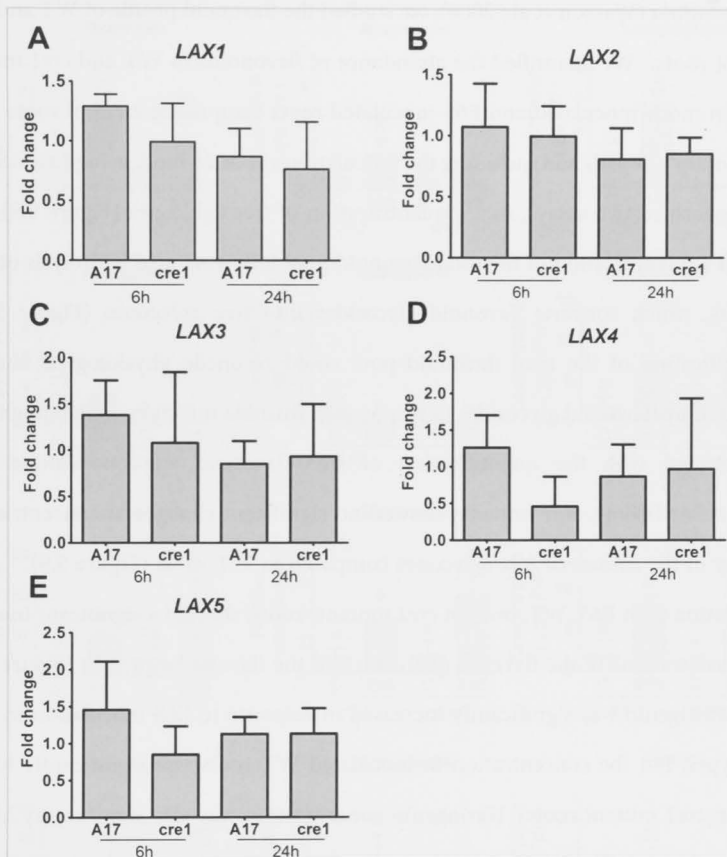


Figure 5.8 Quantitative RT-PCR of MtLAX genes. Transcript abundance was quantified in root segments inoculated for 6 and 24 h with E65 relatively to mock-treated roots. Expression was normalised to the *GAPDh* reference gene. IAA importer-encoding genes *LAX1* (A), *LAX2* (B), *LAX3* (C), *LAX4* (D), and *LAX5* (E) were analysed. A two-way ANOVA with a Tukey-Kramer multiple comparison post-test was used for statistical analysis ($p < 0.05$, $n = 3$). No significant differences were found between any of the treatments. Three biological replicates consisting of at least 50 individual root segments were analysed. Graphs show mean and SD.

5.3.2 The *cre1* mutant shows an altered flavonoid profile

Because flavonoids can act as modulators of auxin transport (Peer and Murphy, 2007) and are required for acropetal auxin transport control during nodulation of *M. truncatula* (Wasson et al., 2006), we studied the flavonoid profile of WT and *cre1* mutant roots. We quantified the abundance of flavonoids in WT and *cre1* mutant roots in mock-inoculated and E65-inoculated roots comprising 2 cm of roots from the root tip upwards and including the inoculation site at 24 h p.i. using LC-MS/MS. We performed two assays, first a quantification of free aglycones (Figure 5.9), and second a quantification of the total flavonoid pool following acid hydrolysis of root extracts, which converts flavonoid glycosides into free aglycones (Figure 5.10). Quantification of the total flavonoid pool could reconcile physiological changes mediated by flavonoid glycosides in response to rhizobia infection, which might not be detected with the quantification of free flavonoid aglycones alone. In uninoculated roots, *cre1* mutants showed no significant changes in concentrations for any of the measured free aglycones compared to WT roots (Figure 5.9). After inoculation with E65, WT, but not *cre1* mutant roots, showed a significant increase in concentrations of the flavonol quercetin and the flavone hesperetin (Figure 5.9). Isoliquiritigenin was significantly increased in response to E65 inoculation in both genotypes, but the concentration in inoculated WT roots was significantly higher than in *cre1* mutant roots. Naringenin concentration was also significantly higher in inoculated WT roots in comparison to inoculated *cre1* mutant roots. The concentration of kaempferol decreased to levels below the detection limit in both genotypes following inoculation. Inoculation significantly elevated the concentrations of the isoflavonoids daidzein, formononetin, medicarpin and biochanin A, with similar responses in both genotypes. Concentrations of liquiritigenin, chrysoeriol and morin were not significantly altered by genotype or inoculation. A summary of differences in flavonoid aglycone abundance between

WT and *cre1* roots in response to E65 inoculation is depicted in Figure 5.11 to correlate the observed defects with the flavonoid metabolic pathway.

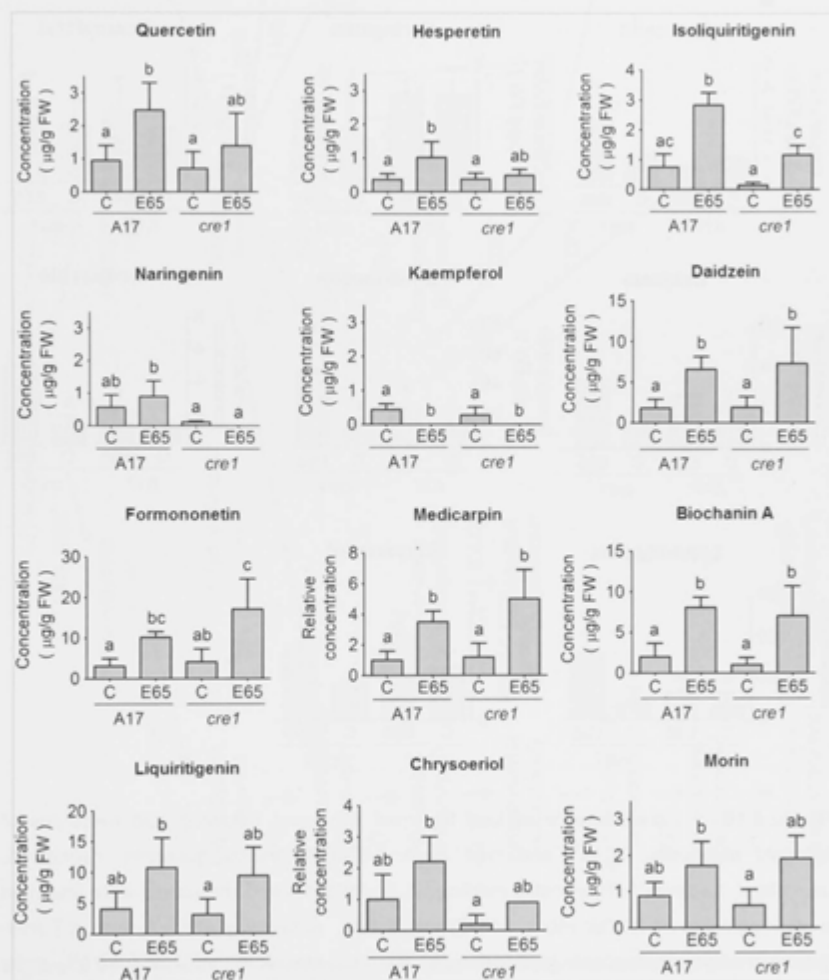


Figure 5.9 Concentrations of major flavonoids in WT (A17) and *cre1* mutant root segments 24 h after mock- or E65 inoculation. Flavonoids analysed include the flavanones (naringenin, hesperetin), flavonols (quercetin, kaempferol, morin), isoflavonoids (isoliquiritigenin, liquiritigenin, medicarpin, formononetin, daidzein, biochanin A), and a flavone (chrysoeriol). Relative quantification was performed on chrysoeriol and medicarpin, where commercial standards were not available. A two-way ANOVA with a Tukey-Kramer

multiple comparison post-test was used for statistical comparison ($p < 0.05$; $n = 3-5$). Different lowercase letters indicate statistically significant difference between treatments. A total of 15 root segments were harvested for each biological replicate. Graphs show mean and SD.

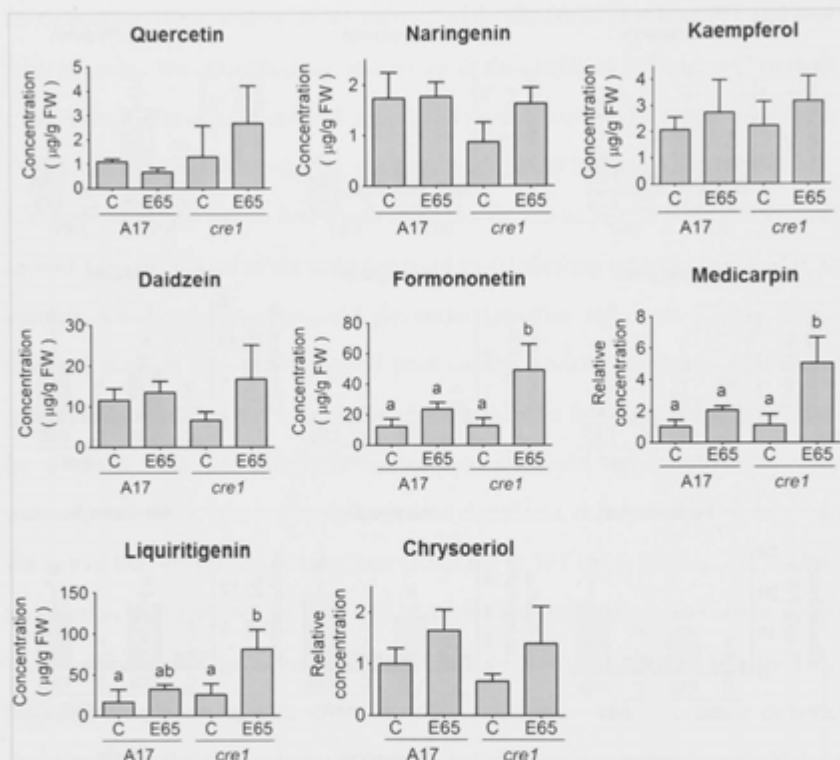


Figure 5.10 Concentrations of total flavonoid aglycones following acid hydrolysis of flavonoid glycosides in WT and *cre1* roots. The flavonoids quercetin, naringenin, kaempferol, daidzein, formononetin, medicarpin, liquiritigenin and chrysoeriol were analysed in root segments 24 h after mock- or E65 inoculation. A two-way ANOVA with a Tukey-Kramer multiple comparison post-test was used for statistical analysis ($p < 0.05$, $n = 3$). Different lower case letters indicate a significant change in flavonoid concentration measured. A total of 15 root segments were harvested for each biological replicate. Graphs show mean and SD.

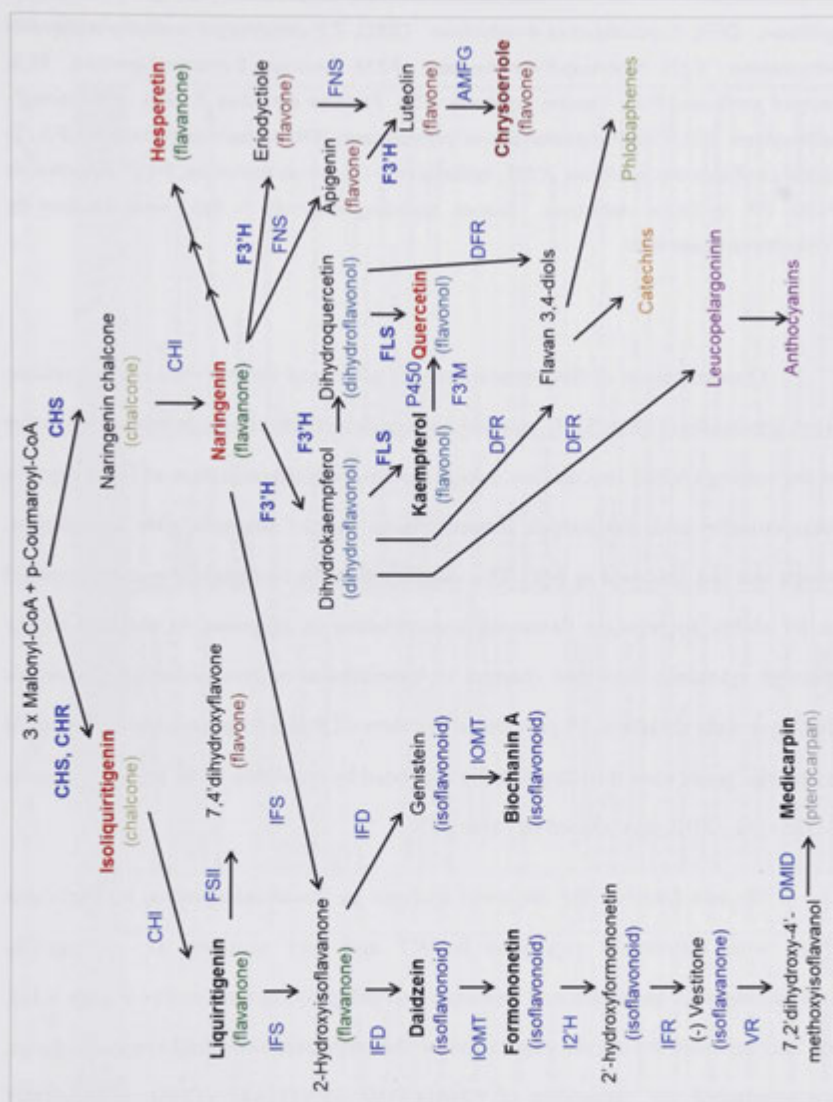


Figure 5.11 Schematic overview of the flavonoid biosynthesis pathway in *Medicago truncatula*. Aglycones that were detected in the roots are shown in bold. Flavonoids shown in bold red showed differences in induction after inoculation between genotypes (isoliquiritigenin, naringenin, hesperetin and quercetin). Different subclasses of flavonoids are indicated in different colours. Note that we could detect genistein/apigenin but could not differentiate between them because of the identical MW and elution time. Enzymes are shown in blue and are abbreviated as follows: AMFG, S-adenosylmethionine:flavonoid 7-O-glucosyltransferase; CHI, chalcone isomerase; CHR, chalcone reductase; CHS, chalcone

synthase; DFR, dihydroflavonol 4-reductase; DMID, 7,2'-dihydroxy-4'-methoxy-isoflavonol dehydratase; F3'H, flavonoid-3'-hydroxylase; F3'M, flavonoid 3'-monooxygenase; FLS, flavonol synthase; FNS, flavone synthase; FSII, Flavone synthase II; I2'H, isoflavone-2'-hydroxylase; IFD, 2-hydroxyisoflavanone dehydratase; IFR, isoflavone reductase; IFS, 2-hydroxyisoflavanone synthase; IOMT, isoflavanone-O-methyltransferase; P450, cytochrome P450; VR, vestitone reductase. Genes encoding enzymes in bold were induced by E65/cytokinin treatment.

Quantification of flavonoid aglycones after acid hydrolysis, i.e. after release from glycosides (Figure 5.10), showed no significant differences between genotypes or depending on E65-inoculation, except for a significant induction of liquiritigenin, formononetin and medicarpin concentrations in *cre1* mutants after inoculation, which was not observed in WT. This suggests that the *cre1* mutant is compromised in its ability to regulate flavonoid accumulation in response to rhizobia either through cytokinin-mediated changes in biosynthesis or conversion of flavonoids during nodule initiation. A previous study showed that a large number of flavonoid metabolic genes were transcriptionally regulated by cytokinin in *M. truncatula* roots (Ariel et al., 2012; genes listed in Table 5.1).

To test whether the observed changes in flavonoid content, in particular those with differential responses in WT and *cre1* mutants, i.e. naringenin, isoliquiritigenin, quercetin and hesperetin (highlighted in bold red in Figure 5.11), are accompanied by altered expression of the respective flavonoid synthesis genes, we monitored the expression of *CHALCONE SYNTHASE (CHS)*, *CHALCONE ISOMERASE (CHI)*, *CHALCONE REDUCTASE (CHR)*, *FLAVONOID-3'-HYDROXYLASE (F3'H)* and *FLAVONOL SYNTHASE (FLS)* by RT-qPCR.

Table 5.1 Induction of flavonoid-related genes by the cytokinin BAP, extracted and modified from the publication by Ariel et al. (2012).

16K-microarray probe ID	Mt genome v4.8 JCVI	Fold Change BAP vs Control	Adj. p-value, (BAP vs control)	MtGI # ID and annotation (TIGR database)	Mt genome v4.8 JCVI annotation	Top UniProt hits
MT00038	Medtr1g31800	2.81	0.00012	TC100176 similar to UPQ267WQ5 (Q267WQ5) UDP-glycose flavonoid glycosyltransferase , partial (83%)	UDP-glycosyltransferase 2B5	UDP-glycose flavonoid glycosyltransferase, Isoflavonoid glycosyltransferase, Triterpene UDP-glycosyl transferase, Putative UDP-glycose (Fragment)
MT000247	Medtr1g042310	4.24	0.00012	TC100520 weakly similar to UPQ540V3 (Q540V3) A2g22590T922.3, partial (25%)	Anthocyanidin 3-O-glucosyltransferase	Putative anthocyanidine rhamnosyl transferase , GT4, GT2, UDP-rhamnose soyasaponin II rhamnosyltransferase
MT001043	Medtr1g075830 Medtr1g075890	2.93	0.00102	TC54829 similar to UPQ8L8C8 (Q8L8C8) Flavanone 3 beta-hydroxylase , complete	Flavanone 3-hydroxylase Naringenin,2-oxoglutarate 3-dioxygenase	Flavanone 3-hydroxylase , Naringenin 2-oxoglutarate 3-dioxygenase Flavanone 3-hydroxylase
MT001070	Medtr1g033675	4.82	3.00E-05	TC107728 similar to UPQ267WQ4 (Q267WQ4) UDP-glycose flavonoid glycosyltransferase (Fragment), partial (96%)	UDP-glycosyl transferase	UDP-glycosyl transferase, (iso)flavonoid glycosyltransferase, Glucosyl transferase
MT001199	Medtr7g013850	4.32	3.00E-05	TC107840 weakly similar to UPQ26URQ7 (Q26URQ7) Anthocyanin 5-aromatic acyltransferase -benzoyltransferase-like protein, partial (21%)	Anthocyanin 5-aromatic acyltransferase	Anthocyanin 5-aromatic acyltransferase , Isoflavonoid malonyl transferase
MT003127	Medtr2g083390 Medtr2g083420	1.51	0.00379	TC97344	UDP-glycosyltransferase family protein UDP-glycosyltransferase family protein	UDP-glycosyltransferase family protein, Anthocyanidin 3-O-glucosyltransferase , Glycosyltransferase UDP-glycosyltransferase family protein, Anthocyanidin 3-O-glucosyltransferase , Glycosyltransferase
MT004805	Medtr3g092890	1.85	0.01454	TC96902 similar to UPQ26FLV0 (Q26FLV0) Flavanone 3-hydroxylase like protein, partial (82%)	1-Aminocyclopropane-1-carboxylate oxidase	1-Aminocyclopropane-1-carboxylate oxidase, Oxidoreductase, Flavanone-3-hydroxylase
MT009572	Medtr3g092890	2.65	0.00011	TC99256 similar to UPQ7XZD6 (Q7XZD6) Isoflavonoid glycosyltransferase , partial (15%)	1-Aminocyclopropane-1-carboxylate oxidase	1-Aminocyclopropane-1-carboxylate oxidase, Oxidoreductase, Flavanone-3-hydroxylase
MT010942	Medtr4g102280	1.90	0.00291	TC111173 weakly similar to UPQ26ST0 (Q26ST0) Flavonoid 3',5'-hydroxylase -like protein (A4g12310), partial (3%)	Cytochrome P450 family protein	Cytochrome P450, Flavonoid 3'-hydroxylase
MT014364	Medtr2g080220 Medtr2g080225	3.47	0.00012	TC100521 weakly similar to UPQ26NV0 (Q26NV0) A2g22590T922.3, partial (15%)	Anthocyanidin 3-O-glucosyltransferase UDP-glycosyltransferase family protein	GT2, GT4, UDP-rhamnose soyasaponin II-rhamnosyltransferase, Putative UDP-rhamnose rhamnosyltransferase, UDP-glycosyltransferase UDP-glycosyltransferase family, GT4, Glycosyltransferase
MT014596	N/A	2.02	0.00112	TC108655 weakly similar to UPQ7XZD0 (Q7XZD0) Isoflavonoid glycosyltransferase , partial (47%)	N/A	N/A
MT014666	Medtr1g032870	1.55	0.0056	TC192386 weakly similar to UPQ84UT8 (Q84UT8) Flavonoid synthase , partial (25%)	1-Aminocyclopropane-1-carboxylate oxidase	oxidoreductase, 1-aminocyclopropane-1-carboxylate oxidase, flavonoid synthase
MT014842	Medtr1g015320	1.72	0.00474	TC110716 weakly similar to UPQ2LJ84 (Q2LJ84) Anthocyanin 5-aromatic acyltransferase like protein, partial (17%)	Malonyl-CoA:isoflavone 7-O-glucoside malonyltransferase	malonyl-CoA:isoflavone 7-O-glucoside malonyltransferase, Putative anthocyanin malonyltransferase , Taxifolin acetyl transferase
MT014912	Medtr2g044620	3.49	0.00032	TC184594 similar to UPQ80VE3 (Q80VE3) Flavonoid 1,2-rhamnosyltransferase , partial (7%)	UDP-glycosyltransferase family protein	UDP-glycosyltransferase family, Anthocyanidin 3-O-glucosyltransferase , Glycosyltransferase
MT015697	Medtr2g035420	1.65	0.00017	TC94915 similar to UPQ7XZD0 (Q7XZD0) Isoflavonoid glycosyltransferase , partial (71%)	UDP-glycosyltransferase family protein	UDP-glycosyltransferase family, Cytosolin-O-glycosyltransferase, Ecdysteroid UDP-glycosyltransferase, Isoflavonoid glycosyltransferase
MT015712	Medtr1g032950	2.03	0.00023	TC198255 similar to UPQ7XZD0 (Q7XZD0) Isoflavonoid glycosyltransferase , partial (47%)	UDP-glycosyltransferase family protein	UDP-glycosyltransferase family, Cytosolin-O-glycosyltransferase, Ecdysteroid UDP-glycosyltransferase, Isoflavonoid glycosyltransferase
MT015750	Medtr1g032950	2.66	0.00034	TC96991 similar to UPQ7XZD0 (Q7XZD0) Isoflavonoid glycosyltransferase , partial (51%)	UDP-glycosyltransferase family protein	UDP-glycosyltransferase family, Cytosolin-O-glycosyltransferase, Ecdysteroid UDP-glycosyltransferase, Isoflavonoid glycosyltransferase
MT015828	Medtr2g035040	1.94	0.00493	TC94917 weakly similar to UPQ7XZD0 (Q7XZD0) Isoflavonoid glycosyltransferase , partial (21%)	Cytosolin-O-glycosyltransferase	GT3, Isoflavonoid glycosyltransferase , Glucosyltransferase, UDP-glycose flavonoid glycosyltransferase

Expression of these flavonoid synthesis genes in response to a short-term cytokinin treatment (10^{-7} M BAP for 30 min) revealed significant induction of *CHR*, *F3'H* and *FLS* expression in BAP-treated WT but not *cre1* mutant roots compared to mock-treated roots (Figure 5.12), indicating that these genes are cytokinin-inducible. A comparison between uninoculated roots of the two genotypes revealed significantly higher expression of *CHS*, *CHR*, *F3'H* and *FLS* in *cre1* mutants roots compared to WT at 24 h, and of *CHR* and *FLS* also at 6 h (Figure 5.13). In response to inoculation with E65, we found a significant induction of *CHS*, *CHR*, and *FLS* in WT but not *cre1* roots at 6 h p.i., and of *CHS* and *F3'H* also at 24 h p.i. (Figure 5.14; shown in bold blue in Figure 5.11). On the contrary, expression of *CHS* and *CHR* was significantly reduced by E65 inoculation in the *cre1* mutant at 24 h p.i. for both genes and at 6 h p.i. for *CHS* (Figure 5.14). *F3'H* was significantly induced in WT and *cre1* roots after E65 inoculation at 6 h, but this increase was only significant in WT at 24 h p.i. (Figure 5.14). *CHI* was neither induced by BAP nor by rhizobia. These gene expression assays support the hypothesis that the observed differential accumulation of isoliquiritigenin (requiring *CHS* and *CHR* activities) and quercetin (requiring *CHS*, *F3'H* and *FLS* activities) in WT roots in response to rhizobia is mediated through cytokinin signalling. For naringenin, which only requires *CHS* activity, there was a discrepancy between induction of *CHS* by rhizobia in WT (but not *cre1* mutants), while *CHS* was not significantly induced by BAP. It is possible that this is due to the different timing of BAP application and rhizobia inoculation or biological variation of the RT-qPCR experiment.

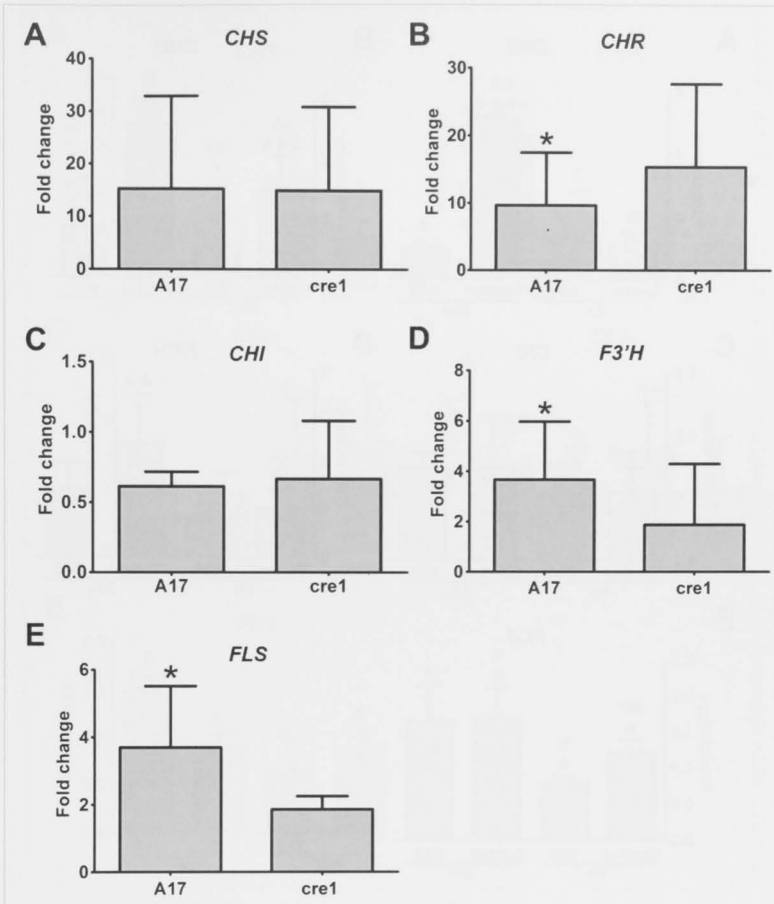


Figure 5.12 Quantitative RT-PCR showing relative transcript abundance of flavonoid-related genes in roots treated with cytokinin (Benzylaminopurine, BAP). Transcript abundance of flavonoid-related genes in WT (A17) and the *cre1* mutant roots treated with 10^{-7} M BAP for 30 min, relatively to mock-treated roots. Expression was normalised to the *RIBOSOMAL BINDING PROTEIN1* (*RBP1*) reference gene (Plet et al., 2011). (A) *CHALCONE SYNTHASE* (*CHS*), (B) *CHALCONE REDUCTASE* (*CHR*), (C) *CHALCONE ISOMERASE* (*CHI*), (D) *FLAVONOID 3'-HYDROXYLASE* (*F3'H*) and (E) *FLAVONOL SYNTHASE* (*FLS*) genes were analysed. A Student's *t*-test was used for statistical analyses ($p < 0.05$, $n = 3$). Asterisks indicate significant inductions by BAP compared to the mock-treatment in WT. Graphs show mean and SD.

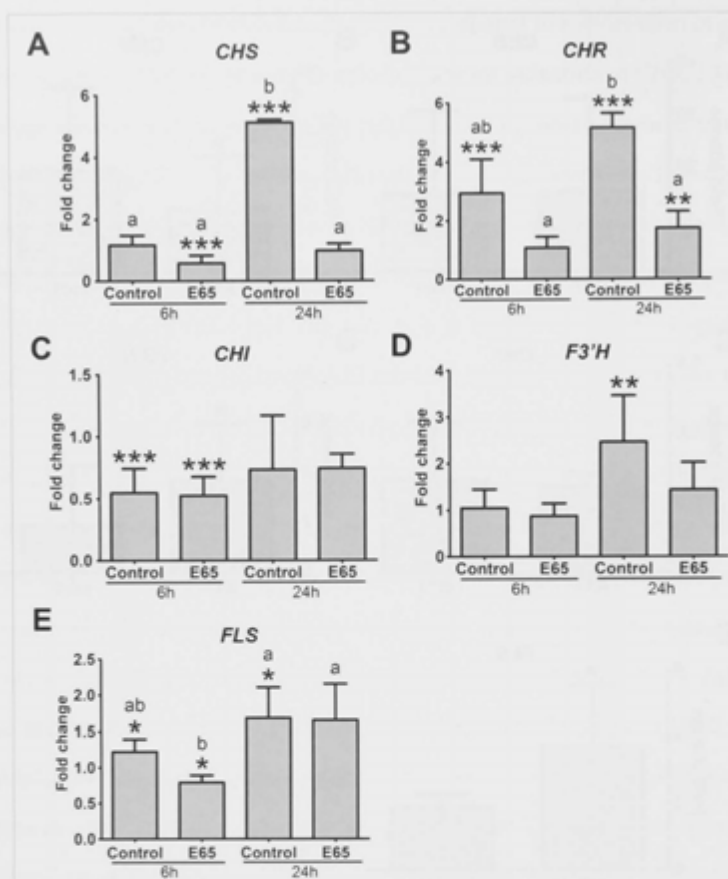


Figure 5.13 Quantitative RT-PCR showing transcript abundance of flavonoid-related genes in root segments. Transcript abundance of flavonoid-related genes in mock-inoculated (control) and inoculated (E65) roots for 6 and 24 h in *cre1* mutants relatively to WT (A17). Expression was normalised to the *GAPDh* reference gene. (A) *CHALCONE SYNTHASE* (*CHS*), (B) *CHALCONE REDUCTASE* (*CHR*), (C) *CHALCONE ISOMERASE* (*CHI*), (D) *FLAVONOID 3'-HYDROXYLASE* (*F3'H*) and (E) *FLAVONOL SYNTHASE* (*FLS*) genes were analysed. A Student's *t*-test was used for statistical analyses between *cre1* mutants and WT (fold change) ($p < 0.05$, $n = 3$). Asterisks indicate significant differences in induction / repression in *cre1* mutants relative to WT. A two-way ANOVA with a Tukey-Kramer multiple comparison post-test was used for statistical analyses between control and E65 treatments ($p < 0.05$, $n = 3$). Different lowercase letters indicate significant differences in induction / repression between control and E65 treatments. Graphs show mean and SD.

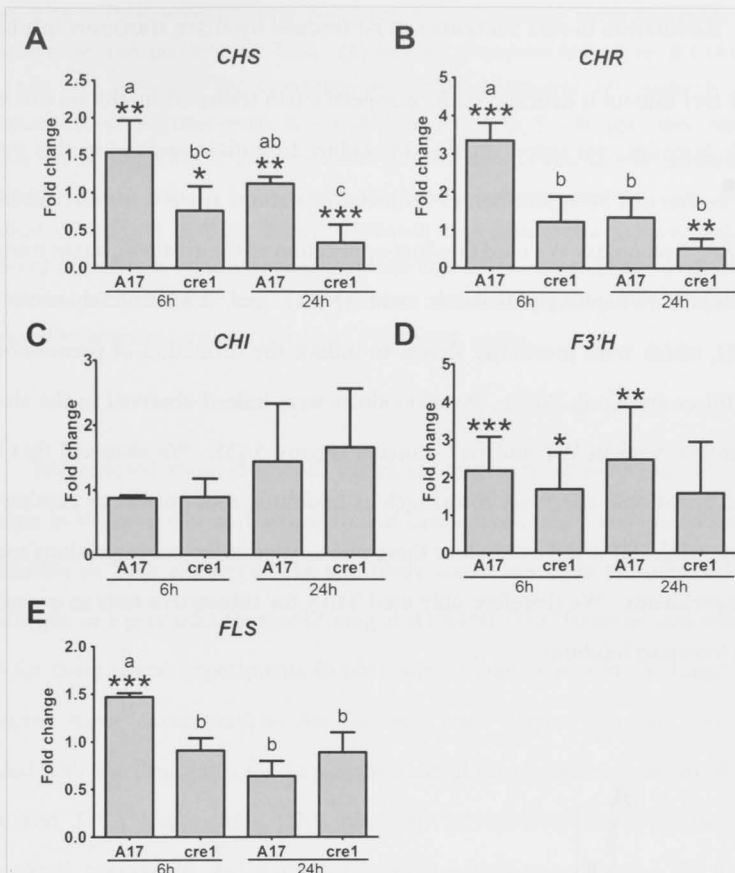


Figure 5.14 Quantitative RT-PCR showing transcript abundance of flavonoid-related genes in root segments. Transcript abundance of flavonoid-related genes in WT (A17) and the *cre1* mutant inoculated for 6 and 24 h with E65 relatively to mock-treated roots. Expression was normalised to the *GAPDh* reference gene. (A) *CHALCONE SYNTHASE* (*CHS*), (B) *CHALCONE REDUCTASE* (*CHR*), (C) *CHALCONE ISOMERASE* (*CHI*), (D) *FLAVONOID 3'-HYDROXYLASE* (*F3'H*) and (E) *FLAVONOL SYNTHASE* (*FLS*) genes were analysed. A Student's *t*-test was used for statistical analyses between roots inoculated with E65 relatively to mock-treated roots (fold change) ($p < 0.05$, $n = 3$). Asterisks indicate significant differences in induction / repression in roots inoculated with E65 relatively to mock-treated roots within individual treatments. A two-way ANOVA with a Tukey-Kramer multiple comparison post-test was used for statistical analyses between genotypes ($p < 0.05$, $n = 3$). Different lowercase letters indicate significant differences in induction / repression between A17 and *cre1* mutants. Graphs show mean and SD.

5.3.3 Nodulation in *cre1* mutants can be rescued by auxin transport inhibitors

As the *cre1* mutant is deficient in the acropetal auxin transport inhibition preceding nodule initiation, we tested whether the failure to initiate nodules in this mutant could be rescued by application of synthetic or natural auxin transport inhibitors, including flavonoids. We used flooding-application of the synthetic auxin transport inhibitors 1-N-naphthylphthalamic acid (NPA) and 2,3,5-triiodobenzoic acid (TIBA), which were previously shown to induce the formation of pseudonodules (Rightmyer and Long, 2011). Pseudonodules were indeed observed in the absence of rhizobia, both in WT and *cre1* mutants (Figure 5.15). We observed that NPA caused pleiotropic effects on roots, such as inhibiting root growth or causing root curling, while TIBA did not induce these phenotypes at the concentrations used in our experiments. We therefore only used TIBA for subsequent tests as a synthetic auxin transport inhibitor.

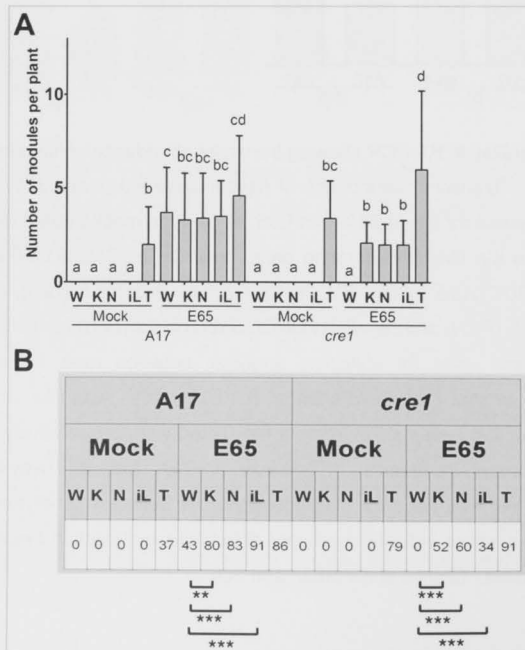


Figure 5.15 Complementation of nodulation in *cre1* mutants using flavonoids or the synthetic auxin transport inhibitor TIBA. (A) Number of nodules forming on WT (A17) and *cre1* roots, with or without E65 inoculation and various treatments: W – water; K – 3 μ M kaempferol; N – 3 μ M naringenin; iL – 3 μ M isoliquiritigenin; T – 50 μ M TIBA. Note that nodules formed with TIBA in the absence of rhizobia were uninfected pseudonodules. A three-way ANOVA with a Tukey-Kramer multiple comparison post-test was used for statistical comparison ($p < 0.05$; $n = 35$). Different lowercase letters indicate statistically significant difference in nodule numbers between treatments. Graph shows mean and SD. (B) Percentage of plants forming nodules in A17 and *cre1* mutants. Two-sample *t*-tests were used for statistical analysis (** $p < 0.01$, *** $p < 0.001$; $n = 35$).

We selected those flavonoid aglycones that were differentially altered by rhizobia in WT and *cre1* mutants, as well as kaempferol, which responded similarly to rhizobia in both genotypes but is a likely auxin transport inhibitor acting in nodulation, or a precursor thereof (Zhang et al., 2009). The flavonoid concentration used for these rescue experiments (3 μ M) was selected as it is in the range of the measured tissue concentrations for free aglycones (Figure 5.9) and roots were flooded with the flavonoids for 10 s at the start of the experiment, identical to the NPA and TIBA treatments. This treatment of seedlings with the flavonoids kaempferol, naringenin, and isoliquiritigenin at a 3 μ M concentration did not lead to pseudonodule formation in either genotype in the absence of rhizobia (Figure 5.15A). Similarly, root growth was not affected by these flavonoids at the 3 μ M concentration (Figure 5.16). We also tested kaempferol application at concentrations up to 100 μ M, but this did not cause pseudonodule formation either. However, when WT or *cre1* mutant roots were inoculated with E65 in the presence of TIBA, kaempferol, naringenin, or isoliquiritigenin, nodules formed on both genotypes with a similar efficiency (Figure 5.15A, B). Addition of quercetin increased percentage of nodulated *cre1* roots and increased nodule numbers in *cre1* mutants such that there was no significant difference in nodule numbers on E65-inoculated roots between mock-treated WT and *cre1* mutants treated with quercetin (Figure 5.17A, B), suggesting a partial rescue effect of quercetin. In contrast,

hesperetin was not able to rescue nodulation of *cre1* mutants to a WT level (Figure 5.17A, B). Overall, naringenin, kaempferol and isoliquiritigenin were able to rescue the *cre1* nodulation phenotype, while quercetin partially rescued nodulation and hesperetin did not rescue nodulation under our conditions.

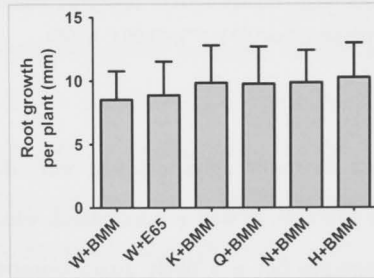


Figure 5.16 Root growth (change in tap root length) on *Medicago truncatula* WT plants with or without flavonoids and E65. A Tukey-Kramer multiple comparisons test was used for statistical comparison between treatments ($p < 0.05$; $n = 15$). Abbreviations: W, water; K, 3 μM kaempferol; Q, 3 μM quercetin; N, 3 μM naringenin; H, 3 μM hesperetin.

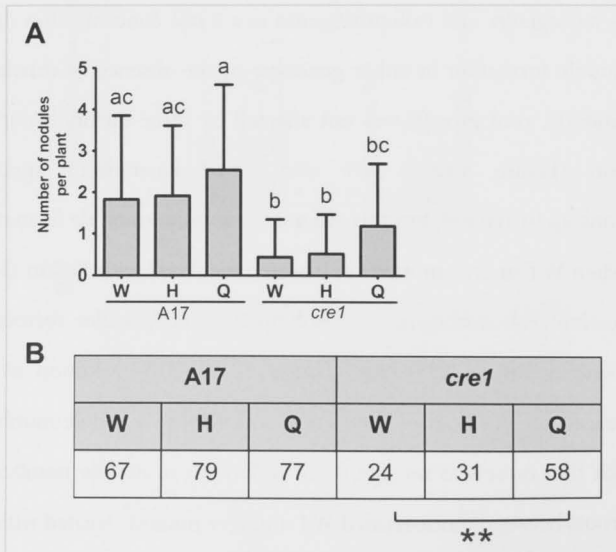


Figure 5.17 Nodulation on WT and *cre1* mutant roots treated with or without quercetin or hesperetin, in the presence of E65. (A) Nodule formation on A17 and *cre1* mutant roots treated with or without quercetin or hesperetin, in the presence of E65. A two-way ANOVA with a Tukey-Kramer multiple comparison post-test was used for statistical comparison between treatments ($p < 0.05$; $n = 35$). (B) Percentage of plants forming nodules on WT (A17) and *cre1* mutant roots treated with or without quercetin or hesperetin, in the presence of E65. A two-sample Student's *t*-test was used for statistical comparison between treatments (** $p < 0.01$; $n = 35$). Abbreviations: W, water; H, 3 μM hesperetin; Q, 3 μM quercetin.

Subsequently, we tested whether application of natural or synthetic auxin transport inhibitors also enabled the induction of *GH3:GUS* expression in nodule primordia. In the absence of rhizobia, pseudonodule primordia that formed in the presence of TIBA expressed *GH3:GUS* in dividing root pericycle, endodermal, and cortical cells similarly in the WT and the *cre1* mutant (Figure 5.5J, K). Likewise, nodules formed in *cre1* mutants in the presence of E65 and naringenin (Figure 5.5L) showed an auxin response in developing nodule primordia. Similar *GH3:GUS* expression was seen in nodule primordia induced in *cre1* roots after addition of either isoliquiritigenin, kaempferol or quercetin (Figure 5.5M-O) but not after addition of hesperetin (Figure 5.5P). To test whether nodules formed in *cre1* mutants in the presence of auxin transport inhibitors were infected, we used a GFP-labelled strain of *S. meliloti* transformed with the E65 plasmid. Nodules that formed on *cre1* mutant roots supplemented with naringenin looked similar to the WT, and were infected with GFP-labelled rhizobia (Figure 5.18). Similarly, supplementation with TIBA, isoliquiritigenin, kaempferol, or quercetin also led to the formation of infected nodules in *cre1* mutants (Figure 5.19).

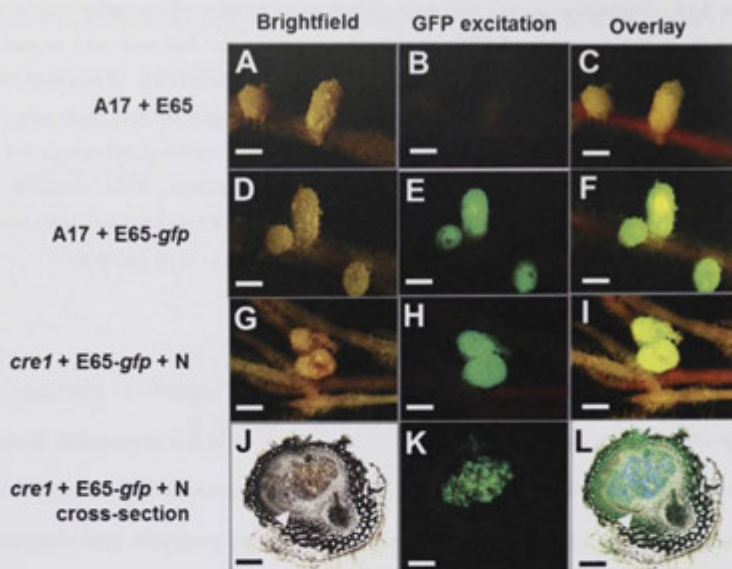


Figure 5.18 Nodules restored on *cre1* mutant roots treated with selected flavonoids are infected by rhizobia. (A-C) WT (A17) roots inoculated with E65 without *gfp* to show background autofluorescence under GFP excitation; (D-F) A17 roots inoculated with a *gfp*-expressing Sm1021 pE65 strain; (G-I) *cre1* mutant roots inoculated with a *gfp*-expressing Sm1021 pE65 strain and treated with naringenin (3 μ M); (J-L) Cross-section of a *cre1* naringenin-rescued nodule shown in (G-I), with *gfp*-expressing Sm1021 pE65 in infected cells of the nodule. (A,D,G,J) Brightfield images; (B,E,H,K) Images taken under GFP excitation (max. excitation 470 nm; 515 nm longpass filter) of the same nodules as in A,D,G,J; (C,F,I,L) Overlay of brightfield and fluorescence images from the same row. More than 20 nodule-forming roots were observed under fluorescence for each treatment. White arrowheads in J and L indicate the nodule peripheral vasculature. Scale bars represent 1 mm in A-I and 500 μ m in J-L.

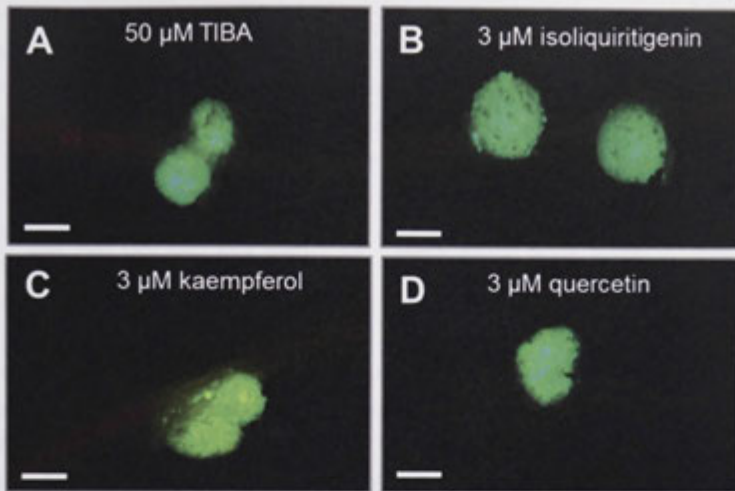


Figure 5.19 Nodules formed on *cre1* mutant roots with addition of auxin transport inhibitors are infected by rhizobia. Roots were co-flood-inoculated with each auxin transport inhibitor and a *gfp*-expressing Sm1021 E65 strain. Nodules were photographed at 3 weeks p.i.. (A) TIBA-, (B) isoliquiritigenin-, (C) kaempferol- and (D) quercetin-rescued nodules. Images were taken under GFP excitation (max. excitation 470 nm; 515 nm longpass filter). More than 20 nodule-forming roots were observed with fluorescence for each treatment. Scale bars represent 1 mm.

To determine whether supplementation with TIBA or flavonoids rescued acropetal auxin transport regulation in *cre1* mutants, we measured auxin transport 24 h after the flood treatment. TIBA alone, which is sufficient to induce pseudonodules, inhibited acropetal auxin transport significantly in WT and *cre1* mutants (Figure 5.20A). Flood treatment with naringenin alone also significantly inhibited acropetal auxin transport in WT and *cre1* roots (Figure 5.20B). Co-treatment with E65 and naringenin, which is sufficient to rescue nodulation in *cre1* mutants, significantly reduced acropetal auxin transport in WT and *cre1* (Figure 5.20B). A comparable result was found with isoliquiritigenin, kaempferol and quercetin (Figure 5.21A, B), but not with hesperetin, (Figure 5.21C, D), which also did not rescue nodulation in *cre1* mutants.

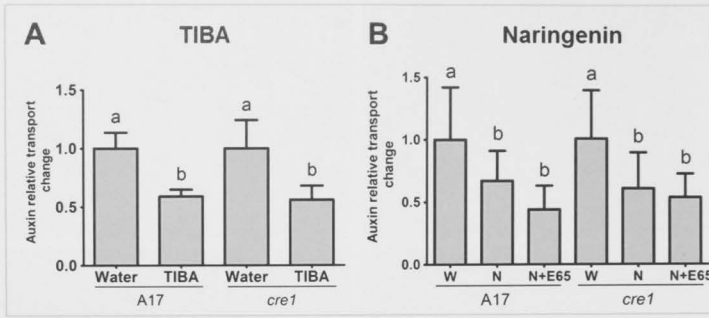


Figure 5.20 Acropetal auxin transport measurements in roots of WT (A17) and the *cre1* mutant. Auxin relative transport rate changes at 24 h post-treatment are shown. Seedlings were treated with (A) TIBA or (B) naringenin, either in the presence or absence of E65. A two-way ANOVA with a Tukey-Kramer multiple comparison post-test was used for statistical comparison ($p < 0.05$; $n = 15-25$). Different lowercase letters indicate significant differences in relative auxin transport rates. Graphs show mean and SD.

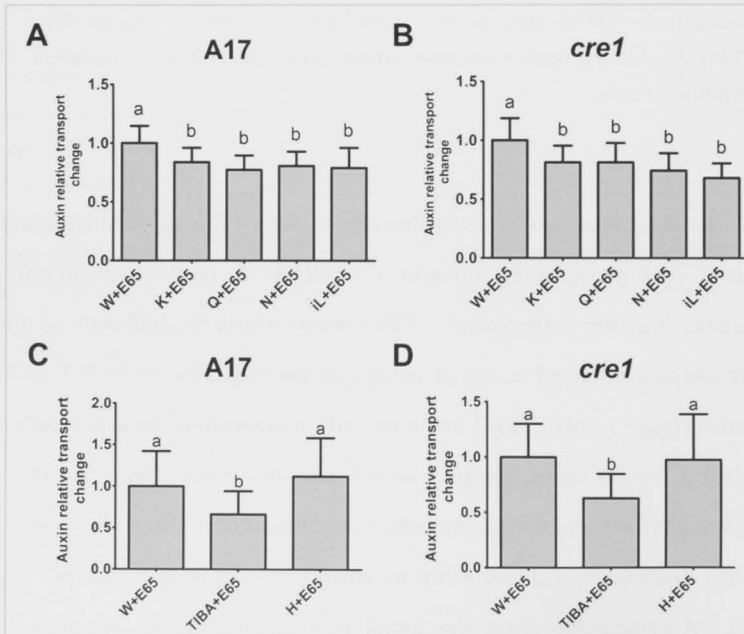


Figure 5.21 Acropetal auxin transport in roots treated with or without flavonoids, in the presence of E65. Acropetal auxin transport in E65-inoculated roots, with a short-term treatment of kaempferol, quercetin, naringenin or isoliquiritigenin on A17 (A) and *cre1* (B) plants. Acropetal auxin transport in E65-inoculated roots, with a short-term treatment of TIBA or hesperetin in A17 (C) and *cre1* (B). A Tukey-Kramer multiple comparison test was used for statistical comparison between treatments ($p < 0.05$; $n = 20$). Different lower case letters indicate a significant change in relative auxin transport. Abbreviations: W, water; K, 3 μM kaempferol; Q, 3 μM quercetin; N, 3 μM naringenin; iL, 3 μM isoliquiritigenin; H, 3 μM hesperetin. Graphs show mean and SD.

In contrast to acropetal auxin transport, basipetal auxin transport was not inhibited by application of TIBA in WT or in *cre1* mutants (Figure 5.22A). Flood treatment of roots with a number of flavonoids also failed to alter basipetal auxin transport (Figure 5.22B). Co-treatment of roots with E65 and quercetin reduced basipetal auxin transport in WT but not in *cre1* mutants (Figure 5.22C). Thus, none of the tested auxin transport inhibitors mimicked the increased basipetal auxin transport that was observed in WT after E65 inoculation (Figure 5.2B), even though they were sufficient to rescue nodulation. This suggests that the acropetal, but not the basipetal, auxin transport changes following *Rhizobium* infection are crucial for successful nodule initiation.

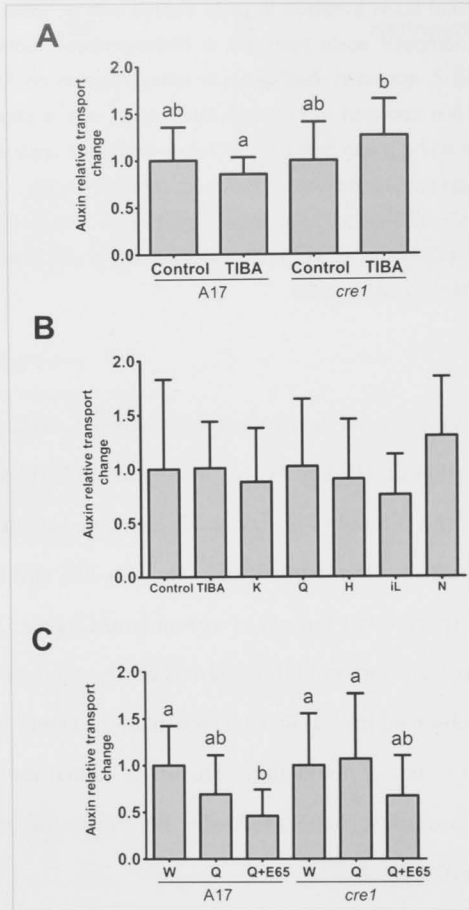


Figure 5.22 Basipetal auxin transport in WT and *cre1* mutant roots in response to auxin transport inhibitors at 24 h.p.i.. (A) TIBA, (B) flavonoids (A17 only) (3 μ M) in the absence of rhizobia, (C) quercetin (3 μ M) in the absence and presence of E65. A two-way ANOVA with a Tukey-Kramer multiple comparison post-test was used for statistical analysis in (A) and (C) ($p < 0.05$, $n = 20$). A Tukey-Kramer multiple comparison test was used for statistical analysis in (B). Different lower case letters indicate a significant change in relative auxin transport. Abbreviations: W, water; TIBA, 2,3,5-triiodobenzoic acid; K, 3 μ M kaempferol; Q, 3 μ M quercetin; H, 3 μ M hesperetin; iL, 3 μ M isoliquiritigenin; N, 3 μ M naringenin. Graphs show mean and SD.

5.4 Discussion

5.4.1 Cytokinin signalling is required for increased auxin accumulation at the infection site

Our results suggest that cytokinin signalling through CRE1 is required for the accumulation of auxin in pericycle, endodermal, and cortical cells targeted to divide to form a nodule. Indeed, *cre1* mutants did not show increased IAA concentrations following *Rhizobium* inoculation, and the auxin reporter *GH3:GUS* was only induced in dividing cells leading to nodule formation in the WT or in the few cases of successful nodulation in *cre1* mutants. Our evidence points to a correlation between IAA concentrations and *GH3:GUS* expression level. However, we cannot exclude the importance of other auxins that were not detectable or not measured in our assays. While we concentrated on auxin amino acids conjugates, which were previously suggested to be present in *M. truncatula* (Campanella et al., 2008), a number of other auxin conjugates exists in plants that could contribute to the dynamics of auxin breakdown, storage and activity (Korasick et al., 2013). In addition, it is likely that the *GH3:GUS* reporter construct does not reflect the exact localization and activity of all different auxins in the root. Nevertheless, auxin activity analyzed through *GH3:GUS* expression agrees with the induction of the *DR5* promoter in nodule primordia of *L. japonicus* (Suzaki et al., 2012) and soybean (Turner et al., 2013) and in the cortex of *M. truncatula* (Breakspear et al., 2014). Interestingly, an auxin response in root hairs at the infection site was visible after 24 h p.i. in both genotypes. A similar auxin response was identified in *M. truncatula* recently, and shown to be involved in the infection process (Breakspear et al., 2014). This suggests that the cortical auxin response is associated with nodule primordium formation, depending on CRE1, while the epidermal auxin response associated with infection still occurs in the *cre1* mutant. In addition, supply of *cre1* mutants with auxin transport inhibitors restored the induction of cortical *GH3:GUS* expression in

nodule primordia and the development of nodules. These results are consistent with the findings that cytokinin application induced expression of *GH3:GUS* in dividing cortical cells in white clover (Mathesius et al., 2000a) and that spontaneous cortical cell divisions in the *Lotus japonicus snf2* mutant are associated with *DR5:GFP* expression (Suzaki et al., 2012). In addition, we also measured a significantly higher transcript abundance of the putative auxin synthesis genes *YUC2* and *YUC3* in WT relatively to the *cre1* mutant, in response to E65 inoculation (Appendix E). These preliminary results suggest a possible role for IAA biosynthesis in generating auxin maxima in the nodule primordia of *M. truncatula*.

These data are reminiscent of studies showing that, in Arabidopsis, cytokinin signaling regulates auxin accumulation during lateral root initiation (Laplaze et al., 2007b). In Arabidopsis, cytokinin was previously shown to control the auxin pool via alteration of PIN protein expression and localization, for example during lateral root initiation (Pernisova et al., 2009; Ruzicka et al., 2009b; Marhavy et al., 2011; Marhavy et al., 2014). In our study, we did not find any clear evidence that the decrease in acropetal auxin transport was accompanied by a reduction in *PIN* or *LAX* gene expression. Indeed, in response to *Rhizobium* inoculation in the WT, we found an increased *PIN4* and *M. truncatula PIN10* expression, the closest homolog of Arabidopsis *PIN1*, which encodes a protein that transports auxin acropetally in Arabidopsis (Petrasek and Friml, 2009). *PIN4* and *PIN10* transcript levels also increased within the first 6 h p.i. with Nod factors in WT but not *cre1* mutant roots (Plet et al., 2011). Therefore it is most likely that *PIN* expression levels are not a sufficient predictor of actual auxin transport capacity. Instead, additional post-transcriptional regulatory mechanisms likely modulate PIN protein activity. Alternatively, *M. truncatula PIN4* and *PIN10* may not be the main transporters mediating acropetal auxin transport, but might be involved in lateral auxin transport.

As both synthetic auxin transport inhibitors as well as certain flavonoids inhibit auxin export (Jacobs and Rubery, 1988), it is expected that the accumulation of auxin in nodule primordia is related to a decreased auxin export from these cells. Reduced acropetal auxin transport was measured below the nodule initiation site in *M. truncatula* in this study, as well as in Plet et al. (2011) and Wasson et al. (2006). Accordingly, in *Vicia sativa* roots, Nod factor application reduced acropetal auxin transport (Boot et al., 1999a). Our evidence thus supports the *in silico* modeling of auxin maximum generation during nodule initiation, which suggested that auxin accumulation in nodule primordia is most likely explained by a reduced auxin export (Deinum et al., 2012). While BAP application to white clover roots did not lead to reduced *GH3:GUS* expression below the application site in white clover (Mathesius et al., 2000), our finding that BAP application to roots significantly reduced acropetal auxin transport in *M. truncatula* supports the hypothesis that the induction of cytokinin signalling during nodulation acts upstream of auxin transport control, in accordance with results from Plet et al. (2011).

We also measured basipetal auxin transport, and found increased basipetal auxin transport in response to rhizobia in the WT at 24 h p.i., which was not detected in *cre1* mutants. This was accompanied in the WT with increased *PIN2* expression; *M. truncatula* *PIN2* is a homolog of the *Arabidopsis* *PIN2* transporter responsible for basipetal auxin transport from the root tip to the elongation zone (Schnabel and Frugoli, 2004b). However, the increased basipetal auxin transport was not mimicked in *cre1* mutants rescued with auxin transport inhibitors, therefore we cannot confirm at this stage whether the increased basipetal auxin transport is necessary for nodule initiation.

Collectively, our results show that the *cre1* mutant is defective in the inhibition of acropetal auxin transport in response to rhizobia. As TIBA and specific flavonoids were able to inhibit acropetal auxin transport similarly in

inoculated *cre1* mutants as in WT roots, this suggests that *cre1* mutants are defective in the induction of an endogenous auxin transport inhibitor.

5.4.2 Flavonoids rescue the *cre1* mutant

Our results showed that mRNA levels of *CHS*, *CHR*, and *FLS* were induced significantly by rhizobia in WT but not in *cre1* mutant roots, and that *cre1* mutant roots did not show increased free naringenin, quercetin, and hesperetin concentrations in E65-inoculated roots, while the concentration of isoliquiritigenin was increased in *cre1* mutants after inoculation with E65, but was significantly lower than in inoculated WT roots. CHS activity is required for the synthesis of all flavonoids, while CHR leads to isoliquiritigenin synthesis and FLS leads to kaempferol and quercetin synthesis (Figure 5.11). Supplementation of *cre1* mutant roots with rhizobia and naringenin, isoliquiritigenin or kaempferol rescued nodulation to a WT level, while hesperetin did not, and quercetin showed a partial rescue. These results strongly suggest that the transcriptional induction of flavonoids during nodule initiation is a (direct or indirect) target of cytokinin signalling. Similarly, results by van Zeijl et al. (2015) showed that a number of flavonoid synthesis genes are induced by Nod factors after 3 h in WT but not in *cre1* roots, including a flavonoid hydroxylase, a dihydroflavonol reductase-like protein, a flavonoid glucosyl transferase, five isoflavone methyltransferases and a malonyl-CoA:isoflavone 7-O-glucoside malonyl transferase, while two copies of flavonol synthase/flavanone-3-hydroxylase were significantly reduced in WT, but not *cre1* roots. In addition, our study showed induction of *CHR*, *F3'H* and *FLS* expression by the cytokinin BAP, while a previous transcriptomic analysis of *M. truncatula* root apices response to cytokinins demonstrated that flavonoid-metabolic genes constituted the most significantly enriched functional category (Ariel et al., 2012 and Table 5.1). Previous results showing that a local BAP treatment of white clover

roots led to cortical cell divisions, *CHS* induction and flavonoid accumulation in the dividing cells also support this model (Mathesius et al., 2000a). In addition, in *Arabidopsis*, expression of some flavonoid genes was also found to be under the control of cytokinins (Bhargava et al., 2013). However, it is likely that BAP treatment does not correctly mimic the induction of specific endogenous cytokinins during nodule initiation (van Zeijl et al., 2015), since BAP also induced changes in flavonoid gene expression in the *cre1* mutant. This suggests that the BAP-induced changes are mediated by CRE1, as well as other cytokinin receptors.

So far, it is unknown which flavonoid(s) is (are) responsible for auxin transport regulation during nodulation. Silencing of the flavonoid pathway in *M. truncatula* indirectly suggested that flavonols, most likely kaempferol, are required for auxin transport control because kaempferol addition to *CHS*-silenced roots, in combination with supplying rhizobia with *nod* gene inducing flavones, rescued nodulation (Zhang et al., 2009b). Our results show that even though nodulation in the *cre1* mutant could be rescued by application of kaempferol, the *cre1* mutant roots were not deficient in free or total kaempferol concentrations compared to WT. However, we detected in *cre1* a deficiency in the induction of free quercetin by rhizobia, which was observed in the WT at 24 h p.i. with E65. Kaempferol can be converted to quercetin (Figure 5.11), and thus it is possible that experiments with kaempferol addition may lead to an increase of the quercetin pool. However, quercetin supplementation only partially rescued nodule formation in *cre1* mutants. Therefore, it is unlikely that flavonol aglycones are sufficient candidates for acropetal auxin transport control during nodulation in *M. truncatula*. We could also rescue nodulation in *cre1* mutants with naringenin and isoliquiritigenin, which accumulated to significantly higher concentrations in inoculated WT compared to inoculated *cre1* roots. In our assays, naringenin and isoliquiritigenin could rescue auxin transport inhibition in *cre1* roots, and are therefore also good candidates for auxin transport inhibitors during nodulation. A

summary of the characteristics of the different flavonoids tested and their relative abundance in WT and *cre1* roots in response to *Rhizobium* inoculation is shown in Table 5.2 and Figure 5.23. From this comparison, the most likely candidates for auxin transport control regulated by the CRE1 cytokinin pathway are naringenin and isoliquiritigenin, or derivatives thereof, formed in the root after supplementation.

Recent studies have suggested that in addition to flavonoid aglycones, flavonoid glycosides might act as auxin transport inhibitors. For example, an *Arabidopsis* flavonoid 3-O-glycosyltransferase mutant, which over-accumulated kaempferol 3-O-rhamnoside-7-O-rhamnoside, showed reduced polar auxin transport (Yin et al., 2014). Similarly, auxin transport phenotypes in several *Arabidopsis* flavonoid mutants have been linked to altered accumulation of flavonoid glycosides as they contain undetectable levels of free kaempferol or quercetin aglycones (Buer et al., 2013). In addition, overexpression of the transcription factor WRKY23 in *Arabidopsis* led to increased levels of quercetin-3-O-rhamnoside, accompanied by a reduced auxin transport in seedling roots (Grunewald et al., 2012). Among the 18 cytokinin-inducible flavonoid-related genes, 14 were putative (iso)flavonoid glycosyl transferases (Ariel et al., 2012; Table 5.1). Thus, future studies could be focused on detailed analysis of flavonoid glycosides during nodulation.

In addition to their activity as endogenous auxin transport inhibitors, flavonoids also play a role as *nod* gene inducers in rhizobia. As the *cre1* mutant was partially defective in the induction of isoliquiritigenin, which can act as a *nod* gene inducer in *S. meliloti* (Zuannazzi et al., 1998), this may affect the ability of rhizobia to induce nodules in the *cre1* mutant. However, in our study we used the A2102 strain harboring the pE65 plasmid, which expresses the *NodD3* gene from a constitutive promoter (Barnett et al., 2004). Therefore, it is unlikely that a

deficiency in *nod* gene inducing flavonoids was the reason for the lack of nodulation in the *cre1* mutant inoculated with this *Sinorhizobium* strain.

Table 5.2 Summary table showing the roles of different flavonoid aglycones identified in this study.

Flavonoid	Differential accumulation between WT and <i>cre1</i> roots after rhizobia inoculation	Rescue of nodulation in <i>cre1</i>	Rescue of acropetal auxin transport inhibition in <i>cre1</i>	Rescue of <i>GH3:GUS</i> response in <i>cre1</i> nodule primordia	Expression of genes leading to flavonoid synthesis induced by rhizobia	Expression of genes leading to flavonoid synthesis induced by cytokinin
Naringenin	Yes ¹	Yes	Yes	Yes	Yes	Yes
Isoliquiritigenin	Yes ²	Yes	Yes	Yes	Yes	Yes
Quercetin	Yes ³	Partial	Yes	Yes	Yes	Yes
Kaempferol	No	Yes	Yes	Yes	Yes	Yes
Hesperetin	Yes ³	No	No	No	Yes	Yes
Chrysoeriol	No	Not tested	Not tested	Not tested	No	Yes
Morin	No	Not tested	Not tested	Not tested	Not tested	Not tested
Liquiritigenin	No	Not tested	Not tested	Not tested	Not tested	Not tested
Daidzein	No	Not tested	Not tested	Not tested	Not tested	Not tested
Formononetin	No	Not tested	Not tested	Not tested	Not tested	Not tested
Medicarpin	No	Not tested	Not tested	Not tested	Not tested	Not tested
Biochanin A	No	Not tested	Not tested	Not tested	Not tested	Not tested

¹ Differential accumulation between E65-inoculated WT and *cre1* mutant roots, but no significant induction in WT inoculated vs WT control roots

² Differential accumulation in response to E65 inoculation, as well as between inoculated WT and *cre1* mutant roots

³ Differential accumulation in response to E65 inoculation only in WT but not in *cre1* mutant roots

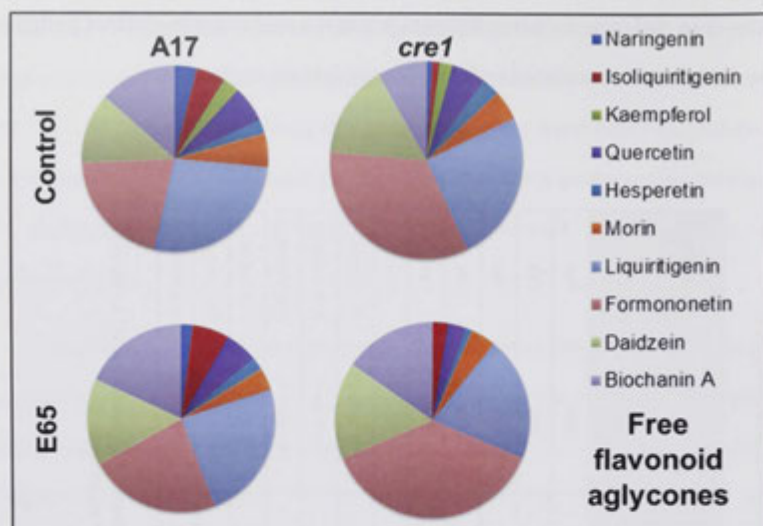


Figure 5.23 Relative flavonoid abundance (free aglycones) in WT and *cre1* mutant roots in control or E65-inoculated roots. The flavonoids shown here only represent those with absolute quantitation data.

To conclude, our results suggest a model in which cytokinin signalling (activated by Nod factor perception) via the CRE1 receptor leads to a transient induction of flavonoid synthesis or release, which is required for local, acropetal auxin transport inhibition and subsequent auxin accumulation in the initiating nodule (Figure 5.24). Our current evidence points to naringenin and isoliquiritigenin as the most likely candidates for flavonoids acting as auxin transport inhibitors and IAA as the most likely active auxin induced during early nodule development. Since the *cre1* mutants is defective in the induction of a large number of transcripts following Nod factor application (van Zeijl et al., 2015), it will be interesting to determine in the future whether these gene expression changes are also dependent on changes in flavonoid accumulation.

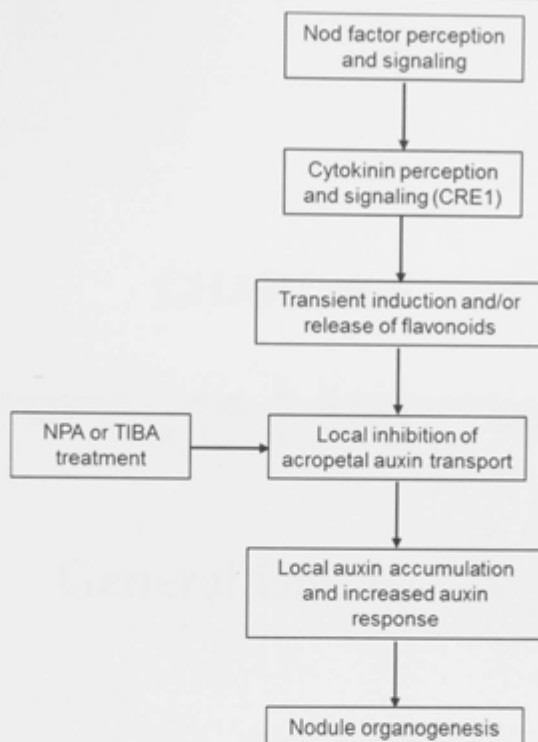
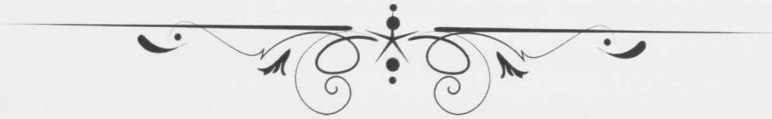


Figure 5.24 Proposed model for the action of cytokinin on auxin transport and accumulation during nodule initiation in *Medicago truncatula*. Our data suggest a model in which cytokinin signalling mediated by the CRE1 receptor transiently activates or releases certain flavonoids (most likely naringenin and / or isoliquiritigenin) in the root, which then act as auxin export inhibitors that cause auxin (IAA) accumulation and subsequently enhance auxin response in cells that will divide to form a nodule primordium. Both transient application of synthetic auxin transport inhibitors like NPA and TIBA, or flavonoids, induce (pseudo)nodules infected by rhizobia.

CHAPTER 6



General Discussion



We aimed to investigate the mechanisms that lead to an increased auxin response in the nodule primordia of both indeterminate and determinate nodules, as demonstrated in previous studies. Since an increase in auxin concentrations is one of the most likely reasons that can explain the increase in auxin response, we aimed to develop a sensitive and reproducible method for quantifying auxins in root tissues. We were also interested in comparing the differences between indeterminate and determinate nodules, in terms of their endogenous auxin concentrations and profile. A recent modelling approach suggested that differences in auxin export at the nodule initiation site could be the defining feature of nodule type. Therefore, we compared auxin transport changes at the nodule initiation site between *M. truncatula* and *L. japonicus*, as well as correlated the differences in auxin transport capacities with their endogenous auxin concentrations. Finally, we aimed to place the regulation of auxin transport and changes in auxin concentrations in context with the known nodulation signalling pathway of *M. truncatula*, in particular with cytokinin signalling.

6.1 Hypothesis one: Mass spectrometry complements qualitative/semi-quantitative results obtained through alternative approaches to study auxin

In Chapter 3, we optimised a method for high sensitivity quantification of auxins in root tissues. This highly sensitive LC-MS/MS method was used to study endogenous auxin concentrations in various legumes and non-legumes in Chapters 4 and 5, in an attempt to elucidate the differences relating to changes in auxin concentrations during indeterminate and determinate nodulation. We interpreted data derived from a combination of: (1) direct quantification of auxins via LC-MS/MS and, (2) various molecular and physiological approaches. We reasoned that metabolomics complements other tools used to study nodulation. In this thesis, we hypothesised that multiple, complementary approaches not only provide important biological information at different cellular regulatory levels, but are also essential at facilitating conclusions based on a more holistic view of complex developmental pathways.

6.1.1 Challenges in the study of auxin at multiple levels

Auxins represent a large class of plant hormones with a complex signalling pathway. Auxin was the earliest hormone to be identified in plants and is implicated in many physiological processes. The idea of comprehensively describing the role of auxins using different approaches at multiple regulatory levels is presented with many hurdles. As described in Section 1.1 in more depth, the auxin signalling pathway is complex. The best-characterised auxin signalling pathway is the TIR1/AFBs-AUX/IAAs signalling module (Dharmasiri et al. 2005). However, previous reports suggest the existence of two other auxin receptors, which could potentially lead to multiple auxin signalling pathways, depending on stimuli (del Pozo et al. 2006;

Napier et al. 2002). One of the most widely utilised auxin reporters is the primary auxin response gene *GH3*. However, since the cloning of the first *GH3* promoter from soybean (Hagen et al. 1991), multiple copies have been identified in various species. In *M. truncatula*, 17 copies of the *GH3* gene have recently been reported (Yang et al. 2014). This complicates the use of one particular *GH3* gene as a universal reporter due to cell or stage-specific promoter activities, in addition to their auxin-responsive elements. Auxin homeostasis is affected by auxin transport, biosynthesis and conjugation/breakdown. The ABCB/PGP subfamily of transporters could potentially be important auxin transport regulators during nodulation, but these are still poorly understood. Auxin biosynthesis was investigated in Chapter 5. However, the *TAA* and *YUC* genes in the IPyA pathway were targeted in this study although other auxin synthesis pathways could contribute significantly, but are yet to be systematically studied in *M. truncatula*. Although multiple IAA-conjugates were identified via LC-MS/MS in Chapters 4 and 5, the genetic and molecular basis of their regulation was not investigated in this study. The scale of experimental work required to uncover the labyrinth of auxin regulation at any given developmental stage is large.

In Chapter 5, we explored the mechanism of nodule formation, focussing on *M. truncatula*. We approached this question by forming several complementary hypotheses surrounding molecular players that either regulate, or are regulated by auxin. Physiological experiments showed that auxin transport regulation in *M. truncatula* requires a functional cytokinin receptor-like kinase. Exogenous application of auxin transport regulators induced nodule-like structures, supporting our hypothesis that auxin transport regulation occurs downstream of the cytokinin receptor-like kinase. This was further supported by transcript analyses showing the involvement of several auxin carriers in response to *Rhizobium* treatment. Transcript analyses also suggest a role played by auxin synthesis genes in generating a proper auxin gradient during nodulation. Reporter-based assays reaffirmed the

auxin transport data, which suggested a potential accumulation of auxin around the *Rhizobium*-treated spot. Finally, auxin quantification via LC-MS/MS supported a change in auxin concentration in response to *Rhizobium* treatment, possibly due to a synergistic contribution by auxin transport and auxin synthesis (Figure 6.1). Curiously, although an increase in *DR5* response has previously been reported in the nodule primordia of *L. japonicus* (Suzaki et al. 2012; Takanashi et al. 2011), we did not detect an increase in IAA concentration after *Rhizobium* treatment. Thus, we speculate that IAA might not be the inducer of *DR5* in *L. japonicus*.

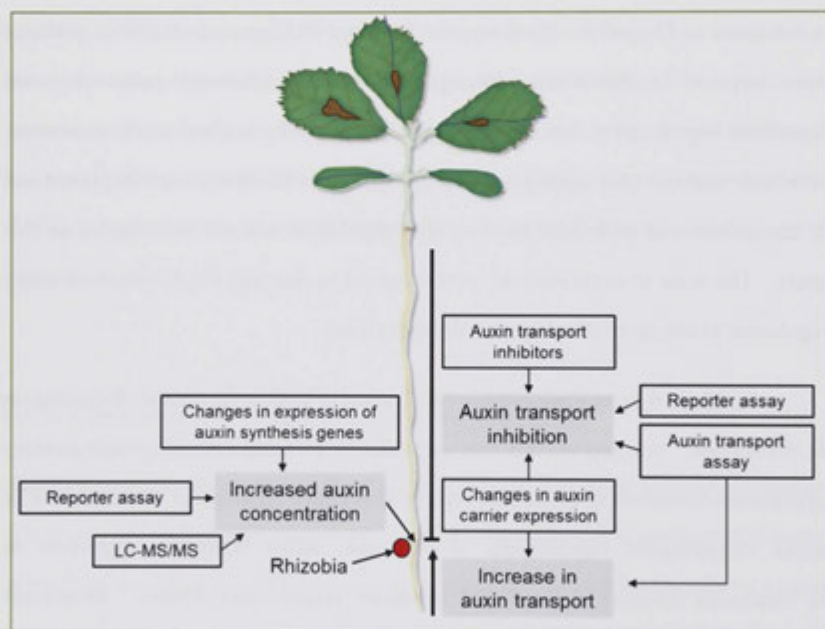


Figure 6.1 Complementary approaches to study auxin regulation of nodulation in *Medicago truncatula*. The regulation of auxin transport surrounding the *Rhizobium* treatment zone was confirmed by direct measurements with radiolabelled auxin. Results from reporter assays and transcript analyses of auxin carriers support data from radiolabelled auxin measurements. Effects from *Rhizobium*-induced changes could be mimicked by auxin transport inhibitors. An increase in auxin concentration thereafter was confirmed by LC-MS/MS analyses and reporter assays. An induction of several auxin

synthesis genes suggests a possible role for auxin synthesis, together with auxin transport, in generating a correct auxin gradient during nodulation. Grey boxes indicate observed/measured experimental outcomes. White boxes indicate experimental techniques/observations used to produce/infer those experimental outcomes. Thick solid lines represent auxin transport flow (upwards)/inhibition (downwards).

6.1.2 Advantages and disadvantages of quantitative hormone measurements using mass spectrometry

Due to technological improvements in recent years, mass spectrometry has emerged as the number one tool for quantitative hormone profiling. Mass spectrometry offers superior specificity and sensitivity, two very important factors for low concentration metabolites like auxins with a large family of similarly-structured compounds. Modern mass spectrometers can target specific compounds by having multiple layers of selection filters (Pan and Wang 2009). This is an advantage over reporter-based techniques, because many promoters are not specific to one activator. For example, the synthetic *DR5* promoter has been shown to respond to brassinosteroids, in addition to auxin (Nakamura et al. 2003). This suggests that reporter outputs might not necessarily represent an equivalent level of input by the intended compound / activator of interest. On the other hand, authentic reference standards can be used to unequivocally identify a specific compound because no two compounds share the same mass fingerprint. Transgenic plants are often limited to one or few reporter constructs, which means only a few compounds can be monitored at once. Mass spectrometry allows profiling of multiple classes of hormones in a single experiment, thus saving experimental material and equipment run cost. Furthermore, by switching the mass spectrometer into “automatic” mode, it allows metabolite discovery by scanning the whole metabolome of the sample and subsequently displays the top hits. One of the limiting steps in metabolite quantitation via mass spectrometry is the extraction procedure. However, the availability of automated workstations would increase data acquisition rate.

Disadvantages of mass spectrometry include the need to optimise the system for specific aims / metabolites, prior to experimentation. For the targeted operational mode, the same method is not transferable to study other compounds. To achieve maximum sensitivity and accuracy, especially for the study of metabolites that are low in concentrations, every parameter of the mass spectrometer needs to be optimised. Moreover, mass spectrometry does not offer spatial and temporal resolution of metabolite concentration due to the inherent need for tissue destruction prior to analysis. In the case of localised metabolite quantification, such as that employed in this project, plant material from multiple organisms is usually needed to achieve sufficient, minimal tissue mass for a single sample.

6.1.3 Advantages and disadvantages of hormone quantitation using alternative techniques

Classical immunolocalisation, particularly with monoclonal antibodies, is a direct tool for *in situ* hormone detection. Immunolocalisation provides subcellular localisation of the target compound. However, although whole-mount immunolocalisation is suitable in small plants (e.g., in *Arabidopsis* roots), the antibodies may not sufficiently penetrate thicker and bigger plants, such as *M. truncatula*. As a consequence, tissue sections are required for sufficient antibody contact with target compounds, which increase labour and experimental time. As mentioned above, promoter:reporter assays are not suitable for hormone quantitation due to potential non-specific promoter activation. Furthermore, in the case of the auxin responsive *GH3* and *DR5* reporters widely used to study auxin response, multiple genetic components are involved between auxin perception and reporter activation (Figure 6.2). The transcription and translation rates of each component may be different. The relationship between auxin abundance and

reporter output is non-linear, making conclusions about auxin concentrations derived from such experiments unreliable. A biosensor was developed for auxin and this presents a more direct approach for auxin quantitation (Brunoud et al. 2012). The use of a fast maturing VENUS protein ensures a rapid response upon auxin perception. The DII-VENUS auxin sensor allows mapping of auxin distribution at the root tip, as well as monitoring auxin concentration during several developmental programs in real-time (Band et al. 2012; Sassi et al. 2012). In addition, it could potentially be used to derive information about auxin transport direction during developmental responses, such as during lateral root and nodule formation. Despite of this, the auxin biosensor is still an indirect detection and quantification approach compared to immunolocalisation and mass spectrometry, because it is still dependent on the TIR1-AUX/IAA signalling pathway. In the last few years, Förster Resonance Energy Transfer (FRET)-based biosensors have been developed (Wells et al. 2013). This type of biosensor provides direct detection of small molecules. Upon binding of a fluorescent protein (FP) to its target small molecule-FP fusion, FRET-induced changes in fluorescence characteristics can be directly detected. This strategy has been used in the identification of sucrose transporters (SWEETs) (Chen et al. 2012). Ribonucleic acid is also an emerging platform for generating fluorescent biosensors that can directly target small molecules and plant hormones (Liang et al. 2011; Paige et al. 2012). The recent use of fluorescent auxin analogues for direct visualisation is also an enticing alternative for studying auxin concentration and transport (Hayashi et al. 2014). Microscopy is generally a labour-intensive and time-consuming process. Hence, the downside for many of the fluorescent-based techniques above is the low throughput. Side effects from exogenous introduction of fluorescent compounds into plants are also subjects for further investigation.

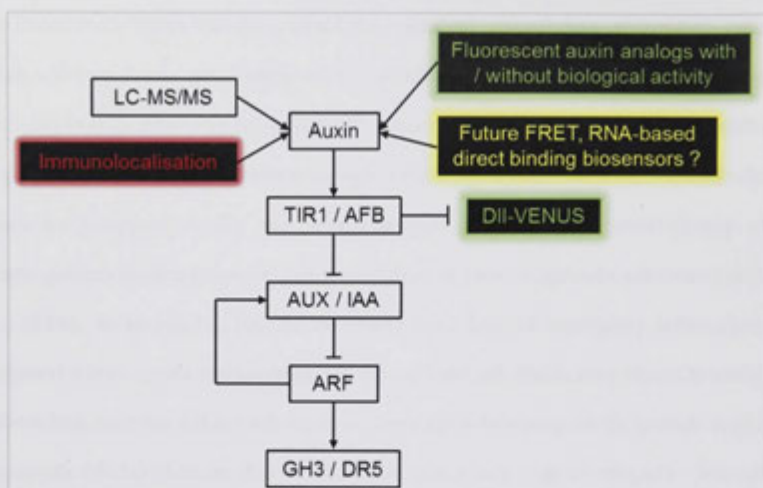


Figure 6.2 Comparison of various techniques to measure auxin transport and concentration. Traditional *GH3* and *DR5*-based reporters are activated following a complex signalling pathway involving transcription, translation and feedback mechanisms. Auxin input and the resulting *GH3* / *DR5* output is not linear. LC-MS/MS, immunolocalisation and fluorescent auxin analogs are direct methods for studying auxin concentration and transport, with several distinct advantages and disadvantages. The auxin biosensor, DII-VENUS interacts with TIR1 / AFB and is degraded along with the AUX / IAA proteins at the proteasome. It is not a direct method for auxin quantitation, but represents a tool which can provide quantitative data with proper mathematical calibration. Future biosensors could be based on FRET methods or RNA molecules.

6.2 Hypothesis two: Auxin transport control is a general mechanism for increasing/decreasing auxin content during nodulation

Auxin transport control has been a major assessment tool throughout this thesis. In Chapter 4, we compared auxin transport regulation between *M. truncatula* and *L. japonicus* in response to *Rhizobium* treatment. These two model legumes represent indeterminate and determinate nodule-forming legumes, respectively. Previous results suggested that auxin transport control in these two groups of legumes differs. By using a combination of physiological, molecular and microscopic techniques on a few leguminous plants, we showed that auxin transport control can be manipulated by rhizobia differently to achieve the same outcome in legumes, i.e. nodulation. Changes in auxin concentrations in response to *Rhizobium* treatment were different between *M. truncatula* and *L. japonicus*. In general, however, only IAA showed significant changes in concentrations in response to rhizobia inoculation, whereas the auxin conjugates that were detected did not show any significant change. Thus, the host auxin transport machinery is not only an important toolbox manipulated by rhizobia during nodulation; it is also a highly tuneable system, as evident by the differences in regulation in two closely-related nodulation programs.

6.2.1 Why does auxin transport inhibition occur?

The importance of auxin transport control during nodule organogenesis was initially demonstrated by Allen et al. (1953) and later by Hirsch et al. (1989). The authors demonstrated that external application of synthetic ATIs could induce nodule-like structures on the roots of leguminous plants. ATI-treated alfalfa roots expressed the nodulation markers *ENOD2* and *Nms-30* (Hirsch et al. 1989), similar

to root responses to *Rhizobium* treatment. Later, Rightmyer and Long (2011) showed that several genes exhibited similar transcriptional responses when treated with either ATI or *S. meliloti*, and that genes that showed opposite transcriptional responses at the early stages upon ATI or *S. meliloti* treatment exhibited similar transcriptional patterns at the later stages. These findings suggest that inhibition of auxin transport acts in the nodulation signalling pathway. Since then, various studies have shown a signature transient acropetal auxin transport inhibition in indeterminate nodule-forming legumes, including *M. truncatula*, white clover and vetch, in response to *Rhizobium* or Nod factor treatment (Boot et al. 1999; Mathesius et al. 1998; Plet et al. 2011; van Noorden et al. 2006; Wasson et al. 2006). Interestingly, this phenomenon has never been reported in determinate nodule-forming legumes. In the determinate nodule-forming legume *L. japonicus*, one study measured an increase in acropetal auxin transport in response to *Rhizobium* treatment at 48 h.p.i. (Pacios-Bras et al. 2003). Another study in soybean (forming determinate nodule) inferred a null requirement for acropetal auxin transport inhibition based on their primary data. The authors, however, did not measure auxin transport directly (Subramanian et al. 2006). By quantifying auxin transport capacity in corresponding segments of *M. truncatula* and *L. japonicus*, we demonstrated that both legumes regulated acro- and basipetal auxin transport in a different manner during the early stages of nodulation.

Interestingly, we discovered more similarities than differences in auxin transport control between both nodulation programs, contradictory to our initial expectations. We detected a temporary inhibition of acro- and basipetal auxin transport in *L. japonicus* following *Rhizobium* treatment at 24-33 h.p.i., both which has never been reported in the literature before. Although whole-root TIBA treatment did not inhibit basipetal auxin transport in either *M. truncatula* or *L. japonicus*, it would be interesting to see if a localised TIBA (or quercetin) treatment at the root could inhibit basipetal auxin transport in both legumes. From

previous results, we know that auxin signalling decreased below the *Rhizobium* infection site in white clover, prior to an increase at the infection zone (Mathesius et al. 1998). Decrease in auxin signalling was suggested to be a mechanism to increase resistance in response to pathogen recognition (Domingo et al. 2009; Wang et al. 2007; Wang and Fu 2011). Up to now, the decrease in auxin transport at the *Rhizobium* infection site observed in indeterminate nodule-forming legumes has been suggested to be a mechanism to increase auxin concentration around the infection zone, correlating with the increased auxin response. An increase in local auxin concentration is believed to promote cell divisions during nodule primordia formation. If this is true for indeterminate nodules, should we not expect a similar mechanism in determinate nodules? Auxin response as indicated by *GH3*- or *DR5*-based reporters shows that auxin response increases in the nodule primordia in both nodulation programs (Figure 6.3) (Suzaki et al. 2012; van Noorden et al. 2007). Why, then, do synthetic ATIs manage to induce nodule-like structures on the roots of indeterminate but not determinate nodule-forming legumes? The idea that both indeterminate and determinate nodule-forming legumes would use a similar mechanism (auxin transport inhibition) to manipulate local auxin concentrations would contradict the inability of determinate nodule-forming legumes to form ATI-induced pseudonodules.

There are two possible explanations to this: (1) the auxin transport inhibition observed in both *M. truncatula* and *L. japonicus* could be a pathogenic rather than a symbiotic response. Recently, the Nod factor receptor in *M. truncatula*, NFP, has been shown to perceive pathogenic signals as well (Rey et al. 2013). Furthermore, non-legumes can perceive Nod factors and downregulate microbe-associated molecular pattern (MAMP)-triggered immunity (Liang et al. 2013); (2) auxin transport inhibition in *M. truncatula* could activate other signalling components not induced in *L. japonicus* to promote cell divisions and formation of a nodule / pseudonodule. Similarly, the fact that gibberellins induce pseudonodules

on *L. japonicus*, but not alfalfa roots supports this idea about alternative signalling pathways in different legumes (Kawaguchi et al. 1996). Taking evidence from Chapter 5 into consideration, where the nodulation-defective *cre1* mutant (which still forms initial infection threads) failed to inhibit acropetal auxin transport, the second explanation looks more plausible. Moreover, flavonoid-deficient roots of *M. truncatula*, which failed to nodulate, also lost their ability to inhibit acropetal auxin transport (Wasson et al. 2006). Thus, at least in indeterminate nodule-forming legumes, auxin transport inhibition seems to be a positive cue for successful nodulation. A possible experiment to test this would be to quantify auxin transport changes in response to *Rhizobium* treatment in all known nodulation-defective *M. truncatula* mutants, including all early mutants, such as *nfp*, *nsp* and *nin*. Auxin transport control in these mutants should be abolished for this model to hold true.

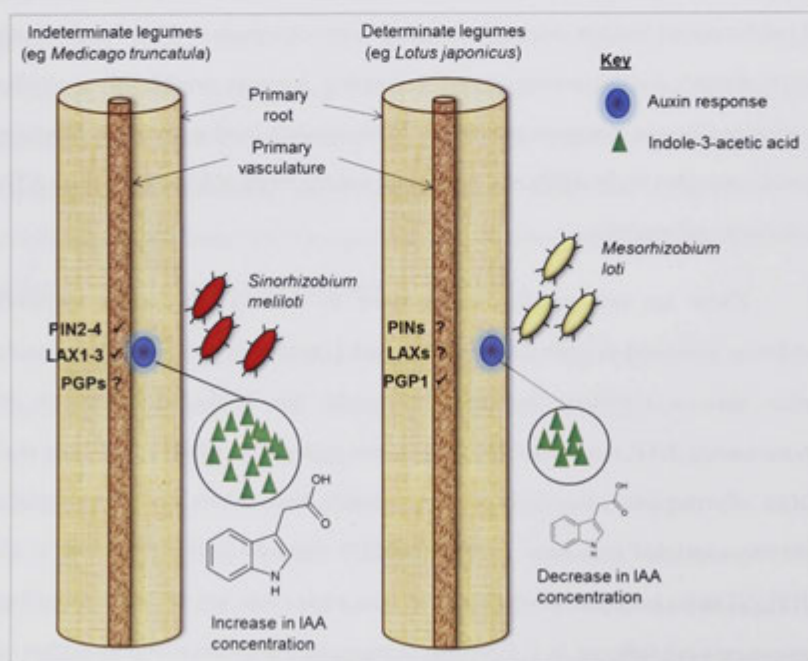


Figure 6.3 Differences in auxin regulation at the site of nodule initiation between indeterminate and determinate nodule-forming legumes. Members of the auxin carriers in the PIN and LAX families have been demonstrated to play a positive role in indeterminate nodulation. Whether a similar role is performed by these proteins in determinate nodules has not been addressed. The role of P-glycoproteins (PGP) has not been investigated in indeterminate nodulation, but has been shown to play an indirect role in determinate nodulation. Differences in the location of initial cell divisions might be contributed by the increase in auxin response in the inner or outer cortical cells of indeterminate and determinate nodule-forming legumes, respectively. Interestingly, a reduced sensitivity to auxin is required for nodule development in soybean (Turner et al. 2013). So far, we have shown that an increase in IAA concentration occurs at the early stages of nodulation in *Medicago truncatula*, but the opposite was observed in *Lotus japonicus*. How this contributes to the differences in the two nodulation programs remains to be explored.

The auxin transport measurements performed in this thesis give a net readout in the form of auxin transport capacity of a given root segment. However, auxin transport may occur passively through the primary vasculature, or actively via cell-to-cell polar auxin transport. In Chapter 5, we examined the gene expression of all known auxin transport carriers of the PIN and LAX family in *M. truncatula*. Auxin transport carriers are directly involved in cell-to-cell auxin transport (Peer et al. 2011). Previous molecular and RNAi studies have strongly pointed towards a positive role for several auxin carriers in *M. truncatula* nodulation (Figure 6.3) (de Billy et al. 2001; Huo et al. 2006; Plet et al. 2011; Prayitno et al. 2006). In Chapter 4, we did not perform a similar expression analysis of auxin carriers, due to limited annotation of the *L. japonicus* genome. Nevertheless, auxin carriers are likely to be directly involved in *L. japonicus*, and indeed nodulation in general. The auxin carriers CgPIN1 and CgAUX1 have been suggested to act synergistically in actinorhizal nodules of *C. glauca* (Péret et al. 2007; Perrine-Walker et al. 2010). Similarly to *M. truncatula*, the redundancy of auxin carriers means that multiple experimental techniques, such as promoter analysis and knockdown approaches of

individual / multiple gene members will be required to understand the role of auxin transport during nodulation in *L. japonicus* and other legumes.

6.2.2 The enigmatic pseudonodule

Pseudonodule is a collective term used to describe non-functional, nodule-like structures. The overexpression of genetic players in the nodulation signalling pathway, such as *DMI3*, *NIN* and *CRE1 / LHK1* produces nodule-like structures, which are devoid of rhizobia (Soyano et al. 2013; Tirichine et al. 2006; Tirichine et al. 2007). Treatment of roots from certain plant species with plant growth regulators, including cytokinins and gibberellins, induces pseudonodules as well (Kawaguchi et al. 1996; Rodriguez-Barrueco and De Castro 1973). Here, we were interested in ATI-induced pseudonodules. We hypothesised that a local, transient auxin transport inhibition is required for proper nodulation, at least in indeterminate nodule-forming legumes. However, pseudonodules were only induced with whole root ATI treatment. Our attempt in promoting pseudonodule formation with local application of ATIs fell short. Perhaps a stronger dose of ATI is required for the latter approach. Crucially, ATI-induced pseudonodules, and indeed pseudonodules formed by overexpression of *DMI3*, *NIN* and *CRE1 / LHK1*, do not exhibit the characteristic peripheral vasculature, as seen in rhizobia-induced nodules (Guan et al. 2013; Soyano et al. 2013; Tirichine et al. 2006; Tirichine et al. 2007). In addition, a partial infection process (normal infection pockets formed but no infection thread initiation), produced nodules without proper vascular patterning as well (Guan et al. 2013). Rhizobia, it seems, are required throughout the nodulation process to coordinate proper vascular development. In agreement with this, our preliminary results showed that the nodulation-defective *cre1* mutant roots cotreated with TIBA and rhizobia formed normal-looking nodules with the characteristic peripheral vasculature. Auxin is involved in the regulation of proper vascular development

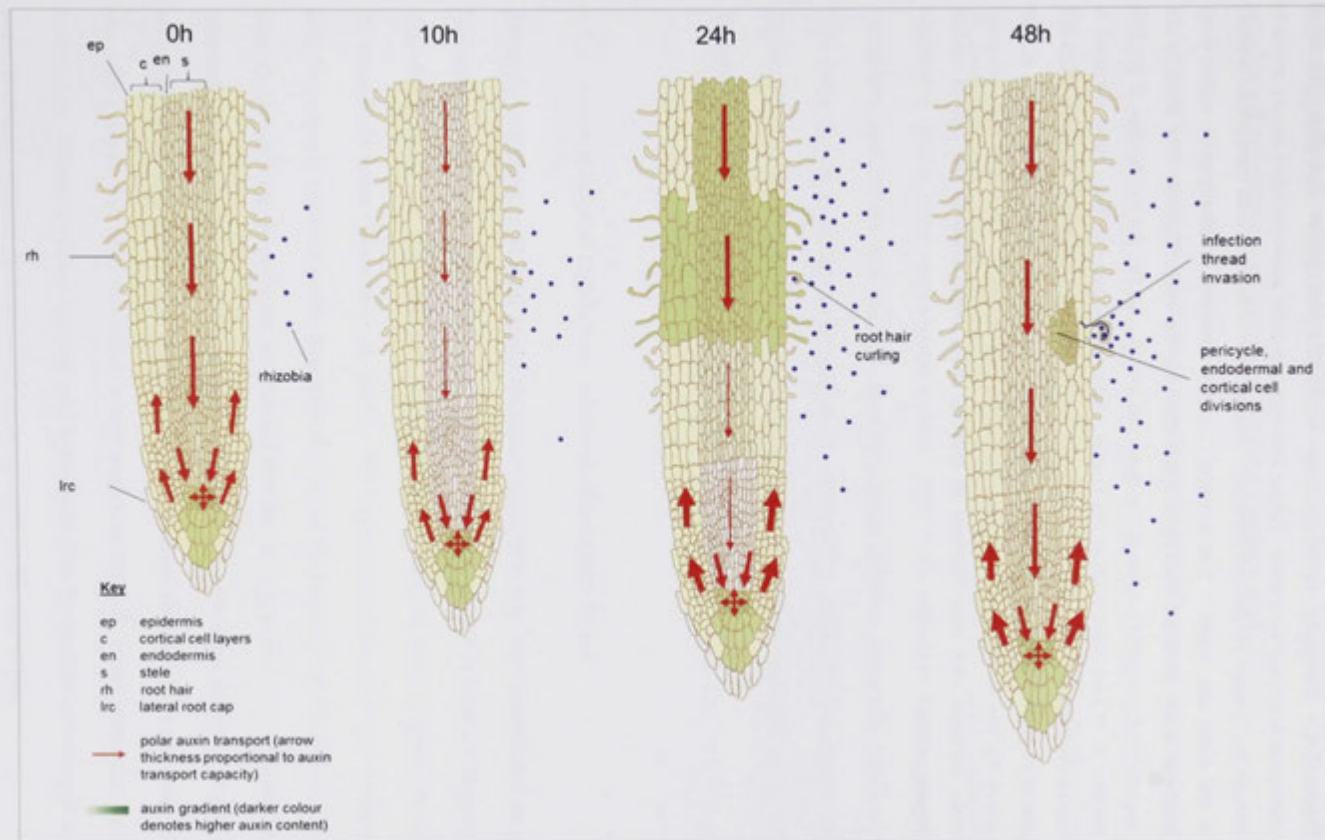
(Lucas et al. 2013). Specifically, correct auxin localisation driven by auxin carriers is important for promoting vascular development and differentiation. A simple external treatment with ATI is unlikely to achieve this result. It would be interesting to see how rhizobia mechanistically affect the host auxin transport machinery and subsequently auxin concentration to make a vascular strand extending from the primary root into the nodule.

6.2.3 Lessons from computer models

Over the last decade, there has been a rise in the “systems biology” approach to biological research. Computer models are generated to understand complex signalling networks and processes. Various auxin transport models focussing on meristem (shoot and root) maintenance and organ initiation in *Arabidopsis* have been proposed (van Berkel et al. 2013). Deinum et al. (2012) modelled auxin transport changes during nodulation and found that inhibition of acropetal auxin transport and subsequent lateral redirection of auxin transport is the most likely mechanism to increase local auxin concentrations sufficiently in the nodule primordia of indeterminate nodule-forming legumes. In determinate nodule-forming legumes, presumably due to differential positioning of cortical auxin carriers, the same auxin transport mechanism does not occur. The authors further suggested that local auxin biosynthesis and breakdown are not sufficiently quick to increase local auxin concentrations. This model reconciles our current knowledge about the molecular players involved in nodulation. However, there are still many unknowns about this process. For example, the localisation of individual auxin carriers in legumes is still unknown. The protein / enzyme kinetics of the auxin carriers, synthesis and hydrolysing enzymes have still not been systematically investigated. Hence, this model forms a very useful baseline for auxin transport modelling in legumes. In the future, information on the localisation, activity and

kinetics of individual molecular players should be integrated into this model to improve its accuracy in predicting auxin transport changes during legume development.

Nevertheless, based on the current *in-silico* model and results from this thesis, we propose a model incorporating acro- and basipetal auxin transport regulation during nodulation in *M. truncatula*, and potentially indeterminate legumes in general (Figure 6.4). Although there were similarities in auxin transport control between *M. truncatula* and *L. japonicus* found in Chapter 4, further molecular experiments on *L. japonicus* need to be completed before a generalised model for all legumes can be constructed. Briefly, consistent with previous studies, we found a temporary inhibition of acropetal auxin transport in *M. truncatula*. We propose basipetal auxin transport as an additional positive player in nodulation, and this hypothesis could be further tested in *Mtpin2* mutants. Bidirectional auxin transport changes most likely contribute increasing auxin concentration at the nodulation site to promote cell divisions and nodule primordia formation.



6.2. Hypothesis two: Auxin transport control is a general mechanism for increasing / decreasing auxin content during nodulation

Figure 6.4 Schematic model for auxin transport routes before and after *Rhizobium* infection in *Medicago truncatula*. Before infection, acropetal auxin transport occurs primarily through the phloem via passive transport. A proportion of auxin is also transported actively in the outer cell layers. The quiescent centre maintains a steady-state auxin level. Basipetal auxin transport transports auxin back up the root. Specific PIN proteins are responsible for exporting auxin in the outer cell layers. So far, the localisation of the PIN proteins in *M. truncatula* roots is not known. After *Rhizobium* infection, auxin transport is transiently inhibited at the point of *Rhizobium* entry. Auxin is temporarily depleted below the site of infection. After the temporary inhibition in auxin transport, auxin increases at, and above the site of *Rhizobium* invasion, promoting cell divisions. On top of that, basipetal auxin transport rate may increase to channel more auxin towards the site of nodule organogenesis.

6.3 Hypothesis three: Cytokinin perception triggers flavonoid-mediated regulation of auxin transport during nodulation

In Chapter 5, we demonstrated flavonoids as potential regulators of auxin transport during nodulation in *M. truncatula*. Although: (1) flavonoids have been shown to regulate auxin transport in general and; (2) auxin transport regulation mediated by auxin carriers affects secondary root organ formation, no study outside *M. truncatula* has placed flavonoids as a direct (co)player in auxin transport regulation during other organogenic events. Flavonoids represent a large class of secondary metabolites and multiple members from different flavonoid subclasses have been shown to inhibit auxin transport. It would be interesting to dissect the individual contribution of candidate flavonoids and to pinpoint the primary auxin transport regulator(s) involved in nodule organogenesis.

6.3.1 Auxin transport regulation - where do flavonoids fit in?

An early, transient, and local auxin transport inhibition has been established as a hallmark of *M. truncatula* nodulation. A previous study in our laboratory showed that flavonoids are required for auxin transport control and nodulation in *M. truncatula* roots (Wasson et al. 2006). We hypothesised that the *cre1* mutant fails to properly regulate auxin transport due to its aberrant flavonoid profile. In accordance with our hypothesis, we showed that the endogenous concentrations of selected flavonoids between WT and the *cre1* mutant roots were different, before and after *Rhizobium* treatment. Supplementation of these flavonoids to the roots of the *cre1* mutant was able to restore auxin transport control, auxin response, and nodulation. These findings support our hypothesis that flavonoids are integral to auxin transport control during nodule organogenesis in *M. truncatula*.

However, there is currently no other organogenic process which necessitates flavonoids as auxin transport regulating agents. During lateral root organogenesis, PIN and AUX1/ LAX auxin carriers positively regulate various stages of lateral root formation (Figure 6.5). Mutations in several AtPIN carriers resulted in several undifferentiated layers of divided pericycle cells (Benková et al. 2003). The AtAUX1 auxin importer plays a role during lateral root initiation via regulation of basipetal auxin transport (De Smet et al. 2007; Swarup et al. 2001). The AtLAX3 auxin importer controls lateral root emergence by regulating auxin gradients in the outer endodermis and cortical layers (Lavenus et al. 2013; Swarup et al. 2008). On the other hand, during nematode gall formation, AtPIN1 is involved at the initiation stage by directing auxin into the syncytium, whereas AtPIN3 and 4 are postulated to redirect auxin in the lateral direction to promote radial cell expansion of the nematode feeding site (Grunewald et al. 2009). Flavonoids were not implicated in these processes. Indeed, flavonoid-deficient roots of *M. truncatula* were not impaired in the total number of lateral roots and nematode galls formed (Wasson et al. 2009). In addition, *Arabidopsis* flavonoid-deficient mutants are not defective in lateral root formation or nematode infection (Brown et al. 2001; Buer and Djordjevic 2009; Wuyts et al. 2006). This suggests that although auxin transport regulation is clearly involved in lateral root and nematode gall formation, flavonoids are not likely to play a role in these processes. Excluding nodulation, flavonoids are not essential for the formation of secondary root structures *per se*.

At the moment, this puts flavonoids in a unique role during nodule organogenesis. Intriguingly, although nodulation in soybean and common bean (both determinate nodule-forming legumes) require the correct set of flavonoids for nod gene induction, flavonoid-mediated auxin transport inhibition is not required during determinate nodulation (Ripodas et al. 2013; Subramanian et al. 2006). From these findings, we can conclude that different flavonoid subclasses play distinct roles during nodulation. Zhang et al. (2009) proposed kaempferol as the

flavonoid / flavonoid precursor involved in auxin transport inhibition during *M. truncatula* nodulation. In general, flavonols (e.g., kaempferol) are considered the primary auxin transport inhibitors with the strongest activity (Kuhn et al. 2011; Murphy et al. 2000), although we found that flavonols and several other flavonoid metabolites to have similar levels of acropetal auxin transport inhibiting activity in *M. truncatula* roots. Indeed, our results demonstrated that flavonols (i.e. kaempferol, quercetin), their precursor (naringenin), or isoliquiritigenin (which has a different structure, and thus unrelated to flavonols) could inhibit acropetal auxin transport when coapplied with rhizobia, and at least partially restore nodulation in the *cre1* mutant. However, multiple flavonols were detected in *M. truncatula* roots, including kaempferol, quercetin and morin. Furthermore, flavonol glycosides, some of which were shown to inhibit auxin transport (Yin et al. 2014), were not investigated in this study. Multiple enzymes could be involved in the interconversion of flavonols and their glycosidic forms, which would determine the steady state concentration of the aglycones (Routaboul et al. 2006). Future experiments could identify if other flavonols or flavonol glycosides play a role during *M. truncatula* nodulation. In addition to a few other flavones which are involved in *Rhizobium* Nod gene induction, there are likely other nodulation-related roles performed by flavonoids which are yet to be identified.

6.3.2 Mechanism of auxin transport regulation during nodulation

In Chapter 4, we showed, at the physiological level, that changes in auxin transport occur bidirectionally in response to *Rhizobium* treatment. We subsequently investigated in more detail the possible molecular mechanisms behind the CRE1-mediated regulation of auxin transport in Chapter 5, by comparing auxin transport changes between WT and the *cre1* mutant. We confirmed a previous finding that the *cre1* mutant fails to transiently inhibit acropetal auxin transport in response to

symbiotic cues (Plet et al. 2011). Additionally, we discovered that the *cre1* mutant failed to alter basipetal auxin transport in response to *Rhizobium* treatment, in contrast to WT seedlings. These defects had a direct impact on the auxin concentrations of the *cre1* mutant. The results obtained suggest that PIN-mediated auxin transport regulation may at least, in part, occur at the transcription level. Indeed, we showed that the transcription of several *PIN* genes was differentially regulated between WT and the *cre1* mutant, in response to *Rhizobium* treatment, and that Plet et al. (2011) found similar results with a Nod factor treatment. Lateral root initiation involves changes in *PIN* expression, which is perturbed by cytokinin treatment (Laplaze et al. 2007). However, cytokinin-induced posttranslational regulation of PIN activity has also been demonstrated during lateral root formation. Cytokinin induces changes in the phosphorylation state of the PIN1 auxin carrier, causing repositioning of AtPIN1 proteins from basal-to-lateral sides of the cell (Marhavý et al. 2014). This redirects auxin to flow in an asymmetrical, horizontal fashion into the lateral root primordia. Moreover, cytokinin treatment increased the population of AtPIN2 auxin carriers at the apical side of epidermal cells to elevate basipetal auxin transport. We hypothesised that a similar regulation occurs during nodulation because of the similarities in the signalling pathway of both organogenic events (Figure 6.5). Furthermore, nematode-induced gall formation in *Arabidopsis* involves the repositioning of the AtPIN3 and AtPIN4 fusion proteins (Grunewald et al. 2009). Our initial attempts to immunolocalise *M. truncatula* PIN auxin carriers using an anti-AtPIN1 antibody yielded positive signals, suggesting that the antibody was able to bind the orthologs in *M. truncatula* (MtPIN4 and 10). However, we did not detect any changes in antibody signal, before and after *Rhizobium* treatment. These results should be interpreted carefully because the antibody used was not specifically raised against *M. truncatula* PIN proteins. We have generated polyclonal antibodies targeting several MtPIN auxin carriers, based on transcript expression changes in response to *Rhizobium* treatment. Future

immunolocalisation experiments on these proteins could shed light on possible changes in posttranslational activity. Alternatively, MtPIN:GFP reporter fusions could be constructed.

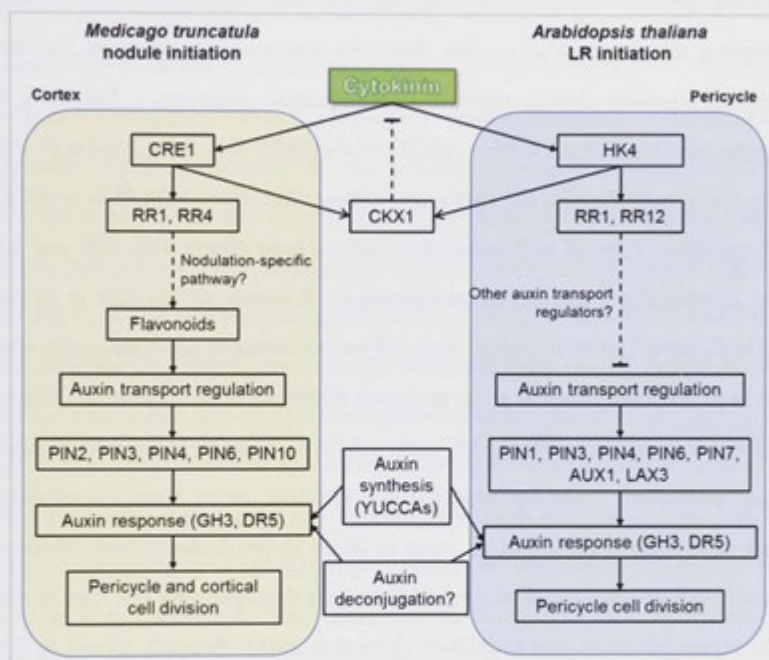


Figure 6.5 Cytokinin regulation of nodule organogenesis and lateral root initiation share many similarities. Cytokinin is perceived by histidine kinases, which activate cytokinin response regulators (RRs). In *Medicago truncatula*, flavonoids are transiently activated / released by cytokinin signalling. Flavonoids are involved in auxin transport regulation during *M. truncatula* nodulation. So far, flavonoids are not implicated in auxin transport regulation during lateral root initiation. The expression and activity of several PIN auxin carriers change during both organogenic events, while the AUX1 / LAX auxin import carriers have only been implicated in lateral root formation. In both cases, cell division is associated with a positive auxin response in founder cells primed to divide to form a primordium. The IAA synthesis genes (*YUCs*) were shown to act during nodulation in this study, while Masiguchi et al (2011) demonstrated that *YUCs* positively affect lateral root numbers in *Arabidopsis*. The role of auxin deconjugation in increasing auxin pools has not been investigated. Abbreviations: CRE, Cytokinin Response; RR, Response Regulator; CKX, Cytokinin Oxidase; HK, Histidine Kinase.

Importantly, we currently do not understand the mechanism in which flavonoids inhibit auxin transport. Flavonoids are unlikely to be specific regulators of auxin transport considering they have multiple proposed targets, including auxin carriers, kinases and the trafficking machinery (Peer et al. 2011). In addition, flavonoid aglycones and glycosides have both been shown to inhibit auxin transport, prompting the question of specific flavonoid compound(s) acting as the auxin transport regulator during separate developmental programs. Flavonols, for example, have been shown to bind ABCB / PGP (Bailly et al. 2008; Ferte et al. 1999). There is currently no evidence for the interaction of flavonols with PINs or AUX1 / LAX proteins. Genetic and molecular evidence have shown that PIN and LAX auxin carriers play a role during nodulation in *M. truncatula* (de Billy et al. 2001; Huo et al. 2006; Plet et al. 2011). It would be interesting to see if flavonols, which have been proposed to act as auxin transport inhibitors in *M. truncatula* (Zhang et al. 2009), interact with PIN / LAX auxin carriers. Moreover, the role of ABCBs during nodulation could be investigated. Synthetic auxin transport inhibitors, which specifically inhibit ABCBs, such as BUM (2-[4-(diethylamino)-2-hydroxybenzoyl]benzoic acid) could be a valuable tool for distinguishing the roles of PIN / LAXs versus ABCBs during nodulation (Kim et al. 2010). Recently, Cho et al. (2014) identified 5-Nitro-2-(3-Phenylpropylamino)-Benzoic Acid as a specific blocking agent of ABCB19, another established auxin transporter. Considering that the absence of flavonoids negatively affect nodulation, but not lateral root and gall formation, identifying the direct targets of flavonoids in the context of auxin transport regulation could be valuable in understanding nodulation-specific molecular players in legumes.

6.3.3 Nodulation - the big picture

We hypothesised flavonoids to act in a linear pathway within the nodulation signalling cascade. The application of synthetic ATIs alone was able to induce pseudonodules on *M. truncatula* roots. However, supplementation of flavonoids alone to WT roots did not induce visible pseudonodules. This was rather contradictory to the known functions of flavonoids and synthetic ATIs. Logically, if synthetic ATIs' only activity is the inhibition of auxin transport, we would assume flavonoids, which are implicated in other cellular processes in addition to inhibiting auxin transport, to be able to induce pseudonodules as well. Nevertheless, this suggests that parallel pathways exist, and it is most likely that the parallel signals are activated upstream of flavonoid induction (Figure 6.6). So far, *NIN* looks like the most plausible candidate to start with the search for these parallel signals, for three reasons. Firstly, *NIN* is proposed to be legume-specific (Schäuser et al. 2005; Yokota and Hayashi 2011), and that the closest homolog of *NIN* in the non-legume, rice (*OsNLP1*) could not rescue the *nin-2* phenotype (Yokota et al. 2010). Secondly, *NIN* is positioned upstream of auxin transport inhibition, and thus is also possible to be upstream of flavonoid induction (Oldroyd et al. 2011). Thirdly, overexpression of *NIN*, the gene furthest down the nodulation signalling pathway compared to prior targets of overexpression, is sufficient to induce pseudonodules (Soyano et al. 2013). Comparison of the flavonoid profile of WT and *nin* mutants after *Rhizobium* treatment would provide insights into *NIN*'s position in the nodulation signalling pathway relative to flavonoid induction.

In Chapter 5, we found that supplementation of selected flavonoids together with *Rhizobium* was sufficient to restore nodulation in the *cre1* mutant. This would suggest that the parallel signal(s) is induced upstream of CRE1, rather than by *NIN*. However, at least two other cytokinin receptors (*MtHK2* and 3) are present in *M. truncatula* and it is likely that these cytokinin receptors play residual but positive roles during nodulation (Frugier 2008). In agreement with this, only loss-of-

function of all cytokinin receptors in *L. japonicus* completely abolished nodulation (Held et al. 2014). The supplementation of flavonoids could have compensated for the insufficient induction / release of flavonoids mediated by the primary cytokinin receptor, CRE1. Moreover, it is unlikely that the cytokinin receptors in legumes encode a nodulation-specific function, because replacement with an *Arabidopsis* ortholog in a loss-of-function mutant completely restored nodulation (Held et al. 2014).

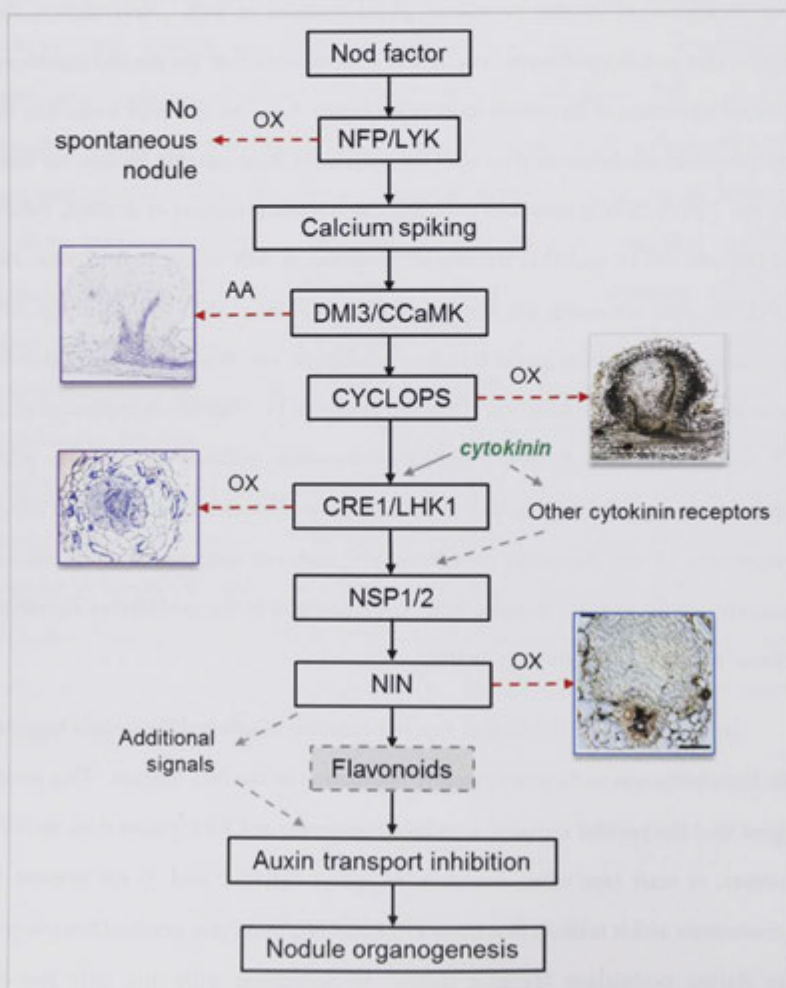


Figure 6.6 Challenges in the identification of signals which are necessary and sufficient for nodulation. The overexpression of several genetic components was sufficient to induce cell division and nodule-like structures on the roots of *Medicago truncatula* and *Lotus japonicus*. The pathway shown here is a simplistic overview of our current understanding of the nodulation signalling pathway. While this pathway includes evidence from *M. truncatula* and *L. japonicus*, it is possible that some of these responses are specific to one of these legumes. Flavonoids are tentatively positioned directly above auxin transport inhibition. Results obtained in this study suggest that parallel signals are likely to operate following cytokinin signalling, because flavonoids alone were not able to induce pseudonodules. We propose that these signals could be induced by NIN, considering its position in the pathway and its ability to induce pseudonodules from overexpression (Singh et al. 2014; Soyano et al. 2013; Tirichine et al. 2006; Tirichine et al. 2007). Abbreviations: AA, autoactivation; OX, overexpression.

86.4 Future perspectives

6.4.1 Improvement in experimental design, suggestions for further experiments and future direction

Mass spectrometry provides a powerful tool for metabolite identification and quantification. Current technology and software offer algorithms for large-scale metabolite discovery, but at the cost of specificity and sensitivity, and vice-versa. In this project, we opted for highly targeted and sensitive detection over large-scale data output from whole metabolome scanning. This targeted operational mode is often limited to 10's of metabolites, as opposed to 1000's that can be detected with non-targeted, whole metabolome mining. Modern mass spectrometers and software, such as the recently-developed AB Sciex TripleTOF® 6600 system, combine discovery and targeted metabolomics to achieve much higher specific hit rates, with potentially up to 100's of targeted metabolite identification and quantification. It is thus possible to measure multiple classes of hormones in tandem with other primary and secondary metabolites in a single run. With such a large amount of data, it is imperative to have improved analytical software, database curation and database search algorithms to facilitate this "next-generation" metabolomics.

The auxin transport measurements performed in this project give us a direct quantification of auxin transport capacity in individual root segments. However, in the case of acropetal auxin transport measurements, the wounding of tissue (see Materials and Methods) would likely have changed the physiological parameters of the root. We performed these assays on the assumption that auxin carriers function normally after wounding. This was not an issue for basipetal auxin transport assays. In addition, quantification in smaller root segments could give a more accurate representation of local auxin transport changes. Recently, fluorescent auxin analogs were introduced as a potential alternative technique to studying auxin transport *in*

planta (Hayashi et al. 2014). These fluorescent auxin analogs are recognised and transported by auxin carriers, but do not activate the TIR1-AUX / IAA-ARF auxin signalling module. Imaging of legume roots treated with *Rhizobium* and these compounds would allow high resolution spatio-temporal visualisation of auxin at the subcellular level. Moreover, the localisation of individual auxin carriers either with protein-GFP fusions or antibodies could link the directionality of auxin transport with specific auxin carriers in legumes. Through the combination of fluorescent auxin analogs and auxin biosynthesis inhibitors, Hayashi and colleagues went on to demonstrate the essential role of auxin biosynthesis in creating auxin maxima at the root apex. Preliminary results (Appendix E) showed that putative *YUC* orthologs in *M. truncatula* were upregulated in response to *Rhizobium* treatment. Thus, we cannot rule out auxin biosynthesis as an equally important component in generating proper auxin gradient during nodule primordia formation. Auxin antibodies are commercially available for the direct localisation and semi-quantitative measurements of auxin. Both IAA and / or PAA have been localised in nodules of the legume *M. truncatula* (Fedorova et al. 2005), and the actinorhizal plants *C. glauca* (Perrine-Walker et al. 2010) and *D. trinervis* (Imanishi et al. 2014). Indeed, we have attempted to perform auxin immunolocalisation assays, but encountered some hurdles, including high background fluorescence, even with a fluorophor that is energised by a high excitation wavelength ($\lambda_{\text{excitation}} = 647 \text{ nm}$). Alternatively, auxin biosensors could be used as the closest proxy to measuring auxin concentration *in planta* (Brunoud et al. 2012). This technique has the additional advantage of being less laborious than immunolocalisation.

Despite the wealth of information that can be generated by mass spectrometry, the lack of temporal information is still a chink in its armour. Reporters and biosensors are valuable tools for providing real-time data on dynamic developmental processes. The non-linear relationship between signal molecules and sensor / reporter output can be corrected by mathematical modelling. Using

mathematical algorithms, Band et al. (2012) demonstrated that the auxin DII-VENUS biosensor can accurately predict auxin distribution and concentration at the root apex during a root gravitropic response. This technique is more feasible if the underlying signalling cascade is well-characterised, such as in the case of auxin and jasmonic acid (Brunoud et al. 2012; Larrieu et al. 2015). In combination with mass spectrometry, these techniques complement each other to provide high spatiotemporal resolution of hormone changes during plant development.

6.4.2 Conclusion

In this thesis, we have developed a sensitive LC-MS/MS method for auxin quantification in root tissue. This method will be a valuable tool in future investigations on plant development via hormone profiling. We showed that auxin transport is a general mechanism employed by nodulating plants to regulate auxin concentration at various stages of nodulation. Different auxin species might play more prominent roles in separate plant tissue and in different nodulating plants. Finally, we demonstrated that flavonoids could be a unique class of secondary metabolites recruited by legumes to regulate auxin transport during nodulation. Proper regulation of flavonoids relies on a functional cytokinin receptor. Flavonoids could increase nodulation capacity in a nodulation-defective mutant via modulation of auxin transport, highlighting the essential role of flavonoid-induced auxin transport changes in shaping the unique nodule organ.

Bibliography

- ABDEL-LATEIF, K., VAISSAYRE, V., GHERBI, H., VERRIES, C., MEUDEC, E., PERRINE-WALKER, F., CHEYNIER, V., SVISTOONOFF, S., FRANCHE, C., BOGUSZ, D. & HOCHER, V. 2013. Silencing of the chalcone synthase gene in *Casuarina glauca* highlights the important role of flavonoids during nodulation. *New Phytologist*, 199, 1012-1021.
- AGUILAR, J. M. M., ASHBY, A. M., RICHARDS, A. J. M., LOAKE, G. J., WATSON, M. D. & SHAW, C. H. 1988. Chemotaxis of *Rhizobium leguminosarum* biovar *phaseoli* towards flavonoid inducers of the symbiotic nodulation genes. *Journal of General Microbiology*, 134, 2741-2746.
- ALLEN, E. K., ALLEN, O. N. & NEWMAN, A. S. 1953. Pseudonodulation of Leguminous Plants Induced by 2-Bromo-3,5- Dichlorobenzoic Acid. *American Journal of Botany*, 40, 429-435.
- ALONI, R. 2004. *The induction of vascular tissues by auxin* Dordrecht, The Netherlands, Kluwer Academic Publishers.
- ANNESLEY, T. M. 2003. Ion Suppression in Mass Spectrometry. *Clinical Chemistry*, 49, 1041-1044.
- ARDOUREL, M., DEMONT, N., DEBELLÉ, F., MAILLET, F., DE BILLY, F., PROMÉ, J. C., DÉNARIÉ, J. & TRUCHET, G. 1994. *Rhizobium meliloti* lipooligosaccharide nodulation factors: different structural requirements for bacterial entry into target root hair cells and induction of plant symbiotic developmental responses. *The Plant Cell Online*, 6, 1357-74.
- ARIEL, F., BRAULT-HERNANDEZ, M., LAFFONT, C., HUAULT, E., BRAULT, M., PLET, J., MOISON, M., BLANCHET, S., ICHANTÉ, J. L., CHABAUD, M., CARRERE, S., CRESPI, M., CHAN, R. L. & FRUGIER, F. 2012. Two Direct Targets of Cytokinin Signaling Regulate Symbiotic Nodulation in *Medicago truncatula*. *The Plant Cell Online*, 24, 3838-3852.
- ARORA, N., SKOOG, F. & ALLEN, O. N. 1959. Kinetin-Induced Pseudonodules on Tobacco Roots. *American Journal of Botany*, 46, 610-613.

- ARRIGHI, J.-F., BARRE, A., BEN AMOR, B., BERSOULT, A., SORIANO, L. C., MIRABELLA, R., DE CARVALHO-NIEBEL, F., JOURNET, E.-P., GHERARDI, M., HUGUET, T., GEURTS, R., DENARIE, J., ROUGE, P. & GOUGH, C. 2006. The *Medicago truncatula* Lysine Motif-Receptor-Like Kinase Gene Family Includes NFP and New Nodule-Expressed Genes. *Plant Physiol.*, 142, 265-279.
- AUGUY, F., ABDEL-LATEIF, K., DOUMAS, P., BADIN, P., GUERIN, V., BOGUSZ, D. & HOCHER, V. 2011. Activation of the isoflavonoid pathway in actinorhizal symbioses. *Functional Plant Biology*, 38, 690-696.
- BAILLY, A., SOVERO, V., VINCENZETTI, V., SANTELIA, D., BARTNIK, D., KOENIG, B. W., MANCUSO, S., MARTINOIA, E. & GEISLER, M. 2008. Modulation of P-glycoproteins by Auxin Transport Inhibitors Is Mediated by Interaction with Immunophilins. *Journal of Biological Chemistry*, 283, 21817-21826.
- BAJGUZ, A. & PIOTROWSKA, A. 2009. Conjugates of auxin and cytokinin. *Phytochemistry*, 70, 957-969.
- BAKER, D. 2000. Vascular transport of auxins and cytokinins in *Ricinus*. *Plant Growth Regulation*, 32, 157-160.
- BAND, L. R., WELLS, D. M., LARRIEU, A., SUN, J., MIDDLETON, A. M., FRENCH, A. P., BRUNOUD, G., SATO, E. M., WILSON, M. H., PÉRET, B., OLIVA, M., SWARUP, R., SAIRANEN, I., PARRY, G., LJUNG, K., BEECKMAN, T., GARIBALDI, J. M., ESTELLE, M., OWEN, M. R., VISSENBERG, K., HODGMAN, T. C., PRIDMORE, T. P., KING, J. R., VERNOUX, T. & BENNETT, M. J. 2012. Root gravitropism is regulated by a transient lateral auxin gradient controlled by a tipping-point mechanism. *Proceedings of the National Academy of Sciences*, 109, 4668-4673.
- BANDYOPADHYAY, A., BLAKESLEE, J., LEE, O., JMRAVEC, J., SAUER, M., TITAPIWATANAKUN, B., MAKAM, S. N., BOUCHARD, R., GEISLER, M., MARTINOIA, E., FRIML, J., PEER, W. A. & MURPHY, A. S. 2007. Interactions of PIN and PGP auxin transport mechanisms. *Biochemical Society Transactions*, 35, 137-141.
- BARBEZ, E., KUBES, M., ROLCIK, J., BEZIAT, C., PENCIK, A., WANG, B., ROSQUETE, M. R., ZHU, J., DOBREV, P. I., LEE, Y., ZAZIMALOVA, E., PETRASEK, J., GEISLER, M., FRIML, J. & KLEINE-VEHN, J. 2012. A novel putative auxin carrier family regulates intracellular auxin homeostasis in plants. *Nature*, advance online publication.

- BARLIER, I., KOWALCZYK, M., MARCHANT, A., LJUNG, K., BHALERAO, R., BENNETT, M., SANDBERG, G. & BELLINI, C. 2000. The *SUR2* gene of *Arabidopsis thaliana* encodes the cytochrome P450 CYP83B1, a modulator of auxin homeostasis. *Proceedings of the National Academy of Sciences*, 97, 14819-14824.
- BARNETT, M. J., TOMAN, C. J., FISHER, R. F. & LONG, S. R. 2004. A dual-genome Symbiosis Chip for coordinate study of signal exchange and development in a prokaryote-host interaction. *Proceedings of the National Academy of Sciences of the United States of America*, 101, 16636-16641.
- BARWICK, V. J. 1999. Sources of uncertainty in gas chromatography and high-performance liquid chromatography. *Journal of Chromatography A*, 849, 13-33.
- BEATTY, P. H. & GOOD, A. G. 2011. Future Prospects for Cereals That Fix Nitrogen. *Science*, 333, 416-417.
- BENJAMINS, R., QUINT, A., WEIJERS, D., HOOYKAAS, P. & OFFRINGA, R. 2001. The PINOID protein kinase regulates organ development in *Arabidopsis* by enhancing polar auxin transport. *Development*, 128, 4057-4067.
- BENKOVÁ, E., MICHNIEWICZ, M., SAUER, M., TEICHMANN, T., SEIFERTOVÁ, D., JÜRGENS, G. & FRIML, J. 2003. Local, Efflux-Dependent Auxin Gradients as a Common Module for Plant Organ Formation. *Cell*, 115, 591-602.
- BENNETT, M. J., MARCHANT, A., GREEN, H. G., MAY, S. T., WARD, S. P., MILLNER, P. A., WALKER, A. R., SCHULZ, B. & FELDMANN, K. A. 1996. *Arabidopsis* AUX1 gene: A permease-like regulator of root gravitropism. *Science*, 273, 948-950.
- BERNASCONI, P. 1996. Effect of synthetic and natural protein tyrosine kinase inhibitors on auxin efflux in zucchini (*Cucurbita pepo*) hypocotyls. *Physiologia Plantarum*, 96, 205-210.
- BHARGAVA, A., CLABAUGH, I., TO, J. P., MAXWELL, B. B., CHIANG, Y.-H., SCHALLER, E. G., LORAINE, A. & KIEBER, J. J. 2013. Identification of Cytokinin Responsive Genes Using Microarray Meta-analysis and RNA-seq in *Arabidopsis thaliana*. *Plant Physiology*.
- BHUVANESWARI, T. V., BHAGWAT, A. A. & BAUER, W. D. 1981. Transient susceptibility of root cells in four common legumes to nodulation by rhizobia. *Plant Physiol*, 68, 1144-1149.

- BIALEK, K. & COHEN, J. D. 1986. Isolation and Partial Characterization of the Major Amide-Linked Conjugate of Indole-3-Acetic Acid from *Phaseolus vulgaris* L. *Plant Physiol*, 80, 99-104.
- BIDLINGMEYER, B. A. & BROSKE, A. D. 2004. The Role of Pore Size and Stationary Phase Composition in Preventing Aqueous-Induced Retention Time Loss in Reversed-Phase HPLC. *Journal of Chromatographic Science*, 42, 100-106.
- BIRKEMEYER, C., KOLASA, A. & KOPKA, J. 2003. Comprehensive chemical derivatization for gas chromatography-mass spectrometry-based multi-targeted profiling of the major phytohormones. *Journal of Chromatography A*, 993, 89-102.
- BISHOPP, A., BENKOVÁ, E. & HELARIUTTA, Y. 2011. Sending mixed messages: auxin-cytokinin crosstalk in roots. *Current Opinion in Plant Biology*, 14, 10-16.
- BITTO, E., BINGMAN, C. A., BITTOVA, L., HOUSTON, N. L., BOSTON, R. S., FOX, B. G. & PHILLIPS, G. N. 2009. X-ray structure of ILL2, an auxin-conjugate amidohydrolase from *Arabidopsis thaliana*. *Proteins: Structure, Function, and Bioinformatics*, 74, 61-71.
- BLAKESLEE, J. J., BANDYOPADHYAY, A., LEE, O. R., MRAVEC, J., TITAPIWATANAKUN, B., SAUER, M., MAKAM, S. N., CHENG, Y., BOUCHARD, R., ADAMEC, J., GEISLER, M., NAGASHIMA, A., SAKAI, T., MARTINOIA, E., FRIML, J., PEER, W. A. & MURPHY, A. S. 2007. Interactions among PIN-FORMED and P-Glycoprotein Auxin Transporters in *Arabidopsis*. *Plant Cell*, 19, 131-147.
- BLAUENFELDT, J., JOSHI, P. A., GRESSHOFF, P. M. & CAETANO-ANOLLÉS, G. 1994. Nodulation of white clover (*Trifolium repens*) in the absence of *Rhizobium*. *Protoplasma*, 179, 106-110.
- BLILOU, L., XU, J., WILDWATER, M., WILLEMSSEN, V., PAPONOV, I., FRIML, J., HEIDSTRA, R., AIDA, M., PALME, K. & SCHERES, B. 2005. The PIN auxin efflux facilitator network controls growth and patterning in *Arabidopsis* roots. *Nature*, 433, 39-44.
- BOISSON-DERNIER, A., CHABAUD, M., GARCIA, F., BECARD, G., ROSENBERG, C. & BARKER, D. 2001. Hairy roots of *Medicago truncatula* as tools for studying nitrogen-fixing and endomycorrhizal symbioses. *Molecular Plant-Microbe Interactions*, 14, 693-700.

- BOOT, K. J. M., VAN BRUSSEL, A. A. N., TAK, T., SPAINK, H. P. & KIJNE, J. W. 1999. Lipochitin Oligosaccharides from *Rhizobium leguminosarum* bv. *viciae* Reduce Auxin Transport Capacity in *Vicia sativa* subsp. *nigra* Roots. *Molecular Plant-Microbe Interactions*, 12, 839-844.
- BREAKSPEAR, A., LIU, C., ROY, S., STACEY, N., ROGERS, C., TRICK, M., MORIERI, G., MYSORE, K. S., WEN, J., OLDROYD, G. E. D., DOWNIE, A. D. & MURRAY, J. D. 2014. The Root Hair "Infectome" of *Medicago truncatula* Uncovers Changes in Cell Cycle Genes and Reveals a Requirement for Auxin Signaling in Rhizobial Infection. *The Plant Cell*, 26, 4680-4701.
- BRECHENMACHER, L., LEE, J., SACHDEV, S., SONG, Z., NGUYEN, T. H. N., JOSHI, T., OEHRLE, N., LIBAULT, M., MOONEY, B., XU, D., COOPER, B. & STACEY, G. 2009. Establishment of a Protein Reference Map for Soybean Root Hair Cells. *Plant Physiology*, 149, 670-682.
- BROGHAMMER, A., KRUSELL, L., BLAISE, M., SAUER, J., SULLIVAN, J. T., MAOLANON, N., VINTHER, M., LORENTZEN, A., MADSEN, E. B., JENSEN, K. J., ROEPSTORFF, P., THIRUP, S., RONSON, C. W., THYGESEN, M. B. & STOUGAARD, J. 2012. Legume receptors perceive the rhizobial lipochitin oligosaccharide signal molecules by direct binding. *Proceedings of the National Academy of Sciences*, 109, 13859-13864.
- BROUGHTON, W. J. & DILWORTH, M. J. 1971. Control of leghaemoglobin synthesis in snake beans. *Biochem. J.*, 125, 1075-1080.
- BROWN, D. E., RASHOTTE, A. M., MURPHY, A. S., NORMANLY, J., TAGUE, B. W., PEER, W. A., TAI, L. & MUDAY, G. K. 2001. Flavonoids Act as Negative Regulators of Auxin Transport in Vivo in Arabidopsis. *Plant Physiology*, 126, 524-535.
- BRUNOUD, G., WELLS, D. M., OLIVA, M., LARRIEU, A., MIRABET, V., BURROW, A. H., BEECKMAN, T., KEPINSKI, S., TRAAS, J., BENNETT, M. J. & VERNOUX, T. 2012. A novel sensor to map auxin response and distribution at high spatio-temporal resolution. *Nature*, 482, 103-106.
- BUER, C., KORDBACHEH, F., TRUONG, T., HOCART, C. & DJORDJEVIC, M. 2013. Alteration of flavonoid accumulation patterns in *transparent testa* mutants disturbs auxin transport, gravity responses, and imparts long-term effects on root and shoot architecture. *Planta*, 238, 171-189.
- BUER, C. S. & MUDAY, G. K. 2004. The *transparent testa4* Mutation Prevents Flavonoid Synthesis and Alters Auxin Transport and the Response of Arabidopsis Roots to Gravity and Light. *The Plant Cell*, 16, 1191-1205.

- BUSTOS-SANMAMED, P., MAO, G., DENG, Y., ELOUET, M., KHAN, G. A., BAZIN, J., TURNER, M., SUBRAMANIAN, S., YU, O., CRESPI, M. & LELANDAIS-BRIÈRE, C. 2013. Overexpression of miR160 affects root growth and nitrogen-fixing nodule number in *Medicago truncatula*. *Functional Plant Biology*, 40, 1208-1220.
- CABO-CALVET, E., ORTIZ-BOLSICO, C., BAEZA-BAEZA, J. J. & GARCÍA-ALVAREZ-COQUE, M. C. 2014. Description of the Retention and Peak Profile for Chromolith Columns in Isocratic and Gradient Elution Using Mobile Phase Composition and Flow Rate as Factors. *Chromatography*, 1, 194-210.
- CAETANO-ANOLLES, G. & GRESSHOFF, P. M. 1991. Plant genetic control of nodulation. *Annual review of Microbiology*, 45, 345-382.
- CALDERÓN VILLALOBOS, L. I. A., LEE, S., DE OLIVEIRA, C., IVETAC, A., BRANDT, W., ARMITAGE, L., SHEARD, L. B., TAN, X., PARRY, G., MAO, H., ZHENG, N., NAPIER, R., KEPINSKI, S. & ESTELLE, M. 2012. A combinatorial TIR1/AFB-Aux/IAA co-receptor system for differential sensing of auxin. *Nat Chem Biol*, 8, 477-485.
- CALDERON-VILLALOBOS, L. I., TAN, X., ZHENG, N. & ESTELLE, M. 2010. Auxin Perception—Structural Insights. *Cold Spring Harbor Perspectives in Biology*, 2.
- CAMPANELLA, J., SMITH, S., LEIBU, D., WEXLER, S. & LUDWIG-MÜLLER, J. 2008. The Auxin Conjugate Hydrolase Family of *Medicago truncatula* and Their Expression During the Interaction with Two Symbionts. *Journal of Plant Growth Regulation*, 27, 26-38.
- CARRARO, N., TISDALE-ORR, T. E., CLOUSE, R. M., KNÖLLER, A. S. & SPICER, R. 2012. Diversification and expression of the PIN, AUX/LAX and ABCB families of putative auxin transporters in *Populus*. *Frontiers in Plant Science*, 3.
- CARRERA, E., HOLMAN, T., MEDHURST, A., PEER, W., SCHMUTHS, H., FOOTITT, S., THEODOULOU, F. L. & HOLDSWORTH, M. J. 2007. Gene Expression Profiling Reveals Defined Functions of the ATP-Binding Cassette Transporter COMATOSE Late in Phase II of Germination. *Plant Physiology*, 143, 1669-1679.
- CASIMIRO, I., MARCHANT, A., BHALERAO, R. P., BEECKMAN, T., DHOOGHE, S., SWARUP, R., GRAHAM, N., INZÉ, D., SANDBERG, G., CASERO, P. J. & BENNETT, M. 2001. Auxin Transport Promotes Arabidopsis Lateral Root Initiation. *The Plant Cell Online*, 13, 843-852.

- CASTILLO, S., GOPALACHARYULU, P., YETUKURI, L. & OREŠIĆ, M. 2011. Algorithms and tools for the preprocessing of LC-MS metabolomics data. *Chemometrics and Intelligent Laboratory Systems*, 108, 23-32.
- CECH, N. B. & ENKE, C. G. 2001. Practical implications of some recent studies in electrospray ionization fundamentals. *Mass Spectrometry Reviews*, 20, 362-387.
- CHAN, C.-C., BOLGAR, M. S., DALPATHADO, D. & LLOYD, D. K. 2012. Mitigation of signal suppression caused by the use of trifluoroacetic acid in liquid chromatography mobile phases during liquid chromatography/mass spectrometry analysis via post-column addition of ammonium hydroxide. *Rapid Communications in Mass Spectrometry*, 26, 1507-1514.
- CHANDLER, J. W. 2011. Founder cell specification. *Trends in Plant Science*, 16, 607-613.
- CHANDLER, J. W. 2011. The Hormonal Regulation of Flower Development. *Journal of Plant Growth Regulation*, 30, 242-254.
- CHARPENTIER, M. & OLDROYD, G. E. D. 2013. Nuclear Calcium Signaling in Plants. *Plant Physiology*, 163, 496-503.
- CHARRON, D., PINGRET, J.-L., CHABAUD, M., JOURNET, E.-P. & BARKER, D. G. 2004. Pharmacological Evidence That Multiple Phospholipid Signaling Pathways Link Rhizobium Nodulation Factor Perception in *Medicago truncatula* Root Hairs to Intracellular Responses, Including Ca²⁺ Spiking and Specific ENOD Gene Expression. *Plant Physiology*, 136, 3582-3593.
- CHEN, L.-Q., QU, X.-Q., HOU, B.-H., SOSSO, D., OSORIO, S., FERNIE, A. R. & FROMMER, W. B. 2012. Sucrose Efflux Mediated by SWEET Proteins as a Key Step for Phloem Transport. *Science*, 335, 207-211.
- CHEN, R., HILSON, P., SEDBROOK, J., ROSEN, E., CASPAR, T. & MASSON, P. H. 1998. The *Arabidopsis thaliana* AGRAVITROPIC 1 gene encodes a component of the polar-auxin-transport efflux carrier. *Proceedings of the National Academy of Sciences*, 95, 15112-15117.
- CHEN, Y., CHEN, W., LI, X., JIANG, H., WU, P., XIA, K., YANG, Y. & WU, G. 2013. Knockdown of *LjIPT3* influences nodule development in *Lotus japonicus*. *Plant and Cell Physiology*.

- CHENG, H.-P. & WALKER, G. C. 1998. Succinoglycan Is Required for Initiation and Elongation of Infection Threads during Nodulation of Alfalfa by *Rhizobium meliloti*. *Journal of Bacteriology*, 180, 5183-5191.
- CHO, M., HENRY, E. M., LEWIS, D. R., WU, G., MUDAY, G. K. & SPALDING, E. P. 2014. Block of ATP-Binding Cassette B19 Ion Channel Activity by 5-Nitro-2-(3-Phenylpropylamino)-Benzoic Acid Impairs Polar Auxin Transport and Root Gravitropism. *Plant Physiology*, 166, 2091-2099.
- CHRISTENSEN, S. K., DAGENAIS, N., CHORY, J. & WEIGEL, D. 2000. Regulation of Auxin Response by the Protein Kinase PINOID. *Cell*, 100, 469-478.
- COOPER, J. B. & LONG, S. R. 1994. Morphogenetic Rescue of *Rhizobium meliloti* Nodulation Mutants by trans-Zeatin Secretion. *Plant Cell*, 6, 215-225.
- CRESPI, M. & FRUGIER, F. 2008. *De Novo Organ Formation from Differentiated Cells: Root Nodule Organogenesis*.
- DAI, J. & MUMPER, R. J. 2010. Plant Phenolics: Extraction, Analysis and Their Antioxidant and Anticancer Properties. *Molecules*, 15, 7313-7352.
- DAKORA, F. D. & PHILLIPS, D. A. 1996. Diverse functions of isoflavonoids in legumes transcend anti-microbial definitions of phytoalexins. *Physiological and Molecular Plant Pathology*, 49, 1-20.
- DAVIES, P. 2010. The Plant Hormones: Their Nature, Occurrence, and Functions. In: DAVIES, P. (ed.) *Plant Hormones*. Springer Netherlands.
- DE BILLY, F., GROSJEAN, C., MAY, S., BENNETT, M. & CULLIMORE, J. V. 2001. Expression Studies on AUX1-like Genes in *Medicago truncatula* Suggest That Auxin Is Required at Two Steps in Early Nodule Development. *Molecular Plant-Microbe Interactions*, 14, 267-277.
- DE SMET, I., TETSUMURA, T., DE RYBEL, B., FREY, N. F. D., LAPLAZE, L., CASIMIRO, I., SWARUP, R., NAUDTS, M., VANNESTE, S., AUDENAERT, D., INZÉ, D., BENNETT, M. J. & BEECKMAN, T. 2007. Auxin-dependent regulation of lateral root positioning in the basal meristem of *Arabidopsis*. *Development*, 134, 681-690.
- DEINUM, E. E., GEURTS, R., BISSELING, T. & MULDER, B. M. 2012. Modeling a cortical auxin maximum for nodulation: different signatures of potential strategies. *Frontiers in Plant Science*, 3.

- DEL POZO, J. C., DIAZ-TRIVINO, S., CISNEROS, N. & GUTIERREZ, C. 2006. The Balance between Cell Division and Endoreplication Depends on E2FC-DPB, Transcription Factors Regulated by the Ubiquitin-SCFSKP2A Pathway in Arabidopsis. *The Plant Cell Online*, 18, 2224-2235.
- DELLO IOIO, R., NAKAMURA, K., MOUBAYIDIN, L., PERILLI, S., TANIGUCHI, M., MORITA, M.T., AOYAMA, T., COSTANTINO, P. & SABATINI, S. 2008. A genetic framework for the control of cell division and differentiation in the root meristem. *Science*, 322, 1380-1384
- DEN HARTOG, M., MUSGRAVE, A. & MUNNIK, T. 2001. Nod factor-induced phosphatidic acid and diacylglycerol pyrophosphate formation: a role for phospholipase C and D in root hair deformation. *The Plant Journal*, 25, 55-65.
- DESBROSSES, GUILHEM J. & STOUGAARD, J. 2011. Root Nodulation: A Paradigm for How Plant-Microbe Symbiosis Influences Host Developmental Pathways. *Cell host and microbe*, 10, 348-358.
- DHARMASIRI, N., DHARMASIRI, S. & ESTELLE, M. 2005. The F-box protein TIR1 is an auxin receptor. *Nature*, 435, 441-445.
- DHARMATILAKE, A. J. & BAUER, W. D. 1992. Chemotaxis of *Rhizobium meliloti* towards Nodulation Gene-Inducing Compounds from Alfalfa Roots. *Applied and Environmental Microbiology*, 58, 1153-1158.
- DHONUKSHE, P., GRIGORIEV, I., FISCHER, R., TOMINAGA, M., ROBINSON, D. G., HAŠEK, J., PACIOREK, T., PETRÁŠEK, J., SEIFERTOVÁ, D., TEJOS, R., MEISEL, L. A., ZAŽÍMALOVÁ, E., GADELLA, T. W. J., STIERHOF, Y.-D., UEDA, T., OIWA, K., AKHMANOVA, A., BROCK, R., SPANG, A. & FRIML, J. 2008. Auxin transport inhibitors impair vesicle motility and actin cytoskeleton dynamics in diverse eukaryotes. *Proceedings of the National Academy of Sciences*, 105, 4489-4494.
- DI PIETRO, A., CONSEIL, G., PÉREZ-VICTORIA, J., DAYAN, G., BAUBICHON-CORTAY, H., TROMPIER, D., STEINFELS, E., JAULT, J. M., DE WET, H., MAITREJEAN, M., COMTE, G., BOUMENDJEL, A., MARIOTTE, A. M., DUMONTET, C., MCINTOSH, D., GOFFEAU, A., CASTANYS, S., GAMARRO, F. & BARRON, D. 2002. Modulation by flavonoids of cell multidrug resistance mediated by P-glycoprotein and related ABC transporters. *Cellular and Molecular Life Sciences*, 59, 307-22.
- DOMINGO, C., ANDRÉS, F., THARREAU, D., IGLESIAS, D. J. & TALÓN, M. 2009. Constitutive Expression of OsGH3.1 Reduces Auxin Content and Enhances Defense Response and Resistance to a Fungal Pathogen in Rice. *Molecular Plant-Microbe Interactions*, 22, 201-210.

- DRDOVÁ, E. J., SYNEK, L., PEČENKOVÁ, T., HÁLA, M., KULICH, I., FOWLER, J. E., MURPHY, A. S. & ŽÁRSKÝ, V. 2013. The exocyst complex contributes to PIN auxin efflux carrier recycling and polar auxin transport in *Arabidopsis*. *The Plant Journal*, 73, 709-719.
- DREYFUS, B. & DOMMERGUES, Y. 1981. Nitrogen-fixing nodules induced by *Rhizobium* on the stem of the tropical legume *Sesbania rostrata*. *FEMS Microbiol. Lett.*, 10, 313-317.
- DUBROVSKY, J. G., SAUER, M., NAPSUCIALY-MENDIVIL, S., IVANCHENKO, M. G., FRIML, J., SHISHKOVA, S., CELENZA, J. & BENKOVÁ, E. 2008. Auxin acts as a local morphogenetic trigger to specify lateral root founder cells. *Proceedings of the National Academy of Sciences*.
- DURGBANSHI, A., ARBONA, V., POZO, O., MIERSCH, O., SANCHO, J. V. & GÓMEZ-CADENAS, A. 2005. Simultaneous Determination of Multiple Phytohormones in Plant Extracts by Liquid Chromatography-Electrospray Tandem Mass Spectrometry. *Journal of Agricultural and Food Chemistry*, 53, 8437-8442.
- EHLERT, B., SCHÖTTLER, M. A., TISCHENDORF, G., LUDWIG-MÜLLER, J. & BOCK, R. 2008. The paramutated SULFUREA locus of tomato is involved in auxin biosynthesis. *Journal of Experimental Botany*, 59, 3635-3647.
- ELIASSON, L. 1972. Translocation of Shoot-Applied Indolylacetic Acid into the Roots of *Populus tremula*. *Physiologia Plantarum*, 27, 412-416.
- EL-SHOWK, S., RUONALA, R. & HELARIUTTA, Y. 2013. Crossing paths: cytokinin signalling and crosstalk. *Development*, 140, 1373-1383.
- ENGELBERTH, J., SCHMELZ, E. A., ALBORN, H. T., CARDOZA, Y. J., HUANG, J. & TUMLINSON, J. H. 2003. Simultaneous quantification of jasmonic acid and salicylic acid in plants by vapor-phase extraction and gas chromatography-chemical ionization-mass spectrometry. *Analytical Biochemistry*, 312, 242-250.
- ERISMAN, J. W., SUTTON, M. A., GALLOWAY, J., KLIMONT, Z. & WINIWARTER, W. 2008. How a century of ammonia synthesis changed the world. *Nature Geosci.*, 1, 636-639.
- ERNST, M., SILVA, D. B., SILVA, R. R., VENCIO, R. Z. N. & LOPES, N. P. 2014. Mass spectrometry in plant metabolomics strategies: from analytical platforms to data acquisition and processing. *Natural Product Reports*, 31, 784-806.

- ESSELING, J. J., LHUISSIER, F. G. P. & EMONS, A. M. C. 2003. Nod Factor-Induced Root Hair Curling: Continuous Polar Growth towards the Point of Nod Factor Application. *Plant Physiology*, 132, 1982-1988.
- FAHRAEUS, G. 1957. The Infection of Clover Root Hairs by Nodule Bacteria Studied by a Simple Glass Slide Technique. *Journal of General Microbiology*, 16, 374-381.
- FANG, Y. & HIRSCH, A. M. 1998. Studying Early Nodulin Gene ENOD40 Expression and Induction by Nodulation Factor and Cytokinin in Transgenic Alfalfa. *Plant Physiology*, 116, 53-68.
- FARAG, M. A., HUHMANN, D. V., LEI, Z. & SUMNER, L. W. 2007. Metabolic profiling and systematic identification of flavonoids and isoflavonoids in roots and cell suspension cultures of *Medicago truncatula* using HPLC-UV-ESI-MS and GC-MS. *Phytochemistry*, 68, 342-354.
- FEDOROVA, E., REDONDO, F. J., KOSHIBA, T., PUEYO, J. J., DE FELIPE, M. R. & LUCAS, M. M. 2005. Aldehyde Oxidase (AO) in the Root Nodules of *Lupinus albus* and *Medicago truncatula*: Identification of AO in Meristematic and Infection Zones. *Molecular Plant-Microbe Interactions*, 18, 405-413.
- FERARU, E., VOSOLSOBE, S., FERARU, M. I., PETRÁŠEK, J. & KLEINE-VEHN, J. 2012. Evolution and structural diversification of PILS putative auxin carriers in plants. *Frontiers in Plant Science*, 3.
- FERGUSON, B. & MATHESIUS, U. 2014. Phytohormone Regulation of Legume-Rhizobia Interactions. *Journal of Chemical Ecology*, 40, 770-790.
- FERGUSON, B. J., INDRASUMUNAR, A., HAYASHI, S., LIN, M.-H., LIN, Y.-H., REID, D. E. & GRESSHOFF, P. M. 2010. Molecular Analysis of Legume Nodule Development and Autoregulation. *Journal of Integrative Plant Biology*, 52, 61-76.
- FERNÁNDEZ-LÓPEZ, M., GOORMACHTIG, S., GAO, M., D'HAENZE, W., VAN MONTAGU, M. & HOLSTERS, M. 1998. Ethylene-mediated phenotypic plasticity in root nodule development on *Sesbania rostrata*. *Proceedings of the National Academy of Sciences*, 95, 12724-12728.
- FERTÉ, J., KÜHNEL, J.-M., CHAPUIS, G., ROLLAND, Y., LEWIN, G. & SCHWALLER, M. A. 1999. Flavonoid-Related Modulators of Multidrug Resistance: Synthesis, Pharmacological Activity, and Structure-Activity Relationships. *Journal of Medicinal Chemistry*, 42, 478-489.

- FORESTAN, C., FARINATI, S. & VAROTTO, S. 2012. The maize PIN gene family of auxin transporters. *Frontiers in Plant Science*, 3.
- FOWLER, D., COYLE, M., SKIBA, U., SUTTON, M. A., CAPE, J. N., REIS, S., SHEPPARD, L. J., JENKINS, A., GRIZZETTI, B., GALLOWAY, J. N., VITOUSEK, P., LEACH, A., BOUWMAN, A. F., BUTTERBACH-BAHL, K., DENTENER, F., STEVENSON, D., AMANN, M. & VOSS, M. 2013. The global nitrogen cycle in the twenty-first century. *Philosophical Transactions of the Royal Society B: Biological Sciences*, 368.
- FRESCHI, L. 2013. Nitric oxide and phytohormone interactions: current status and perspectives. *Frontiers in Plant Science*, 4.
- FRIML, J. 2003. Auxin transport -- shaping the plant. *Current Opinion in Plant Biology*, 6, 7-12.
- FRIML, J., YANG, X., MICHNIEWICZ, M., WEIJERS, D., QUINT, A., TIETZ, O., BENJAMINS, R., OUWERKERK, P. B. F., LJUNG, K., SANDBERG, G., HOOYKAAS, P. J. J., PALME, K. & OFFRINGA, R. 2004. A PINOID-Dependent Binary Switch in Apical-Basal PIN Polar Targeting Directs Auxin Efflux. *Science*, 306, 862-865.
- FRUGIER, F., KOSUTA, S., MURRAY, J.D., CRESPI, M. & SZCZYGLOWSKI, K. 2008. Cytokinin: secret agent of symbiosis. *Trends in Plant Science*, 13, 115-120.
- FUKAKI, H. & TASAKA, M. 2009. Hormone interactions during lateral root formation. *Plant Molecular Biology*, 69, 437-449.
- GAMOH, K., ABE, H., SHIMADA, K. & TAKATSUTO, S. 1996. Liquid Chromatography/Mass Spectrometry with Atmospheric Pressure Chemical Ionization of Free Brassinosteroids. *Rapid Communications in Mass Spectrometry*, 10, 903-906.
- GANGULY, A., LEE, S. H., CHO, M., LEE, O. R., YOO, H. & CHO, H.-T. 2010. Differential Auxin-Transporting Activities of PIN-FORMED Proteins in Arabidopsis Root Hair Cells. *Plant Physiology*, 153, 1046-1061.
- GAO, Y., ZHANG, Y., ZHANG, D., DAI, X., ESTELLE, M. & ZHAO, Y. 2015. Auxin binding protein 1 (ABP1) is not required for either auxin signaling or Arabidopsis development. *Proceedings of the National Academy of Sciences*, 112, 2275-2280.

- GEISLER, M., BLAKESLEE, J. J., BOUCHARD, R., LEE, O. R., VINCENZETTI, V., BANDYOPADHYAY, A., TITAPIWATANAKUN, B., PEER, W. A., BAILLY, A., RICHARDS, E. L., EJENDAL, K. F. K., SMITH, A. P., BAROUX, C., GROSSNIKLAUS, U., MÜLLER, A., HRYCYNA, C. A., DUDLER, R., MURPHY, A. S. & MARTINOIA, E. 2005. Cellular efflux of auxin catalyzed by the Arabidopsis MDR/PGP transporter AtPGP1. *The Plant Journal*, 44, 179-194.
- GEISLER, M., KOLUKISAOGLU, H. Ü., BOUCHARD, R., BILLION, K., BERGER, J., SAAL, B., FRANGNE, N., KONCZ-KÁLMÁN, Z., KONCZ, C., DUDLER, R., BLAKESLEE, J. J., MURPHY, A. S., MARTINOIA, E. & SCHULZ, B. 2003. TWISTED DWARF1, a Unique Plasma Membrane-anchored Immunophilin-like Protein, Interacts with Arabidopsis Multidrug Resistance-like Transporters AtPGP1 and AtPGP19. *Molecular Biology of the Cell*, 14, 4238-4249.
- GELDNER, N., ANDERS, N., WOLTERS, H., KEICHER, J., KORNBERGER, W., MULLER, P., DELBARRE, A., UEDA, T., NAKANO, A. & JÜRGENS, G. 2003. The Arabidopsis GNOM ARF-GEF Mediates Endosomal Recycling, Auxin Transport, and Auxin-Dependent Plant Growth. *Cell*, 112, 219-230.
- GELDNER, N., FRIML, J., STIERHOF, Y.-D., JURGENS, G. & PALME, K. 2001. Auxin transport inhibitors block PIN1 cycling and vesicle trafficking. *Nature*, 413, 425-428.
- GILAR, M., JAWORSKI, A. & MCDONALD, T. S. 2014. Solvent selectivity and strength in reversed-phase liquid chromatography separation of peptides. *Journal of Chromatography A*, 1337, 140-146.
- GLEASON, C., CHAUDHURI, S., YANG, T., MUNOZ, A., POOVAIAH, B. W. & OLDROYD, G. E. D. 2006. Nodulation independent of rhizobia induced by a calcium-activated kinase lacking autoinhibition. *Nature*, 441, 1149-1152.
- GODFRAY, H. C. J., BEDDINGTON, J. R., CRUTE, I. R., HADDAD, L., LAWRENCE, D., MUIR, J. F., PRETTY, J., ROBINSON, S., THOMAS, S. M. & TOULMIN, C. 2010. Food Security: The Challenge of Feeding 9 Billion People. *Science*, 327, 812-818.
- GOETHALS, K., GAO, M., TOMEKPE, K., VAN MONTAGU, M. & HOLSTERS, M. 1989. Common nodABC genes in Nod locus 1 of *Azorhizobium caulinodans*: Nucleotide sequence and plant-inducible expression. *Mol Gen Genet*, 219, 289-298.
- GONZALEZ-RIZZO, S., CRESPI, M. & FRUGIER, F. 2006. The *Medicago truncatula* CRE1 Cytokinin Receptor Regulates Lateral Root Development and Early Symbiotic Interaction with *Sinorhizobium meliloti*. *Plant Cell*, 18, 2680-2693.

- GREBE, M., FRIML, J., SWARUP, R., LJUNG, K., SANDBERG, G., TERLOU, M., PALME, K., BENNETT, M. J. & SCHERES, B. 2002. Cell Polarity Signaling in Arabidopsis Involves a BFA-Sensitive Auxin Influx Pathway. *Current Biology*, 12, 329-334.
- GRIMME, S. 2013. Towards First Principles Calculation of Electron Impact Mass Spectra of Molecules. *Angewandte Chemie International Edition*, 52, 6306-6312.
- GRUNEWALD, W., CANNOOT, B., FRIML, J. & GHEYSEN, G. 2009. Parasitic Nematodes Modulate PIN-Mediated Auxin Transport to Facilitate Infection. *PLoS Pathog*, 5, e1000266.
- GRUNEWALD, W., DE SMET, I., LEWIS, D. R., LÖFKE, C., JANSEN, L., GOEMINNE, G., VANDEN BOSSCHE, R., KARIMI, M., DE RYBEL, B., VANHOLME, B., TEICHMANN, T., BOERJAN, W., VAN MONTAGU, M. C. E., GHEYSEN, G., MUDAY, G. K., FRIML, J. & BEECKMAN, T. 2012. Transcription factor WRKY23 assists auxin distribution patterns during Arabidopsis root development through local control on flavonol biosynthesis. *Proceedings of the National Academy of Sciences*, 109, 1554-1559.
- GRUNEWALD, W., VAN NOORDEN, G., VAN ISTERDAEL, G., BEECKMAN, T., GHEYSEN, G. & MATHESIUS, U. 2009. Manipulation of Auxin Transport in Plant Roots during Rhizobium Symbiosis and Nematode Parasitism. *The Plant Cell Online*, 21, 2553-2562.
- GUAN, D., STACEY, N., LIU, C., WEN, J., MYSORE, K. S., TORRES-JEREZ, I., VERNIE, T., TADEGE, M., ZHOU, C., WANG, Z.-Y., UDVARDI, M. K., OLDROYD, G. E. D. & MURRAY, J. D. 2013. Rhizobial infection is associated with the development of peripheral vasculature in nodules of *Medicago truncatula*. *Plant Physiology*.
- GUO, J., LIU, D., NIKOLIC, D., ZHU, D., PEZZUTO, J. M. & VAN BREEMEN, R. B. 2008. In Vitro Metabolism of Isoliquiritigenin by Human Liver Microsomes. *Drug Metabolism and Disposition*, 36, 461-468.
- HAGEN, G., MARTIN, G., LI, Y. & GUILFOYLE, T. J. 1991. Auxin-induced expression of the soybean GH3 promoter in transgenic tobacco plants. *Plant Molecular Biology*, 17, 567-579.
- HASSAN, S. & MATHESIUS, U. 2012. The role of flavonoids in root-rhizosphere signalling: opportunities and challenges for improving plant-microbe interactions. *Journal of Experimental Botany*.

- HAVENS, K. A., GUSEMAN, J. M., JANG, S. S., PIERRE-JEROME, E., BOLTEN, N., KLAVINS, E. & NEMHAUSER, J. L. 2012. A Synthetic Approach Reveals Extensive Tunability of Auxin Signaling. *Plant Physiology*, 160, 135-142.
- HAYASHI, K.-I., NAKAMURA, S., FUKUNAGA, S., NISHIMURA, T., JENNESS, M. K., MURPHY, A. S., MOTOSE, H., NOZAKI, H., FURUTANI, M. & AOYAMA, T. 2014. Auxin transport sites are visualized in planta using fluorescent auxin analogs. *Proceedings of the National Academy of Sciences*.
- HECKMANN, A. B., SANDAL, N., BEK, A. S., MADSEN, L. H., JURKIEWICZ, A., NIELSEN, M. W., TIRICHINE, L. & STOUGAARD, J. 2011. Cytokinin Induction of Root Nodule Primordia in *Lotus japonicus* Is Regulated by a Mechanism Operating in the Root Cortex. *Molecular Plant-Microbe Interactions*, 24, 1385-1395.
- HELD, M., HOU, H., MIRI, M., HUYNH, C., ROSS, L., HOSSAIN, M. S., SATO, S., TABATA, S., PERRY, J., WANG, T. L. & SZCZYGLOWSKI, K. 2014. *Lotus japonicus* Cytokinin Receptors Work Partially Redundantly to Mediate Nodule Formation. *The Plant Cell Online*.
- HERRBACH, V., REMBLIÈRE, C., GOUGH, C. & BENSMIHEN, S. 2014. Lateral root formation and patterning in *Medicago truncatula*. *Journal of Plant Physiology*, 171, 301-310.
- HERRERA, L. C., GROSSERT, J. S. & RAMALEY, L. 2008. Quantitative Aspects of and Ionization Mechanisms in Positive-Ion Atmospheric Pressure Chemical Ionization Mass Spectrometry. *Journal of the American Society for Mass Spectrometry*, 19, 1926-1941.
- HERRIDGE, D., PEOPLES, M. & BODDEY, R. 2008. Global inputs of biological nitrogen fixation in agricultural systems. *Plant and Soil*, 311, 1-18.
- HIRSCH, A. M. 1992. Developmental biology of legume nodulation. *New Phytologist*, 122, 211-237.
- HIRSCH, A. M., BHUVANESWARI, T. V., TORREY, J. G. & BISSELING, T. 1989. Early nodulin genes are induced in alfalfa root outgrowths elicited by auxin transport inhibitors. *Proceedings of the National Academy of Sciences*, 86, 1244-1248.
- HIRSCH, A. M., LARUE, T. A. & DOYLE, J. 1997. Is the Legume Nodule a Modified Root or Stem or an Organ sui generis? *Critical Reviews in Plant Sciences*, 16, 361-392.

- HIRSCH, S., KIM, J., MUÑOZ, A., HECKMANN, A. B., DOWNIE, J. A. & OLDROYD, G. E. D. 2009. GRAS Proteins Form a DNA Binding Complex to Induce Gene Expression during Nodulation Signaling in *Medicago truncatula*. *The Plant Cell Online*, 21, 545-557.
- HOFGEN, R. & WILLMITZER, L. 1988. Storage of competent cells for *Agrobacterium* transformation. *Nucleic Acids Research*, 16, 9877.
- HOLLOWAY, J. M., DAHLGREN, R. A., HANSEN, B. & CASEY, W. H. 1998. Contribution of bedrock nitrogen to high nitrate concentrations in stream water. *Nature*, 395, 785-788.
- HORAI, H., ARITA, M., KANAYA, S., NIHEI, Y., IKEDA, T., SUWA, K., OJIMA, Y., TANAKA, K., TANAKA, S., AOSHIMA, K., ODA, Y., KAKAZU, Y., KUSANO, M., TOHGE, T., MATSUDA, F., SAWADA, Y., HIRAI, M. Y., NAKANISHI, H., IKEDA, K., AKIMOTO, N., MAOKA, T., TAKAHASHI, H., ARA, T., SAKURAI, N., SUZUKI, H., SHIBATA, D., NEUMANN, S., IIDA, T., TANAKA, K., FUNATSU, K., MATSUURA, F., SOGA, T., TAGUCHI, R., SAITO, K. & NISHIOKA, T. 2010. MassBank: a public repository for sharing mass spectral data for life sciences. *Journal of Mass Spectrometry*, 45, 703-714.
- HUA, Y. & JENKE, D. 2012. Increasing the Sensitivity of an LC-MS Method for Screening Material Extracts for Organic Extractables via Mobile Phase Optimization. *Journal of Chromatographic Science*, 50, 213-227.
- HUIE, C. 2002. A review of modern sample-preparation techniques for the extraction and analysis of medicinal plants. *Analytical and Bioanalytical Chemistry*, 373, 23-30.
- HUO, X., SCHABEL, E., HUGHES, K. & FRUGOLI, J. 2006. RNAi phenotypes and the localisation of a protein::GUS fusion imply a role for *Medicago truncatula* PIN genes in nodulation. *Journal of Plant Growth Regulation*, 25, 156-165.
- HUTANGURA, P., MATHESIUS, U., JONES, M. G. K. & ROLFE, B. G. 1999. Auxin induction is a trigger for root gall formation caused by root-knot nematodes in white clover and is associated with the activation of the flavonoid pathway. *Functional Plant Biology*, 26, 221-231.
- IMAIZUMI-ANRAKU, H., KOUCHI, H., SYONO, K., AKAO, S. & KAWAGUCHI, M. 2000. Analysis of ENOD40 expression in alb1, a symbiotic mutant of *Lotus japonicus* that forms empty nodules with incompletely developed nodule vascular bundles. *Mol Gen Genet*, 264, 402-410.

- IMANISHI, L., PERRINE-WALKER, F. M., NDOUR, A., VAYSSIERES, A., CONEJERO, G., LUCAS, M., CHAMPION, A., LAPLAZE, L., WALL, L. & SVISTOONOFF, S. 2014. Role of auxin during intercellular infection of *Discaria trinervis* by *Frankia*. *Frontiers in Plant Science*, 5.
- ITOH, H., KINOSHITA, T. & NIMURA, N. 1993. Reversed-Phase High Performance Liquid Chromatographic Separation of Small Molecules on Nonporous C18 Silica Gel Column. *Journal of Liquid Chromatography*, 16, 809-823.
- JACKSON, R. G., KOWALCZYK, M., LI, Y., HIGGINS, G., ROSS, J., SANDBERG, G. & BOWLES, D. J. 2002. Over-expression of an Arabidopsis gene encoding a glucosyltransferase of indole-3-acetic acid: phenotypic characterisation of transgenic lines. *The Plant Journal*, 32, 573-583.
- JACOBS, M. & RUBERY, P. H. 1988. Naturally occurring auxin transport regulators. *Science*, 241, 346-349.
- JIN, J., WATT, M. & MATHESIUS, U. 2012. The Autoregulation Gene SUNN Mediates Changes in Root Organ Formation in Response to Nitrogen through Alteration of Shoot-to-Root Auxin Transport. *Plant Physiology*, 159, 489-500.
- JONES, B., GUNNERAS, S. A., PETERSSON, S. V., TARKOWSKI, P., GRAHAM, N., MAY, S., DOLEZAL, K., SANDBERG, G. & LJUNG, K. 2010. Cytokinin Regulation of Auxin Synthesis in Arabidopsis Involves a Homeostatic Feedback Loop Regulated via Auxin and Cytokinin Signal Transduction. *Plant Cell*, tpc.110.074856.
- JOSHI, P., CAETANO-ANOLLÉS, G., GRAHAM, E. & GRESSHOFF, P. M. 1991. Ontogeny and ultrastructure of spontaneous nodules in alfalfa (*Medicago sativa*). *Protoplasma*, 162, 1-11.
- JOURNET, E. P., PICHON, M., DEDIEU, A., DE BILLY, F., TRUCHET, G. & BARKER, D. G. 1994. *Rhizobium meliloti* Nod factors elicit cell-specific transcription of the ENOD12 gene in transgenic alfalfa. *The Plant Journal*, 6, 241-249.
- JURADO, S., ABRAHAM, Z., MANZANO, C., LOPEZ-TORREJON, G., PACIOS, L. F. & DEL POZO, J. C. 2010. The Arabidopsis Cell Cycle F-Box Protein SKP2A Binds to Auxin. *The Plant Cell*, 22, 3891-3904.
- KAI, K., HORITA, J., WAKASA, K. & MIYAGAWA, H. 2007. Three oxidative metabolites of indole-3-acetic acid from *Arabidopsis thaliana*. *Phytochemistry*, 68, 1651-1663.

- KALLENBACH, M., BALDWIN, I. & BONAVENTURE, G. 2009. A rapid and sensitive method for the simultaneous analysis of aliphatic and polar molecules containing free carboxyl groups in plant extracts by LC-MS/MS. *Plant Methods*, 5, 17.
- KALÓ, P., GLEASON, C., EDWARDS, A., MARSH, J., MITRA, R. M., HIRSCH, S., JAKAB, J., SIMS, S., LONG, S. R., ROGERS, J., KISS, G. B., DOWNIE, J. A. & OLDROYD, G. E. D. 2005. Nodulation Signaling in Legumes Requires NSP2, a Member of the GRAS Family of Transcriptional Regulators. *Science*, 308, 1786-1789.
- KARIMI, M., INZÉ, D. & DEPICKER, A. 2002. GATEWAY™ vectors for Agrobacterium-mediated plant transformation. *Trends in Plant Science*, 7, 193-195.
- KAWAGUCHI, M., IMAIZUMI-ANRAKU, H., FUKAI, S. & SYONO, K. 1996. Unusual Branching in the Seedlings of *Lotus japonicus*—Gibberellins Reveal the Nitrogen-sensitive Cell Divisions within the Pericycle on Roots. *Plant and Cell Physiology*, 37, 461-470.
- KIM, J.-Y., HENRICH, S., BAILLY, A., VINCENZETTI, V., SOVERO, V., MANCUSO, S., POLLMANN, S., KIM, D., GEISLER, M. & NAM, H.-G. 2010. Identification of an ABCB/P-glycoprotein-specific Inhibitor of Auxin Transport by Chemical Genomics. *Journal of Biological Chemistry*, 285, 23309-23317.
- KLEINE-VEHN, J., DHONUKSHE, P., SWARUP, R., BENNETT, M. & FRIML, J. 2006. Subcellular Trafficking of the Arabidopsis Auxin Influx Carrier AUX1 Uses a Novel Pathway Distinct from PIN1. *The Plant Cell Online*, 18, 3171-3181.
- KLEINE-VEHN, J., HUANG, F., NARAMOTO, S., ZHANG, J., MICHNIEWICZ, M., OFFRINGA, R. & FRIML, J. 2009. PIN Auxin Efflux Carrier Polarity Is Regulated by PINOID Kinase-Mediated Recruitment into GNOM-Independent Trafficking in Arabidopsis. *The Plant Cell Online*, 21, 3839-3849.
- KORASICK, D. A., ENDERS, T. A. & STRADER, L. C. 2013. Auxin biosynthesis and storage forms. *Journal of Experimental Botany*.
- KOWALCZYK, M. & SANDBERG, G. 2001. Quantitative Analysis of Indole-3-Acetic Acid Metabolites in Arabidopsis. *Plant Physiology*, 127, 1845-1853.
- KRAMER, E. M., RUTSCHOW, H. L. & MABIE, S. S. 2011. AuxV: a database of auxin transport velocities. *Trends in Plant Science*, 16, 461-463.

- KRECEK, P., SKUPA, P., LIBUS, J., NARAMOTO, S., TEJOS, R., FRIML, J. & ZAZIMALOVA, E. 2009. The PIN-FORMED (PIN) protein family of auxin transporters. *Genome Biology*, 10, 249.
- KUEGER, S., STEINHAUSER, D., WILLMITZER, L. & GIAVALISCO, P. 2012. High-resolution plant metabolomics: from mass spectral features to metabolites and from whole-cell analysis to subcellular metabolite distributions. *The Plant Journal*, 70, 39-50.
- KUHN, B. M., GEISLER, M., BIGLER, L. & RINGLI, C. 2011. Flavonols Accumulate Asymmetrically and Affect Auxin Transport in Arabidopsis. *Plant Physiology*, 156, 585-595.
- KUPPUSAMY, K. T., IVASHUTA, S., BUCCIARELLI, B., VANCE, C. P., GANTT, J. S. & VANDENBOSCH, K. A. 2009. Knockdown of CELL DIVISION CYCLE16 Reveals an Inverse Relationship between Lateral Root and Nodule Numbers and a Link to Auxin in *Medicago truncatula*. *Plant Physiology*, 151, 1155-1166.
- LAFFONT, C., BLANCHET, S., LAPIERRE, C., BROCARD, L., RATET, P., CRESPI, M., MATHESIUS, U. & FRUGIER, F. 2010. The Compact Root Architecture 1 gene regulates lignification, flavonoid production and polar auxin transport in *Medicago truncatula*. *Plant Physiology*.
- LANCKMANS, K., SARRE, S., SMOLDERS, I. & MICHOTTE, Y. 2007. Use of a structural analogue versus a stable isotope labeled internal standard for the quantification of angiotensin IV in rat brain dialysates using nano-liquid chromatography/tandem mass spectrometry. *Rapid Communications in Mass Spectrometry*, 21, 1187-1195.
- LAPLAZE, L., BENKOVA, E., CASIMIRO, I., MAES, L., VANNESTE, S., SWARUP, R., WEIJERS, D., CALVO, V., PARIZOT, B., HERRERA-RODRIGUEZ, M. B., OFFRINGA, R., GRAHAM, N., DOUMAS, P., FRIML, J., BOGUSZ, D., BECKMAN, T. & BENNETT, M. 2007. Cytokinins Act Directly on Lateral Root Founder Cells to Inhibit Root Initiation. *The Plant Cell Online*, 19, 3889-3900.
- LARRIEU, A., CHAMPION, A., LEGRAND, J., LAVENUS, J., MAST, D., BRUNOUD, G., OH, J., GUYOMARC'H, S., PIZOT, M., FARMER, E. E., TURNBULL, C., VERNOUX, T., BENNETT, M. J. & LAPLAZE, L. 2015. A fluorescent hormone biosensor reveals the dynamics of jasmonate signalling in plants. *Nat Commun*, 6.
- LAVENUS, J., GOH, T., ROBERTS, I., GUYOMARC'H, S., LUCAS, M., DE SMET, I., FUKAKI, H., BECKMAN, T., BENNETT, M. & LAPLAZE, L. 2013. Lateral root development in Arabidopsis: fifty shades of auxin. *Trends in Plant Science*, 18, 450-458.

- LECLERE, S., TELLEZ, R., RAMPEY, R. A., MATSUDA, S. P. T. & BARTEL, B. 2002. Characterization of a Family of IAA-Amino Acid Conjugate Hydrolases from *Arabidopsis*. *Journal of Biological Chemistry*, 277, 20446-20452.
- LEHMANN, T., HOFFMANN, M., HENTRICH, M. & POLLMANN, S. 2010. Indole-3-acetamide-dependent auxin biosynthesis: A widely distributed way of indole-3-acetic acid production? *European Journal of Cell Biology*, 89, 895-905.
- LE SIGNOR, C., SAVOIS, V., AUBERT, G., VERDIER, J., NICOLAS, M., PAGNY, G., MOUSSY, F., SANCHEZ, M., BAKER, D., CLARKE, J. & THOMPSON, R. 2009. Optimizing TILLING populations for reverse genetics in *Medicago truncatula*. *Plant Biotechnology Journal*, 7, 430-441.
- LI, G., LU, S., WU, H., CHEN, G., LIU, S., KONG, X., KONG, W. & YOU, J. 2015. Determination of multiple phytohormones in fruits by high-performance liquid chromatography with fluorescence detection using dispersive liquid-liquid microextraction followed by precolumn fluorescent labeling. *Journal of Separation Science*, 38, 187-196.
- LI, T., YAN, Z., ZHOU, C., SUN, J., JIANG, C. & YANG, X. 2013. Simultaneous quantification of paeoniflorin, nobiletin, tangeretin, liquiritigenin, isoliquiritigenin, liquiritin and formononetin from Si-Ni-San extract in rat plasma and tissues by liquid chromatography-tandem mass spectrometry. *Biomedical Chromatography*, 27, 1041-1053.
- LI, X., LEI, M., YAN, Z., WANG, Q., CHEN, A., SUN, J., LUO, D. & WANG, Y. 2014. The REL3-mediated TAS3 ta-siRNA pathway integrates auxin and ethylene signaling to regulate nodulation in *Lotus japonicus*. *New Phytologist*, 201, 531-544.
- LIANG, JOE C., BLOOM, RYAN J. & SMOLKE, CHRISTINA D. 2011. Engineering Biological Systems with Synthetic RNA Molecules. *Molecular Cell*, 43, 915-926.
- LIANG, Y., CAO, Y., TANAKA, K., THIBIVILLIERS, S., WAN, J., CHOI, J., KANG, C. H., QIU, J. & STACEY, G. 2013. Nonlegumes Respond to Rhizobial Nod Factors by Suppressing the Innate Immune Response. *Science*.
- LIBBENGA, K., VAN IREN, F., BOGERS, R., SCHRAAG-LAMERS, M. & 1973. The role of hormones and gradients in the initiation of cortex proliferation and nodule formation in *Pisum sativum* L. *Planta*, 114, 29-39.

- LIU, S., CHEN, W., QU, L., GAI, Y. & JIANG, X. 2013. Simultaneous determination of 24 or more acidic and alkaline phytohormones in femtomole quantities of plant tissues by high-performance liquid chromatography-electrospray ionization-ion trap mass spectrometry. *Analytical and Bioanalytical Chemistry*, 405, 1257-1266.
- LIU, X., BARKAWI, L., GARDNER, G. & COHEN, J. D. 2012. Transport of Indole-3-Butyric Acid and Indole-3-Acetic Acid in Arabidopsis Hypocotyls Using Stable Isotope Labeling. *Plant Physiology*, 158, 1988-2000.
- LIU, X., HEGEMAN, A., GARDNER, G. & COHEN, J. 2012. Protocol: High-throughput and quantitative assays of auxin and auxin precursors from minute tissue samples. *Plant Methods*, 8, 31.
- LJUNG, K. 2013. Auxin metabolism and homeostasis during plant development. *Development*, 140, 943-950.
- LJUNG, K., BHALERAO, R. P. & SANDBERG, G. 2001. Sites and homeostatic control of auxin biosynthesis in Arabidopsis during vegetative growth. *The Plant Journal*, 28, 465-474.
- LJUNG, K., HULL, A. K., CELENZA, J., YAMADA, M., ESTELLE, M., NORMANLY, J. & SANDBERG, G. 2005. Sites and Regulation of Auxin Biosynthesis in Arabidopsis Roots. *The Plant Cell Online*, 17, 1090-1104.
- LJUNG, K., SANDBERG, G. & MORITZ, T. 2010. Methods of Plant Hormone Analysis. In: DAVIES, P. (ed.) *Plant Hormones*. Springer Netherlands.
- LUCAS, W. J., GROOVER, A., LICHTENBERGER, R., FURUTA, K., YADAV, S.-R., HELARIUTTA, Y., HE, X.-Q., FUKUDA, H., KANG, J., BRADY, S. M., PATRICK, J. W., SPERRY, J., YOSHIDA, A., LÓPEZ-MILLÁN, A.-F., GRUSAK, M. A. & KACHROO, P. 2013. The Plant Vascular System: Evolution, Development and Functions. *Journal of Integrative Plant Biology*, 55, 294-388.
- LUDWIG-MÜLLER, J. 2011. Auxin conjugates: their role for plant development and in the evolution of land plants. *Journal of Experimental Botany*, 62, 1757-1773.
- LUDWIG-MÜLLER, J. & COHEN, J. D. 2002. Identification and quantification of three active auxins in different tissues of *Tropaeolum majus*. *Physiologia Plantarum*, 115, 320-329.
- MA, Z., GE, L., LEE, A. S. Y., YONG, J. W. H., TAN, S. N. & ONG, E. S. 2008. Simultaneous analysis of different classes of phytohormones in coconut (*Cocos nucifera* L.) water using high-performance liquid chromatography and liquid chromatography-tandem mass spectrometry after solid-phase extraction. *Analytica Chimica Acta*, 610, 274-281.

- MACK, A. E. 2011. Several ZORBAX RRHD 1.8 μ m Selectivities Facilitate Method Development. *Agilent Technologies Inc.*
- MACLEAN, B., TOMAZELA, D. M., ABBATIello, S. E., ZHANG, S., WHITEAKER, J. R., PAULOVICH, A. G., CARR, S. A. & MACCOSS, M. J. 2010. Effect of Collision Energy Optimization on the Measurement of Peptides by Selected Reaction Monitoring (SRM) Mass Spectrometry. *Analytical Chemistry*, 82, 10116-10124.
- MADSEN, E. B., MADSEN, L. H., RADUTOIU, S., OLBRYT, M., RAKWALSKA, M., SZCZYGLOWSKI, K., SATO, S., KANEKO, T., TABATA, S., SANDAL, N. & STOUGAARD, J. 2003. A receptor kinase gene of the LysM type is involved in legume perception of rhizobial signals. *Nature*, 425, 637-640.
- MAO, G., TURNER, M., YU, O. & SUBRAMANIAN, S. 2013. miR393 and miR164 influence indeterminate but not determinate nodule development. *Plant Signaling and Behavior*, 8, e26753.
- MARCHANT, A., BHALERAO, R., CASIMIRO, I., EKLÖF, J., CASERO, P. J., BENNETT, M. & SANDBERG, G. 2002. AUX1 Promotes Lateral Root Formation by Facilitating Indole-3-Acetic Acid Distribution between Sink and Source Tissues in the Arabidopsis Seedling. *The Plant Cell Online*, 14, 589-597.
- MARHAVÝ, P., BIELACH, A., ABAS, L., ABUZEINEH, A., DUCLERCQ, J., TANAKA, H., PAYEZOVÁ, M., PETRÁAEK, J., FRIML, J., KLEINE-VEHN, J. & BENKOVÁ, E. 2011. Cytokinin Modulates Endocytic Trafficking of PIN1 Auxin Efflux Carrier to Control Plant Organogenesis. *Developmental cell*, 21, 796-804.
- MARHAVÝ, P., DUCLERCQ, J., WELLER, B., FERARU, E., BIELACH, A., OFFRINGA, R., FRIML, J., SCHWECHHEIMER, C., MURPHY, A. & BENKOVÁ, E. 2014. Cytokinin Controls Polarity of PIN1-Dependent Auxin Transport during Lateral Root Organogenesis. *Current Biology*, 24, 1031-1037.
- MASHIGUCHI, K., TANAKA, K., SAKAI, T., SUGAWARA, S., KAWAIDE, H., NATSUME, M., HANADA, A., YAENO, T., SHIRASU, K., YAO, H., MCSTEEN, P., ZHAO, Y., HAYASHI, K.-I., KAMIYA, Y. & KASAHARA, H. 2011. The main auxin biosynthesis pathway in Arabidopsis. *Proceedings of the National Academy of Sciences*.
- MATHESIUS, U. 2001. Flavonoids induced in cells undergoing nodule organogenesis in white clover are regulators of auxin breakdown by peroxidase. *Journal of Experimental Botany*, 52, 419-426.

- MATHESIUS, U. 2008. Auxin: at the root of nodule development? *Functional Plant Biology* 35, 651-668.
- MATHESIUS, U. 2008. Goldacre paper: Auxin: at the root of nodule development? *Functional Plant Biology*, 35, 651-668.
- MATHESIUS, U., BAYLISS, C., WEINMAN, J. J., SCHLAMMAN, H. R. M., SPAINK, H. P., ROLFE, B. G., MCCULLY, M. E. & DJORDJEVIC, M. A. 1998. Flavonoids Synthesized in Cortical Cells During Nodule Initiation Are Early Developmental Markers in White Clover. *Molecular Plant-Microbe Interactions*, 11, 1223-1232.
- MATHESIUS, U., SCHLAMMAN, H. R. M., SPAINK, H. P., OF SAUTTER, C., ROLFE, B. G. & DJORDJEVIC, M. A. 1998. Auxin transport inhibition precedes root nodule formation in white clover roots and is regulated by flavonoids and derivatives of chitin oligosaccharides. *The Plant Journal*, 14, 23-34.
- MATHESIUS, U., WEINMAN, J. J., ROLFE, B. G. & DJORDJEVIC, M. A. 2000. Rhizobia Can Induce Nodules in White Clover by "Hijacking" Mature Cortical Cells Activated During Lateral Root Development. *Molecular Plant-Microbe Interactions*, 13, 170-182.
- MATSUDA, F., MIYAZAWA, H., WAKASA, K. & MIYAGAWA, H. 2005. Quantification of Indole-3-Acetic Acid and Amino Acid Conjugates in Rice by Liquid Chromatography-Electrospray Ionization-Tandem Mass Spectrometry. *Bioscience, Biotechnology, and Biochemistry*, 69, 778-783.
- MCMASTER, M. C. 2005. Appendix B: Solvents and Volatile Buffers for LC/MS. *LC/MS*. John Wiley & Sons, Inc.
- MICHNIEWICZ, M., ZAGO, M. K., ABAS, L., WEIJERS, D., SCHWEIGHOFER, A., MESKIENE, I., HEISLER, M. G., OHNO, C., ZHANG, J., HUANG, F., SCHWAB, R., WEIGEL, D., MEYEROWITZ, E. M., LUSCHNIG, C., OFFRINGA, R. & FRIML, J. 2007. Antagonistic Regulation of PIN Phosphorylation by PP2A and PINOID Directs Auxin Flux. *Cell*, 130, 1044-1056.
- MIKKELSEN, M. D., NAUR, P. & HALKIER, B. A. 2004. Arabidopsis mutants in the C-S lyase of glucosinolate biosynthesis establish a critical role for indole-3-acetaldoxime in auxin homeostasis. *The Plant Journal*, 37, 770-777.
- MIWA, H., SUN, J., OLDROYD, G. E. D. & DOWNIE, J. A. 2006. Analysis of Nod-Factor-Induced Calcium Signaling in Root Hairs of Symbiotically Defective Mutants of *Lotus japonicus*. *Molecular Plant-Microbe Interactions*, 19, 914-923.

- MOREIRA, S., BISHOPP, A., CARVALHO, H. & CAMPILHO, A. 2013. AHP6 Inhibits Cytokinin Signaling to Regulate the Orientation of Pericycle Cell Division during Lateral Root Initiation. *PLoS ONE*, 8, e56370.
- MORRIS, D. A. & JOHNSON, C. 1987. Regulation of auxin transport in pea (*Pisum sativum* L.) by phenylacetic acid: inhibition of polar auxin transport in intact plants and stem segments. *Planta*, 172, 408-416.
- MORTIER, V., WASSON, A., JAWOREK, P., DE KEYSER, A., DECROOS, M., HOLSTERS, M., TARKOWSKI, P., MATHESIUS, U. & GOORMACHTIG, S. 2014. Role of LONELY GUY genes in indeterminate nodulation on *Medicago truncatula*. *New Phytologist*, 202, 582-593.
- MOUBAYIDIN, L., DI MAMBRO, R. & SABATINI, S. 2009. Cytokinin-auxin crosstalk. *Trends in Plant Science*, 14, 557-562.
- MRAVEC, J., KUBEŠ, M., BIELACH, A., GAYKOVA, V., PETRÁŠEK, J., SKŮPA, P., CHAND, S., BENKOVÁ, E., ZAŽÍMALOVÁ, E. & FRIML, J. 2008. Interaction of PIN and PGP transport mechanisms in auxin distribution-dependent development. *Development*, 135, 3345-3354.
- MRAVEC, J., SKUPA, P., BAILLY, A., HOYEROVA, K., KRECEK, P., BIELACH, A., PETRASEK, J., ZHANG, J., GAYKOVA, V., STIERHOF, Y.-D., DOBREV, P. I., SCHWARZEROVA, K., ROLCIK, J., SEIFERTOVA, D., LUSCHNIG, C., BENKOVA, E., ZAZIMALOVA, E., GEISLER, M. & FRIML, J. 2009. Subcellular homeostasis of phytohormone auxin is mediated by the ER-localized PIN5 transporter. *Nature*, 459, 1136-1140.
- MULLER, M. & MUNNE-BOSCH, S. 2011. Rapid and sensitive hormonal profiling of complex plant samples by liquid chromatography coupled to electrospray ionization tandem mass spectrometry. *Plant Methods*, 7, 37.
- MURAKAMI, Y., MIWA, H., IMAIZUMI-ANRAKU, H., KOUCHI, H., DOWNIE, J. A., KAWAGUCHI, M. & KAWASAKI, S. 2007. Positional Cloning Identifies *Lotus japonicus* NSP2, A Putative Transcription Factor of the GRAS Family, Required for NIN and ENOD40 Gene Expression in Nodule Initiation. *DNA Research*, 13, 255-265.
- MURPHY, A., PEER, W. & TAI, L. 2000. Regulation of auxin transport by aminopeptidases and endogenous flavonoids. *Planta*, 211, 315-324.

- MURPHY, A. S., HOOGNER, K. R., PEER, W. A. & TAIZ, L. 2002. Identification, Purification, and Molecular Cloning of N-1-Naphthylphthalamic Acid-Binding Plasma Membrane-Associated Aminopeptidases from Arabidopsis. *Plant Physiology*, 128, 935-950.
- MURRAY, J. D., KARAS, B. J., SATO, S., TABATA, S., AMYOT, L. & SZCZYGLOWSKI, K. 2007. A Cytokinin Perception Mutant Colonized by Rhizobium in the Absence of Nodule Organogenesis. *Science*, 315, 101-104.
- NAKAMURA, A., HIGUCHI, K., GODA, H., FUJIWARA, M. T., SAWA, S., KOSHIBA, T., SHIMADA, Y. & YOSHIDA, S. 2003. Brassinolide Induces IAA5, IAA19, and DR5, a Synthetic Auxin Response Element in Arabidopsis, Implying a Cross Talk Point of Brassinosteroid and Auxin Signaling. *Plant Physiology*, 133, 1843-1853.
- NAPIER, R., DAVID, K. & PERROT-RECHENMANN, C. 2002. A short history of auxin-binding proteins. *Plant Molecular Biology*, 49, 339-348.
- NISHIO, S., MORIGUCHI, R., IKEDA, H., TAKAHASHI, H., TAKAHASHI, H., FUJII, N., GUILFOYLE, T., KANAHAMA, K. & KANAYAMA, Y. 2010. Expression analysis of the auxin efflux carrier family in tomato fruit development. *Planta*, 232, 755-764.
- NOH, B., MURPHY, A. S. & SPALDING, E. P. 2001. Multidrug Resistance-like Genes of Arabidopsis Required for Auxin Transport and Auxin-Mediated Development. *The Plant Cell Online*, 13, 2441-2454.
- NORDSTRÖM, A., TARKOWSKI, P., TARKOWSKA, D., NORBAEK, R., ÅSTOT, C., DOLEZAL, K. & SANDBERG, G. 2004. Auxin regulation of cytokinin biosynthesis in *Arabidopsis thaliana*: A factor of potential importance for auxin-cytokinin-regulated development. *Proceedings of the National Academy of Sciences of the United States of America*, 101, 8039-8044.
- NORMANLY, J., COHEN, J. D. & FINK, G. R. 1993. *Arabidopsis thaliana* auxotrophs reveal a tryptophan-independent biosynthetic pathway for indole-3-acetic acid. *Proc Natl Acad Sci U S A.*, 90, 10355-10359.
- NOVÁK, O., HĚNYKOVÁ, E., SAIRANEN, I., KOWALCZYK, M., POSPÍŠIL, T. & LJUNG, K. 2012. Tissue-specific profiling of the *Arabidopsis thaliana* auxin metabolome. *The Plant Journal*, 72, 523-536.

- NOVÁK, O., TARKOWSKI, P., TARKOWSKÁ, D., DOLEŽAL, K., LENOBEL, R. & STRNAD, M. 2003. Quantitative analysis of cytokinins in plants by liquid chromatography–single-quadrupole mass spectrometry. *Analytica Chimica Acta*, 480, 207-218.
- OLDROYD, G. E. D. & DIXON, R. 2014. Biotechnological solutions to the nitrogen problem. *Current Opinion in Biotechnology*, 26, 19-24.
- OLDROYD, G. E. D. & DOWNIE, J. A. 2008. Coordinating Nodule Morphogenesis with Rhizobial Infection in Legumes. *Annual Review of Plant Biology*, 59, 519-546.
- OLDROYD, G. E. D. & LONG, S. R. 2003. Identification and Characterization of Nodulation-Signaling Pathway 2, a Gene of *Medicago truncatula* Involved in Nod Factor Signaling. *Plant Physiology*, 131, 1027-1032.
- OLDROYD, G. E. D., MURRAY, J., POOLE, P. S. & DOWNIE, A. 2013. Speak, friend, and enter: signalling systems that promote beneficial symbiotic associations in plants. *Nat Rev Micro*, 11, 252-263.
- OLDROYD, G. E. D., MURRAY, J. D., POOLE, P. S. & DOWNIE, J. A. 2011. The Rules of Engagement in the Legume-Rhizobial Symbiosis. *Annual Review of Genetics*, 45, 119-144.
- ORR, C. H., JAMES, A., LEIFERT, C., COOPER, J. M. & CUMMINGS, S. P. 2011. Diversity and Activity of Free-Living Nitrogen-Fixing Bacteria and Total Bacteria in Organic and Conventionally Managed Soils. *Applied and Environmental Microbiology*, 77, 911-919.
- ÖSTIN, A., CATALÁ, C., CHAMARRO, J. & SANDBERG, G. 1995. Identification of glucopyranosyl- β -1,4-glucopyranosyl- β -1-N-oxindole-3-acetyl-N-aspartic acid, a new IAA catabolite, by liquid chromatography/tandem mass spectrometry. *Journal of Mass Spectrometry*, 30, 1007-1017.
- ÖSTIN, A., ILIĆ, N. & COHEN, J. D. 1999. An in Vitro System from Maize Seedlings for Tryptophan-Independent Indole-3-Acetic Acid Biosynthesis. *Plant Physiology*, 119, 173-178.
- OUYANG, J., SHAO, X. & LI, J. 2000. Indole-3-glycerol phosphate, a branchpoint of indole-3-acetic acid biosynthesis from the tryptophan biosynthetic pathway in *Arabidopsis thaliana*. *The Plant Journal*, 24, 327-334.
- OVERVOORDE, P., FUKAKI, H. & BEECKMAN, T. 2010. Auxin Control of Root Development. *Cold Spring Harbor Perspectives in Biology*, 2.

- PACIOS-BRAS, C., SCHLAMMAN, H. M., BOOT, K., ADMIRAAL, P., MATEOS LANGERAK, J., STOUGAARD, J. & SPAINK, H. 2003. Auxin distribution in *Lotus japonicus* during root nodule development. *Plant Molecular Biology*, 52, 1169-1180.
- PAIGE, J. S., NGUYEN-DUC, T., SONG, W. & JAFFREY, S. R. 2012. Fluorescence Imaging of Cellular Metabolites with RNA. *Science*, 335, 1194.
- PAN, X. & WANG, X. 2009. Profiling of plant hormones by mass spectrometry. *Journal of Chromatography B*, 877, 2806-2813.
- PAN, X., WELTI, R. & WANG, X. 2010. Quantitative analysis of major plant hormones in crude plant extracts by high-performance liquid chromatography-mass spectrometry. *Nat. Protocols*, 5, 986-992.
- PARK, S., COHEN, J. & SLOVIN, J. 2006. Strawberry fruit protein with a novel indole-acyl modification. *Planta*, 224, 1015-1022.
- PARRY, G., CALDERON-VILLALOBOS, L. I., PRIGGE, M., PERET, B., DHARMASIRI, S., ITOH, H., LECHNER, E., GRAY, W. M., BENNETT, M. & ESTELLE, M. 2009. Complex regulation of the TIR1/AFB family of auxin receptors. *Proceedings of the National Academy of Sciences*, 106, 22540-22545.
- PARRY, G., MARCHANT, A., MAY, S., SWARUP, R., SWARUP, K., JAMES, N., GRAHAM, N., ALLEN, T., MARTUCCI, T., YEMM, A., NAPIER, R., MANNING, K., KING, G. & BENNETT, M. 2001. Quick on the uptake: characterization of a family of plant auxin influx carriers. *Journal of Plant Growth Regulation*, 20, 217-225.
- PATTISON, R. J. & CATALÁ, C. 2012. Evaluating auxin distribution in tomato (*Solanum lycopersicum*) through an analysis of the PIN and AUX/LAX gene families. *The Plant Journal*, 70, 585-598.
- PAWLOWSKI, K. & DEMCHENKO, K. 2012. The diversity of actinorhizal symbiosis. *Protoplasma*, 249, 967-979.
- PEAT, T. S., BÖTTCHER, C., NEWMAN, J., LUCENT, D., COWIESON, N. & DAVIES, C. 2012. Crystal Structure of an Indole-3-Acetic Acid Amido Synthetase from Grapevine Involved in Auxin Homeostasis. *The Plant Cell Online*, 24, 4525-4538.
- PEER, W. A. 2013. From perception to attenuation: auxin signalling and responses. *Current Opinion in Plant Biology*, 16, 561-568.

- PEER, W. A., BANDYOPADHYAY, A., BLAKESLEE, J. J., MAKAM, S. N., CHEN, R. J., MASSON, P. H. & MURPHY, A. S. 2004. Variation in Expression and Protein Localization of the PIN Family of Auxin Efflux Facilitator Proteins in Flavonoid Mutants with Altered Auxin Transport in *Arabidopsis thaliana*. *Plant Cell*, 16, 1898-1911.
- PEER, W. A., BLAKESLEE, J. J., YANG, H. & MURPHY, A. S. 2011. Seven Things We Think We Know about Auxin Transport. *Molecular Plant*, 4, 487-504.
- PEER, W. A., BROWN, D. E., TAGUE, B. W., MUDAY, G. K., TAIZ, L. & MURPHY, A. S. 2001. Flavonoid Accumulation Patterns of *Transparent Testa* Mutants of *Arabidopsis*. *Plant Physiol.*, 126, 536-548.
- PEER, W. A., CHENG, Y. & MURPHY, A. S. 2013. Evidence of oxidative attenuation of auxin signalling. *Journal of Experimental Botany*, 64, 2629-2639.
- PEER, W. A. & MURPHY, A. S. 2007. Flavonoids and auxin transport: modulators or regulators? *Trends in Plant Science*, 12, 556-563.
- PÉRET, B., DE RYBEL, B., CASIMIRO, I., BENKOVÁ, E., SWARUP, R., LAPLAZE, L., BEECKMAN, T. & BENNETT, M. J. 2009. Arabidopsis lateral root development: an emerging story. *Trends in Plant Science*, 14, 399-408.
- PÉRET, B., SWARUP, R., JANSEN, L., DEVOS, G., AUGUY, F., COLLIN, M., SANTI, C., HOCHER, V., FRANCHE, C., BOGUSZ, D., BENNETT, M. & LAPLAZE, L. 2007. Auxin Influx Activity Is Associated with Frankia Infection during Actinorhizal Nodule Formation in *Casuarina glauca*. *Plant Physiology*, 144, 1852-1862.
- PERNISOVÁ, M., KLÍMA, P., HORÁK, J., VÁLKOVÁ, M., MALBECK, J., SOUČEK, P., REICHMAN, P., HOYEROVÁ, K., DUBOVÁ, J., FRIML, J., ZA, ŽÍMALOVÁ, E. & HEJÁTKO, J. 2009. Cytokinins modulate auxin-induced organogenesis in plants via regulation of the auxin efflux. *Proceedings of the National Academy of Sciences*, 106, 3609-3614.
- PERRINE-WALKER, F., DOUMAS, P., LUCAS, M., VAISSAYRE, V., BEAUCHEMIN, N. J., BAND, L. R., CHOPARD, J., CRABOS, A., CONEJERO, G., PÉRET, B., KING, J. R., VERDEIL, J.-L., HOCHER, V., FRANCHE, C., BENNETT, M. J., TISA, L. S. & LAPLAZE, L. 2010. Auxin Carriers Localization Drives Auxin Accumulation in Plant Cells Infected by Frankia in *Casuarina glauca* Actinorhizal Nodules. *Plant Physiology*, 154, 1372-1380.

- PETERSSON, S. V., JOHANSSON, A. I., KOWALCZYK, M., MAKOVEYCHUK, A., WANG, J. Y., MORITZ, T., GREBE, M., BENFEY, P. N., SANDBERG, G. & LJUNG, K. 2009. An Auxin Gradient and Maximum in the Arabidopsis Root Apex Shown by High-Resolution Cell-Specific Analysis of IAA Distribution and Synthesis. *The Plant Cell Online*, 21, 1659-1668.
- PETRASEK, J., CERNA, A., SCHWARZEROVA, K., ELCKNER, M., MORRIS, D. A. & ZAZIMALOVA, E. 2003. Do Phytotropins Inhibit Auxin Efflux by Impairing Vesicle Traffic? *Plant Physiol*, 131, 254-263.
- PETRAŠEK, J. & FRIML, J. 2009. Auxin transport routes in plant development. *Development*, 136, 2675-2688.
- PETRASEK, J., MRAVEC, J., BOUCHARD, R., BLAKESLEE, J. J., ABAS, M., SEIFERTOVA, D., WISNIEWSKA, J., TADELE, Z., KUBES, M., COVANOVA, M., DHONUKSHE, P., SKUPA, P., BENKOVA, E., PERRY, L., KRECEK, P., LEE, O. R., FINK, G. R., GEISLER, M., MURPHY, A. S., LUSCHNIG, C., ZAZIMALOVA, E. & FRIML, J. 2006. PIN Proteins Perform a Rate-Limiting Function in Cellular Auxin Efflux. *Science*, 312, 914-918.
- PFAFFL, M. W. 2001. A new mathematical model for relative quantification in real-time RT-PCR.
- PIETRASZEWSKA-BOGIEL, A., LEFEBVRE, B., KOINI, M. A., KLAUS-HEISEN, D., TAKKEN, F. L. W., GEURTS, R., CULLIMORE, J. V. & GADELLA, T. W. J. 2013. Interaction of *Medicago truncatula* Lysin Motif Receptor-Like Kinases, NFP and LYK3, Produced in *Nicotiana benthamiana* Induces Defence-Like Responses. *PLoS ONE*, 8, e65055.
- PII, Y., CRIMI, M., CREMONESE, G., SPENA, A. & PANDOLFINI, T. 2007. Auxin and nitric oxide control indeterminate nodule formation. *BMC Plant Biology*, 7, 21.
- PLET, J., WASSON, A., ARIEL, F., LE SIGNOR, C., BAKER, D., MATHESIUS, U., CRESPI, M. & FRUGIER, F. 2011. MtCRE1-dependent cytokinin signaling integrates bacterial and plant cues to coordinate symbiotic nodule organogenesis in *Medicago truncatula*. *The Plant Journal*, 65, 622-633.
- PRAYITNO, J., ROLFE, B. G. & MATHESIUS, U. 2006. The Ethylene-Insensitive sickle Mutant of *Medicago truncatula* Shows Altered Auxin Transport Regulation during Nodulation. *Plant Physiology*, 142, 168-180.

- QUITTENDEN, L. J., DAVIES, N. W., SMITH, J. A., MOLESWORTH, P. P., TIVENDALE, N. D. & ROSS, J. J. 2009. Auxin Biosynthesis in Pea: Characterization of the Tryptamine Pathway. *Plant Physiology*, 151, 1130-1138.
- RADUTOIU, S., MADSEN, L. H., MADSEN, E. B., FELLE, H. H., UMEHARA, Y., GRONLUND, M., SATO, S., NAKAMURA, Y., TABATA, S., SANDAL, N. & STOUGAARD, J. 2003. Plant recognition of symbiotic bacteria requires two LysM receptor-like kinases. *Nature*, 425, 585-592.
- RADUTOIU, S., MADSEN, L. H., MADSEN, E. B., JURKIEWICZ, A., FUKAI, E., QUISTGAARD, E. M. H., ALBREKTSEN, A. S., JAMES, E. K., THIRUP, S. & STOUGAARD, J. 2007. LysM domains mediate lipochitin-oligosaccharide recognition and Nfr genes extend the symbiotic host range. *EMBO J*, 26, 3923-3935.
- RAMPEY, R. A., LECLERE, S., KOWALCZYK, M., LJUNG, K., SANDBERG, G. & BARTEL, B. 2004. A Family of Auxin-Conjugate Hydrolases That Contributes to Free Indole-3-Acetic Acid Levels during Arabidopsis Germination. *Plant Physiology*, 135, 978-988.
- RANOCHA, P., DIMA, O., NAGY, R., FELTEN, J., CORRATGÉ-FAILLIE, C., NOVÁK, O., MORREEL, K., LACOMBE, B., MARTINEZ, Y., PFRUNDER, S., JIN, X., RENOU, J.-P., THIBAUD, J.-B., LJUNG, K., FISCHER, U., MARTINOIA, E., BOERJAN, W. & GOFFNER, D. 2013. Arabidopsis WAT1 is a vacuolar auxin transport facilitator required for auxin homeostasis. *Nat Commun*, 4.
- RASHOTTE, A. M., BRADY, S. R., REED, R. C., ANTE, S. J. & MUDAY, G. K. 2000. Basipetal Auxin Transport Is Required for Gravitropism in Roots of Arabidopsis. *Plant Physiology*, 122, 481-490.
- REDDY, S. M., HITCHIN, S., MELAYAH, D., PANDEY, A. K., RAFFIER, C., HENDERSON, J., MARMEISSE, R. & GAY, G. 2006. The auxin-inducible GH3 homologue Pp-GH3.16 is downregulated in *Pinus pinaster* root systems on ectomycorrhizal symbiosis establishment. *New Phytologist*, 170, 391-400.
- REY, T., NARS, A., BONHOMME, M., BOTTIN, A., HUGUET, S., BALZERGUE, S., JARDINAUD, M.-F., BONO, J.-J., CULLIMORE, J., DUMAS, B., GOUGH, C. & JACQUET, C. 2013. NFP, a LysM protein controlling Nod factor perception, also intervenes in *Medicago truncatula* resistance to pathogens. *New Phytologist*, 198, 875-886.

- RIBNICKY, D. M., COOKE, T. J. & COHEN, J. D. 1997. A microtechnique for the analysis of free and conjugated indole-3-acetic acid in milligram amounts of plant tissue using a benchtop gas chromatograph-mass spectrometer. *Planta*, 204, 1-7.
- RIGHTMYER, A. P. & LONG, S. R. 2011. Pseudonodule Formation by Wild-Type and Symbiotic Mutant *Medicago truncatula* in Response to Auxin Transport Inhibitors. *Molecular Plant-Microbe Interactions*, 24, 1372-1384.
- RÍPODAS, C., VIA, V. D., AGUILAR, O. M., ZANETTI, M. E. & BLANCO, F. A. 2013. Knock-down of a member of the isoflavone reductase gene family impairs plant growth and nodulation in *Phaseolus vulgaris*. *Plant Physiology and Biochemistry*, 68, 81-89.
- RODRIGUEZ-BARRUECO, C. & DE CASTRO, F. B. 1973. Cytokinin-induced Pseudonodules on *Alnus glutinosa*. *Physiologia Plantarum*, 29, 277-280.
- ROLFE, B. G. & GRESSHOFF, P. M. 1988. Genetic analysis of legume nodule initiation. *Annual Review of Plant Physiology and Plant Molecular Biology*, 39, 297-319.
- ROUTABOUL, J.-M., KERHOAS, L., DEBEAUJON, I., POURCEL, L., CABOCHE, M., EINHORN, J. & LEPINIEC, L. 2006. Flavonoid diversity and biosynthesis in seed of *Arabidopsis thaliana*. *Planta*, 224, 96-107.
- RŮŽIČKA, K., ŠIMÁŠKOVÁ, M., DUCLERCQ, J., PETRÁŠEK, J., ZAŽÍMALOVÁ, E., SIMON, S., FRIML, J., VAN MONTAGU, M. C. E. & BENKOVÁ, E. 2009. Cytokinin regulates root meristem activity via modulation of the polar auxin transport. *Proceedings of the National Academy of Sciences*, 106, 4284-4289.
- SABATINI, S., BEIS, D., WOLKENFELT, H., MURFETT, J., GUILFOYLE, T., MALAMY, J., BENFEY, P., LEYSER, O., BECHTOLD, N., WEISBEEK, P. & SCHERES, B. 1999. An Auxin-Dependent Distal Organizer of Pattern and Polarity in the Arabidopsis Root. *Cell*, 99, 463-472.
- SANTELIA, D., HENRICH, S., VINCENZETTI, V., SAUER, M., BIGLER, L., KLEIN, M., BAILLY, A., LEE, Y., FRIML, J. Í., GEISLER, M. & MARTINOIA, E. 2008. Flavonoids Redirect PIN-mediated Polar Auxin Fluxes during Root Gravitropic Responses. *Journal of Biological Chemistry*, 283, 31218-31226.
- SANTELIA, D., VINCENZETTI, V., AZZARELLO, E., BOVET, L., FUKAO, Y., DÜCHTIG, P., MANCUSO, S., MARTINOIA, E. & GEISLER, M. 2005. MDR-like ABC transporter AtPGP4 is involved in auxin-mediated lateral root and root hair development. *FEBS Letters*, 579, 5399-5406.

- SANTI, C., BOGUSZ, D. & FRANCHE, C. 2013. Biological nitrogen fixation in non-legume plants. *Annals of Botany*.
- SANTNER, A. A. & WATSON, J. C. 2006. The WAG1 and WAG2 protein kinases negatively regulate root waving in Arabidopsis. *The Plant Journal*, 45, 752-764.
- SASAKI, T., SUZAKI, T., SOYANO, T., KOJIMA, M., SAKAKIBARA, H. & KAWAGUCHI, M. 2014. Shoot-derived cytokinins systemically regulate root nodulation. *Nat Commun*, 5.
- SASSI, M., LU, Y., ZHANG, Y., WANG, J., DHONUKSHE, P., BLILOU, I., DAI, M., LI, J., GONG, X., JAILLAIS, Y., YU, X., TRAAS, J., RUBERTI, I., WANG, H., SCHERES, B., VERNOUX, T. & XU, J. 2012. COP1 mediates the coordination of root and shoot growth by light through modulation of PIN1- and PIN2-dependent auxin transport in Arabidopsis. *Development*, 139, 3402-3412.
- SAUER, M., ROBERT, S. & KLEINE-VEHN, J. 2013. Auxin: simply complicated. *Journal of Experimental Botany*.
- SCHAUSER, L., WIELOCH, W. & STOUGAARD, J. 2005. Evolution of NIN-Like Proteins in Arabidopsis, Rice, and *Lotus japonicus*. *Journal of Molecular Evolution*, 60, 229-237.
- SCHERES, B., MCKHANN, H. I., ZALENSKY, A., LOBLER, M., BISSELING, T. & HIRSCH, A. M. 1992. The PsENOD12 Gene Is Expressed at Two Different Sites in Afghanistan Pea Pseudonodules Induced by Auxin Transport Inhibitors. *Plant Physiol*, 100, 1649-1655.
- SCHMELZ, E. A., ENGELBERTH, J., TUMLINSON, J. H., BLOCK, A. & ALBORN, H. T. 2004. The use of vapor phase extraction in metabolic profiling of phytohormones and other metabolites. *The Plant Journal*, 39, 790-808.
- SCHMITZ, R., KLOPPROGGE, K. & GRABBE, R. 2002. Regulation of nitrogen fixation in *Klebsiella pneumoniae* and *Azotobacter vinelandii*: NifL, transducing two environmental signals to the nif transcriptional activator NifA. *J Mol Microbiol Biotechnol.*, 4, 235-242.
- SCHNABEL, E. L. & FRUGOLI, J. 2004. The PIN and LAX families of auxin transport genes in *Medicago truncatula*. *Molecular Genetics and Genomics*, 272, 420-432.
- SCHNEIDER, E. A., KAZAKOFF, C. W. & WIGHTMAN, F. 1985. Gas chromatography-mass spectrometry evidence for several endogenous auxins in pea seedling organs. *Planta*, 165, 232-241.

- SEO, M., AKABA, S., ORITANI, T., DELARUE, M., BELLINI, C., CABOCHE, M. & KOSHIBA, T. 1998. Higher Activity of an Aldehyde Oxidase in the Auxin-Overproducing *superroot1* Mutant of *Arabidopsis thaliana*. *Plant Physiology*, 116, 687-693.
- SHIMIZU-MITAO, Y. & KAKIMOTO, T. 2014. Auxin Sensitivities of All Arabidopsis Aux/IAAs for Degradation in the Presence of Every TIR1/AFB. *Plant and Cell Physiology*, 55, 1450-1459.
- SIEMENS, J., KELLER, I., SARX, J., KUNZ, S., SCHULLER, A., NAGEL, W., SCHMÜLLING, T., PARNISKE, M. & LUDWIG-MÜLLER, J. 2006. Transcriptome Analysis of Arabidopsis Clubroots Indicate a Key Role for Cytokinins in Disease Development. *Molecular Plant-Microbe Interactions*, 19, 480-494.
- SINGH, S., KATZER, K., LAMBERT, J., CERRI, M. & PARNISKE, M. 2014. CYCLOPS, A DNA-Binding Transcriptional Activator, Orchestrates Symbiotic Root Nodule Development. *Cell host and microbe*, 15, 139-152.
- SLININGER, P. J., BURKHEAD, K. D. & SCHISLER, D. A. 2004. Antifungal and sprout regulatory bioactivities of phenylacetic acid, indole-3-acetic acid, and tyrosol isolated from the potato dry rot suppressive bacterium *Enterobacter cloacae* S11:T:07. *Journal of Industrial Microbiology and Biotechnology*, 31, 517-524.
- SMIT, P., RAEDTS, J., PORTYANKO, V., DEBELLÉ, F., GOUGH, C., BISSELING, T. & GEURTS, R. 2005. NSP1 of the GRAS Protein Family Is Essential for Rhizobial Nod Factor-Induced Transcription. *Science*, 308, 1789-1791.
- SOMERS, E., PTACEK, D., GYSEGOM, P., SRINIVASAN, M. & VANDERLEYDEN, J. 2005. *Azospirillum brasilense* Produces the Auxin-Like Phenylacetic Acid by Using the Key Enzyme for Indole-3-Acetic Acid Biosynthesis. *Applied and Environmental Microbiology*, 71, 1803-1810.
- SOYANO, T., KOUCHI, H., HIROTA, A. & HAYASHI, M. 2013. NODULE INCEPTION Directly Targets NF-Y Subunit Genes to Regulate Essential Processes of Root Nodule Development in *Lotus japonicus*. *PLoS Genet*, 9, e1003352.
- SPAEPEN, S. & VANDERLEYDEN, J. 2010. Auxin and Plant-Microbe Interactions. *Cold Spring Harbor Perspectives in Biology*.
- STACEY, G., LIBAULT, M., BRECHENMACHER, L., WAN, J. & MAY, G. D. 2006. Genetics and functional genomics of legume nodulation. *Current Opinion in Plant Biology*, 9, 110-121.

- STASWICK, P. E. 2009. The Tryptophan Conjugates of Jasmonic and Indole-3-Acetic Acids Are Endogenous Auxin Inhibitors. *Plant Physiology*, 150, 1310-1321.
- STENLID, G. 1976. Effects of Flavonoids on the Polar Transport of Auxins. *Physiologia Plantarum*, 38, 262-266.
- STEPANOVA, A. N., ROBERTSON-HOYT, J., YUN, J., BENAVENTE, L. M., XIE, D.-Y., DOLEŽAL, K., SCHLERETH, A., JÜRGENS, G. & ALONSO, J. M. 2008. TAA1-Mediated Auxin Biosynthesis Is Essential for Hormone Crosstalk and Plant Development. *Cell*, 133, 177-191.
- STEPANOVA, A. N., YUN, J., LIKHACHEVA, A. V. & ALONSO, J. M. 2007. Multilevel Interactions between Ethylene and Auxin in Arabidopsis Roots. *The Plant Cell*, 19, 2169-2185.
- STEPANOVA, A. N., YUN, J., ROBLES, L. M., NOVAK, O., HE, W., GUO, H., LJUNG, K. & ALONSO, J. M. 2011. The Arabidopsis YUCCA1 Flavin Monooxygenase Functions in the Indole-3-Pyruvic Acid Branch of Auxin Biosynthesis. *The Plant Cell Online*, 23, 3961-3973.
- STRADER, L. C. & BARTEL, B. 2011. Transport and Metabolism of the Endogenous Auxin Precursor Indole-3-Butyric Acid. *Molecular Plant*.
- SU, Y.-H., LIU, Y.-B. & ZHANG, X.-S. 2011. Auxin-Cytokinin Interaction Regulates Meristem Development. *Molecular Plant*, 4, 616-625.
- SUBRAMANIAN, S., STACEY, G. & YU, O. 2006. Endogenous isoflavones are essential for the establishment of symbiosis between soybean and *Bradyrhizobium japonicum*. *The Plant Journal*, 48, 261-273.
- SUGAWARA, S., HISHIYAMA, S., JIKUMARU, Y., HANADA, A., NISHIMURA, T., KOSHIBA, T., ZHAO, Y., KAMIYA, Y. & KASAHARA, H. 2009. Biochemical analyses of indole-3-acetaldoxime-dependent auxin biosynthesis in Arabidopsis. *Proceedings of the National Academy of Sciences*, 106, 5430-5435.
- SUKUMAR, P., EDWARDS, K. S., RAHMAN, A., DELONG, A. & MUDAY, G. K. 2009. PINOID Kinase Regulates Root Gravitropism through Modulation of PIN2-Dependent Basipetal Auxin Transport in Arabidopsis. *Plant Physiology*, 150, 722-735.
- SUZAKI, T., ITO, M. & KAWAGUCHI, M. 2013. Genetic basis of cytokinin and auxin functions during root nodule development. *Frontiers in Plant Science*, 4.

- SUZAKI, T., ITO, M. & KAWAGUCHI, M. 2013. Induction of localized auxin response during spontaneous nodule development in *Lotus japonicus*. *Plant Signaling and Behavior*, 8, e23359.
- SUZAKI, T., YANO, K., ITO, M., UMEHARA, Y., SUGANUMA, N. & KAWAGUCHI, M. 2012. Positive and negative regulation of cortical cell division during root nodule development in *Lotus japonicus* is accompanied by auxin response. *Development*, 139, 3997-4006.
- SVEC, F. 2010. Porous polymer monoliths: Amazingly wide variety of techniques enabling their preparation. *Journal of Chromatography A*, 1217, 902-924.
- SWARUP, K., BENKOVA, E., SWARUP, R., CASIMIRO, I., PERET, B., YANG, Y., PARRY, G., NIELSEN, E., DE SMET, I., VANNESTE, S., LEVESQUE, M. P., CARRIER, D., JAMES, N., CALVO, V., LJUNG, K., KRAMER, E., ROBERTS, R., GRAHAM, N., MARILLONNET, S., PATEL, K., JONES, J. D. G., TAYLOR, C. G., SCHACHTMAN, D. P., MAY, S., SANDBERG, G., BENFEY, P., FRIML, J., KERR, I., BEECKMAN, T., LAPLAZE, L. & BENNETT, M. J. 2008. The auxin influx carrier LAX3 promotes lateral root emergence. *Nat Cell Biol*, 10, 946-954.
- SWARUP, R., FRIML, J., MARCHANT, A., LJUNG, K., SANDBERG, G., PALME, K. & BENNETT, M. 2001. Localization of the auxin permease AUX1 suggests two functionally distinct hormone transport pathways operate in the Arabidopsis root apex. *Genes & Development*, 15, 2648-2653.
- SWARUP, R., KARGUL, J., MARCHANT, A., ZADIK, D., RAHMAN, A., MILLS, R., YEMM, A., MAY, S., WILLIAMS, L., MILLNER, P., TSURUMI, S., MOORE, I., NAPIER, R., KERR, I. D. & BENNETT, M. J. 2004. Structure-Function Analysis of the Presumptive Arabidopsis Auxin Permease AUX1. *The Plant Cell Online*, 16, 3069-3083.
- SZABÓ, K., BAKOS, É., WELKER, E., MÜLLER, M., GOODFELLOW, H. R., HIGGINS, C. F., VÁRADI, A. & SARKADI, B. 1997. Phosphorylation Site Mutations in the Human Multidrug Transporter Modulate Its Drug-stimulated ATPase Activity. *Journal of Biological Chemistry*, 272, 23165-23171.
- TAKANASHI, K., SUGIYAMA, A., SATO, S., TABATA, S. & YAZAKI, K. 2012. LjABCBI, an ATP-binding cassette protein specifically induced in uninfected cells of *Lotus japonicus* nodules. *Journal of Plant Physiology*, 169, 322-326.
- TAKANASHI, K., SUGIYAMA, A. & YAZAKI, K. 2011. Involvement of auxin distribution in root nodule development of *Lotus japonicus*. *Planta*, 234, 73-81.

- TAM, Y. Y., EPSTEIN, E. & NORMANLY, J. 2000. Characterization of Auxin Conjugates in Arabidopsis. Low Steady-State Levels of Indole-3-Acetyl-Aspartate, Indole-3-Acetyl-Glutamate, and Indole-3-Acetyl-Glucose. *Plant Physiology*, 123, 589-596.
- TAN, X., CALDERON-VILLALOBOS, L. I. A., SHARON, M., ZHENG, C., ROBINSON, C. V., ESTELLE, M. & ZHENG, N. 2007. Mechanism of auxin perception by the TIR1 ubiquitin ligase. *Nature*, 446, 640-645.
- TANSENGCO, M., HAYASHI, M., KAWAGUCHI, M., IMAIZUMI-ANRAKU, H. & YOSHIKATSU, M. 2003. crinkle, a Novel Symbiotic Mutant That Affects the Infection Thread Growth and Alters the Root Hair, Trichome, and Seed Development in *Lotus japonicus*. *Plant Physiol*, 131, 1054-1063.
- TAO, Y., FERRER, J.-L., LJUNG, K., POJER, F., HONG, F., LONG, J. A., LI, L., MORENO, J. E., BOWMAN, M. E., IVANS, L. J., CHENG, Y., LIM, J., ZHAO, Y., BALLARÉ, C. L., SANDBERG, G., NOEL, J. P. & CHORY, J. 2008. Rapid Synthesis of Auxin via a New Tryptophan-Dependent Pathway Is Required for Shade Avoidance in Plants. *Cell*, 133, 164-176.
- TERASAKA, K., BLAKESLEE, J. J., TITAPIWATANAKUN, B., PEER, W. A., BANDYOPADHYAY, A., MAKAM, S. N., LEE, O. R., RICHARDS, E. L., MURPHY, A. S., SATO, F. & YAZAKI, K. 2005. PGP4, an ATP Binding Cassette P-Glycoprotein, Catalyzes Auxin Transport in *Arabidopsis thaliana* Roots. *Plant Cell*, 17, 2922-2939.
- TIAN, H., KLÄMBT, D. & JONES, A. M. 1995. Auxin-binding Protein 1 Does Not Bind Auxin within the Endoplasmic Reticulum Despite This Being the Predominant Subcellular Location for This Hormone Receptor *Journal of Biological Chemistry*, 270, 26962-26969.
- TIAN, Q., NAGPAL, P. & REED, J. W. 2003. Regulation of Arabidopsis SHY2/IAA3 protein turnover. *The Plant Journal*, 36, 643-651.
- TIRICHINE, L., IMAIZUMI-ANRAKU, H., YOSHIDA, S., MURAKAMI, Y., MADSEN, L. H., MIWA, H., NAKAGAWA, T., SANDAL, N., ALBREKTSSEN, A. S., KAWAGUCHI, M., DOWNIE, A., SATO, S., TABATA, S., KOUCHI, H., PARNISKE, M., KAWASAKI, S. & STOUGAARD, J. 2006. Dereglulation of a Ca²⁺/calmodulin-dependent kinase leads to spontaneous nodule development. *Nature*, 441, 1153-1156.

- TIRICHINE, L., SANDAL, N., MADSEN, L. H., RADUTOIU, S., ALBREKTSSEN, A. S., SATO, S., ASAMIZU, E., TABATA, S. & STOUGAARD, J. 2007. A Gain-of-Function Mutation in a Cytokinin Receptor Triggers Spontaneous Root Nodule Organogenesis. *Science*, 315, 104-107.
- TITAPIWATANAKUN, B., BLAKESLEE, J. J., BANDYOPADHYAY, A., YANG, H., MRAVEC, J., SAUER, M., CHENG, Y., ADAMEC, J., NAGASHIMA, A., GEISLER, M., SAKAI, T., FRIML, J., PEER, W. A. & MURPHY, A. S. 2009. ABCB19/PGP19 stabilises PIN1 in membrane microdomains in Arabidopsis. *The Plant Journal*, 57, 27-44.
- TIVENDALE, N. D., DAVIES, N. W., MOLESWORTH, P. P., DAVIDSON, S. E., SMITH, J. A., LOWE, E. K., REID, J. B. & ROSS, J. J. 2010. Reassessing the Role of N-Hydroxytryptamine in Auxin Biosynthesis. *Plant Physiology*, 154, 1957-1965.
- TIVENDALE, N. D., ROSS, J. J. & COHEN, J. D. 2014. The shifting paradigms of auxin biosynthesis. *Trends in Plant Science*, 19, 44-51.
- TRUCHET, G., ROCHE, P., LEROUGE, P., VASSE, J., CAMUT, S., DE BILLY, F., PROME, J.-C. & DENARIE, J. 1991. Sulphated lipo-oligosaccharide signals of *Rhizobium meliloti* elicit root nodule organogenesis in alfalfa. *Nature*, 351, 670-673.
- TURNER, M., NIZAMPATNAM, N. R., BARON, M., COPPIN, S., DAMODARAN, S., ADHIKARI, S., ARUNACHALAM, S. P., YU, O. & SUBRAMANIAN, S. 2013. Ectopic Expression of miR160 Results in Auxin Hypersensitivity, Cytokinin Hyposensitivity, and Inhibition of Symbiotic Nodule Development in Soybean. *Plant Physiology*, 162, 2042-2055.
- UDVARDI, M. K., CZECHOWSKI, T. & SCHEIBLE, W.-R. 2008. Eleven Golden Rules of Quantitative RT-PCR. *Plant Cell*, 20, 1736-1737.
- UEDA, J., TODA, Y., KATO, K., KURODA, Y., ARAI, T., HASEGAWA, T., SHIGEMORI, H., HASEGAWA, K., KITAGAWA, J., MIYAMOTO, K. & UHEDA, E. 2013. Identification of dehydrocostus lactone and 4-hydroxy- β -thujone as auxin polar transport inhibitors. *Acta Physiologiae Plantarum*, 35, 2251-2258.
- VAN BERKEL, K., DE BOER, R. J., SCHERES, B. & TEN TUSSCHER, K. 2013. Polar auxin transport: models and mechanisms. *Development*, 140, 2253-2268.
- VAN NOORDEN, G. E., KERIM, T., GOFFARD, N., WIBLIN, R., PELLERONE, F. I., ROLFE, B. G. & MATHESIUS, U. 2007. Overlap of Proteome Changes in *Medicago truncatula* in Response to Auxin and *Sinorhizobium meliloti*. *Plant Physiology*, 144, 1115-1131.

- VAN NOORDEN, G. E., ROSS, J. J., REID, J. B., ROLFE, B. G. & MATHESIUS, U. 2006. Defective Long-Distance Auxin Transport Regulation in the *Medicago truncatula* super numeric nodules Mutant. *Plant Physiology*, 140, 1494-1506.
- VAN SPRONSEN, P. C., GRÖNLUND, M., BRAS, C. P., SPAINK, H. P. & KIJNE, J. W. 2001. Cell Biological Changes of Outer Cortical Root Cells in Early Determinate Nodulation. *Molecular Plant-Microbe Interactions*, 14, 839-847.
- VAN ZEIJL, A., OP DEN CAMP, RIK H. M., DEINUM, EVA E., CHARNIKHOVA, T., FRANSSSEN, H., OP DEN CAMP, HUUB J. M., BOUWMEESTER, H., KOHLEN, W., BISSELING, T. & GEURTS, R. 2015. Rhizobium Lipo-chitoooligosaccharide Signaling Triggers Accumulation of Cytokinins in *Medicago truncatula* Roots. *Molecular Plant* (in press)
- VASSE, J., DE BILLY, F., CAMUT, S. & TRUCHET, G. 1990. Correlation between ultrastructural differentiation of bacteroids and nitrogen fixation in alfalfa nodules. *Journal of Bacteriology*, 172, 4295-4306.
- VERRIER, P. J., BIRD, D., BURLA, B., DASSA, E., FORESTIER, C., GEISLER, M., KLEIN, M., KOLUKISA OGLU, Ü., LEE, Y., MARTINOIA, E., MURPHY, A., REA, P. A., SAMUELS, L., SCHULZ, B., SPALDING, E. P., YAZAKI, K. & THEODOULOU, F. L. 2008. Plant ABC proteins – a unified nomenclature and updated inventory. *Trends in Plant Science*, 13, 151-159.
- VILLAGRASA, M., GUILLAMÓN, M., ELJARRAT, E. & BARCELÓ, D. 2007. Matrix effect in liquid chromatography–electrospray ionization mass spectrometry analysis of benzoxazinoid derivatives in plant material. *Journal of Chromatography A*, 1157, 108-114.
- VITOUSEK, P. M., MENGE, D. N. L., REED, S. C. & CLEVELAND, C. C. 2013. Biological nitrogen fixation: rates, patterns and ecological controls in terrestrial ecosystems. *Philosophical Transactions of the Royal Society B: Biological Sciences*, 368.
- VOSS, M., BANGE, H. W., DIPPNER, J. W., MIDDELBURG, J. J., MONTOYA, J. P. & WARD, B. 2013. The marine nitrogen cycle: recent discoveries, uncertainties and the potential relevance of climate change. *Philosophical Transactions of the Royal Society B: Biological Sciences*, 368.
- WALKER, S. A. & DOWNIE, J. A. 2000. Entry of *Rhizobium leguminosarum* bv. *viciae* into Root Hairs Requires Minimal Nod Factor Specificity, but Subsequent Infection Thread Growth Requires nodO or nodE. *Molecular Plant-Microbe Interactions*, 13, 754-762.

- WALZ, A., PARK, S., SLOVIN, J. P., LUDWIG-MÜLLER, J., MOMONOKI, Y. S. & COHEN, J. D. 2002. A gene encoding a protein modified by the phytohormone indoleacetic acid. *Proceedings of the National Academy of Sciences*, 99, 1718-1723.
- WALZ, A., SEIDEL, C., RUSAK, G., PARK, S., COHEN, J. D. & LUDWIG-MÜLLER, J. 2008. Heterologous expression of IAP1, a seed protein from bean modified by indole-3-acetic acid, in *Arabidopsis thaliana* and *Medicago truncatula*. *Planta*, 227, 1047-61.
- WANG, D., PAJEROWSKA-MUKHTAR, K., CULLER, A. H. & DONG, X. 2007. Salicylic Acid Inhibits Pathogen Growth in Plants through Repression of the Auxin Signaling Pathway. *Current Biology*, 17, 1784-1790.
- WANG, J.-R., HU, H., WANG, G.-H., LI, J., CHEN, J.-Y. & WU, P. 2009. Expression of PIN Genes in Rice (*Oryza sativa* L.): Tissue Specificity and Regulation by Hormones. *Molecular Plant*, 2, 823-831.
- WANG, S. & FU, J. 2011. Insights into auxin signaling in plant-pathogen interactions. *Frontiers in Plant Science*, 2.
- WASSON, A. P., PELLERONE, F. I. & MATHESIUS, U. 2006. Silencing the Flavonoid Pathway in *Medicago truncatula* Inhibits Root Nodule Formation and Prevents Auxin Transport Regulation by Rhizobia. *The Plant Cell Online*, 18, 1617-1629.
- WASSON, A. P., RAMSAY, K., JONES, M. G. K. & MATHESIUS, U. 2009. Differing requirements for flavonoids during the formation of lateral roots, nodules and root knot nematode galls in *Medicago truncatula*. *New Phytologist*, 183, 167-179.
- WELLS, D. M., LAPLAZE, L., BENNETT, M. J. & VERNOUX, T. 2013. Biosensors for phytohormone quantification: challenges, solutions, and opportunities. *Trends in Plant Science*, 18, 244-249.
- WENT, F. W. 1926. On growth accelerating substances in the coleoptile of *Avena sativa*. *Proc. K. Akad. Wet.*, 30, 10-19.
- WIGHTMAN, F. & LIGHTY, D. L. 1982. Identification of phenylacetic acid as a natural auxin in the shoots of higher plants. *Physiologia Plantarum*, 55, 17-24.
- WISNIEWSKA, J., XU, J., SEIFERTOVA, D., BREWER, P. B., RUZICKA, K., BLILOU, I., ROQUIE, D., BENKOVA, E., SCHERES, B. & FRIML, J. 2006. Polar PIN Localization Directs Auxin Flow in Plants. *Science*, 1121356.

- WON, C., SHEN, X., MASHIGUCHI, K., ZHENG, Z., DAI, X., CHENG, Y., KASAHARA, H., KAMIYA, Y., CHORY, J. & ZHAO, Y. 2011. Conversion of tryptophan to indole-3-acetic acid by TRYPTOPHAN AMINOTRANSFERASES OF ARABIDOPSIS and YUCCAs in Arabidopsis. *Proceedings of the National Academy of Sciences*.
- WRIGHT, A. D., SAMPSON, M. B., NEUFFER, M. G., MICHALCZUK, L., SLOVIN, J. P. & COHEN, J. D. 1991. Indole-3-Acetic Acid Biosynthesis in the Mutant Maize *orange pericarp*, a Tryptophan Auxotroph. *Science*, 254, 998-1000.
- WU, C., DICKSTEIN, R., CARY, A. J. & NORRIS, J. H. 1996. The Auxin Transport Inhibitor N-(1-Naphthyl)phthalamic Acid Elicits Pseudonodules on Nonnodulating Mutants of White Sweetclover. *Plant Physiology*, 110, 501-510.
- WU, Z., GAO, W., PHELPS, M. A., WU, D., MILLER, D. D. & DALTON, J. T. 2004. Favorable Effects of Weak Acids on Negative-Ion Electrospray Ionization Mass Spectrometry. *Analytical Chemistry*, 76, 839-847.
- WUYTS, N., LOGNAY, G., SWENNEN, R. & DE WAELE, D. 2006. Nematode infection and reproduction in transgenic and mutant Arabidopsis and tobacco with an altered phenylpropanoid metabolism. *Journal of Experimental Botany*, 57, 2825-2835.
- XIAO, T. T., SCHILDERINK, S., MOLING, S., DEINUM, E. E., KONDOROSI, E., FRANSEN, H., KULIKOVA, O., NIEBEL, A. & BISSELING, T. 2014. Fate map of *Medicago truncatula* root nodules. *Development*, 141, 3517-3528.
- XU, T., DAI, N., CHEN, J., NAGAWA, S., CAO, M., LI, H., ZHOU, Z., CHEN, X., DE RYCKE, R., RAKUSOVÁ, H., WANG, W., JONES, A. M., FRIML, J., PATTERSON, S. E., BLEECKER, A. B. & YANG, Z. 2014. Cell Surface ABP1-TMK Auxin-Sensing Complex Activates ROP GTPase Signaling. *Science*, 343, 1025-1028.
- YANG, H. & MURPHY, A. S. 2009. Functional expression and characterization of Arabidopsis ABCB, AUX 1 and PIN auxin transporters in *Schizosaccharomyces pombe*. *The Plant Journal*, 59, 179-191.
- YANG, Y., HAMMES, U. Z., TAYLOR, C. G., SCHACHTMAN, D. P. & NIELSEN, E. 2006. High-Affinity Auxin Transport by the AUX1 Influx Carrier Protein. *Current Biology*, 16, 1123-1127.
- YANG, Y., YUE, R., SUN, T., ZHANG, L., CHEN, W., ZENG, H., WANG, H. & SHEN, C. 2014. Genome-wide identification, expression analysis of GH3 family genes in *Medicago truncatula* under stress-related hormones and *Sinorhizobium meliloti* infection. *Applied Microbiology and Biotechnology*, 1-14.

- YIN, R., HAN, K., HELLER, W., ALBERT, A., DOBREV, P. I., ZAŽÍMALOVÁ, E. & SCHÄFFNER, A. R. 2014. Kaempferol 3-O-rhamnoside-7-O-rhamnoside is an endogenous flavonol inhibitor of polar auxin transport in Arabidopsis shoots. *New Phytologist*, 201, 466-475.
- YOKOTA, K. & HAYASHI, M. 2011. Function and evolution of nodulation genes in legumes. *Cellular and Molecular Life Sciences*, 68, 1341-1351.
- YOKOTA, K., SOYANO, T., KOUCHI, H. & HAYASHI, M. 2010. Function of GRAS Proteins in Root Nodule Symbiosis is Retained in Homologs of a Non-Legume, Rice. *Plant and Cell Physiology*, 51, 1436-1442.
- ZAŽÍMALOVÁ, E., MURPHY, A. S., YANG, H., HOYEROVÁ, K. & HOŠEK, P. 2010. Auxin Transporters—Why So Many? *Cold Spring Harbor Perspectives in Biology*, 2.
- ZHAN, J. & SUN, Q. 2012. Diversity of free-living nitrogen-fixing microorganisms in the rhizosphere and non-rhizosphere of pioneer plants growing on wastelands of copper mine tailings. *Microbiological Research*, 167, 157-165.
- ZHANG, J., SUBRAMANIAN, S., STACEY, G. & YU, O. 2009. Flavones and flavonols play distinct critical roles during nodulation of *Medicago truncatula* by *Sinorhizobium meliloti*. *The Plant Journal*, 57, 171-183.
- ZHANG, Z., LI, Q., LI, Z., STASWICK, P. E., WANG, M., ZHU, Y. & HE, Z. 2007. Dual Regulation Role of GH3.5 in Salicylic Acid and Auxin Signaling during Arabidopsis-*Pseudomonas syringae* Interaction. *Plant Physiology*, 145, 450-464.
- ZHAO, Y., CHRISTENSEN, S. K., FANKHAUSER, C., CASHMAN, J. R., COHEN, J. D., WEIGEL, D. & CHORY, J. 2001. A Role for Flavin Monooxygenase-Like Enzymes in Auxin Biosynthesis. *Science*, 291, 306-309.
- ZHAO, Y., HULL, A. K., GUPTA, N. R., GOSS, K. A., ALONSO, J., ECKER, J. R., NORMANLY, J., CHORY, J. & CELENZA, J. L. 2002. Trp-dependent auxin biosynthesis in Arabidopsis: involvement of cytochrome P450s CYP79B2 and CYP79B3. *Genes and Development*, 16, 3100-3112.
- ZHOU, Z.-Y., ZHANG, C.-G., WU, L., ZHANG, C.-G., CHAI, J., WANG, M., JIA, A., JIA, P.-F., CUI, S.-J., YANG, M., CHEN, R. & GUO, G.-Q. 2011. Functional characterization of the CKRC1/TAA1 gene and dissection of hormonal actions in the Arabidopsis root. *The Plant Journal*, 66, 516-527.

ZUANAZZI, J. A. S., CLERGEOT, P. H., QUIRION, J.-C., HUSSON, H.-P., KONDOROSI, A. & RATET, P. 1998. Production of *Sinorhizobium meliloti* nod Gene Activator and Repressor Flavonoids from *Medicago sativa* Roots. *Molecular Plant-Microbe Interactions*, 11, 784-794.

Appendix A - Growth media

1. Fahraeus medium (Fahraeus, 1957)

Chemical	Stock conc.	ml / L dH ₂ O
Calcium chloride dihydrate, CaCl ₂ ·2H ₂ O	13.2 g / 100 ml	1
Magnesium sulphate heptahydrate, MgSO ₄ ·7H ₂ O	12 g / 100 ml	1
Potassium dihydrogen phosphate, KH ₂ PO ₄	10 g / 100 ml	1
Disodium hydrogen phosphate dodecahydrate, Na ₂ HPO ₄ ·12H ₂ O	15 g / 100 ml	1
Ferric citrate	0.5 g / 100 ml	1
Gibson's trace elements*	See below	1
Agar (J3 grade)	NA	10 g / L

* *Gibson's trace elements*

Chemical	Conc.
Boric acid, H ₃ BO ₃	2.96 g / L
Manganese sulphate tetrahydrate, MnSO ₄ ·4H ₂ O	2.03 g / L
Zinc sulphate heptahydrate, ZnSO ₄ ·7H ₂ O	220 mg / L
Copper sulphate pentahydrate, CuSO ₄ ·5H ₂ O	80 mg / L
Molybdic acid monohydrate, H ₂ MoO ₄ ·H ₂ O	90 mg / L
Sodium molybdate dihydrate, Na ₂ MoO ₄ ·2H ₂ O	121 mg / L

2. Modified Fahraeus medium (for *Agrobacterium rhizogenes* transformation)

Chemical	Stock conc.	Final conc.
Macroelements		
Calcium chloride, CaCl ₂	0.9 M	0.9 mM
Magnesium sulphate, MgSO ₄	0.5 M	0.5 mM
Potassium dihydrogen phosphate, KH ₂ PO ₄	0.7 M	0.7 mM
Disodium hydrogen phosphate, Na ₂ HPO ₄	0.4 M	0.8 mM
Ferric citrate	20 mM	20 µM
Ammonium nitrate, NH ₄ NO ₃	1 M	0.5 mM
Microelements		
Manganese chloride, MnCl ₂	1 mg / ml	100 µg / L
Copper sulphate, CuSO ₄	1 mg / ml	100 µg / L
Zinc chloride, ZnCl ₂	1 mg / ml	100 µg / L
Boric acid, H ₃ BO ₃	1 mg / ml	100 µg / L
Sodium molybdate, Na ₂ MoO ₄	1 mg / ml	100 µg / L
Agar (J3 grade)	NA	10 g / L

Kanamycin is added to autoclaved medium to a final concentration of 25 mg / l

3. Broughton and Dilworth medium (Broughton and Dilworth, 1971)

Chemical	Amount in 100 ml	Stock conc. (1000x)	Final conc.
CaCl ₂ .2H ₂ O	14.7 g	1.0 M	1.0 mM
KH ₂ PO ₄	6.8 g	0.5 M	0.5 mM
FeCitrate.H ₂ O	0.26 g	0.01 M	10 µM
MgSO ₄ .7H ₂ O	6.2 g	0.25 M	0.25 mM
K ₂ SO ₄	4.4 g	0.25 M	0.25 mM
MnSO ₄ .H ₂ O	16.9 mg	1.0 mM	1.0 µM
H ₃ BO ₃	12.4 mg	2.0 mM	2.0 µM
ZnSO ₄ .7H ₂ O	14.4 mg	0.5 mM	0.5 µM
CuSO ₄ .5H ₂ O	5.0 mg	0.2 mM	0.2 µM
CoCl ₂ .6H ₂ O	2.4 mg	0.1 mM	0.1 µM
Na ₂ MoO ₄ .2H ₂ O	2.4 mg	0.1 mM	0.1 µM

4. Bergensen's modified medium (Rolfe and Gresshoff, 1988)

Chemical	Stock conc.	Amount / conc.
Calcium chloride, CaCl ₂	4 g / 100 ml	1 ml / L
Magnesium sulphate, MgSO ₄	8 g / 100 ml	1 ml / L
Disodium hydrogen phosphate, Na ₂ HPO ₄	36 g / 100 ml	4 ml / L
Iron(III) chloride, FeCl ₃	0.3 g / 100 ml	1 ml / L
Gamborg's trace elements**	NA	1 ml / L
Vitamins***	NA	1 ml / L
Glutamic acid (sodium salt)	NA	0.5 g
Yeast extract	NA	0.5 g
Mannitol		
- for solid media	NA	3.0 g
- for liquid media		10.0 g
Agar (J3 grade)	NA	12 g / L

** *Gamborg's trace elements (filter-sterilised; Gamborg et al., 1968)*

Chemical	Conc. (g / L)
Boric acid, H ₃ BO ₃	3.0
Manganese sulphate tetrahydrate, MnSO ₄ ·4H ₂ O	10.0
Zinc sulphate heptahydrate, ZnSO ₄ ·7H ₂ O	3.0
Copper sulphate pentahydrate, CuSO ₄ ·5H ₂ O	0.25
Copper chloride hexahydrate, CoCl ₂ ·6H ₂ O	0.25
Sodium molybdate dihydrate, Na ₂ MoO ₄ ·2H ₂ O	0.25

*** Vitamins

Microwave to boiling 90 ml dH₂O, add 20 mg biotin and stir. Add 200 mg thiamine.

Adjust to 100 ml. Add 1 drop of 1 M HCl. Filter-sterilise into autoclaved bottle.

Appendix B - Quality parameters for auxin detection method using LC-MS/MS

1. Quality parameters for auxin detection method in the positive ion polarity

Analyte	Molecular formulae	MW (g/mol)	Parent Ion [M+H] ⁺	Collision energy (eV)	t _R (min)	Product ions (from most intense to least)					LOD ^a (pg/mg)	LOQ ^b (pg/mg)	Linearity (y =)	Correlation coefficient (R ²)
D5-IAA	C ₁₀ H ₄ D ₅ NO ₂	180.21	181.1014	12	12.3 ± 0.004	134.0892	133.0826	135.0961	116.9742	95.9716	0.54	0.91	-	-
IAA	C ₁₀ H ₉ NO ₂	175.19	176.0710	10	12.4 ± 0.005	130.0643	131.0663	158.0582	103.0522	77.0336	1.01	1.69	20.9120x - 0.1716	0.9991
IBA	C ₁₂ H ₁₃ NO ₂	203.24	204.1033	12	15.7 ± 0.007	186.0890	130.0624	168.0787	158.0934	144.0790	0.20	0.51	34.5990x - 0.3430	0.9976
4-Cl-IAA	C ₁₀ H ₈ ClNO ₂	209.63	210.0295	10	15.1 ± 0.063	164.0256	165.0275	166.0226	169.9534	129.0527	3.13	5.22	1.6144x + 0.0239	0.9915
IAA-Ala	C ₁₃ H ₁₄ N ₂ O ₃	246.27	247.1095	10	11.7 ± 0.014	130.0651	90.0553	131.0686	201.1019	-	0.75	1.26	30.9550x - 0.1009	0.9991
IAA-Asp	C ₁₄ H ₁₄ N ₂ O ₅	290.28	291.0939	10	9.7 ± 0.064	130.0661	134.0462	88.0396	273.0922	245.0932	3.86	6.44	13.073x - 0.2022	0.9950
IAA-Ile	C ₁₆ H ₂₀ N ₂ O ₃	288.35	289.1538	12	16.5 ± 0.016	130.0648	132.1011	86.0967	243.1486	271.1419	0.35	0.59	54.773x - 0.3395	0.9990
IAA-Leu	C ₁₆ H ₂₀ N ₂ O ₃	288.35	289.1538	12	16.5 ± 0.016	130.0648	132.1011	86.0967	243.1486	271.1419	0.35	0.59	54.773x - 0.3395	0.9990
IAA-Phe	C ₁₉ H ₁₈ N ₂ O ₃	322.37	323.1418	12	16.9 ± 0.008	130.0646	166.0853	120.0803	277.1325	121.0828	1.03	1.71	18.175x - 0.0959	0.9996
IAA-Trp	C ₂₁ H ₁₉ N ₃ O ₃	361.39	362.1491	15	16.4 ± 0.006	130.0648	188.0709	205.0974	185.0713	159.0923	1.90	3.16	9.3314x - 0.0524	0.9988
IAA-Val	C ₁₅ H ₁₈ N ₂ O ₃	274.32	275.1407	12	15.2 ± 0.003	130.0662	229.1349	118.0867	72.0818	131.0692	0.55	0.91	27.522x - 0.2154	0.9984

Injection precision (n=10), data show mean and SD

^a Limit of detection (LOD) ≥ 3 x S/N; ^b Limit of quantification (LOQ) ≥ 5 x S/N, S/N, signal-to-noise ratio

2. Quality parameters for auxin detection method in the negative ion polarity

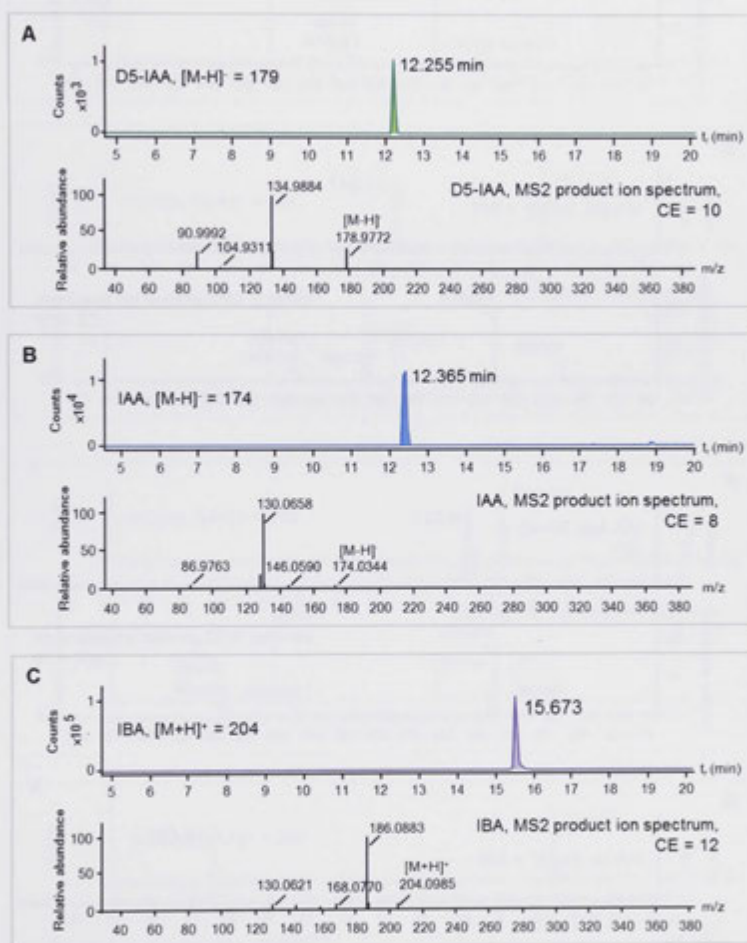
Analyte	Molecular formulae	MW (g/mol)	Parent Ion [M-H] ⁻	Collision energy (eV)	t _R (min)	Product ions (from most intense to least)					LOD ^a (pg/mg)	LOQ ^b (pg/mg)	Linearity (y =)	Correlation coefficient (R ²)
D5-IAA	C ₁₀ H ₄ D ₅ NO ₂	180.21	179.0874	10	12.2 ± 0.020	135.0960	90.9979	159.6305	59.1363	104.9311	3.71	6.18	-	-
IAA	C ₁₀ H ₉ NO ₂	175.19	174.0561	8	12.4 ± 0.008	130.0647	128.0479	131.0660	136.2874	86.9760	3.04	5.07	2.6951x + 0.0041	0.9986
IBA	C ₁₂ H ₁₃ NO ₂	203.24	202.0874	25	15.6 ± 0.033	116.0517	158.0970	73.0278	59.0133	-	52.64	87.74	0.4795x + 0.0037	0.9991
PAA	C ₈ H ₈ O ₂	136.05	135.0452	3	11.7 ± 0.047	91.0526	72.0207	117.4564	50.2836	-	6.90	11.50	1.2736x - 0.0050	0.9922
4-Cl-IAA	C ₁₀ H ₈ ClNO ₂	209.63	208.0171	8	15.0 ± 0.006	164.0287	165.0275	128.0468	-	-	0.25	0.41	21.5260x + 0.1375	0.9956
IAA-Ala	C ₁₃ H ₁₄ N ₂ O ₃	246.27	245.0932	12	11.6 ± 0.009	88.0404	156.0444	128.0499	89.0436	-	0.29	0.49	35.567x + 0.1561	0.9992
IAA-Asp	C ₁₄ H ₁₄ N ₂ O ₅	290.28	289.0830	17	9.6 ± 0.059	88.0423	132.0311	115.0051	173.0723	156.0472	1.55	2.58	9.1470x + 0.0279	0.9975
IAA-Ile	C ₁₆ H ₂₀ N ₂ O ₃	288.35	287.1361	15	16.5 ± 0.002	130.0854	131.0887	156.0425	243.1475	-	0.05	0.09	97.2150x + 1.1548	0.9959
IAA-Leu	C ₁₆ H ₂₀ N ₂ O ₃	288.35	287.1385	10	16.5 ± 0.002	130.0854	131.0887	156.0425	243.1475	-	0.05	0.09	97.2150x + 1.1548	0.9959
IAA-Phe	C ₁₉ H ₁₈ N ₂ O ₃	322.37	321.1245	15	16.9 ± 0.007	164.0718	165.0749	147.0453	103.0548	277.1341	0.14	0.24	45.3370x + 0.3456	0.9974
IAA-Trp	C ₂₁ H ₁₉ N ₃ O ₃	361.39	360.1354	17	16.4 ± 0.003	203.0829	204.0864	74.0254	116.0514	156.0455	0.76	1.27	6.3667x + 0.1310	0.9914
IAA-Val	C ₁₅ H ₁₈ N ₂ O ₃	274.32	273.1243	15	15.1 ± 0.006	116.0739	117.0765	156.0478	128.0522	229.1371	0.11	0.18	58.1590x + 0.3346	0.9987

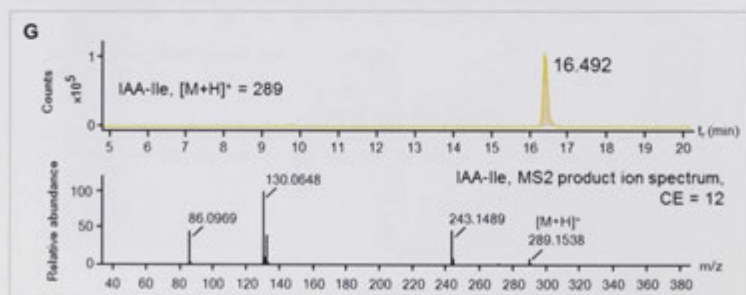
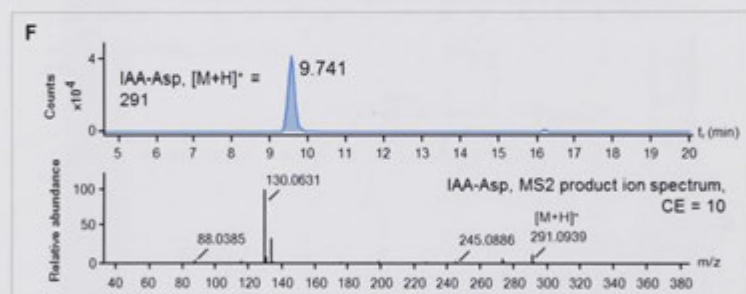
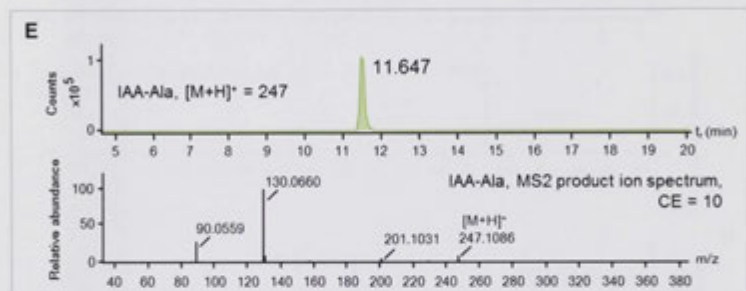
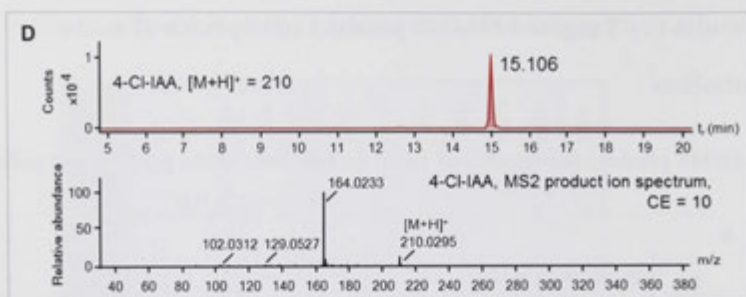
Injection precision (n=10); data show mean and SD

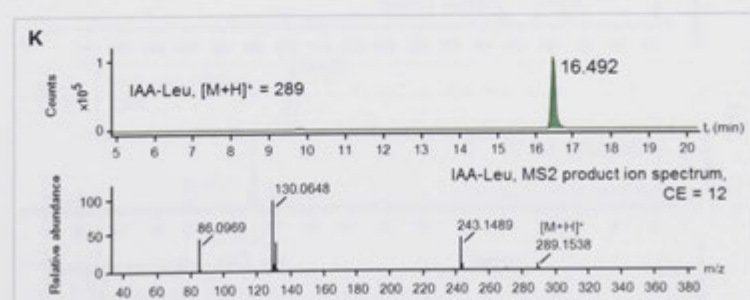
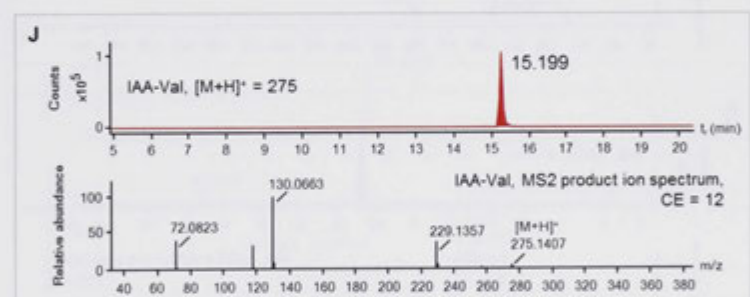
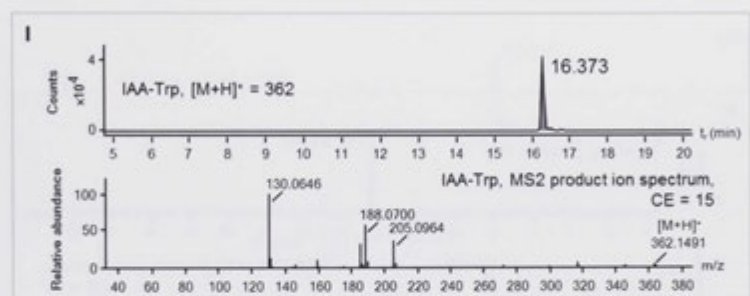
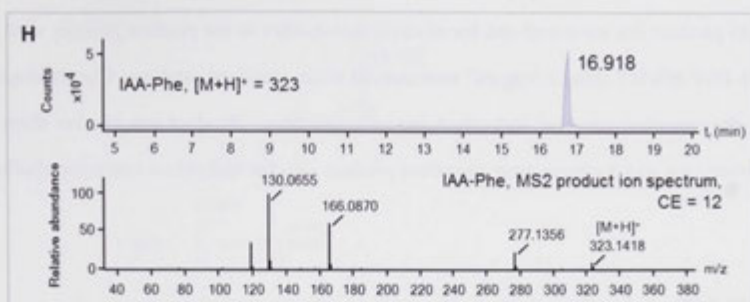
^a Limit of detection (LOD) ≥ 3 x S/N; ^b Limit of quantification (LOQ) ≥ 5 x S/N; S/N, signal-to-noise ratio

Appendix C - Targeted MS/MS product ion spectra of auxin metabolites

1. MS/MS product ion spectra of auxin metabolites in the positive ion polarity

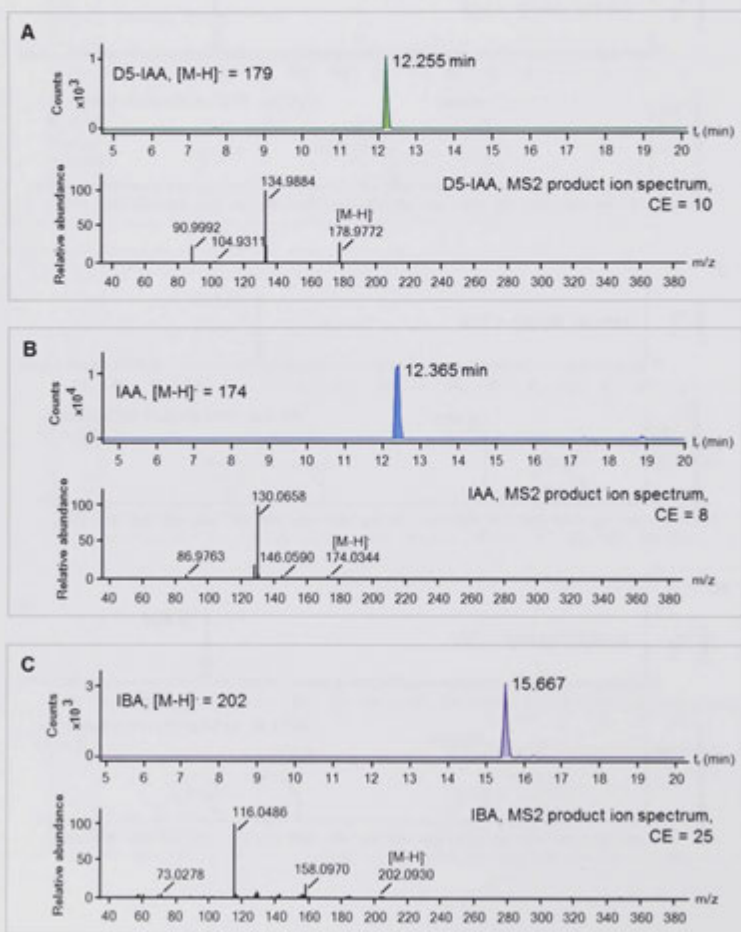


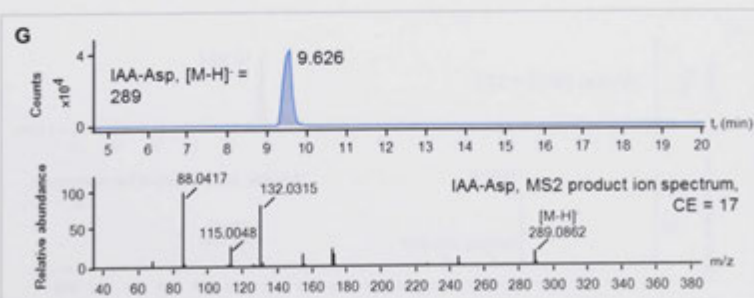
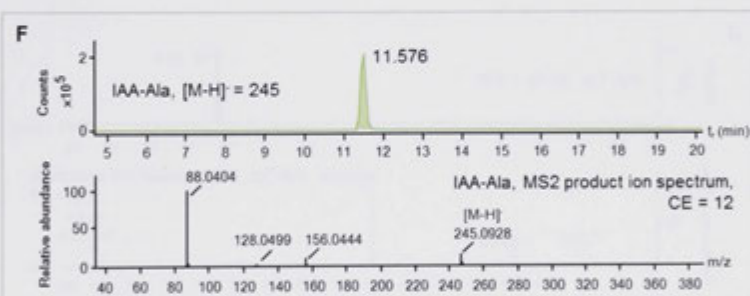
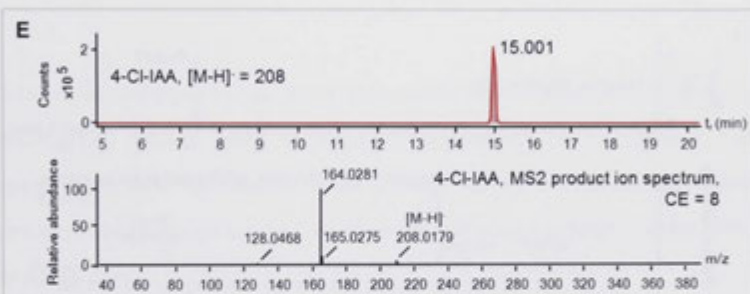
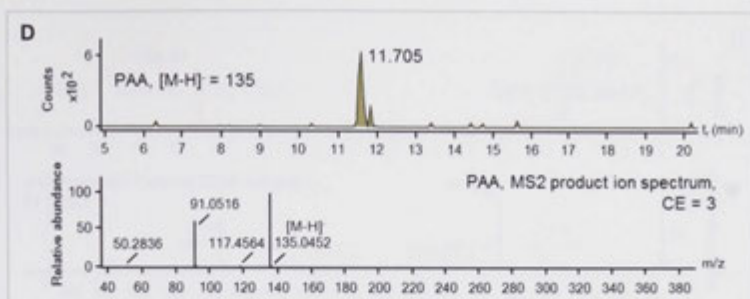


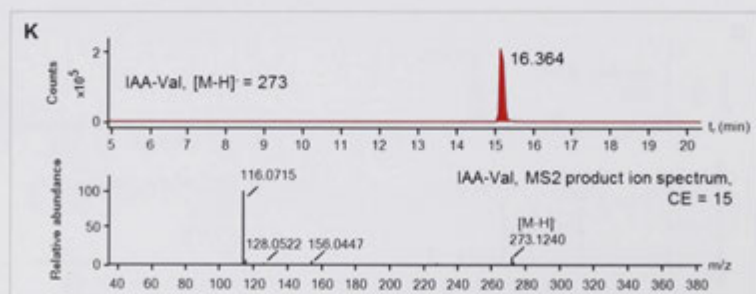
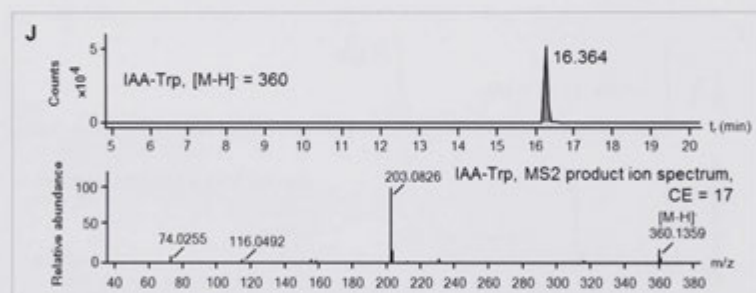
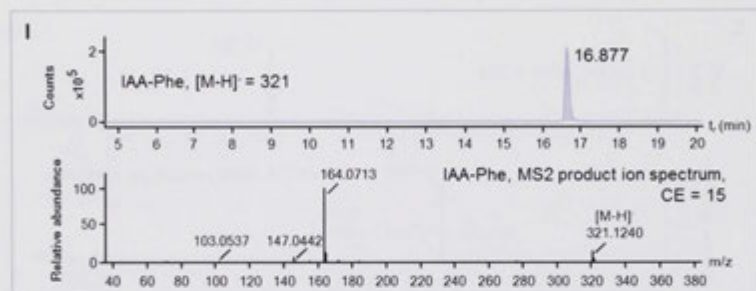
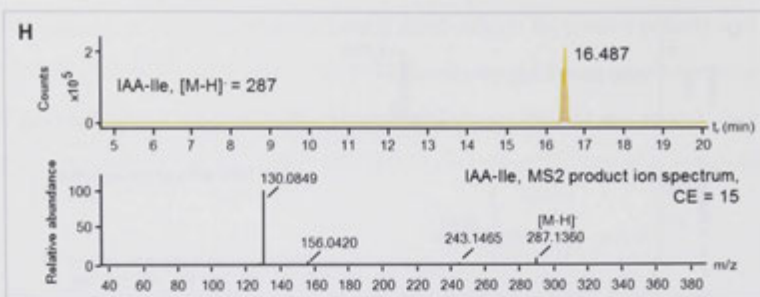


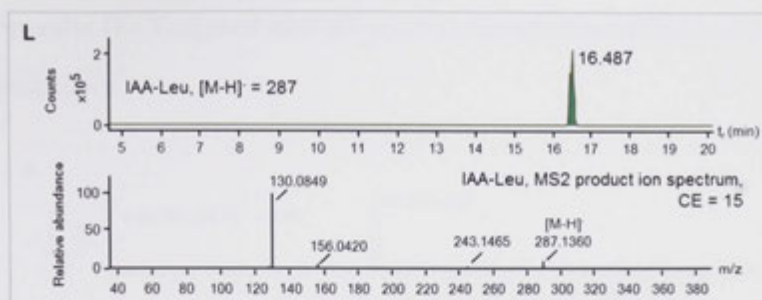
MS/MS product ion scans and spectra of auxin metabolites in the positive polarity with LC-ESI-Q-TOF MS/MS using a $5 \mu\text{g ml}^{-1}$ commercial auxin standard mixture. Chromatograms show the retention times of individual auxin metabolites. Product ion spectra show the precursor ions and the three most abundant product ions for individual auxin metabolites.

2. MS/MS product ion spectra of auxin metabolites in the negative ion polarity



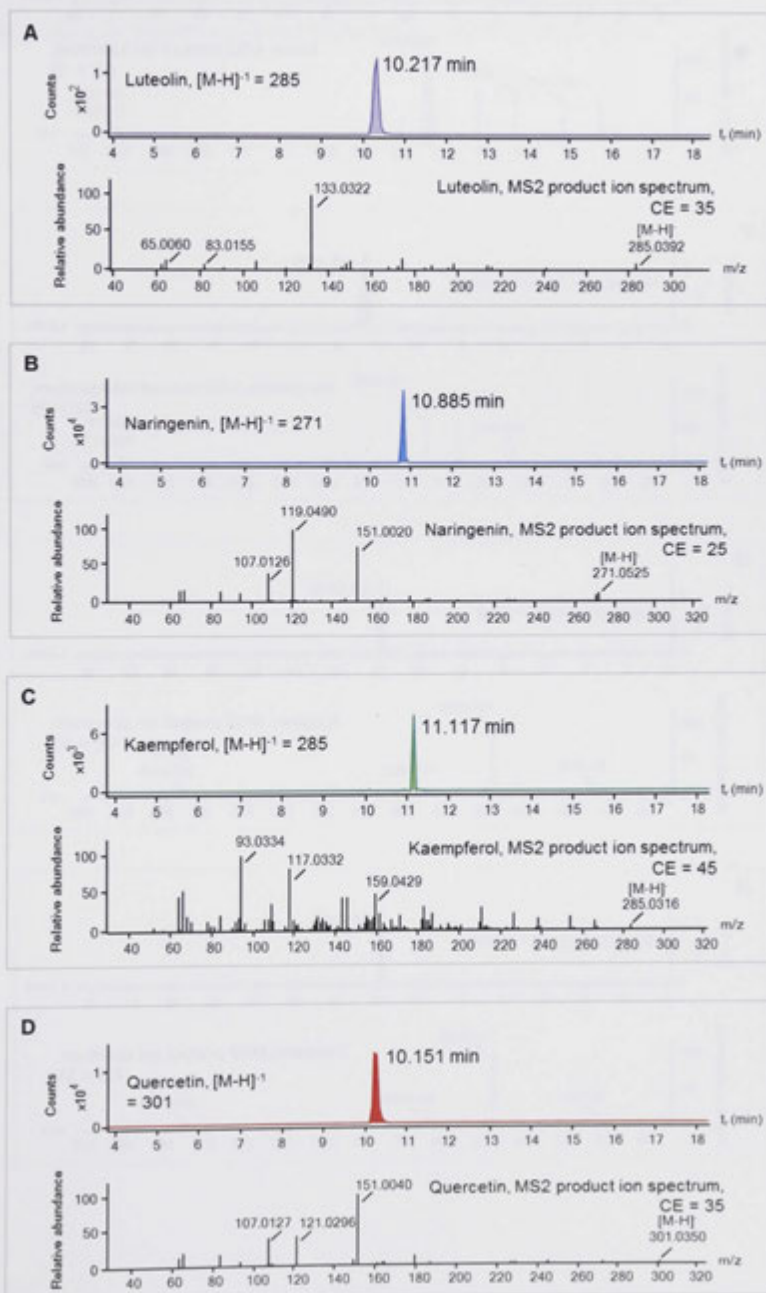


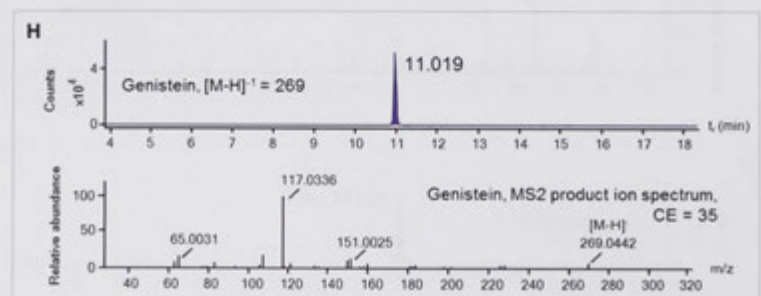
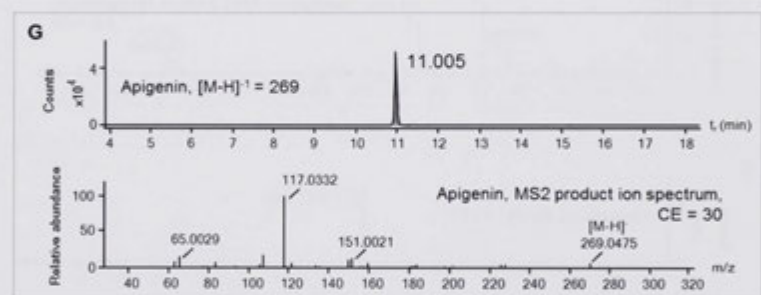
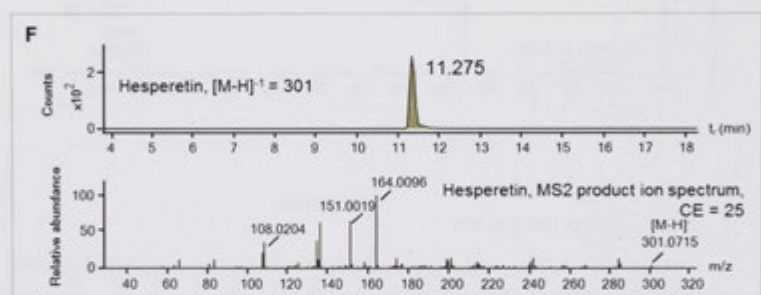
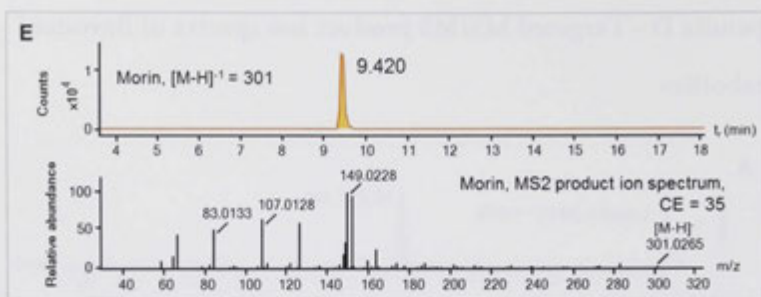




MS/MS product ion scans and spectra of auxin metabolites in the negative ion polarity with LC-ESI-Q-TOF MS/MS using a 5 $\mu\text{g ml}^{-1}$ commercial auxin standard mixture. Chromatograms show the retention times of individual auxin metabolites. Product ion spectra show the precursor ions and the three most abundant product ions for individual auxin metabolites.

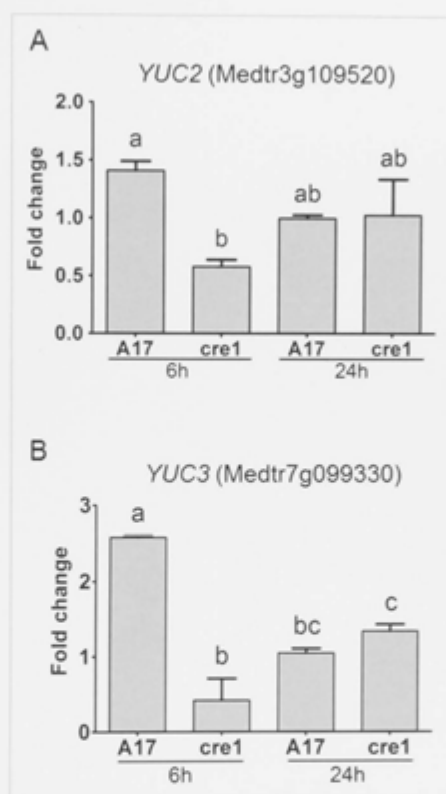
Appendix D - Targeted MS/MS product ion spectra of flavonoid metabolites





MS/MS product ion scans and spectra of flavonoid metabolites in the negative ion polarity with LC-ESI-Q-TOF MS/MS using $5 \mu\text{g ml}^{-1}$ commercial flavonoid standards. Chromatograms show the retention times of individual flavonoid compounds. Product ion spectra show the precursor ions and the three most abundant product ions.

Appendix E - Transcriptional changes in putative auxin synthesis genes in response to E65 inoculation



Transcriptional abundance of putative *YUC* genes in WT and the *cre1* mutant in response to E65 inoculation. Expression was normalised to the *GLYCERALDEHYDE 3-PHOSPHATE DEHYDROGENASE (GAPDh)* reference gene. A two way ANOVA with a Tukey-Kramer multiple comparison post-test was used for statistical analysis ($p < 0.05$; $n = 3$). Different lowercase letters indicate statistically significant difference in transcript abundance.